Investigation of the role of sialo-glycoproteins in oral biofilms

By:

Katherine Ka Yee Ansbro

A thesis submitted for the degree of Doctor of Philosophy

School of Clinical Dentistry
Faculty of Medicine, Dentistry and Health
University of Sheffield

30/09/2022

Acknowledgements

This work would not have been possible without the support of many people, as well as my funders the University of Sheffield and GlaxoSmithKline.

Firstly, I would like to say a huge thank you to my supervisor Professor Graham Stafford. You were always there to provide support and guidance, and I am grateful for your invaluable insight as well as your dedication to your students.

I would also like to thank Professor William Wade, Dr David Bradshaw, Dr Jonathan Pratten and Dr Joey Shepherd for your advice and guidance. Your supervision and input were always valued. Thank you also to Dr Keyvan Moharamzadeh, Dr Sarah Pollington, Katy D'Apice and Dr Emma Bird for your tireless help with obtaining ethical approval, recruiting volunteers, and collecting clinical samples. I am also incredibly grateful to all of the volunteers who took part in our study and who very kindly provided the clinical samples. Thanks also to Dr Matt Parker and Matt Wyles for their help with Nanopore sequencing.

I am greatly indebted to our technical staff Jason and Brenka who provided endless support throughout their years at the Dental School. Many thanks also to the PhD students, post-docs and other staff members (past and present) I have encountered along the way. I have greatly enjoyed our friendships and time spent together. It's not possible to mention everyone by name but a special thanks must go to the Stafford/Shepherd research group, as well as to Anita, Ash, Beth, and Cher who I was lucky enough to start my PhD with.

I am grateful for the love and support from my Mum and Dad, Karen, Dawn, and Derek throughout these years so thank you to you all. To my husband Simon, I could not have done this without you, and I am so thankful for the laughter, support and love you have given me. To our beautiful daughter Jennifer who was part of this PhD journey without her realising it at the time, I love you and this is for you.

Contents

List of Figures

List of Tables

Abbreviations

4-MU- 4-methylumbelliferone

BCA- bicinchoninic acid

bp- base pair

BSM- bovine submaxillary mucin

CDC- Centre for Disease Control and Prevention

CDFF- constant depth film fermentor

CFU- colony forming unit

CLSM- confocal laser scanning microscopy

C_t - cycle threshold

DANA- 2,3-dehydro-2-deoxy-N-acetylneuraminic acid

DNA- deoxyribonucleic acid

ECM- extracellular matrix

eDNA- extracellular deoxyribonucleic acid

eHOMD- expanded Human Oral Microbiome Database

EPS- extracellular polymeric substance

FAA- Fastidious Anaerobe Agar

FAB- Fastidious Anaerobe Blood Agar

FDA- Food and Drug Administration

FISH- fluorescence in situ hybridisation

GalNAc- N-acetylgalactosamine

GCF- gingival crevicular fluid

GH33- glycoside hydrolase family 33

GlcNAc- N-acetylglucosamine

GST- glutathione-S-transferase tagged

HA- hydroxyapatite

His- histidine

HOMD- Human Oral Microbiome Database

IC_{50} - half-maximal inhibitory concentration

kDa- kilo Dalton

LPS- lipopolysaccharide

MBEC- minimum eradication concentration (a.k.a. Calgary Biofilm Device)

MFUM- modified fluid universal medium

MIC- minimum inhibitory concentration

mNOS- modified NOS medium (a.k.a. ATCC 1494 medium)

MUNANA- 4-methylumbelliferyl N-acetyl-a-D-neuraminic acid

MurNAc- N-acetylmuramic acid (a.k.a. NAM)

MWCO- molecular weight cut-off

NAM- N-acetylmuramic acid (a.k.a. MurNAc)

Neu5,9Ac- 5-N,9-O-acetylneuraminic acid

Neu5Ac- 5-N-acetylneuraminic (a.k.a. sialic acid)

Neu5Gc- 5-N-glycolylneuraminic acid

OD- optical density

OTU- operational taxonomic unit

PCoA- principal coordinates analysis

PMA- propidium monoazide

pNp- p-nitrophenol

pNP-Ac- p-nitrophenyl acetate

qPCR- quantitative polymerase chain reaction

PAGE- polyacrylamide gel electrophoresis

PBS- phosphate buffered saline

PCR- polymerase chain reaction

rRNA- ribosomal ribonucleic acid

SDS- sodium dodecyl sulphate

SEM- scanning electron microscopy

TBA- thiobarbituric acid

Abstract

Background: Periodontitis affects >700 million people worldwide and is characterised by a shift in the oral microbiota to one with higher abundances of anaerobes. Several oral bacteria can synthesise sialidases to cleave sialic acid from host glycoproteins. Sialidases are thought to be virulence factors and previous work has suggested the potential role for sialidase inhibitors such as zanamivir, oseltamivir and DANA to reduce sialidase activity as well as biofilm formation.

Aims: Considering this, the aim of this thesis was to develop *in vitro* multispecies mock and plaque biofilm models and use these as tools in expanding the current understanding of the role sialo-glycoproteins play in driving dysbiotic biofilm growth.

Methods: The MBEC biofilm inoculator was used to culture the mock and plaque biofilms under anaerobic conditions. Using cultural analysis, qPCR, Illumina MiSeq and Nanopore sequencing, the biofilms were assessed for their compositions upon the influence of various factors such as the duration of biofilm growth, the addition of sialidase inhibitors and the use of deglycosylated growth medium.

Results: An *in vitro* mock 13-species biofilm model was developed, which was inoculated with *Actinomyces oris, Campylobacter rectus, Dialister invisus, Filifactor alocis, Fusobacterium nucleatum* subsp. *nucleatum*, *Neisseria subflava, Parvimonas micra, Porphyromonas gingivalis, Prevotella intermedia, Streptococcus oralis, Tannerella forsythia, Treponema denticola* and *Veillonella dispar*. The 16S rRNA gene profiling of both mock and plaque biofilm communities using Nanopore sequencing revealed both models supported the growth of aerobes, facultative and strict oral anaerobes, although the red microbial complex was not consistently recovered. Through MUNANA assays and the use of the two models, this study demonstrated the combination of 100 μM oseltamivir and 250 μM DANA in unison resulted in the reduction of sialidase activity and contributed to alterations in the microbial community compositions such as increased community diversity and changes to the relative abundance of several genera.

Conclusion: This study has expanded the current toolset in investigating the mechanisms of periodontitis progression and has shown the use of the sialidase inhibitors oseltamivir and DANA can alter multispecies oral microbial communities.

Chapter 1 – Introduction and literature review

1.1 General introduction

The oral cavity- or mouth- is a body site that connects the external environment to the human body. Consequently, the oral cavity holds one of the most diverse assortment of microorganisms in the body that includes archaea, bacteria, fungi, protozoa and viruses (Wade, 2013a). These microorganisms are collectively known as the oral microbiome. The term microbiome was introduced in 2001 by the late Nobel prize laureate Joshua Lederberg (Lederberg and McCray, 2001) to describe all the microorganisms, along with their genetic material found in a distinct ecological niche. When this community of microorganisms are attached to a surface such as a tooth, this is known as a biofilm community.

Over 700 bacterial taxa from 14 phyla: *Actinobacteria; Bacteroidetes; Chlamydiae; Chlorobi; Chloroflexi; Firmicutes; Fusobacteria; Gracilibacteria* (GN02*); Proteobacteria; Spirochaetes;* SR1*; Synergistetes; Saccharibacteria (*formerly the candidate division TM7) and WPS-2 have been detected in the mouth (Dewhirst *et al.*, 2010; Chen *et al.*, 2010). Of these, the majority of oral taxa detected were from the six phyla *Firmicutes, Bacteroidetes, Proteobacteria, Actinobacteria, Spirochaetes* and *Fusobacteria*. It is estimated half are currently uncultivated (Wade, 2013b) although research into cultivating these uncultured oral bacteria are ongoing. Wade *et al.* (2016) for instance, have recently summarised the approaches attempted for this although the list is not limited to oral bacteria. The key difficulties with culturing oral bacteria are that many are nutritionally fastidious and slow growing requiring complex media or growth conditions. This means appropriate sample collection and transport are crucial, so selection bias towards easy-to-grow strains is a concern. Bacterial culture may also require the presence of other members of the community for synergistic or symbiotic growth such as the successful isolation of TM7 strains by co-culturing with *Actinomyces* spp. for example (Soro *et al.*, 2014; He *et al.*, 2015), which led to the naming of the TM7 division as the phylum *Saccharibacteria*. These were significant achievements as the candidate phylum TM7 (part of the so-called “microbial dark matter”) which are frequently detected in culture-independent studies and associated with

periodontal disease (Liu *et al.*, 2012), were until recently lacking in cultivated representatives.

It is perhaps unsurprising that certain bacteria which have previously only been detected in DNA studies, depend on other members of the community for growth, as bacteria are frequently found as multi-species community in nature. They therefore cannot be easily grown in pure culture on agar plates in the laboratory. Whether this dependence is nutritional or signalling-based is important to understand. The recent advancements described previously therefore highlight the importance of using *in vitro* multi-species biofilm models for investigating the human microbiome in health and disease. They can for example, be valuable for understanding the role bacteria play in the aetiology of periodontal diseases.

Dental caries and periodontal diseases are common oral diseases, with periodontitis (an inflammatory disease) estimated to affect over 700 million people worldwide. Periodontitis develops as the result of an inappropriate host response to the normal microbiota in susceptible individuals. A healthy microbial community in the oral cavity is dominated by facultative Gram-positive bacteria but in periodontitis, the composition of the community shifts to one that is dysbiotic (Marsh, 1994), resulting in increased abundances of Gram-negative strict anaerobes that may provoke further host inflammation and lead to the loss of supporting tissues surrounding the teeth. The World Health Organisation has estimated 5-15% of the world's population suffer from the severe forms of periodontitis, leading to tooth loss in affected individuals (Newman *et al.*, 2012).

This doctoral project is therefore focused on investigating the community dynamics occurring during biofilm maturation in the development of periodontitis by using *in vitro* multi-species biofilm community models.

1.2 Resident microbiome in the healthy oral cavity

1.2.1 Fungi

Investigations into the resident organisms within the oral cavity are heavily dominated by those focused solely on bacteria but fungi (the so-called "oral mycobiome") also make up the oral microbiota. While approximately 700 bacterial species-level taxa are detected in the mouth, only 101 fungal species are estimated so far (Ghannoum *et al.*, 2010). The study by Ghannoum *et al.* (2010) involved 20 healthy individuals rinsing their mouth with 15 ml sterile phosphate buffered saline and the contents analysed by taking a Multitag Pyrosequencing (MTPS) approach for the universal internal transcribed spacer (ITS) regions. This technique enabled a broader fungal detection range when compared to 18S rRNA gene-based PCR amplification that is employed in other studies (e.g. Aas *et al*. (2007)). A basal oral mycobiome profile was generated in Ghannoum's study by considering only the fungi present in at least 4 of the 20 study participants. It revealed *Candida albicans* was most frequently detected in the oral cavity of healthy individuals. The potential role of *C. albicans* as a keystone pathogen alongside the early and intermediate colonisers *Streptococcus mutans* and *Fusobacterium nucleatum* in oral disease was described by Baker *et al.* (2017), and the inter-domain physical, chemical and metabolic interactions were reviewed by Krom *et al.* (2014). The second most frequently detected fungal genus in Ghannoum's study was *Cladosporium,* followed by *Aureobasidium, Aspergillus, Fusarium* and *Cryptococcus.* It is likely spores from the sporulating moulds *Cladosporium* and *Aspergillus* entered the oral cavity from the external environment and are not true colonisers. DNA from non-culturable fungi was also detected in every individual. The diversity of fungal organisms was also detected in agreement to another study from the saliva samples of healthy participants (Dupuy *et al.*, 2014) although notably, *Malassezia* was additionally isolated at 13-96 % abundances across the six study participants in the more recent study. The genus *Malassezia* is now thought to be frequently present in the commensal oral mycobiome (Diaz *et al.*, 2017; Hong *et al.*, 2020).

Furthermore, the genera *Candida* and *Aspergillus* were detected in oral rinses from a high proportion of healthy participants in a study by Peters *et al.* (2017).

Curiously, this study did not find a significant difference between healthy compared to diseased participants. It was possibly limited by the study's sampling method for periodontal patients as subgingival plaque was not collected.

1.2.2 Viruses and bacteriophages

"Virome" is the term given to viral communities and much work investigating the virome in the human body has emerged in recent years due to the availability of next-generation sequencing methods. The study by Pérez-Brocal and Moya (2018) used the Illumina MiSeq sequencing platform to profile the viral metagenome of oral wash samples from 72 healthy subjects. The sample size of this study was greater than previous studies although the age of the subjects were only in the 18-25 range. A limitation of this study was that only DNA viruses were studied. Regardless, the study demonstrated the eukaryotic viral family *Herpesviridae*, the bacteriophage families *Siphoviridae* and *Myoviridae,* plus prophages directed putatively infecting and resident within the bacterial families *Streptococcaceae*, *Neisseriaceae* and *Veillonellaceae* were distributed across >75 % of subject population. Bacteriophages however, are known to dominate in the oral virome, particularly those within the *Siphoviridae*, *Myoviridae* and *Podoviridae* families (Ly *et al.*, 2014).

Like the study by Pérez-Brocal and Moya (2018), bacteriophages were detected in a study of saliva samples from 5 healthy individuals, which were predominately viruses of *Veillonella* (such as *Veillonella dispar*) and *Streptococcus* (Pride *et al.*, 2012). Furthermore, bacteriophages specific for oral bacteria such as *Fusobacterium nucleatum, Enterococcus faecalis* and *Streptococcus mutans* have also been isolated (Machuca *et al.*, 2010; Dalmasso *et al.*, 2015). Prophages were also found in the genome of *F. nucleatum* subsp. *polymorphum* for example (Karpathy *et al.*, 2007). It has also since been reported that the viromes were relatively stable over a 60-day period (Pride *et al.*, 2012; Abeles *et al.*, 2014) and is individual-specific. These individual-specific virome profiles were further observed in a much larger study comprising multi-site sampling of 102 healthy adults. The multi-site sampling also included the mouth. In agreement to the previously

described studies, the study by Wylie *et al.* (2014) demonstrated 98 % of the study population harboured viruses belonging to the *Herpesvirales* order (HHV-6 and HHV-7) in the mouth. Furthermore, these viruses were also detected in the samples collected on second visits (which ranged from 30-359 days after first visit) in 90 % cases, suggesting HHV-6 and HHV-7 are not transient oral viruses. For such a large-scale study, it was limited however by the few results provided on the oral virome. Also, like many other studies, it also overlooked the characterisation of RNA viruses in the oral community. Hopefully in time, further follow-up studies will address this.

1.2.3 Archaea

Archaea, a prokaryotic domain that is distinct from *Bacteria* was initially isolated from the healthy oral cavity and observed under a fluorescence microscope in the late 1980s (Brusa *et al.*, 1987). In a study of 20 healthy individuals, 45 % of subjects harboured *Archaea* in both saliva and subgingival plaque samples (Brusa *et al.*, 1993). Later investigations by the same research group described the novel oral species *Methanobrevibacter oralis* (Ferrari *et al.*, 1994) which we now know to belong in *Archaea* due to phylogenetic analysis. Its potential role in periodontal disease has also been investigated, as it was previously isolated from subgingival plaque by cultural and PCR analyses (Belay *et al.*, 1988; Lepp *et al.*, 2004; Nguyen-Hieu *et al.*, 2013). DNA sequence analysis based on detecting the archaeal small subunit ribosomal DNA using *Archaea*-specific PCR primers in recent years also found *M. oralis* to be in high abundance in the subgingival plaque of periodontal patients (Kulik *et al.*, 2001). *M. oralis* is particularly prevalent in the oral cavity but other reported archaeal species have included *Methanobacterium congelese/curvum, Methanosarcina mazeii*, *Methanobrevitacter smithii, Methanobrevibacter massiliense* (Belkacemi *et al.*, 2018; Sogodogo *et al.*, 2019; Radaic and Kapila, 2021). It is likely these strict anaerobic *Archaea* live in a mutualistic manner with other anaerobic bacteria within the periodontal pocket community (Lepp *et al.*, 2004).

1.2.4 Bacteria

The majority of studies characterising the resident microorganisms within the oral cavity are focused on the bacterial domain. Its dominance is evident particularly because of the availability of the Human Oral Microbiome Database (HOMD) that is curated and specific to solely bacteria detected within the oral cavity (Chen *et al.*, 2010). The database has since been expanded into the eHOMD to now include bacteria present in the upper respiratory and digestive tracts. eHOMD is a landmark web-accessible resource where each of its reference 16S rRNA gene sequences can be used to match against user datasets in 16S rRNA gene community profiling studies. Combining this with next-generation sequencing methods has greatly improved the description of the oral microbiota. The first published iteration of the HOMD (version 10) included 619 taxa representing the 13 phyla: *Actinobacteria; Bacteroidetes; Chlamydiae; Chloroflexi; Euryarchaeota; Firmicutes; Fusobacteria; Proteobacteria; Spirochaetes;* SR1; *Synergistetes; Tenericutes* and TM7 (Dewhirst *et al.*, 2010). The distribution of the 619 taxa is shown in Figure 1.1 although approximately half remained uncultivated. Most taxa belonged in the four phyla: *Firmicutes* (227 taxa, 36.7 %); *Bacteroidetes* (107 taxa, 17.3 %); *Proteobacteria* (106 taxa, 17.1 %) and *Actinobacteria* (72 taxa, 11.6 %).

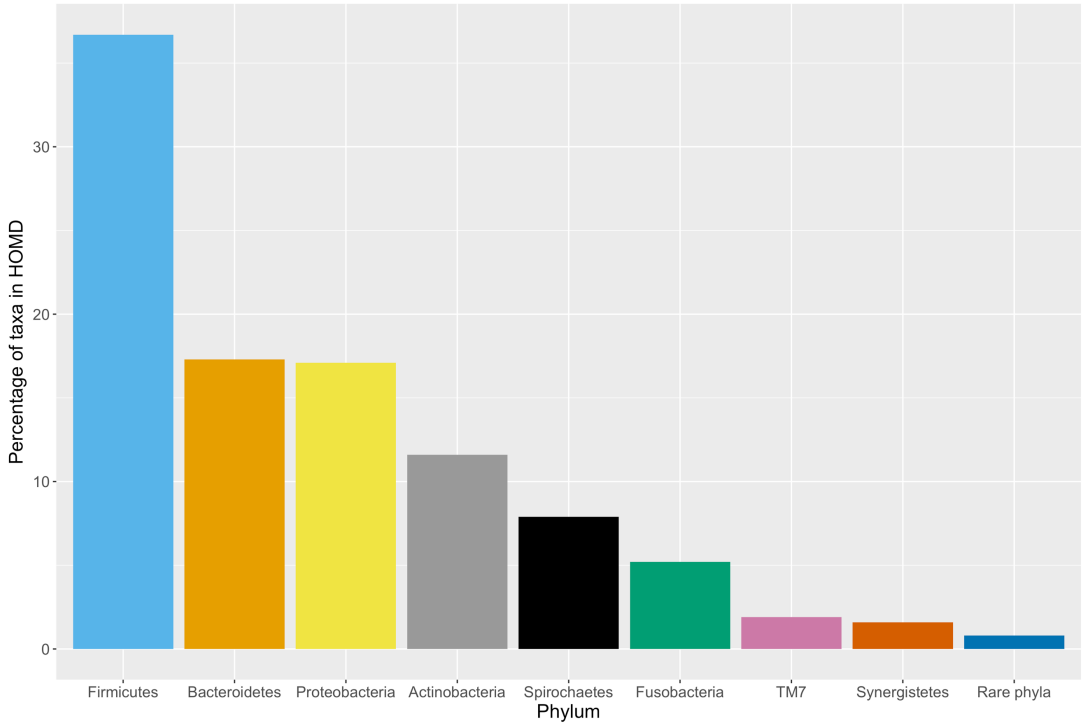

Figure 1.1. Phylogenetic distribution of phylum level taxa in HOMD. The 619 bacterial taxa published within HOMD version 10 (data taken from Dewhirst *et al*. (2010)) are distributed among the phyla. Rare phyla are described as those with <1 % abundance in the database.

Many years prior to this work, the first experiment to describe the bacterial composition of the mouth originated with the famous 'father of microbiology', Antony van Leeuwenhoek in the late 1600s. He sampled his saliva and tooth scrapings with his rudimentary but effective microscopes (Figure 1.2) (Leeuwenhoek, 1683; Porter, 1976). Culture-dependent studies then followed, with examples such as *Bacillus, Staphylococcus* and *Micrococcus* spp. amongst others isolated from the human mouth (Miller, 1890), the cultivation of the anaerobic filamentous bacterium *Leptothrix buccalis* by Robin (1853) and the first isolation of the oral bacterium *S. mutans* in 1924 (Verma, Garg and Dubey, 2018) although culture-based techniques are slow and require previous knowledge of optimum growth conditions for certain bacteria which may be fastidious in nature. Culture-independent methods such as DNA cloning and sequencing can address these shortcomings.

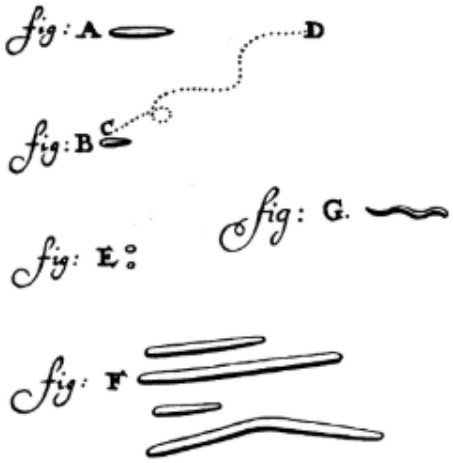

Figure 1.2 Leeuwenhoek's drawings of different bacterial types. Original drawings by Leeuwenhoek in 1683 of bacilli, cocci and spirillum sampled from the human mouth used with permission from Leeuwenhoek (1683).

A particularly informative culture-independent based study was completed by Bik *et al.* (2010). Here, the 16S rRNA gene sequences in saliva and plaque samples of 10 healthy individuals were investigated by using broad-range bacteria-specific primers, cloning and Sanger sequencing. All 10 healthy individuals carried the following 11 bacterial species in their mouth, suggesting these may make up the core oral microbiome: *Haemophilus parainfluenzae; Streptococcus oralis; Streptococcus sanguinis; Granulicatella adiacens; Veillonella parvula; Veillonella dispar; Rothia aeria; Actinomyces naeslundii; Actinomyces odontolyticus; Prevotella melaninogenica* and *Capnocytophaga gingivalis.* Sequences belonging to the uncultivated group TM7 were also detected in all the participants. *Firmicutes* was the most abundant phylum. These results were in almost complete agreement with those described by Lazarevic *et al.* (2010), who sequenced the hypervariable regions V1-V3 of the 16S rRNA gene of bacterial communities in saliva samples collected from 5 healthy individuals. Here, microbiome analysis was performed whereby the variable regions within the 16S rRNA gene which is universally present in all bacteria in the communities were sequenced. The sequence reads were identified against an oral reference sequence dataset by using next-generation sequencing platforms. The process is described in Figure 1.3 by Kilian *et al.* (2016).

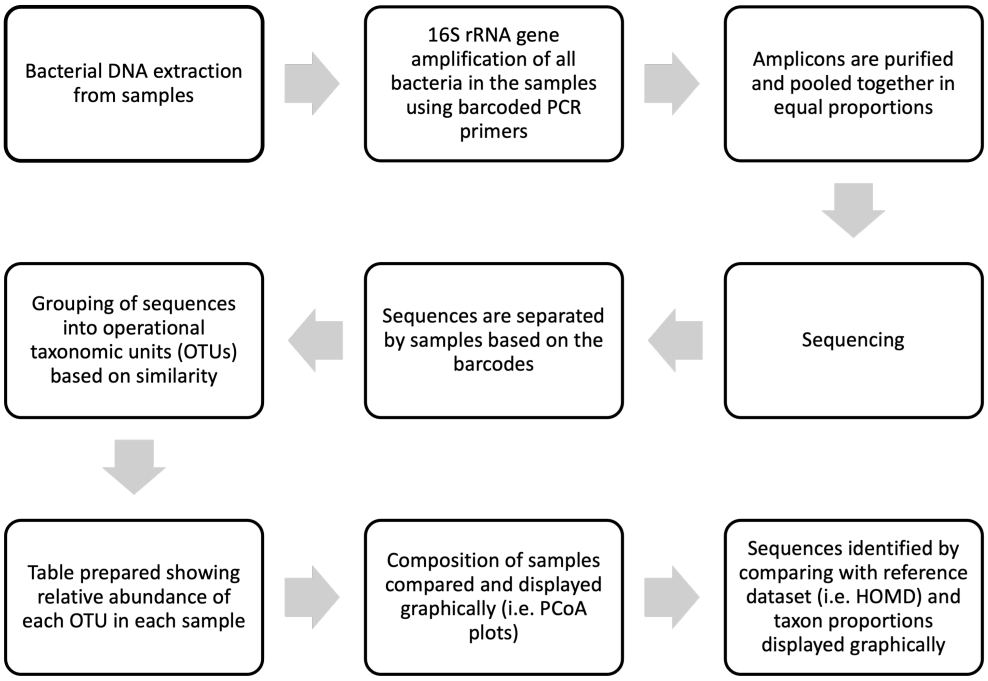

Figure 1.3 Overview of process involved in 16S rRNA gene microbiome analysis. As described by Kilian et al. (2016), steps typically involve 1) DNA extraction, 2) PCR using barcoded primers to amplify the 16S rRNA gene, 3) amplicon purification and pooling, 4) sequencing, 5) sequences separated by samples based on the barcodes, 6) grouping of sequences into operational taxonomic units (OTUs) based on similarity, 7) table prepared, 8) composition of samples compared and displayed graphically, 9) sequences identified by comparing to a reference dataset such as HOMD and the proportions of taxa displayed graphically.

The authors in the study by Lazarevic *et al.* (2010) found the genera *Streptococcus, Veillonella, Haemophilus, Granulicatella, Actinomyces, Campylobacter* and *Selenomonas* were present in all 5 subjects. As shown in both studies, there is also an inter-individual variability among the individuals. For example in the Bik *et al.* (2010) study, the oral cavity of certain individuals was dominated by *Prevotella* whereas a variety of other genera dominated the mouths of the remaining individuals. Furthermore, different species belonging to the genera *Neisseria, Fusobacterium* and *Corynebacterium* were detected in the subjects. Although other studies have in the past described the bacterial composition of the mouth to be unique to individuals (Nasidze *et al.*, 2009; Lazarevic *et al.*, 2010; Human microbiome project consortium, 2012; Hall *et al.*, 2017), this study by Bik *et al.* (2010) was able to sequence nearly the full-length of the 16S rRNA gene sequences and thus offered a high-resolution phylogenetic approach. This contrasts with many microbiome studies that sequenced only a limited number of hypervariable regions in the 16S rRNA gene.

The majority of oral microbiota characterisation studies are now focused on profiling the 16S rRNA gene sequences in bacterial communities (Paster *et al.*, 2001; Aas *et al.*, 2005; Diaz *et al.*, 2006, 2012). Zaura *et al.* (2009) pyrosequenced the V5-V6 hypervariable region of the 16S rRNA gene to demonstrate a core oral microbiome existing in the mouths of three healthy adults. An average of 266 species-level taxa were detected in each sample and similar to the studies described previously, the predominant genera present in all three individuals in order of relative abundance were as follows: *Streptococcus; Corynebacterium; Neisseria; Rothia; Actinomyces; Granulicatella; Porphyromonas* and *Fusobacterium.* However, it should be highlighted that though Zaura *et al.* (2009) selected the V5-V6 hypervariable region to amplify, it is thought the V1-V2 hypervariable region best discriminates between *Streptococcus* species, making this region a superior choice for classifying sequences obtained from the oral microbiome, as *Streptococcus* is one of the most common genera in the mouth (Wade and Prosdocimi, 2020). Adding to the findings obtained by Zaura *et al.* (2009), Naginyte *et al.* (2019) used a metagenomic approach on supragingival plaque, tongue and saliva samples and found high levels of *Streptococcus, Haemophilus, Veillonella* and *Prevotella* spp.. The profiling of the 16S rRNA gene in microbial communities is credited to technology advancements such as PCR, next-generation sequencing platforms and metagenomics that have permitted the description of uncultivable taxa which traditional culture methods have previously disregarded. A major advantage of culture-independent techniques is they do not distort the description of the human microbiota composition the way culturing does. An example is the detection of the moderately abundant previously uncultivable TM7 sequences in saliva samples, alongside many abundant genera including *Streptococcus, Prevotella, Veillonella, Neisseria* and *Haemophilus* in a study by Hasan *et al.* (2014). Culture-independent techniques do however also contain disadvantages. For example, it is argued 16S rRNA gene microbiome analysis cannot profile non-bacterial species, non-viable bacterial cells might not be excluded from analysis, bacterial load is not easily quantified and bias from primer design can also occur (Wade and Prosdocimi, 2020).

The most updated version of eHOMD contains 774 bacterial-species level taxa, with only 26 % remaining as uncultivated phylotypes (homd.org, accessed on 5th September 2022). It is also estimated that 100-300 oral bacterial species are present in a single individual (Griffen *et al.*, 2012). Yet, because the oral cavity sits at the interface between the human body and the external environment, it is difficult to determine which bacteria are truly commensals and which are transient, as the oral microbiome can be influenced by the last food ingestion, oral contact, or oral hygiene prior to sampling. Furthermore, oral bacterial compositions can vary depending on site of sample collection. It was reported by (Mark Welch *et al.*, 2019) that oral microbes are spatially organised at distinct sites. Different sites of the mouth for example, vary in their surface features so the ability of bacteria to adhere and thrive in distinct habitats is an important consideration. As confirmed by oligotyping analysis (based on identifying exact sequence variants), the site-specialist hypothesis therefore suggests that different strains of the same bacterial species might thrive at different sites if the distinct sites such as plaque, buccal mucosa or tongue is preferential (Eren *et al.*, 2014; Mark Welch *et al.,* 2019). Variation is also observed between individuals, which is contributed by antibiotic use, the host's age, genetics, changes in host defences, diet and habits (e.g. smoking) (Kilian *et al.*, 2016). Time-series studies on analysing the compositions of collected saliva and supragingival plaque have shown variability arose between individuals and over time (Jiang *et al.*, 2015; Utter *et al.,* 2016; Eriksson *et al.*, 2017; Esberg *et al.*, 2022). Interestingly, no major differences were found between the plaque compositions of individuals living in China and the United States (Utter *et al.*, 2016). Sampling sites also led to inter-individual differences (Esberg *et al.*, 2022). Nonetheless, it is widely understood the commensal bacteria play an essential role in maintaining the mouth in a "healthy" state and the prevention of oral diseases. Examples of their roles are described in the review by Wade (2013b) that included the prevention of pathogen colonisation and maintaining an appropriate tolerant immune response in the mouth. Furthermore, certain bacterial species are thought to be antagonistic to potential oral pathogens such as the production of the Gram-negative bacteria inhibiting-bacteriocins by *Streptococcus salivarius* K12 strain (Wescombe *et al.*, 2009). A second example is

the production of the anti-microbial nitric oxide by nitrate-reducing bacteria (Schreiber *et al.*, 2010) such as *Streptococci* and *Veillonella* spp. (Doel *et al.*, 2005; Hyde *et al.*, 2014). Nitric oxide is considered anti-microbial due to its presence leading to the clearance of gut pathogens such as *Salmonella, Yersinia* and *Shigella* species, as well as in the clearance of *Pseudomonas aeruginosa* in a cystic fibrosis animal model (Lundberg, Weitzberg and Gladwin, 2008). Loss of the previously described protective mechanisms in susceptible individuals can lead to inappropriate host responses to the normal oral microbiota, which may eventually cause oral diseases such as dental caries, gingivitis, and periodontitis.

1.3 Dysbiosis of the oral microbiota in oral diseases

1.3.1 Caries

Dental caries is characterised by the demineralisation of the tooth enamel. It was as early as 1890 when it was demonstrated that caries lesions are formed as a consequence of acid production by bacteria fermenting dietary carbohydrates in the mouth (Miller, 1890). Many studies since then have attributed the role acidogenic *S. mutans* plays in caries development because of its tolerance to acidic environments (Bender *et al.*, 1986; Sansone *et al.*, 1993; Balakrishnan *et al.*, 2000). The lactic acid produced by acidogenic bacteria such as *S. mutans* and lactobacilli in turn produces a positive-feedback loop as it further promotes acid-tolerating strains and inhibits the growth of many commensal oral bacteria such as *Veillonella* spp. and other streptococcal species. A prime example of competition involves the negative association observed between the growth of *S. mutans* and *S. sanguinis* in dual-species biofilms (Kreth *et al.*, 2005b). It was found in this study that the first species to colonise first was able to inhibit the growth of the second species. The suggested mechanisms of how *S. mutans* inhibits *S. sanguinis* involve *S. mutans* excreting and tolerating higher amounts of acid in the environment, as well as the production of mutacin which are proteinaceous broad-spectrum antibacterial compounds (Kreth *et al.*, 2005a). *S. mutans* in addition reduces the production of hydrogen peroxide by *S. sanguinis* which can suppress *S. mutans* growth, thus conferring ecological advantage for *S. mutans* (Ritz, 1967). It is important to note

however that caries can exist in the absence of *S. mutans*. Likewise, *S. mutans* have also been isolated from caries-free sites.

However, whether certain bacteria such as *S. mutans* dominate in the caries microbiome is dependent on the sensitivity of the methodology used in the studies. For instance, a higher detection of *S. mutans* was observed in culture-based and PCR studies using specific DNA probes, whereas the absence of *S. mutans* was apparent in various 16S rRNA gene community profiling studies (Tanner *et al.*, 2018). Instead, a wider range of bacteria including both Gram-positive and Gram-negative species was observed. In addition to *Actinomyces* and *Lactobacillus,* this included species within the genera *Atopobium, Bifidobacterium, Corynebacterium, Scardovia, Neisseria, Selenomonas, Fusobacterium* and *Haemophilus* (Corby *et al.*, 2005; Aas *et al.*, 2008; Gross *et al.*, 2010).

It is therefore now widely accepted *S. mutans* is not the sole aetiology of dental caries (Marsh, 2003). Instead, a whole community of bacteria drives caries development to cause a shift in the oral microbiota composition which we call dysbiosis. The “ecological plaque hypothesis” is a term that describes changes in the environmental factors. It is thought the major influencers of a shift in the microbial communities include pH, a rise in host glycoproteins during an inflammatory response to plaque, as well as essential nutrients and cofactors for growth composition (Marsh, 2003) (Figure 1.4). It is therefore a change in the dynamic relationship between the resident bacteria and the ecological environment that is responsible for this shift and not merely the presence of a specific pathogen. In relation to dental caries as an example, increased consumption of sugars in the host diet will repeatedly expose the microbial community to lower pH conditions in the microbial environment and over time, shifts the microbial composition to one where acidogenic and acid-tolerant Gram-positive bacteria dominate. This ecological plaque hypothesis can also be applied to periodontal diseases such as gingivitis and periodontitis. Here, ecological pressures again will lead to another shift in the microbial community composition whereby Gram-negative strict anaerobes outcompete other members of the community.

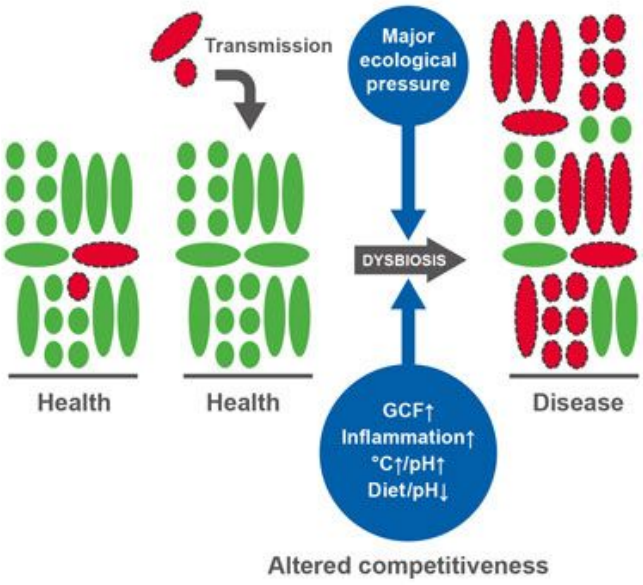

Figure 1.4. Ecological plaque hypothesis. As described by Marsh (2003) the ecological plaque hypothesis describes the changes that occur from major ecological pressures to cause altered competitiveness of the low abundant potentially periodontopathic bacteria (red) at health sites, and consequently increase their abundances at disease sites. Illustration taken from Kilian *et al.* (2016) with permission.

The caries ecological hypothesis was further extended by Takahashi and Nyvad (2008) by explaining that the constant exposure to low pH conditions, which leads to the population increase of acidogenic and acid-tolerant Gram-positive bacteria (i.e. *Actinomyces* spp. and non-mutans *streptococci*), can cause tooth de-mineralisation and initiate lesion development. Interestingly, this cascade of events can be reversed if the acidic environment is removed. Once the acidic environment is established however, the growth of *S. mutans* and lactobacilli can follow and this further promotes lesion development and alters the enamel surface texture from smooth to rough, and dentin from hard to soft.

1.3.2 Gingivitis

As described previously, a healthy oral microbiota is relatively stable over time because homeostatic mechanisms occur between the host and microorganisms. When this microbial homeostasis breaks down in susceptible individuals, significant changes in the oral microbiota composition can ensue and lead to periodontal diseases. Factors associated with the collapse of homeostasis include individuals

who smoke, are immunosuppressed, are taking antibiotics, or when oral hygiene is reduced.

Gingivitis is the mildest but also commonest form of periodontal disease, thought to affect 90 % of the population worldwide (Pihlstrom, Michalowicz and Johnson, 2005). It is an oral polymicrobial disease stemming from poor dental hygiene that can result in plaque build-up around the gingival margins so that over time, this can lead to increased host inflammatory response. This can occur alongside increased gingival crevicular fluid (GCF) flow which brings about additional nutrient availability for the bacteria within the tooth crevice. This ultimately causes inflammation and bleeding of the gums (gingiva) where if left untreated, persistent gingivitis can progress to periodontitis. It is however a reversible disease. This was first demonstrated by Löe, Theilade and Jensen in 1965, when 12 healthy volunteers developed experimental gingivitis after 10-21 days of withholding oral hygiene. During this period, the plaque composition shifted from a predominantly coccal community to one with a higher abundance of filaments within a day and spirilla and spirochaetes appeared by day 7 (Loe, Theilade and Jensen, 1965). When oral hygiene was reinstated after 15 days, the plaque composition reverted back to a pre-gingivitis state with spirilla and spirochaetes disappearing within 24 h in 82 % subjects and fusobacteria within 48 h in 64 % subjects (Theilade *et al.*, 1966). Kistler *et al.* (2013) expanded on this culture work by 16S rRNA gene pyrosequencing the bacterial communities in plaque samples collected from 20 healthy volunteers who developed experimental gingivitis after refraining from oral hygiene for two weeks. Again, changes in the plaque composition were observed in the transition from health to gingivitis. For example, Gram-positive aerobes such as *Streptococcus, Rothia* and *Actinomyces* levels reduced as gingivitis developed over the two weeks, whereas predominately Gram-negative bacteria such as *Campylobacter, Fusobacterium, Leptotrichia, Porphyromonas, Selenomonas* and *Tannerella* increased in relative abundance. The mean volume of GCF and % sites bleeding were also significantly raised after the first and second week. However, species richness did not significantly differ between health and experimental gingivitis

plaque communities, although a more even distribution was observed in gingivitis after 2 weeks.

These experimental gingivitis studies are in accordance with other work focused on characterising the bacterial community in gingivitis. Traditional culture methods have previously implicated *Fusobacterium* spp., *Actinomyces* spp., *Parvimonas micra* and *Porphyromonas gingivalis* in gingivitis (Jenkinson, 2011). Molecular studies, however, have since determined the aetiologies of gingivitis include *Eubacterium nodatum, Eikenella corrodens* and *F. nucleatum* too. Likewise, Zaura *et al.* (2009) determined that as gingivitis progresses, the subgingival plaque composition shifts from a dominance of aerobic *Streptococcus* to one comprising predominately *Actinomyces, Capnocytophaga, Campylobacter, Eikenella, Fusobacterium* and *Prevotella*. This dysbiotic shift in the community composition therefore results in a community with fewer streptococci but are richer in anaerobes and proteolytic species.

Dental plaque is continuously found on the tooth surface, but bacterial attachment is transient in a healthy mouth due to for instance, the mechanical removal force of salivary flow. This attachment becomes more permanent when oral hygiene ceases, allowing bacteria within the dental biofilm to colonise and multiply further. Plaque forms in distinct stages, with an orderly succession of early-, intermediate-, and late-colonising species. Initial adhesion occurs (as demonstrated in Figure 1.5) when oral bacteria bind to salivary glycoproteins such as mucin, proline-rich proteins, salivary acidic phospho-protein statherine (Tabak *et al.*, 1982; Bennick *et al.*, 1983; Levine *et al.*, 1987). These are found in a conditioning film of acquired pellicle that forms to cover the tooth surface by a range of forces such as hydrogen bonds, hydrophobic interactions and electrostatic interactions (Hannig and Hannig, 2009). These oral bacteria are the primary colonisers and they are typically Gram-positive aerobes and facultative anaerobes which include species belonging to the genera *Actinomyces, Streptococcus, Haemophilus, Capnocytophaga, Veillonella, Gemella* and *Neisseria* (Aas *et al.*, 2005; Huang *et al.*, 2011). After initial adhesion, bacteria secrete extracellular polymeric substance (EPS) and form further

interactions to allow the primary colonisers to co-aggregate. Interaction is highly specific though, as it was estimated interaction with ≥1 co-aggregation partner exists in approximately 1000 bacterial strains which were examined (Kolenbrander *et al.*, 2010). An example of this highly-specific coaggregation involves *S. mutans* aggregating with *F. nucleatum* but never with *P. gingivalis* (Hojo *et al.*, 2009).

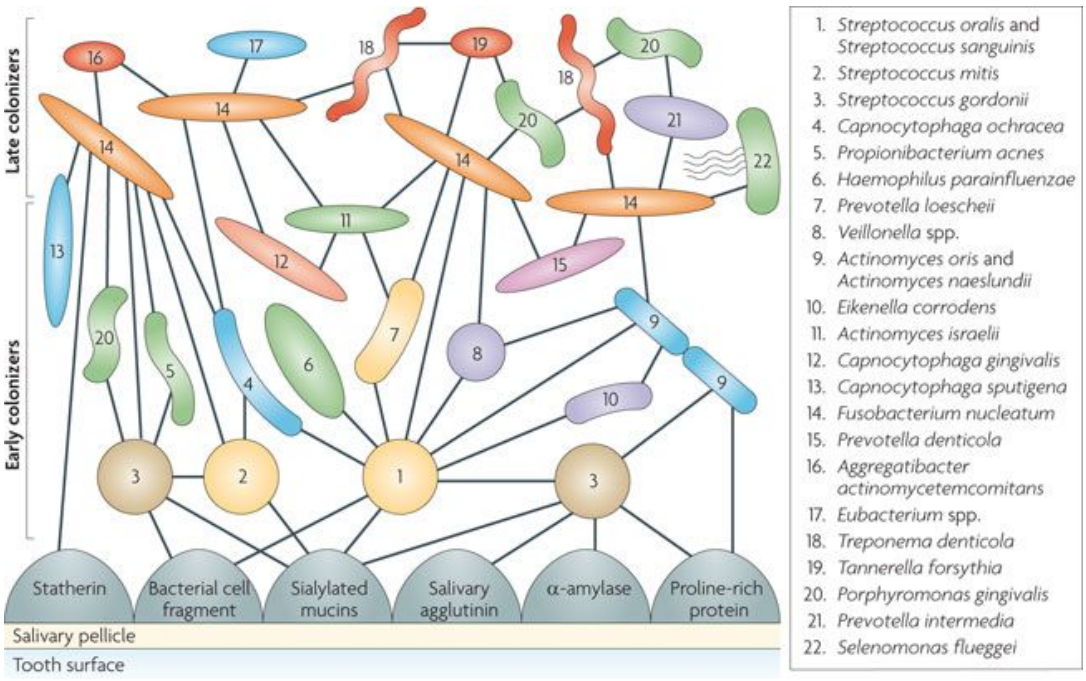

Figure 1.5. Interactions occurring between different bacteria within oral communities. Model illustrating the proposed interactions between early colonisers and the complementary receptors on surface of salivary statherin, bacterial cell fragment, sialylated mucins, agglutinin, α-amylase and proline-rich protein. Specific co-aggregation is observed between specific partners and late colonisers sequentially bind to those already present in the biofilm community. Image taken from Kolenbrander et al. (2010) with permission.

An example of reported interspecies cell-cell interactions include type II fimbriae in *Actinomyces* spp. that bind to the phosphopolysaccharides expressed on the surfaces of several *Streptococcus* spp. (Yang *et al.*, 2009). A wide variety of adhesion and colonisation factors for streptococci have been described, including glucan-binding proteins, pili, fimbriae, fibrils and the surface adhesion protein AgI/II as reviewed by Nobbs *et al.* (2009). In addition, *S. gordonii* has been shown to produce a sialic-acid binding protein Hsa/GspB (Bensing, López and Sullam, 2004). Sialic acids which are also known as neuraminic acids, are found as terminal 9-carbon amino-sugars on host glycoproteins (Varki, 2008).

Maturing biofilms are therefore often thought to be spatially and functionally organised due to the synergistic bacterial interactions that also include the transfer of antibiotic resistant genes, metabolic cooperation and cell-cell signalling. Quorum sensing is also thought to contribute to biofilm development as auto-inducers are released by oral bacteria associated with periodontitis such as *P. gingivalis* to attract further bacteria (Gerits, Verstraeten and Michiels, 2017). These are in addition to the antagonistic interactions through the secretion of certain inhibitory molecules such as H_2O_2, mutacins and bacteriocins (Marsh, 2010; Jenkinson, 2011). Mutualism between interspecies was also demonstrated using *in vitro* biofilm models. Examples include the reduction of *P. gingivalis* abundance in a multi-species model inoculated without the early colonising *Streptococcus* (Ammann *et al.*, 2013), and the synergy between *F. nucleatum* and *Tannerella forsythia* which promoted greater inflammation and alveolar bone loss in murine models compared to single-species infections (Settem *et al.*, 2012). In the latter example, it is likely *F. nucleatum* provided the amino sugar N-acetylmuramic acid (MurNAc) that *T. forsythia* required for peptidoglycan synthesis, as it lacked the enzyme required for its biosynthesis (Wyss, 1989). It is likely the source of MurNAc is from the outer surfaces of *F. nucleatum* (*nucleatum* and *polymorphum* subspecies included) which are known to be decorated with sialic acids (Yoneda *et al.*, 2014). Conversely, *F. nucleatum* utilises sialic acid which becomes freed by the action of sialidase enzymes secreted by *T. forsythia*. Many oral bacteria secrete these enzymes to promote their growth and the role microbial glycobiology plays in oral communities will be discussed in further detail in section 1.5.

Following the initial adhesion by primary colonisers, the bacteria that are in close proximity to one another provide additional adhesion sites for the sequential binding of other phylogenetically distinct bacteria. Examples include the intermediate colonisers such as *F. nucleatum*. It is understood *F. nucleatum* is an important 'bridging' microorganism that binds to both early and late colonisers, as well as reducing the local environment to optimise the growth of oxygen-intolerant strict anaerobes. The latter bacteria are typically fastidious strict anaerobes such as

P. gingivalis, T. forsythia and *Treponema* spp., allowing further maturation of the developing biofilm that becomes thicker and more diverse in composition. It is suggested the interspecies communication occurring throughout microbial succession is also due to the universal signalling molecule autoinducer 2 (AI2) and its concentration was greatest in mature biofilm communities (Kolenbrander *et al.*, 2010). The detachment and dispersion of the bacterial cells within biofilms to colonise new sites generally define the last stage of biofilm formation. In periodontal disease, this may lead to bacteria entering the bloodstream and potentially contributing to systemic diseases.

1.3.3 Periodontitis

Chronic periodontitis is a severe form of periodontal disease that is estimated to affect ~10 % of the world's population (Frencken *et al.*, 2017). Recently though, there have been revisions in the classification framework for the staging and grading of periodontitis. The new framework replaces the previous 1999 classification of periodontitis as chronic, aggressive, necrotising, and as a manifestation of systemic disease (Armitage, 1999). Briefly, four stages are described for the disease severity and are as follows: stage I described for initial periodontitis; stage II for moderate periodontitis; stage III for severe periodontitis with the potential for tooth loss and stage IV for advanced periodontitis with extensive tooth loss (Tonetti, Greenwell and Kornman, 2018). Each stage is further graded by A-C based on the risk of progression and its potential risk of systemic disease.

At the root of the tooth in periodontitis, a dense subgingival biofilm forms and propagates further into the gingival tissues. This is shown in Figure 1.6 and is compared to health. As the biofilm grows, it induces inflammation at this site, forms a periodontal pocket and causes further destruction to the supporting tissues of the tooth, that can eventually cause receding gum line and alveolar bone loss (Armitage, 1999). Patients typically then experience the slow progressive loss of tissue attachment and tooth. In contrast to gingivitis, periodontitis is an irreversible oral disease. Its aetiology is thought to be primarily bacteria although

the tissue destruction is due to a dysregulated and exaggerated host immune response, such as from the production of proteolytic enzymes, damage-associated molecular peptides and reactive oxygen species in susceptible individuals (Meyle and Chapple, 2015).

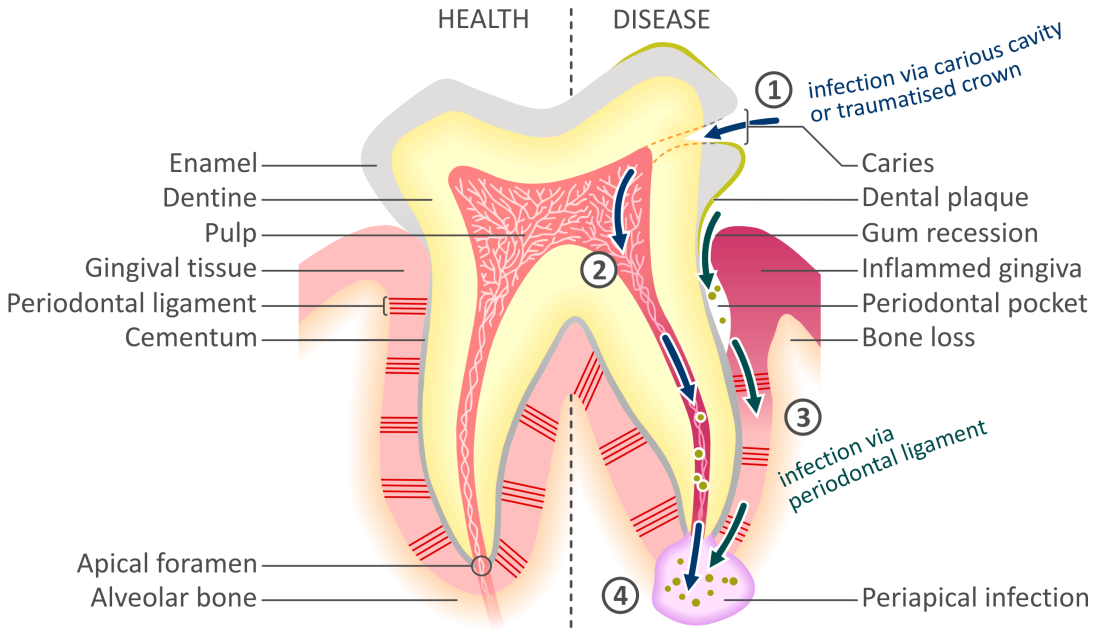

Figure 1.6. Structure of tooth as seen in health vs disease. Features such as subgingival plaque, periodontal pocket, inflammation in gingiva and bone loss can be seen in periodontal disease in relation to health. Figure taken from Douglas *et al.* (2014) and used with permission.

In periodontitis, the community composition changes from one dominated by facultative anaerobic Gram-positive bacteria, to one with an increasing abundance of Gram-negative strict anaerobes (Christersson *et al.*, 1991). Table 1.1 summarises the bacterial taxa commonly associated with health as early pioneer species and with periodontitis as later Gram-negative strict anaerobes in key literature.

Table 1.1 Relevant oral bacterial species determined from literature. Summary of bacterial taxa commonly associated with health as pioneer species and with periodontitis in key literature.

Bacterial species	**Likely role in oral microbiota from key literature**
Actinomyces oris	Pioneer species (Cisar *et al.*, 1984)
Campylobacter rectus	Periodontitis-associated (von Troil-Lindén *et al.*, 1995)
Campylobacter showae	Periodontitis-associated (Socransky *et al.*, 1982)
Dialister invisus	Periodontitis-associated (Kistler *et al.*, 2013)
Filifactor alocis	Periodontitis-associated (Kumar *et al.*, 2005; Griffen *et al.*, 2012; Kistler *et al.*, 2013)
Fusobacterium nucleatum subsp. *nucleatum* and subsp. *polymorphum*	'Bridging' organism between early and late oral colonisers (Socransky *et al.*, 1982; Moore *et al.*, 1983; Kistler *et al.*, 2013)
Neisseria subflava	Pioneer species (Liu *et al.*, 2015)
Parvimonas micra	Periodontitis-associated (Socransky *et al.*, 1982; von Troil-Lindén *et al.*, 1995; Kistler *et al.*, 2013)
Porphyromonas gingivalis	Periodontitis-associated (Socransky *et al.*, 1998; Hajishengallis, 2011; Griffen *et al.*, 2012; Kistler *et al.*, 2013)
Prevotella intermedia	Periodontitis-associated (Socransky *et al.*, 1982; von Troil-Lindén *et al.*, 1995; Griffen *et al.*, 2012)
Prevotella nigrescens	Periodontitis-associated (Socransky *et al.*, 1982)
Streptococcus gordonii	Pioneer species (Nyvad and Fejerskov, 1987)
Streptococcus oralis	Pioneer species (Nyvad and Fejerskov, 1987)
Tannerella forsythia	Periodontitis-associated (Socransky *et al.*, 1998; Kistler *et al.*, 2013)
Treponema denticola	Periodontitis-associated (Socransky *et al.*, 1998; Griffen *et al.*, 2012)
Veillonella dispar	Early coloniser (Periasamy and Kolenbrander, 2010)

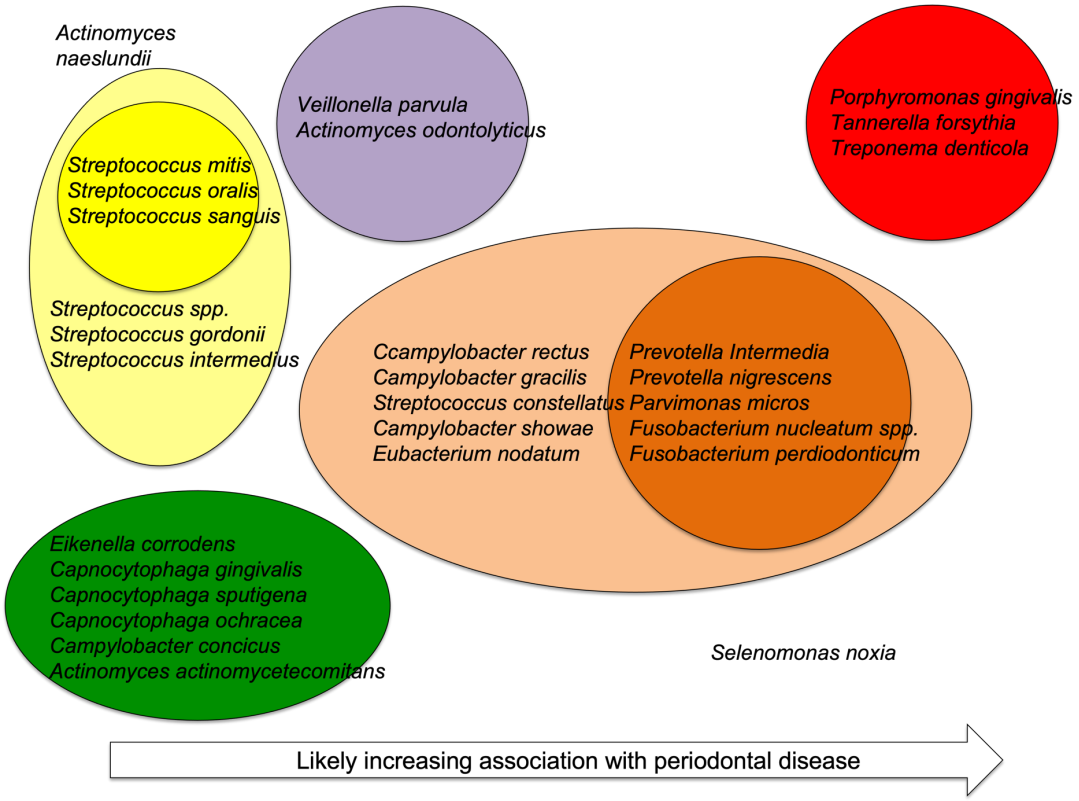

Figure 1.7. Microbial complexes in subgingival plaque. A diagrammatic representation of the microbial complexes in subgingival plaque as described by Socransky *et al.* (1998), with each complex and their likely association with periodontal disease. Image adapted from Socransky *et al.* (1998) with permission.

Strict anaerobes include those in the so-called red microbial complex as described by Socransky *et al.* (1998) (Figure 1.7) and are notably in low abundance in healthy patients (Aas *et al.*, 2005). The microbial red complex include *P. gingivalis, Treponema denticola* and *T. forsythia* and are frequently detected together in subgingival plaque of periodontitis patients (Socransky *et al.*, 1998). Mouse models are often used to establish pathogenicity and *P. gingivalis* has been extensively studied as a 'keystone pathogen' for their role in tissue inflammation and destruction. A study by Hajishengallis *et al.* (2011) demonstrated that introducing *P. gingivalis* to mice with commensal oral microbiota shifted the composition to a dysbiotic state and induced periodontal bone loss. A variety of pathogenic factors are known to facilitate *P. gingivalis* virulence, which includes cysteine proteinases (also known as gingipains) that inhibit host complement activation, lipo-polysaccharide (LPS) layer to evade host immune response and fimA fimbriae for the adhesion, colonisation and inhibition of phagocytosis (Hajishengallis, 2011). The remaining members of the red microbial complex *T. denticola* and *T. forsythia* have

similarly been demonstrated to induce alveolar bone loss in murine models (Sharma, S. Inagaki, *et al.*, 2005; Lee *et al.*, 2009). Besides other putative virulence factors that have been reported in the literature, It has been shown the secretion of the protein BspA induces the upregulation of host pro-inflammatory cytokine and chemokine activity (Sharma, S. Inagaki, *et al.*, 2005). Furthermore, it is suggested NanH sialidase production by *T. forsythia* provide a nutrient source via the removal of sialic acids present in the salivary pellicle as well as exposing receptors to allow bacterial adherence to oral epithelial cells and the evasion of host immune response (Honma *et al*, 2011; Roy *et al.*, 2011; Sekot *et al.*, 2011). These red complex microorganisms were initially associated with periodontitis in culture and DNA-DNA hybridisation studies, as described by Socransky and confirmed later on using culture-independent methods such as DNA probes.

A closely related orange complex was described by Socransky *et al.* (1982) and is one comprising *F. nucleatum*, *P. micra, Prevotella intermedia*, *Prevotella nigrescens*, *Streptococcus constellatus*, *E. nodatum*, *Campylobacter showae*, *Campylobacter gracilis* and *Campylobacter rectus*. These microorganisms are also associated with increased pocket depth. Higher levels of *P. micra*, *P. intermedia* and *C. rectus* from this complex were also found in saliva obtained from periodontitis patients than those with no or initial periodontitis (von Troil-Lindén *et al.*, 1995). It has been suggested members of the yellow, green, blue, and purple complexes are involved in the initial bacterial colonisation of the oral epithelia. Microbial succession subsequently follows and involves the attachment of the orange complex and lastly the red complex (Socransky and Haffajee, 2005). It is clear many bacteria within the oral microbial community exploit what is available in the environment which ultimately aids biofilm formation after adhesion, such as the secretion of the previously mentioned sialidases by *T. forsythia* which shall be described in greater detail in section 1.5. A second example involves the fact that some bacteria within subgingival plaque are proteolytic, such as the previously described black-pigmented anaerobes *P. gingivalis, P. nigrescens* and *P. intermedia*. These asaccharolytic bacteria likely largely gain nutrients from proteins by releasing proteases as virulence factors to obtain iron derived from erythrocyte haemoglobin

(Douglas *et al.*, 2014). Other proteolytic oral bacteria include *T. forsythia, T. denticola* and some commensal streptococci such as *S. gordonii*.

Other bacteria that have been implicated in periodontal disease from culture work have included *E. corrodens* and *F. nucleatum* subsp. *nucleatum* (Moore *et al.*, 1983). *F. nucleatum* subsp. *polymorphum* and subsp. *animalis* have also been significantly correlated with a community shift from health to periodontal disease state (Kistler *et al.*, 2013). Recent culture-independent techniques such as 16S rRNA gene community profiling has furthered the list of putative pathobionts associated with periodontal disease and this includes: *Filifactor alocis; Anaeroglobus geminatus; Prevotella denticola; Treponema socranskii; Selenomonas sputigena; S. anginosus; Dialister invisus; Capnocytophaga granulosa; Kingella oralis; Eubacterium saburreum; Eubacterium saphenum; Peptostreptococcus stomatis; Dialister pneumosintes; V. dispar; Peptostreptococcus anaerobius*; *Mogibacterium timidum* and species-level representatives within the candidate TM7 division (Paster *et al.*, 2001; Brinig *et al.*, 2003; Kumar *et al.*, 2005; Griffen *et al.*, 2012; Kistler *et al.*, 2013). Griffen *et al.* (2012) conducted a particularly comprehensive study involving pyrosequencing the V1-2 and V4 regions of the 16S rRNA gene of subgingival plaque samples to compare between 29 healthy controls and 29 periodontal patients. Here, community diversity as well as 123 species were significantly raised in disease-associated subjects than in control subjects. The genera *Treponema, Prevotella* and *Fusobacterium* were particularly prevalent with periodontitis. Interestingly, *F. alocis* was also highly associated with periodontitis in this study where its abundance is often not discussed as frequently as the species within the red complex. Multiple studies have also demonstrated a high abundance of *Prevotella* species in the bacterial communities within periodontitis subjects (Griffen *et al.*, 2012; Hong *et al.*, 2015).

As well as investigating the abundance of specific bacteria in periodontitis, it is also important to highlight the effect that periodontitis has on microbial community diversity. It is thought oral dysbiosis is described by the combination of the loss of beneficial microbes, the increased abundance of bacteria associated with disease,

and the overall loss of microbial diversity (Petersen and Round, 2014). As such, the progression of periodontitis has been linked to a reduction in microbial diversity due to lower measures of α-diversity found in periodontal patient samples compared to healthy controls, which measures the richness and distribution of the samples (Ai *et al.*, 2017; Almeida *et al.*, 2020). However, the opposite effect has also been reported and the increase in diversity was explained by the increase in nutrients during inflammation (Griffen *et al.*, 2012; Lamont, Koo and Hajishengallis, 2018; Van Dyke, Bartold and Reynolds, 2020). It is important to note however that sample numbers were limited in these studies and other confounding factors such as variation in sampling and microbial community metabolic requirements might have contributed to the discrepancy in opinion.

1.4 *In vitro* approaches to studying biofilms

1.4.1 Historical perspective on *in vitro* biofilm studies

It is widely understood that microorganisms in nature grow and aggregate as complex biofilm communities rather than as individual planktonic cells. *In vitro* models offer a way of understanding the complexity of biofilms by mimicking biofilms occurring naturally within the human body, by replicating the natural environment under laboratory conditions. Thus, researchers can investigate biofilm formation and development as well as antimicrobial susceptibility in biofilms. The latter has been widely explored as antimicrobial action is generally known to be less effective against biofilm-associated bacteria than in their free-living counterparts. Many studies have therefore applied *in vitro* models to testing antibiotic efficacy. A prime example relevant to periodontal disease is the study by Wright *et al.* (1997), who compared the metronidazole minimum inhibitory concentration (MIC) of planktonic *P. gingivalis* cells and also as biofilms grown on hydroxyapatite-coated coupons suspended in equivalent broth. They reported MIC of metronidazole was up to 160x higher in biofilms than for planktonic *P. gingivalis*. The higher MICs seen are likely due to the structural nature of biofilms, possibly because cells are embedded in an extracellular matrix that allows for firmer attachment to surfaces. This can provide bacteria their protection from antibiotics. Medically relevant biofilms are thus important to study and there are a variety of

tools available to explore this in laboratory settings under controlled conditions. An ideal *in vitro* model would be one encompassing the following properties:

- Be standardised and reproducible
- Be inexpensive and simple to set up
- Promotes high biofilm mass growth
- Allows for high throughput testing and parallel biofilm comparisons grown under different environmental conditions such as the addition of antimicrobial agents
- Supports a broad range of microbial growth and thus reflects the complexity of biofilms in nature
- Allows for direct visualisation whilst maintaining intact community biogeography and preferably in real-time

In vitro models can be separated into two major categories. A closed system (also known as batch culture) is one where throughout the duration of an experiment, nutrients in the system are not replenished and waste is not removed. This can result in the eventual end of population growth. On the other hand, an open system (also known as continuous culture) allows for the continuous flow of nutrients and waste respectively into and out of the system so that population growth is maintained. Both systems have their benefits and examples of biofilm models previously reported in the literature will be described in detail later. A variety of model systems therefore currently exist although it is typical to use model substrata coated in hydroxyapatite to simulate the tooth enamel environment when studying periodontal disease. Pratten *et al.* (1998) compared biofilm growth of *S. sanguinis* (formerly known as *S. sanguis*) in an open system called a constant depth film fermentor (CDFF) on discs either coated in hydroxyapatite or bovine enamel to study the microbicidal effect of various mouthwash compositions together with a placebo control lacking in sodium fluoride and antimicrobial compounds. The authors demonstrated biofilm formation and viable bacterial counts were similar between the two substrata under placebo conditions, although the antibacterial effect of mouthwash was dependent on the type of substratum used.

1.4.2 Batch culture model system

The major advantage offered by batch culture models is they are generally far simpler to set up, and to some degree, nutrients are replenished by regularly replacing the model communities with fresh growth media. The commonly used *in vitro* batch culture model systems described in this review are summarised in Figure 1.8.

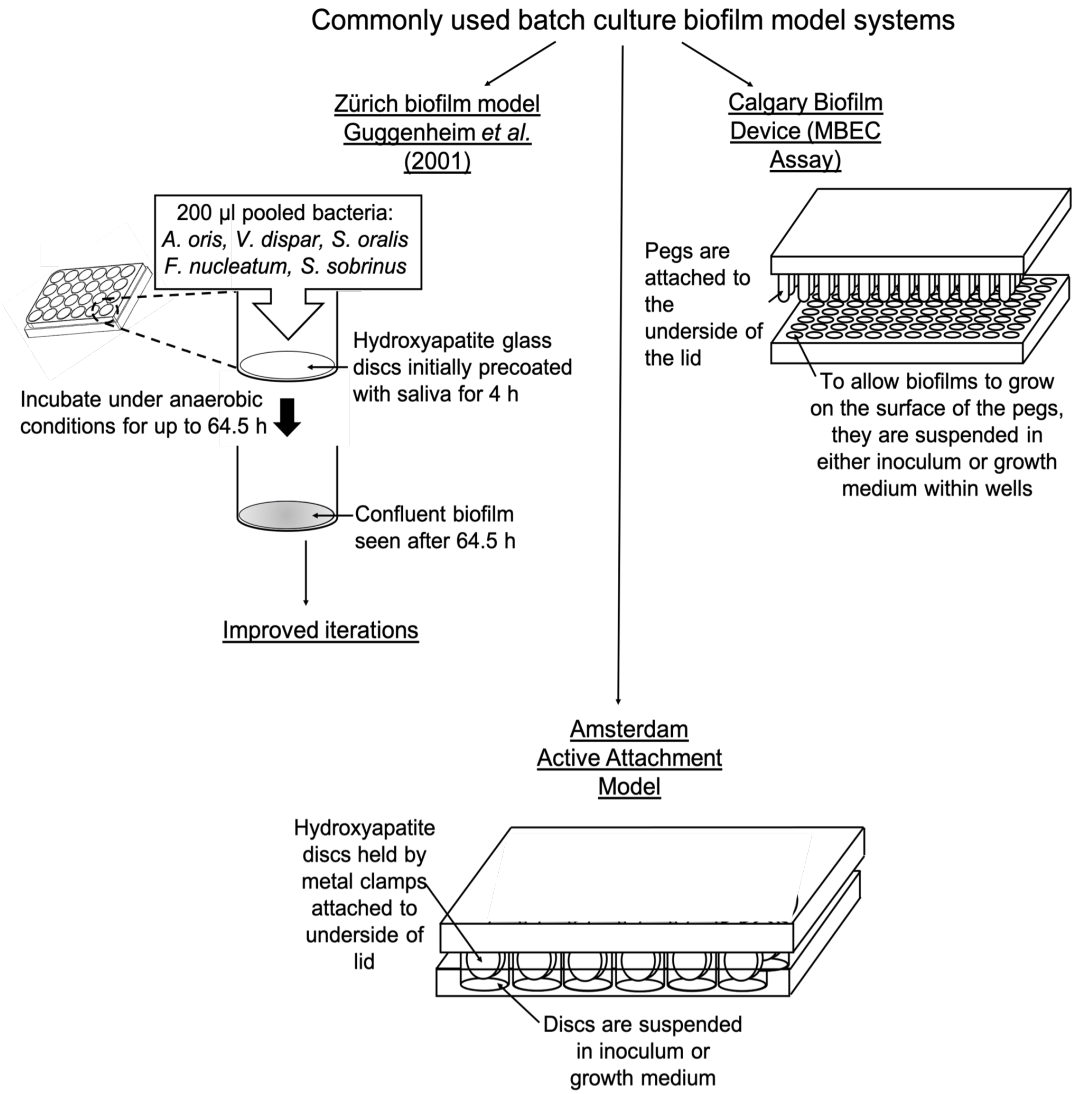

Figure 1.8 Commonly used in vitro batch biofilm systems described in this review. This includes the Zürich biofilm model which was initially developed by Guggenheim *et al.* (2001) and its improved iterations thereafter, the Amsterdam Active Attachmemt model, and the Calgary Biofilm Device (also known as MBEC).

Early laboratory models simulating periodontal disease such as dental caries historically involved growing biofilms on extracted teeth (Magitot, 1878; Miller,

1890; Dietz, 1943; Pigman *et al.*, 1952), which in its simplest form was on agar plates. However, it would not be possible to replenish nutrients in the agar plates. Furthermore, the heterogenous nature of teeth and even obtaining large numbers of extracted tooth for studies were this early technique's major shortcomings.

1.4.2.1 Zürich biofilm model

An improvement on *in vitro* batch biofilm models then came with the use of microtitre plates (known as microtitre plate-based systems). It is now very common for biofilm models grown under batch culture systems to involve the formation of biofilms on a specific surface within the wells of a microtitre plate. This permits the statistical analysis of multiple replicate biofilms as well as the examination of biofilm growth under numerous test conditions. As described in a review by Salli and Ouwehand (2015), biofilms may form on "the surface of discs, coupons, pegs, on human or bovine enamel within wells". The most simplistic approach would involve inoculating the wells of a microtitre plate with inoculum (whether it be a defined bacterial community or a patient oral sample) and replacing it with fresh growth medium on a regular basis to maintain the levels of nutrients. The biofilms grown at the bottom of the microtitre plate can be scraped off and harvested for compositional analysis.

The Zürich biofilm model was initially developed by Guggenheim *et al.* (2001) who used hydroxyapatite discs, as illustrated in Figure 1.8, left. The discs are inexpensive and it is easy to purchase numerous identical discs to warrant many replicate biofilm models. With that, it is unsurprising the Zürich biofilm model is arguably the most commonly used approach and especially for growing multi-species models. This model has since been improved upon over the years. In the first iteration of the Zürich biofilm model, Guggenheim *et al.* (2001) mimicked dental supragingival plaque by co-culturing the following five species in the model: *A. oris; V. dispar; F. nucleatum; Streptococcus sobrinus* and *S. oralis* on reusable circular hydroxyapatite (HA) discs that were first preconditioned with salivary pellicle for 4 h. Each disc sat in an individual well of a 24-well cell culture plate and was incubated at 37 °C for up to 64.5 h, with the growth medium being replenished

at 24 h intervals. The authors were able to track over time the formation of biofilms by using confocal laser scanning microscopy (CLSM) on the HA discs which revealed initial cell adhesion to the discs within 30 min of incubation. These early colonisers were predominately single cells and chains of *Streptococcus* and a confluent biofilm was seen by 64.5 h. Colony-forming units were also counted for each of the five species harvested from the biofilms after plating the cells onto agar plates and by direct microscopy. Yet, a greater understanding may have been achieved were the authors to report on the CFU counts plated out from the harvested cells at separate timepoints of biofilm formation. This study nonetheless crucially advanced biofilm modelling techniques for their time by demonstrating the repeatability of their dental plaque model because comparable populations of cells in 40.5 h and 64.5 h biofilms replicated on six separate occasions were observed.

1.4.2.2 Improvements on the Zürich biofilm model

Improvements for analysing the communities grown in the Zürich biofilm model followed, although the principle of the model set-up largely remained the same. Improved techniques included the use of fluorescent *in situ* hybridisation (FISH)- a technique for using fluorescently-tagged species-specific 16S rRNA gene oligonucleotide probes to label different species- following CLSM, colony forming unit counts, immunofluorescence and PCRs (Thurnheer *et al.*, 2004; Guggenheim *et al.*, 2009; Sánchez *et al.*, 2011; Ammann *et al.*, 2012). Additional microbial species were also introduced into the community inoculum to better simulate supra- and subgingival plaque. For example, *C. albicans* were added to the Guggenheim's 2001 Zürich biofilm model (Thurnheer *et al.*, 2004), as were species associated with a more mature biofilm such as *C. rectus, P. gingivalis, P. intermedia, T. forsythia, Treponema lecithinolyticum, V. dispar* and *T. denticola* in *in vitro* subgingival plaque biofilm models (Guggenheim *et al.*, 2009; Ammann *et al.*, 2012; Belibasakis and Thurnheer, 2014). Whether they used the Zürich biofilm model or not, many previously reported oral biofilm models were commonly inoculated with ten or fewer bacterial species (Guggenheim *et al.*, 2001; Sánchez *et al.*, 2011; Belibasakis and Thurnheer, 2014; Kommerein *et al.*, 2017). Earlier models even contained only

single- or dual-species. The majority of the aforementioned models have generally included *F. nucleatum, Veillonella spp., Streptococcus spp.* and *Actinomyces naeslundii* (renamed as *A. oris*) (Guggenheim *et al.*, 2001; Peyyala *et al.*, 2011; Sánchez *et al.*, 2011; Kommerein *et al.*, 2017), where *S. oralis* and *A. oris* were often chosen as early colonisers of the biofilm. Ammann *et al.* (2013) investigated the effect on biofilm models by excluding early colonising bacteria such as *S. oralis, S. anginosus* and *A. oris* entirely, or by adding *Streptococcus* spp. only after 16.5 h incubation compared to a 10-species subgingival plaque model that were initially inoculated with the colonisers from the start. It was reported from this study that although the early colonisers did not impact total bacterial counts in the community, their presence did produce denser yet less spatially uniform biofilms. Additionally, streptococcal colonisation even when delayed significantly impeded the growth of *A. oris* but it promoted the growth of *P. gingivalis*. Omitting all three early colonising species in contrast significantly reduced the late-colonising *P. gingivalis* cell numbers but it increased *P. intermedia* growth. This highlighted a possible synergistic relationship between the early colonisers and *P. gingivalis* that allowed the latter keystone species to become established as the biofilm community matured.

Many of these simplistic models are however perhaps not representative of naturally occurring complex multi-species communities. Although it is impractical to inoculate models with the hundreds of bacterial species that are reported in subgingival plaque due to the time and resources required for their growth and maintenance, a selection of periodontitis-relevant keystone bacteria would have to suffice. Ammann *et al.* (2012) for example, made further advances on the Zürich biofilm model by optimising the growth of treponemes in the communities to include *T. denticola* which is another member of the red complex. Impressively, an approximately 10,000-fold increase of *T. denticola* cell number was achieved by using growth medium in their model that contained 50% human serum. In another biofilm model set up, the local environment within the microbial community was shifted from aerobic to microaerophilic to anaerobic conditions by methodically inoculating at various phases of biofilm maturation with various different key

bacteria (Thurnheer *et al.*, 2016). Here, only early colonisers and *F. nucleatum* were inoculated into the model after an initial pellicle formation. *C. rectus, P. intermedia* and *S. anginosus* were inoculated after 72 h and finally, the three members of the red complex added 168 h (7 days) after the model set up and the biofilms were harvested throughout. Whilst this approach was intended to model the shift from a supragingival plaque to a subgingival plaque community, it may be hindered by the fact that introducing fresh cultures of new species to the establishing communities could cause the overgrowth of the new species. Alternatively, it is also possible that all species that are added sequentially may not remain viable throughout biofilm growth. However, these possible limitations were unfounded in the species cell number counts. Furthermore, strict anaerobes such as *F. nucleatum* and *V. dispar* would have to rely on the formation of anaerobic pockets for their growth during the initial aerobic phase as the biofilm initially developed. This might explain the large variances in their cell numbers seen at this stage. Yet, this model did allow biofilm structural changes to be observed such as the development of extracellular polysaccharide (EPS) and interestingly, also the reduction of cell viability during the microaerophilic phase before recovery occurred in the final switch to anaerobic conditions.

Besides modelling mock bacterial communities, the Zürich biofilm model has also been used to study the antimicrobial effect of incorporating antimicrobials, probiotic bifidobacteria and mutant strains of pathogenic species such as *T. forsythia* with defective cell surfaces (Soares *et al.*, 2015; Jäsberg *et al.*, 2016; Bloch *et al.*, 2017). These approaches further emphasise the capacity of this model to observe shifts in the biofilm communities when tested under multiple exposure and test conditions. Furthermore, the Zürich biofilm model has been successfully used for modelling subgingivival plaque and saliva in a reproducible manner (Walker and Sedlacek, 2007; Shaddox *et al.*, 2010; Edlund *et al.*, 2013; Lamont *et al.*, 2021).

1.4.2.3 Amsterdam active attachment model

A drawback to the Zürich biofilm model is the risk planktonic bacteria may settle on the horizontally-placed HA discs instead of establishing tight attachments. This becomes particularly problematic when during the biofilm-harvesting step, discs are often washed in PBS to wash off any non-adherent cells. Therefore to avoid bacterial sedimentation, the active attachment biofilm model can be used. As shown in Figure 1.8 middle, this model was initally custom-made and it involved readily-autoclavable metal clamps which were attached to a metal lid, each holding a HA disc that hung vertically into the inoculum of a 24 well microtitre plate (Deng *et al.*, 2009; Exterkate *et al.*, 2010). This model has since been used for profiling subgingival plaque (Fernandez y Mostajo *et al.,* 2017) and in an *ex vivo* biofilm model using saliva from orally-healthy volunteers (Janus *et al.*, 2017). On a related note, it will be interesting to see with the advent of tabletop 3D printers how custom 3D printing may allow researchers to adapt existing models to create novel custom-made versions that are more suited to the needs of the researcher.

1.4.2.4 Calgary biofilm device (MBEC Assay)

Based on a similar principle, a commerically available model called the minimum biofilm eradication concentration (MBEC) assay (formerly known as Calgary Biofilm Device) currently exists and this was developed in the 1990s (Ceri *et al.*, 1999). The assay consists of 96 pegs attached to the underside of a lid where each peg is suspended in either bacterial inoculum or in growth medium contained within the individual wells of a corresponding 96-well base (as illustrated in Figure 1.8 right). Different varieties are available such as pegs that are coated in hydroxyapatite, or the corresponding base may contain troughs instead of wells.

This assay was developed as a high-throughput way of testing the antimicrobial susceptibility of biofilms but it has since been developed for use in oral biofilm models too (Kistler *et al.,* 2015). Here, HA pegs were bathed in three separate batches of pooled saliva samples, with each batch containing saliva from 6 participants. The MBEC wells were incubated under anaerobic conditions for up to 14 days. At days 7 and 14, biofilms were scraped off, with triplicate biofilms pooled

into one sample and the community DNA within each sample was extracted and pyrosequenced. This study is particularly noteworthy as replicate biofilm communities formed on separate HA pegs exhibited high similarity to one another, suggesting the reproducible nature of the MBEC assays for modelling. However, community membership and their structure did significantly differ between the three batches of different participants, especially at day 14. This is perhaps surprising as community membership and structure are considered to be more settled in more mature biofilms. 250 operational-taxonomic units (OTUs) were also detected from the pooled samples although the subjects were healthy and without periodontal disease. Naginyte *et al.*, (2019) also inoculated MBEC plates with inoculum comprising oral samples from dentally-healthy subjects, so an *ex vivo* subgingival plaque model from periodontitis patients would therefore also be beneficial to the current understanding of periodontal disease.

An example of this was by Baraniya *et al.* (2020), who analysed the composition of 7-day old biofilms grown on saliva-conditioned MBEC pegs. The pegs were inoculated with subgingival plaque samples pooled from 5 subjects with periodontitis and separately, from subgingival plaque samples pooled from 5 healthy donors. The aim of the study here was to test several growth medium types by varying the concentrations of sucrose and heat-inactivated human serum, and whether there were differences between normal- and periodontitis-associated biofilms. The authors found regardless of the sucrose concentration; periodontitis-associated biofilms had a higher biomass when assessed with 16S rRNA gene community profiling using the MiSeq platform. However, lower viability assessed with ATP assays was also observed with periodontitis-associated biofilms. Increasing the serum concentration to 10 % (v/v) increased the biomass and viability in periodontitis-associated biofilm communities. Interestingly, *Haemophilus, Aggregigatibacter* and *Capnocytophaga* amongst other genera were under-represented in the biofilms compared to the clinical inoculum. *Parvimonas, Dialister, Atopobium* and *Peptostreptococcus* amongst others were in contrast over-represented in the biofilms compared to the clinical inoculum.

Soares *et al.* (2015) used the same assay to model subgingival plaque by developing a 40 multi-species model and tested the eradication of biofilms after their exposure to antibiotics. The focus of the study was on the effect of antibiotics but the large number of different bacterial species inoculated in the model means this was one of the most significant studies yet, in attempting to create mock communities that are representative of the natural diversity of the oral microbiota. Unfortunately, due to the large number of species, 5 of the 40 species were not consistently recovered from the mature biofilms, although checkerboard DNA-DNA hybridisation was used which does not differentiate DNA from viable or non-viable bacteria. It is also possible that the large number might have impeded certain bacteria to become established in the community under a laboratory setting where there is no constant flow of fluids and nutrients. This would be different to a natural setting where the flow of GCF fluid is present. Because the lids with the attached biofilms can easily be moved to a new baseplate containing different wells of varying serial dilutions of antibiotics, many other studies have reported the use of the MBEC plate for this purpose (Bardouniotis *et al.*, 2001; Finelli *et al.*, 2003; Harrison *et al.*, 2005; Melchior *et al.*, 2007; Arias-Moliz *et al.*, 2010).

1.4.2.5 xCELLigence RTCA Single Plate

A novel biofilm device named the xCELLigence RTCA Single Plate system is commercially available from ACEA Biosciences (part of Agilent Technologies, USA), and this was trialled by Mira *et al.* (2019). The authors grew biofilms from saliva, tongue and plaque samples and using the electrode-based biosensors embedded on the bottom of the plate, enabled the progression of biofilm formation to be observed in real-time. A measure of total biofilm mass (cell index CI) was observed without the need for labels or stains because the methodology relies on cell-electrode impedance in the wells. Biofilms were also recovered from the wells, their DNA extracted, and 16S rNA gene sequencing was performed. Amoxicillin treatment on the saliva-derived biofilms was also tested for its inhibitory effect. Like the pros and cons afforded by biofilms grown in microtitre plates, susceptibility testing can be performed in the xCELLigence RTCA Single Plate and biofilms can be grown in a high-throughput manner. However, bacterial cells are

prone to settling on the bottom instead of forming strong attachments to the substratum.

1.4.3 Continuous culture model system

Many continuous culture biofilm models exist although only a few of the more recently and widely used systems are described in this review. These are summarised in Figure 1.9.

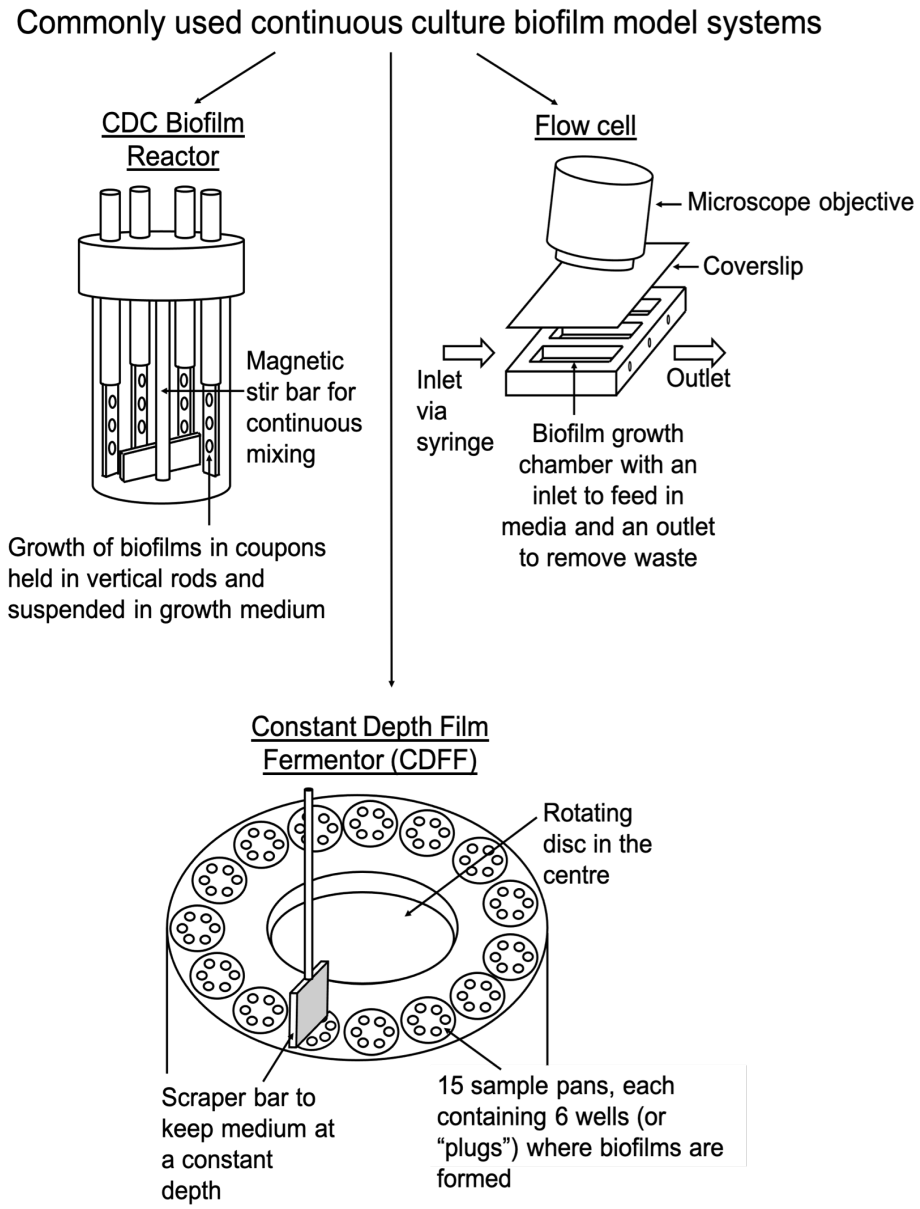

Figure 1.9 Commonly used in vitro continuous biofilm model systems described in this review. This includes the CDC Biofilm Reactor, the Constant Depth Film Fermentor, and the Flow Cell.

1.4.3.1 CDC biofilm reactor

As introduced earlier, batch culture model systems lack growth medium flow and consequently may not be as representative of the oral cavity as continuous culture model systems. However, salivary flow has a higher flow rate than the flow of GCF in periodontal pockets, so site is also an important factor to consider. The lack of growth medium flow may subsequently reduce bacterial adherence as some bacteria have shown to attach to surfaces better when shear forces are present, although this was disproved by Song *et al.* (2017). The study here compared the biofilms formed on hydroxyapatite discs in wells to those grown in a Centre for Disease Control and Prevention (CDC) biofilm reactor (illustrated in Figure 1.9 left). This is a device that enables biofilms to grow on coupons incorporated into long rods which are positioned vertically and are fully submerged in growth medium. Shear forces and the flow of nutrients are introduced by a baffled stir bar that continuously stir at moderate to high speeds (Goeres *et al.*, 2005) to mimic the continuous salivary flow in the oral cavity. The continuous mixing can also promote nutrient concentration stability during biofilm formation. A drawback to this is the constant flow of growth medium would require much larger volumes than those that are required in batch cultures. Song *et al.* (2017) grew single- and dual-species biofilms comprising *F. nucleatum* and *P. gingivalis* and reported the lower adherence and bacterial numbers in a CDC biofilm reactor than in wells. For this, they suggested the shear forces occurring in a CDC biofilm reactor reduced the adherence of bacteria. A less dense accumulation of *F. nucleatum* in CDC models was also reported and shown by scanning electron microscopy and confocal laser scanning microscopy. Nevertheless, the CDC biofilm reactor has successfully been shown to support the growth of reproducible multispecies oral biofilms (Rudney *et al.*, 2012; An *et al.*, 2022).

1.4.3.2 Constant depth film fermentor (CDFF)

Another well-established continuous culture model system is the constant depth film fermentor (CDFF) (Peters and Wimpenny, 1988). This is a glass vessel (as illustrated in Figure 1.9 middle) with a rotating disc in the centre that houses 15 sample pans, with each pan containing 5 or 6 wells (or “plugs”) where biofilms are

formed. The vessel contains an entry port for fresh growth medium and gas, as well as an output medium outlet to continuously replenish nutrients. A scraper bar is also present to continuously smear growth medium over the wells at a constant predetermined depth, thus maintaining bacterial density and a predetermined constant thickness across all developing biofilms. Salivary flow in the human mouth is reported at approximately 0.35 ml/min and together with the chewing, tongue, and jaw movements, they control the thickness of biofilms in the mouth (Chevalier, Ranque and Prêcheur, 2018). Furthermore, the continuous scraping also mimics the natural continuous removal of the uppermost layer of dental plaque by chewing and the tongue movement. This was suggested by Pratten *et al.* (1998) who studied the bactericidal effect of antimicrobial-containing mouthwashes on biofilms. This may be less appropriate for subgingival plaque samples though. Hydroxyapatite discs can also be placed within the plugs to better suit oral bacteria growth and up to 90 biofilms can be grown in one CDFF, allowing multiple test conditions and technical replicates to be included in one experiment. Hope *et al.* (2012) ran two CDFFs concurrently in a single incubator, with identical inoculum and growth medium to check for any biofilm variability between the two CDFFs. In addition, two further CDFF runs were carried out separately in series. It was shown that the variability in bacterial counts was reduced when biofilms were grown in concurrently-ran CDFFs compared to those run-in series. However, a disadvantage of these continuous culture model systems is that only one type of media can be used for a single experiment so testing different antimicrobial-containing growth media will require separate systems. Although concurrently-operated runs may be useful for gathering data under separate test conditions when not testing any antimicrobial agents, biological repeats which are carried out on separate occasions will still be important in evaluating the reproducibility of biofilm models. Unfortunately, as mentioned, this study has highlighted the variability in CDFF biofilms run in series. An amendment to the CDFF was made though by Deng *et al.* (2005) to create a ‘split-mode’ CDFF, consisting of the rotating disc which holds the sample pans to rotate 180 ° instead of 360 °, thus enabling the testing of two growth conditions simultaneously in one CDFF. A further drawback to CDFF biofilm models is the need for specialised equipment.

1.4.3.3 Flow cells

Flow cells used in biofilm modelling differ to the previously described CDC biofilm reactor and CDFF because flow cells are designed so that they can be mounted with microscope coverslips (which act as the substrata) on top of the flow cell base for easy microscopic analysis such as CLSM without disrupting the biofilms. Real-time analysis during biofilm development can also be carried out. A flow cell chamber designed by Wolfaardt *et al.* (1994) (shown in Figure 1.9 right) was as small as a 45 x 50 mm coverslip and contained up to 10 growth chambers. Microscope coverslips sit on top of the flow cell base for easy microscopic analysis such as CLSM without disrupting the biofilms. Inlets and outlets are present to maintain continuous culture conditions via the use of syringes to feed in liquid. Unfortunately, because mixing in flow cells is by diffusion and not by a stirrer, environmental conditions can differ within the biofilm model. Regardless, the flow cells may be preconditioned with saliva first and various studies have used flow cells for investigating the development of multispecies oral biofilm communities (Foster and Kolenbrander, 2004; Pamp *et al.*, 2009; Periasamy and Kolenbrander, 2009).

1.4.3.4 BioFlux system

Biofilms can also be viewed in real-time under controlled shear flow by using the BioFlux system (Fluxion Biosciences, USA), which allows the user to precisely mimic the salivary flow within models in a high-throughput manner. This is due to the use of multiple channel plates under light microscopy. In place of crystal violet assays, this can be advantageous in observing and quantifying the architecture of biofilms (i.e. surface area, fluffiness and porosity) over time and under specific conditions if the use of a live/dead stain is combined with CLSM and software programmes such as BAIT (Biofilm Architecture Interference Tool) (Luo *et al.*, 2019). Like the flow cell biofilm model, small volumes of fresh growth medium are pushed through the microchannels from an inlet by a pneumatic pressure pump and an outlet is present to remove spent medium. Numerous studies have since made use of this commercially available microfluidic system to study oral biofilms although these studies have focused on caries (Tao *et al.*, 2011; Ding *et al.*, 2014; Volgenant *et al.*,

2016). The downside to this microfluidic device, however, is the cost, training and availability of the equipment involved and it may not be as relevant to studying subgingival plaque because GCF flow within periodontal pockets is low.

1.4.4 Alternatives to *in vitro* biofilm models

This PhD project is focused solely on developing *in vitro* oral biofilm models, but it is still essential to briefly describe other alternatives, such as *in vivo* models. The key benefits of *in vitro* models compared to the latter include its inexpensive cost, its reproducibility, and it is relatively easy to set up. *In vivo* biofilm model systems on the other hand involve using animals to model the biofilm communities and this therefore requires stringent and sometimes lengthy ethical applications, specialised equipment and facilities, training, and regular audits. There are also ethical limitations to what can be tested in animal models when investigating periodontal disease development. *In vivo* studies also do not allow high-throughput applications and the data obtained from animal models may not be applicable to humans.

Despite these limitations, *in vivo* studies in general offer a huge wealth of knowledge and most importantly, allow causative agents to be definitively understood. For example, it is understood *P. gingivalis* induced alveolar bone loss due to the inoculation of this bacterium in immunocompetent gnotobiotic mice (Baker et al., 1994). The mouse model is often the classic animal model (Abe and Hajishengallis, 2013) although canines are the most frequently used in periodontal research as dogs have a high incidence of periodontal disease. Other animals include and are not limited to non-human primates, rabbits and hamsters have been used in modelling experimental gingivitis and periodontitis for instance (Jordan and Keyes, 1964; Ericsson *et al.*, 1975; Schou *et al.*, 1993; Tyrrell *et al.*, 2002; Polak *et al.*, 2009). Relating once again to the synergy between streptococci and *P. gingivalis*, a mouse model was used to show streptococci promoted the colonisation of *P. gingivalis* and hence, it played a role in periodontal disease development (Kuboniwa *et al.*, 2006). Animal models also complement *in vitro* studies for testing novel treatments.

The use of non-mammalian models can circumvent some of the disadvantages of their mammalian counterparts such as ethical conflicts, cost, and throughput. For example, a novel zebrafish larvae model was recently demonstrated to model the role of *P. gingivalis* gingipains and proteases in the bacterium disseminating into the cardiovascular system to cause systemic infections (Widziolek *et al.*, 2016). This model offered a non-invasive real-time method on investigating bacterial molecular mechanisms and is an innovative powerful tool in helping to expand the current knowledge of the role of bacteria in periodontitis.

1.5 Role of microbial glycobiology in bacterial communities

1.5.1 Microbial glycobiology

Glycans in the broadest sense are also known as carbohydrates, saccharides, attached sugars or chains, and microbial glycobiology is the study of these glycans in relation to microorganisms. Glycans are highly branched molecules and are typically found on the surface of all cells and numerous cellular and secreted macromolecules in nature (Varki and Kornfeld, 2015). They are for instance conjugated to the macromolecules proteins and lipids to form glycoproteins and glycolipids respectively. As shown in Figure 1.10, glycan chains are bound to proteins by either a nitrogen atom (side group of asparagine on proteins) to form N-linked glycans, or an oxygen atom (side groups serine or threonine) to form O-linked glycans (Dwek, 1996).

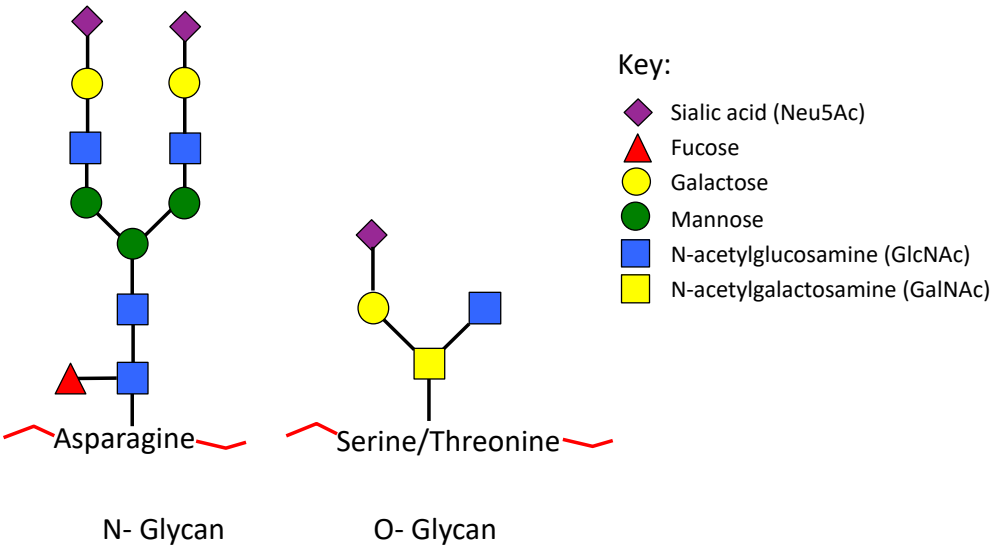

Figure 1.10 Examples of a N-Glycan and an O-Glycan. Glycan chains can be bound to proteins by a nitrogen atom to the side group of asparagine to form N-glycans, or by an oxygen atom to the side groups serine or threonine to form O-glycans.

From their positions on the cell surfaces, glycans are therefore able to recognise and mediate cell-cell, cell-matrix, cell-molecule plus host-microorganism interactions (Varki and Kornfeld, 2015). Furthermore, host-associated glycans also act as sources of sugar-based carbon for oral bacteria. This is particularly useful as sugars derived from the diet are often transient and would be insufficient to sustain the cohabiting bacteria within the oral community. In addition, the salivary pellicle layer on tooth surfaces is rich in glycoproteins and this is shown in Figure 1.11.

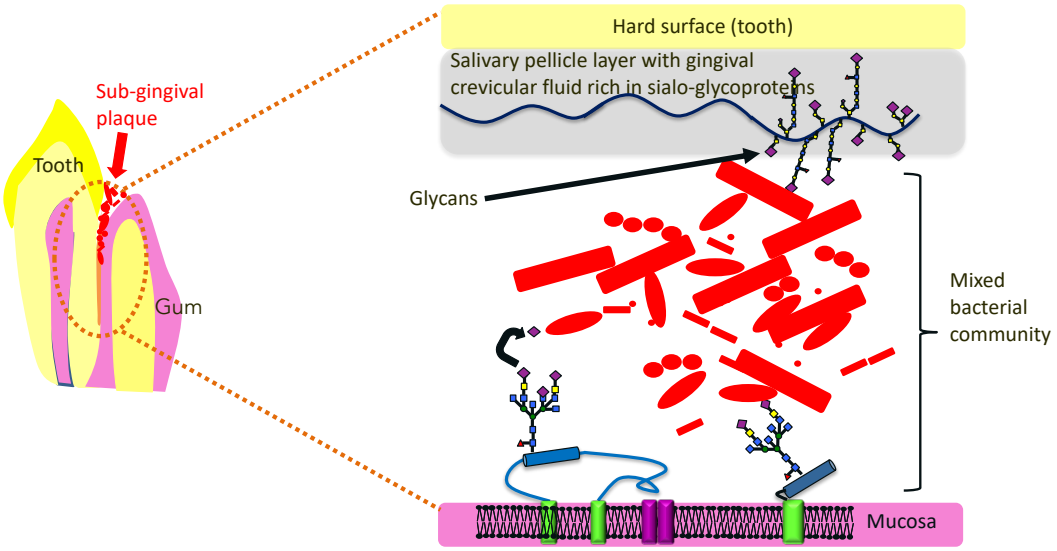

Figure 1.11 The periodontal pocket in periodontitis. An illustration representing the salivary pellicle layer seen in the oral cavity associated with periodontitis. The tooth surface is covered in a salivary pellicle layer that is covered with gingival crevicular fluid that is rich in glycoproteins.

1.5.2 Structure of sialic acids

Sialic acids are part of a family of *N*- and *O*-linked derivatives of neuraminic acid which are 9-carbon polyhydroxyaminoketoacid sugars (Varki and Diaz, 1983) that are often found at the termini of glycan chains of eukaryotic and bacterial cells. The name sialic acid is derived from sialon, the Greek word for saliva as it was first found in saliva in 1937 by the biochemist Gunnar Blix (Blix G, 1936; Lundblad, 2015). Sialic acids function in host cells include self-labelling for protection from immune cells by sialic acid-binding immunoglobulin-like lectins (receptors), cell signalling, the masking of host surface proteins, binding of hormones and maintenance of negatively-charged cell surface (Varki and Diaz, 1983).

In mammals, 5-*N*-acetylneuraminic acid (a.k.a. Neu5Ac), is the most abundant type of sialic acid and it was initially discovered after its release as the major product after the acid hydrolysis of salivary mucin (Varki and Schauer, 2009). Mucin is a sialo-glycoprotein. Most mammals except humans can also produce large amounts of N-glycolylneuraminic acid (Neu5Gc) which is structurally and chemical similar to Neu5Ac. This is demonstrated in Figure 1.12 (Douglas *et al.*, 2014). Neu5Gc is hydroxylated and contains an additional O-atom in place of the acetyl group at the 5-carbon position present in Neu5Ac. It is thought modern humans have since lost the ability to synthesise Neu5Gc sometime after the last common ancestor with

the great apes, caused by a mutation in the gene for the synthesis of CMP-N-acetylneuraminic acid hydroxylase (Varki, 2001). Neu5Ac is present on all human cell surfaces and its function is essential, as demonstrated by the fatality of early mouse embryos in the absence of sialic acids (Varki, 2001).

Furthermore, Neu5Ac may be diacetylated and as examples, form Neu5,7Ac_2, Neu5,8Ac_2 and Neu5,9Ac_2. These sialic acids contain a second acetyl group that is found at the 7-carbon, 8-carbon and 9-carbon positions respectively. High levels of the diacetylated Neu5,9Ac_2 sialic acid are found in humans, which are thought to play a protective role for the host as bacterial access to Neu5,9Ac_2 and subsequent cleavage for carbon use are hampered. Although the 9-carbon backbone is present in all sialic acids, many derivatives of sialic acids exist due to some modifications. This diversity can be due to the combinations of different glycosidic linkages, substitutions at the hydroxyl groups at different carbon positions for different chemical groups such as O-sulphate and phosphate among many others (Varki and Schauer, 2009). These can all affect their recognition (Cohen and Varki, 2010).

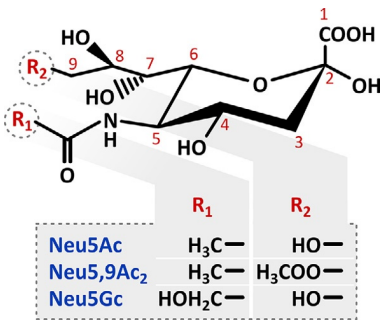

Figure 1.12. Structures of different sialic acids. Schematic illustrating the structures of the different sialic acids Neu5Ac, Neu5,9Ac_2 plus Neu5Gc, and how they differ to one another. Image taken from Douglas *et al.* (2014) with permission.

Proportions of sialic acids such as those in mucin can also vary between different host species, although *N*-acetylneuraminic acid is only found in humans. Generally, sialic acids are covalently attached to mucin by a 2-6' glycosidic bond (Mizan *et al.*, 2000). For another glycoprotein fetuin which is found in blood, sialic acids are linked by both 2-3' and 2-6' glycosidic bonds. The sialyated nature of mucin was shown by Roy *et al.* (2011) to provide a source of nutrition and to facilitate

attachment to mucin-coated surfaces by *T. forsythia* during biofilm formation. The mechanism behind this is via the secretion of sialidase enzymes by certain bacteria and this will be discussed in section 1.5.4.

1.5.3 Function of sialic acids

The function of sialic acids can also be structural and physical. For example, the negatively-charged sialic acids can provide a repulsion to help separate circulating cells in the bloodstream, as well as contributing to neuronal plasticity by separating neurons and neuronal extensions in the brain (Varki, 2001). Further functions of host sialic acids also include: the maintenance of negatively-charged cell surface; ion transport and signalling; stabilisation of protein conformations and increasing mucin viscosity (Varki and Schauer, 2009). Mucin makes up approximately 16 % protein content in saliva and thus is considered the most abundant protein that is present in whole saliva (Payment *et al.*, 2000). Salivary mucin is heavily glycosylated and their O-glycosylated sugar chains, which are attached to the protein backbone by serine/threonine linkages, encompass 40-80 % of their mass (Levine *et al.*, 1987; Zalewska *et al.*, 2000). N-glycans linked to asparagine are also present in salivary mucin. Other heavily glycosylated proteins present in saliva also include salivary agglutinin, proline-rich glycoprotein and secretory immunoglobulin A (Cross and Ruhl, 2018). The majority of salivary mucin are sialyated, with the two dominant mucin proteins in human saliva MUC5B (also called MG1) and MUC7 (also called MG2) containing α2,6-linkages with N-acetylglucosamine in MUC5B and both α2,3-linkages and α2,6-linkages in MUC7 (Shori *et al.*, 2001; Limsuwat *et al.*, 2016). MUC5B has a high molecular weight of 20,000-40,000 kDa, is secreted and plays a role in gel-forming. In contrast, MUC7 has a low molecular weight of 130-180 kDa and is secreted in mucous secretions such as saliva (Oppenheim *et al.*, 2007; Douglas *et al.*, 2014). As shown in Figure 1.13, mucins typically contain N-acetylgalactosamine (GalNAc) which is bound to serine/threonine residues to form an O-glycan core structure. This is then further elongated by the linkages of GalNAc, galactose (Gal) or N-acetylglucosamine (GlcNAc) (Brockhausen *et al.,* 2009; Juge *et al*., 2016). A highly variable part may contain fucose and terminal sialic acid.

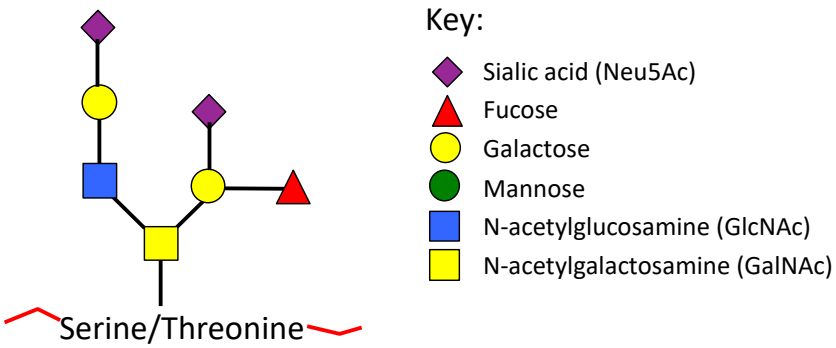

Typical mucin structure

Figure 1.13 A typical mucin structure. The typical structure of a mucin O-glycan contains N-acetylgalactosamine (GalNAc) that is linked to serine/threonine, a backbone elongated by N-acetylgalactosamine (GalNAc), N-acetylglucosamine (GlcNAc) or galactose, and a highly variable peripheral part containing fucose and terminal sialic acid.

The mass and size of mucins are increased during mucin synthesis, whereby O-glycosylation and multimerisation occurs. This provides mucus its viscoelastic property that aids in the lubrication of the oral mucosa, providing a thick barrier to the oral epithelium. It also contributes to the trapping, agglutination and clearance of pathogens thereby providing an antimicrobial role (Ramsey *et al.*, 2016). It is also thought the predominance of α2,6-linked sialic acids in membrane-bound human salivary mucin inhibit human influenza A viruses binding to host cells, as the sialic acids present as ligands to viral haemagglutinin, thereby acting as decoy α2,6-linked sialic acid receptors (Limsuwat *et al.*, 2016). Furthermore, sialic acids present in mucin also contribute to an overall negative charge to provide charge repulsion, the protection of mucin from proteolytic degradation, as well as modulating the clearance of proteins (Takehara *et al.*, 2013).

Sialic acids also play an important role by marking and therefore recognising host cells as “self”, but bacteria are however able to utilise this system by procuring and coating their cell surfaces with the sugars. This is a form of molecular mimicry, which allows them to evade the host immune system. Lastly, sialic acids additionally help in the modulation of the host immune system, as sialic acids are recognised by host receptors as “self” by Siglecs (Varki and Diaz, 1983). Siglecs are sialic acid-recognising lectins which are members of the immunoglobulin

superfamily that work by binding to the sialic acids present on host immune cells. These immune cells include macrophages, dendritic cells, and B-cells. As an example, it results in the suppression of the immune response by limiting the activation of Toll-like receptors (TLRs) and hence, prevents the release of inflammatory cytokines (Crocker *et al.*, 2007; Paulson and Kawasaki, 2011). However, bacteria can use sialic acids present on host cell surfaces for nutrition, and for attachment and invasion into host cells.

1.5.4 Bacterial sialidases

Sialic acids can be obtained by bacteria in two ways. The first route is *de novo* biosynthesis, which is where sialic acids can be synthesised by certain bacteria such as *Escherichia coli* K1, *Neisseria meningitidis* and *Camplyobacter jejuni* (Severi *et al.*, 2007). Briefly, a precursor metabolite UDP-N-acetylglucosamine (UDP-GlcNAc) is converted to N-acetylmannosamine (ManNAc) by the NeuC protein, before being converted to Neu5Ac by the NeuB protein. The second route of obtaining sialic acids is by scavenging them from the environment, for example by secreting sialidases, which is also known as neuraminidases.

Sialidases are enzymes that function to remove sialic acid residues from the terminal branches of glycans in glycoproteins, glycolipids and polysaccharides by cleaving the α-2,3 and α-2,6 glycosidic linkages. Sialidases can be cell-bound which are stored before their release but they can also remain surface-located. It is widely understood sialidases act as virulence factors to help promote bacterial growth through a wide variety of means for both resident and pathogenic bacteria. Sialic acids can be catabolised inside bacterial cells into N-acetylmannosamine (ManNAc) by the enzyme acetylneuraminate pyruvate lyase after transport into cells (Corfield, 1992), which can then be used as a precursor for bacterial sialic acid biosynthesis and incorporated into sialic acid-containing cell-surface macromolecules, which as mentioned previously can aid in molecular mimicry. Alternatively, through further metabolism stages, an eventual end-product such as GlcNAc-6-P is used as a substrate for the peptidoglycan amino sugar N-acetylmuramic acid (NAM) biosynthesis, as is the case for *T. forsythia*. Furthermore,

Jansen *et al.* (1994) showed immunoglobulin G (IgG) which is a major glycoprotein in GCF, provided not only a source of amino acids for bacterial growth but likewise, also inhibited host immune response.

Even in the 1950s, sialidases were isolated from a range of bacteria such as *Vibrio cholerae* and *Clostridium perfringens* (Popenoe and Drew, 1957; Schramm and Mohr, 1959). As mentioned previously, commensal bacteria within the oral cavity are constantly exposed to sialic-acid rich mucin. Many commensal oral bacteria such as *S. oralis* and *S. intermedius* (Beighton and Whiley, 1990) and those associated with periodontal disease such as *P. gingivalis* and *T. forsythia* from the red microbial complex have therefore been shown to express genes for sialidases. Besides exposing the oral epithelium for adhesion and invasion, they do this to access the additional energy source. Sialidases that were previously isolated from oral bacteria in the human mouth is summarised in Table 1.2 below. In the canine microbiome, the commensal bacterium *Capnocytophaga canimorsus* has also been reported to exhibit sialidase activity (Mally and Cornelis, 2008).

Table 1.2 Sialidases previously isolated from bacteria in the human mouth.

Bacteria	**References**
Porphyromonas gingivalis	Moncla *et al.*, 1990
Bacteroides fragilis	Vonnicolai *et al.*, 1983
Tannerella forsythia	Thompson *et al.*, 2009
Streptococcus oralis	Byers *et al.*, 2000
Streptococcus mitis	Beighton and Whiley, 1990
Streptococcus intermedius	Beighton and Whiley, 1990
Haemophilus parainfluenzae	Tuyau and Sims, 1974
Actinomyces oris (naeslundii)	Moncla and Braham, 1989
Actinomyces odontolyticus	Moncla and Braham, 1989
Treponema denticola	Kurniyati *et al.*, 2013

The role of bacterial sialidases in biofilm formation have also been extensively studied. Examples have included a *P. gingivalis* mutant absent of sialidases, which prevented capsule synthesis and also reduced biofilm formation (Li *et al.*, 2012). Likewise, as the *nanH* enzyme is thought to cleave sialic acids from glycoproteins, a

T. forsythia mutant with a *nanH* sialidase deletion reduced biofilm growth. When sialic acid is the sole carbon source, it also reduced the initial adhesion to the glycoprotein-coated surfaces by up to four-fold compared to an equivalent wild-type strain (Roy *et al.*, 2011).

Some bacteria such as *Hamophilus influenzae* which is found at respiratory sites lack genes for sialidase but they are still able to utilise free sialic acid accessed by other sialidase-expressing bacteria that are present in the same community (Bouchet *et al.*, 2003). Interestingly, although *T. forsythia* expresses sialidase activity, another species in this genus, *Tannerella serpentiformis* (Ansbro, Wade and Stafford, 2020), was recently found to be sialidase-negative under the same test conditions and also lacking the *nan* operon in its genome (Beall *et al.*, 2014; Frey *et al.*, 2018). For those bacteria not expressing genes for the sialidase enzymes, it is also thought free sialic acids may become available during host inflammatory processes by the host sialidases as a method to cope with oxidative stress (Severi *et al.*, 2007). More related to periodontal disease, sialidase activity was also previously detected in subgingival plaque from adults with gingivitis through measuring the release of sialic acid from bovine mucoprotein, although which bacteria were present in samples were not revealed (Thonard *et al.*, 1965). Most recently, higher levels of sialidase concentrations were evidenced in periodontal communities than in healthy counterparts by Gul *et al.* (2016), suggesting the role of these enzymes in the development of dysbiotic communities. This is yet to be fully understood.

As mentioned above, a particularly relevant oral bacterium capable of expressing genes for sialidases is *T. forsythia*, as it is highly associated with periodontitis. Interestingly, *T. forsythia* can produce two sialidase enzymes to carry out different functions. *T. forsythia* can firstly produce the enzyme NanH, which functions to remove the mono-N-acetylated sialic acids (Neu5Ac) from terminal N-acetylglucosamine branches of host glycoproteins by cleaving the α2,3 and α2,6 glycosidic bonds (Douglas *et al.*, 2014). Approximately 20 % of sialic acids in humans are however diacetylated, via the O-acetylation at the C4,8 or most

commonly at the C9 position (Robbe *et al.*, 2003). In other words, they contain a second O-acetyl group in the C9 position of human sialic acids (Neu5,9Ac_2). NanH can cleave the mono-N-acetylated form of sialic acids, but it is unable to cleave the diacetylated version (Corfield, 1992). Therefore, *T. forsythia* also produces the second enzyme NanS (sialate-O-acetylesterase), as shown in Figure 1.14.

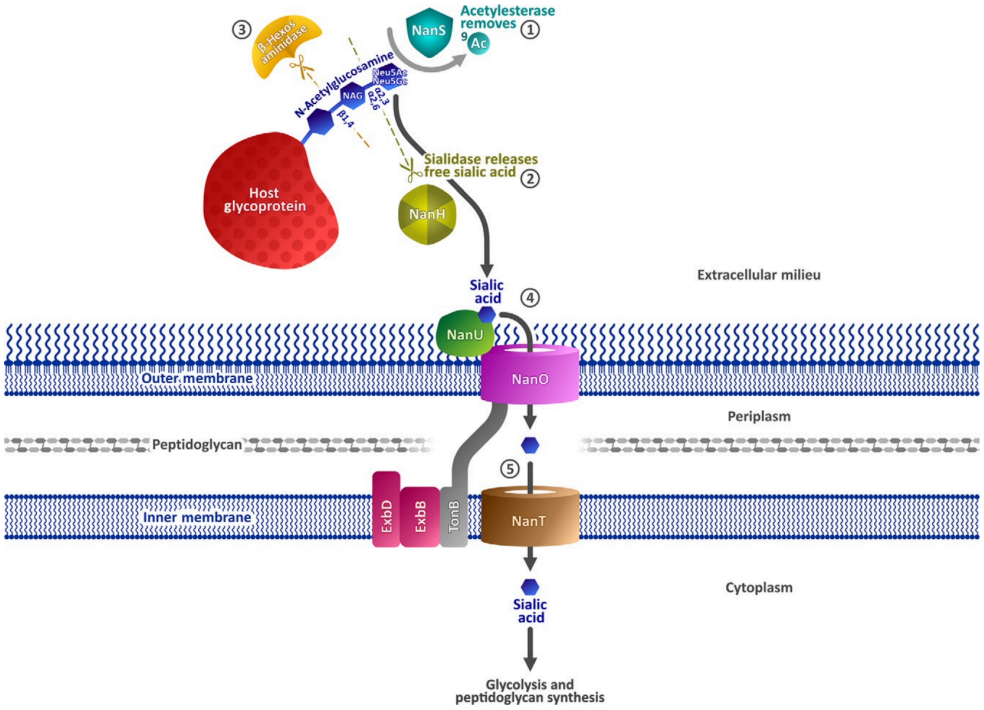

Figure 1.14 Sialic acid uptake and harvesting system in *T. forsythia*. Illustration from Douglas *et al.* (2014) representing the sialic acid uptake system in T. forsythia. The steps involved include 1) removal of the second O-acetyl group in the C9 position of diacetylated sialloglycoproteins by NanS, 2) removal of the mono-N-acetylated sialic acids (Neu5Ac) from terminal N-acetylglucosamine branches of host glycoproteins by cleaving the α2,3 and α2,6 glycosidic bonds, 3) removal of β-linked sugar residues by β-hexosaminidase, 4) cleaved sialic acid bound to the cell surface protein NanU prior to transportation through the outer membrane by the NanO TonB-dependent transporter and then 5) through the inner membrane into the cytoplasm by NanT permease. Image adapted from Douglas *et al.* (2014) with permission.

NanS functions to specifically cleave the second acetyl group within diacetylated sialic acids first (Douglas *et al.*, 2014; Phansopa *et al.*, 2015), thus allowing *T. forsythia* to efficiently harvest and make use of sialic acids. Likewise, the sialidase enzyme SiaPG also required NanS to maximise its harvesting of sialic acids (Frey *et al.*, 2019). A recent study used enzyme-linked lectin assays to show that the combined activities of the N- and C-terminal domains of the NanS enzyme allowed efficient de-acetylation at the O-acetyl groups in the C7 and C9 positions present in the sialic acid on the termini of bovine submaxillary mucin (Albers *et al.*, 2021).

Having the additional NanS in *T. forsythia* may confer a competitive advantage over the other bacteria present within the same community. In *T. forsythia*, it is thought due to the exposure of β-linked glucosamine or β-linked galactosamine after the removal of terminal sialic acids, these β-linked sugar residues are then removed by β-hexosaminidase enzymes (Hughes *et al.*, 2003). Roy *et al.* (2011) confirmed this by demonstrating that at least three putative β-hexosaminidase were present in the genome of *T. forsythia*. The cleaved Neu5Ac then binds to the cell surface protein NanU prior to transportation through the outer membrane by the NanO TonB-dependent transporter and then through the inner membrane into the cytoplasm by NanT permease (Douglas *et al.*, 2014). As mentioned earlier, Neu5Ac can then be incorporated onto bacterial surfaces as a method of mimicking host cells to evade the host's immune response.

1.5.5 Inhibitors of bacterial sialidases

Sialidases can however be inhibited and sialidase inhibitors were historically manufactured as anti-influenza drugs. Zanamivir and oseltamivir as examples, are licensed and are commercially known as Relenza and Tamiflu respectively. They are available as anti-influenza drugs, which act to inhibit viral neuraminidase (McKimm-Breschkin, 2013). This enzyme normally functions to cleave host cell sialic acids, breaking the interaction between the viral membrane and host glycans, thus allowing the release of newly synthesised viral particles from the infected host cells. Zanamivir and oseltamivir therefore act as antiviral compounds to limit further viral infection in the host. As shown in Figure 1.15, both are analogues of the transition molecule of the sialic acid analogue 2,3-dehydro-2-deoxy-N-acetylneuraminic acid (DANA), during the cleavage of glycosidic linkages by sialidases. They are thus based on the structure of DANA, which was first shown to weakly inhibit influenza neuraminidase. A 10,000-fold improvement in binding affinity was achieved with substituting the C4-OH group with a 4-guanidino group to produce zanamivir (McKimm-Breschkin, 2013). The design of oseltamivir then followed, and its structure involves the substitution of the C4-OH group in DANA with a C4-NH_2 group, as well as replacing DANA's glycerol side chain with a bulky hydrophobic pentyl ether side chain. Studies have since shown the mediation of

oral bacterial virulence with the use of these three inhibitors. For example, the presence of DANA reduced the activity of *T. denticola* sialidase (TDE0471) (Kurniyati *et al.*, 2013). Treatment with DANA in another study also recently reported to reduce the growth and biofilm formation of *P. gingivalis,* as well as the reduction of several gene expressions that are associated with virulence factors (Yu *et al.*, 2021). The genes affected included gingipains and those associated with fimbriae. Furthermore, DANA also significantly reduced *T. forsythia* attachment to the epithelial cells (Kurniyati *et al.*, 2013). The presence of oseltamivir was likewise demonstrated to reduce the growth and adhesion of *T. forsythia* to bovine submaxillary mucin by approximately two-fold and up to threefold to human serum (Roy *et al.*, 2011). It was also recently reported that zanamivir reduced the activity of SiaPG and inhibited *P. gingivalis* attachment and invasion into oral epithelial cells (Frey *et al.*, 2019).

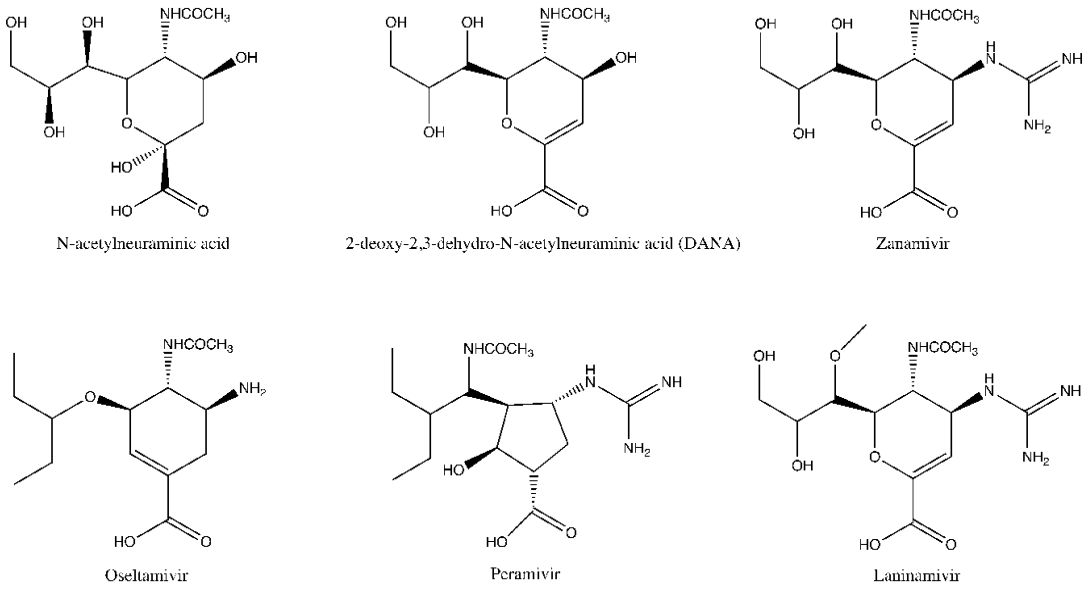

Figure 1.15 N-acetylneuraminic acid and its inhibitors. The chemical structures of N-acetylneuraminic acid (Neu5Ac) and the neuraminidase inhibitors DANA, zanamivir, oseltamivir, peramivir and laninamivir (adapted from Mckimm-Breschkin (2013)).

There is an apparent sialidase-specific preference in the efficacy of sialidase inhibitors though. As an example, both DANA and oseltamivir were demonstrated to require concentrations in the micromolar range for inhibiting *T. forsythia* NanH activity by 50 % compared to requiring zanamivir concentrations in the millimolar

range under the same scenario (Satur, 2019). Of those tested, DANA was therefore the most potent inhibitor of NanH activity. In contrast, zanamivir more efficiently inhibited the sialidase activity (SiaPG) of *P. gingivalis* than the NanH sialidase activity of *T. forsythia* (Frey *et al.*, 2019). A nearly 20-fold difference in the zanamivir concentration was also required to inhibit *T. forsythia* NanH activity by 50 % compared to inhibiting the activity of *P. gingivalis* SiaPG by 50 %. This observation is particularly relevant in a multispecies community whereby the addition of *T. forsythia* NanS has been shown to enhance the removal of sialic acids from mucin by *P. gingivalis* SiaPG sialidase (Frey *et al.*, 2019). As bacteria are known to act in synergy, the authors here have also tested and revealed the combination of *T. forsythia, P. gingivalis* and *F. nucleatum* significantly reduced their attachment and invasion of oral epithelial cells.

Other subsequent sialidase inhibitors have since been developed and licenced in Japan, including peramivir and laninamivir but they have yet to be tested in the context of inhibiting the virulence of oral bacterial associated with periodontitis. Derived from DANA, peramivir was also recently FDA-approved and it contains a cyclopentane ring instead of a cyclohexene ring. It also contains the 4-guanidino group as seen in zanamivir and the hydrophobic pentyl ether side chain in oseltamivir. Laninamivir is based on the structure of zanamivir but with the substitution of the 7-OH group with a 7-OCH_3 group (Babu *et al.*, 2000; Koyama *et al.*, 2010).

As previously described, the exposed β-linked sugar residues after the removal of terminal sialic acids can then be removed by β-hexosaminidase enzymes. These enzymes can however then be inhibited by the addition of the β-hexosaminidase inhibitor PugNAc ((O-(2- acetamido-2-deoxy-D-glucopyranosylidene)amino N-phenyl carbamate)) but crucially only in combination with sialidase to first expose the β-linked sugar residues (Roy *et al.*, 2012). The important role of β-hexosaminidase was also demonstrated in this study as *T. forsythia* biofilm growth on mucin and fetuin was significantly reduced in the presence of the inhibitor PugNAc.

1.6 Aims and objectives of this study

1.6.1 Aims and research questions

The primary aim of this study was to create an *in vitro* multi-species biofilm model that was representative of the microbial community found within the periodontal pockets of the human oral cavity. In parallel, a second aim was to address the question of how microbial sialo-glycobiology influences microbial community structure using this model.

1.6.2 Objectives

The objectives for achieving the aims of this study are listed below:

1. Conduct a literature review to determine the oral bacterial species relevant to periodontitis development.
2. Design and validation of PCR primers specific to each bacterial species selected for inclusion in the *in vitro* mock biofilm model.
3. Construction of an *in vitro* defined mock community biofilm model.
4. Construction of an *in vitro* periodontal plaque biofilm model inoculated directly from periodontal plaque.
5. Assessment of microbial composition changes in the biofilm models using culture, qPCR, and microbiome analysis over time and under influence of addition of specific factors such as sialidase inhibitors.

Chapter 2 – Materials and methods

2.1 Literature search

A literature search was conducted using the PubMed and Scopus databases to determine oral bacteria important in periodontitis development. The following key words were used: “biofilm”, “microbial community”, “bacteria*”, “multispecies” and “dental”, “t??th”, “oral”, “plaque”, “gum”, “gum disease”, “periodont*”, “caries”, gingivitis”, “mouth” to identify papers of interest. Culture media supportive of the growth of each of the chosen bacteria was also selected from previously reported studies focused on oral bacterial community modelling.

2.2 Bacterial strains used in this study

Eighteen bacterial strains were selected for mock community modelling and are listed in Table 2.1. All strains except the spirochaete *T. denticola* were cultured on Fastidious Anaerobe Agar (FAA) (Neogen, UK) supplemented with 5 % oxalated horse blood (Thermo Scientific, USA). Both strains of *T. forsythia* were also cultured on FAA but supplemented with 5 % oxalated horse blood and 1 % N-acetylmuramic acid (NAM). The fastidious oral spirochaete *T. denticola* ATCC 35405 was grown anaerobically at 37 °C in both mNOS (ATCC medium 1494) semi-solid agar and liquid broth (provided in Appendix 8.1). The *A. oris* and *S. gordonii* strains were provided by Nick Jakubovics (Newcastle University). *C. showae, D. invisus* and *P. intermedia* were supplied by William Wade (King’s College London). Angela Nobbs and Jane Brittan (University of Bristol) provided cultures and training for maintaining the growth of *T. denticola*.

Table 2.1 Bacterial culture. Bacterial strains selected for use in this study, with their growth conditions.

Oxygen requirement	Bacterial species	Strain	Growth conditions
Aerobe	*Neisseria. subflava*	ATCC 49275	37 °C in 5 % CO_2
Facultative anaerobes	*Actinomyces oris*	MF1	37 °C in 5 % CO_2
	Streptococcus gordonii	DL1 (Challis)	37 °C in 5 % CO_2
	Streptococcus oralis	C647	37 °C in 5 % CO_2
Strict anaerobes	*Campylobacter rectus*	ATCC 33238	37 °C in 85 % N_2, 10 % H_2, 5% CO_2
	Campylobacter showae	ATCC 51146	37 °C in 85 % N_2, 10 % H_2, 5% CO_2
	Dialister invisus	DSM 15470	37 °C in 85 % N_2, 10 % H_2, 5% CO_2
	Filifactor alocis	ATCC 35896	37 °C in 85 % N_2, 10 % H_2, 5% CO_2
	Fusobacterium nucleatum subsp. nucleatum	ATCC 25586	37 °C in 85 % N_2, 10 % H_2, 5% CO_2
	Fusobacterium nucleatum subsp. *polymorphum*	ATCC 10953	37 °C in 85 % N_2, 10 % H_2, 5% CO_2
	Parvimonas micra	ATCC 33270	37 °C in 85 % N_2, 10 % H_2, 5% CO_2
	Porphyromonas gingivalis	NCTC 11834	37 °C in 85 % N_2, 10 % H_2, 5% CO_2
	Prevotella intermedia	ATCC 25611	37 °C in 85 % N_2, 10 % H_2, 5% CO_2
	Prevotella nigrescens	ATCC 25261	37 °C in 85 % N_2, 10 % H_2, 5% CO_2
	Treponema denticola	ATCC 35405	37 °C in 85 % N_2, 10 % H_2, 5% CO_2
	Tannerella forsythia	ATCC 43037	37 °C in 85 % N_2, 10 % H_2, 5% CO_2
	Tannerella forsythia	UB4	37 °C in 85 % N_2, 10 % H_2, 5% CO_2
	Veillonella dispar	WT	37 °C in 85 % N_2, 10 % H_2, 5% CO_2

2.3 Colony-forming unit counts

Except for *T. denticola*, the bacterial cell concentration was measured for all bacterial strains by determining the bacterial colony-forming units grown on the surface of agar plates and based on the Miles and Misa method (Miles *et al.*, 1938). In brief, an inoculum of optical density 1.0 at 600 nm wavelength was made for each bacterial strain except for *P. micra* and *D. invisus* for whom OD_{600} = 0.5 was used. Ten-fold serial dilutions up to 10^{-7} were subsequently prepared with sterile PBS. Five µl of 10^{-4}, 10^{-5} and 10^{-6} dilutions were pipetted in triplicates onto an agar plate so that discrete colonies could be measured from a volume of 5 µl. The plates were air-dried and incubated under appropriate conditions as described previously for each strain. Enumeration of the colony-forming units was completed when full-size discrete colonies were observed (as demonstrated for *S. oralis* in Figure 2.1). The CFU/ml for each strain was calculated by multiplying the average number of colonies for a dilution by 200 and again by the dilution factor. A third biological repeat was obtained for strains where duplicate counts differed considerably.

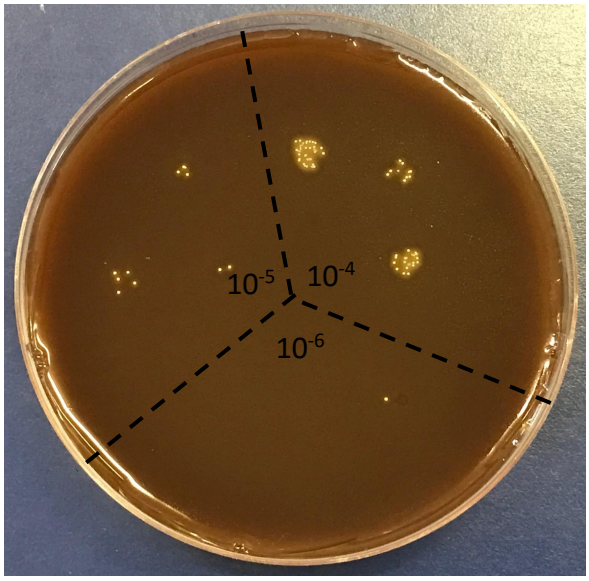

Figure 2.1 Colony-forming units (CFUs) on agar plates. *S. oralis* coony-forming units observed on FAA+5 % horse blood agar plate at dilutions 10^{-4}, 10^{-5} and 10^{-6}.

For spirochaete cell concentration measurements, a 0.2 OD_{600} inoculum of a 4-day old *T. denticola* was serially diluted to 10^{-8} and 1 ml of the dilutions 10^{-6}, 10^{-7} and 10^{-8} was inoculated into 30 ml cooled yet molten semi-solid mNOS agar containing 0.5 % gelatin and 0.5 % agar in separate flasks and completed in triplicate. The flasks were incubated under anaerobic conditions at 37 °C to allow the medium to

gel and the colony-forming units were counted after an 8-day incubation (Figure 2.2).

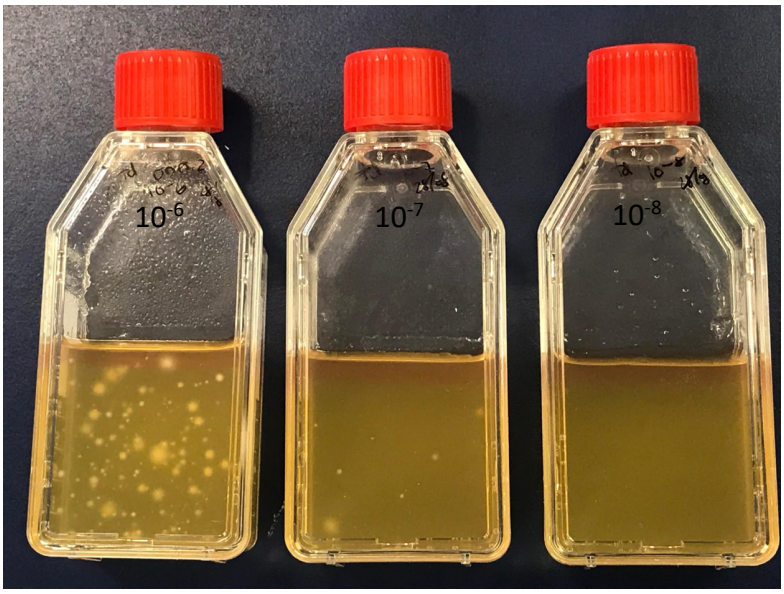

Figure 2.2 Colony-forming units (CFUs) for *T. denticola*. An example of the CFUs recovered for *T. denticola* at dilutions 10^{-6}, 10^{-7} and 10^{-8} in mNOS semi-solid agar.

2.4 DNA extraction and DNA quantitation

For each bacterial strain, a large loopful of bacterial cells from solid medium growth was resuspended in 300 µl PBS and its DNA extracted using the Wizard® Genomic DNA Purification Kit according to the manufacturer's guidelines (Promega, USA) for Gram-positive and Gram-negative bacteria. The extracted genomic DNA was initially quantitated using a NanoDrop™ spectrophotometer (ThermoFisher, USA) following manufacturer's guidelines. For comparison of the DNA quantitation techniques, DNA concentration measurements were also taken using a Qubit™ dsDNA HS Assay kit (ThermoFisher, USA) and measured on a Qubit™ 2 Fluorometer (Invitrogen, USA) following the manufacturer's guidelines. After DNA quantitation by Qubit™, all genomic DNA were diluted to 1 ng/µl and stored at -20 °C until further use.

2.5 Species-specific primer design and validation

2.5.1 Primer search and design

For the 18 bacterial taxa selected for inclusion in the community modelling, species-specific PCR (subspecies-specific or strain-specific where applicable)

oligonucleotide primer sequences with an optimum product size 90-100 bp were sought from the literature. For those species where primers were unavailable and that therefore required primer design, the 16S rRNA gene sequences of species from the same genus as the bacterial species of interest were downloaded from the GenBank nucleotide sequence database (Benson *et al.*, 2013). A multiple sequence alignment was constructed using ClustalW2 in BioEdit Sequence Alignment Editor (v7.2.5) (Hall, 1999) and the variable regions identified. An alternative gene to the 16S rRNA gene was used when the 16S rRNA gene sequences were too highly conserved and primer specificity was further verified by using a BLAST search. The PrimerQuest Tool (idtdna.com) was then used to design potential primers that matched specific parameters such as having an optimum primer annealing temperature of 60 °C, an optimum amplicon size of 90-100 bp and absence of hairpin loops. A primer pair was selected from the resultant list of potential primer sequences provided it mapped to the variable regions highlighted in the multiple sequence alignment mentioned previously. The primers were synthesised by Sigma-Aldrich, UK. Further details and explanation are provided in the results section 3.2.2.

2.5.2 Primer optimisation and validation using end-point PCR

Each of the PCR oligonucleotide primers were checked for their specificity by testing against DNA from each of the different bacterial species in multiplex end-point PCR reactions. Briefly, reactions were performed in total volumes of 25 µl comprising 12.5 µl 2X DreamTaq Green PCR MasterMix (Thermo Fisher Scientific, USA), 6.5 µl nuclease-free water, 0.5 µl each of forward and reverse primers (10 µM each) and 5 µl template DNA (1 ng/µl). PCR amplification was performed under the conditions: initial denaturation at 95 °C for 3 min, followed by 30 cycles of denaturation at 95 °C for 30 s, annealing step at an optimised temperature which was determined post-testing for 30 s, and extension at 72 °C for 1 min. A final extension step of 72 °C for 5 min followed. Some primer sets required re-amplification at various annealing temperatures for PCR condition optimisation.

Amplicons were analysed on a 2 % agarose gel electrophoresis stained with ethidium bromide and GeneRuler 50 bp DNA ladder (ThermoFisher Scientific, USA) was used as the molecular weight marker. DNA was visualised under UV light. Species-specific amplification was demonstrated when a single band was observed only in the lane containing DNA specific to the primer set and at the correct predicted molecular size. No amplification was to have been detected in the remaining lanes containing DNA that was not specific to the primer set of interest. Otherwise, primers were redesigned following the steps as described earlier.

2.6 PMA-qPCR

2.6.1 Propidium monoazide (PMA) treatment

Propidium monoazide (PMA) treatment (Biotium, USA) of cell samples allows for differentiation between intracellular DNA from viable bacteria and extracellular DNA (Nocker *et al.*, 2007). The principle behind this treatment is that when combined with end-point PCR or quantitative qPCR (qPCR), the photo-activating PMA dye selectively binds only to extracellular DNA or DNA within membrane-compromised bacterial cells during a photoactivation step. Its subsequent covalent binding to the DNA then blocks DNA amplification in downstream qPCR reactions as shown in Figure 2.3.

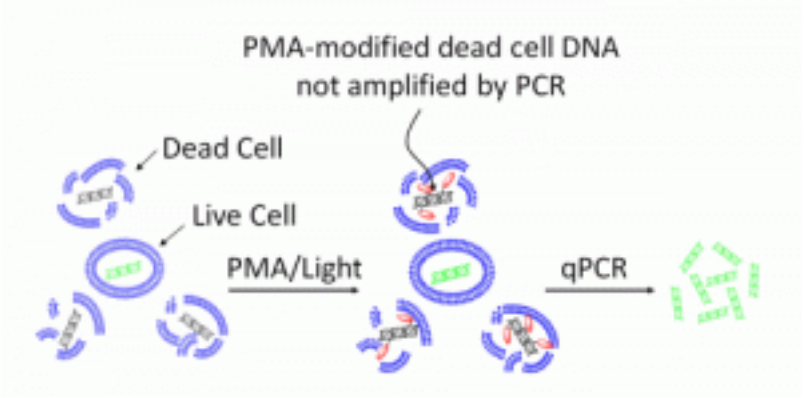

Figure 2.3 Propidium monoazide (PMA) treatment on samples. The principle behind PMA treatment involves the photoactivation of PMA dye, which allows selective binding of PMA dye to extracellular DNA or DNA within membrane-compromised dead cells. Any PMA-modified dead cell DNA is subsequently not amplified by downstream qPCR reaction. Image taken from Biotium, USA.

A stock solution of 20 mM PMA dye (Biotium, USA) was diluted 1:100 and stored at -20 °C. Six aliquots each containing 5 µl of 1 ng/µl *F. nucleatum* subsp. *nucleatum* DNA were prepared and kept on ice. Of these aliquots, one remained untreated with PMA and kept on ice. Next, 1.25 µl of the 0.2 mM stock solution of PMA dye (Biotium, USA) was added to each of the remaining five aliquots at a final PMA concentration of 50 µM. Following 5 min incubation in the dark with occasional shaking, the five aliquots were placed on ice and subjected to a 10,000 lumen LED light source (Super Bright LED Torch, TFCFL, USA), which is an approximate equivalence to the 650 W halogen lamp as described by Nocker *et al.* (2007) at a distance of 20 cm for various durations: 1 min, 3 min, 5 min, 10 min and 20 min with occasional shaking to avoid excessive heating. The tubes were kept on ice in the dark and qPCR immediately followed the photo-induced cross-linkage of the PMA dye to any extracellular DNA.

2.6.2 Quantitative PCR (qPCR)

qPCR reactions for each DNA sample were run in triplicate and in total reaction volumes of 10 µl containing 1 µl template genomic DNA, 9 µl 2x SYBR Green PCR Master Mix (PCR Biosystems, UK), 0.5 µl forward primer (10 µM, 5'-GTCAGAACTAAGATATCCAGC-3' in this example which is specific for *F. nucleatum* subsp. *nucleatum*) and 0.5 µl reverse primer (10 µM, 5'-ATAAACTGAATAAGCAAGTC-3' in this example which is specific for *F. nucleatum* subsp. *nucleatum*). To generate a standard curve, *F. nucleatum* subsp. *nucleatum* DNA was adjusted to 1 ng/µl (based on Qubit DNA concentration measurements as described earlier) with nuclease-free water, with subsequent ten-fold dilutions to $1x10^{-5}$ ng/µl and used as template genomic DNA. The reactions were run on a Rotor-Gene Q cycler (Qiagen, UK) and the cycling parameters were as follows: initial incubation of 95 °C for 10 min, followed by 40 cycles of 95 °C for 10 s, 50 °C for 15 s and 75 °C for 20 s. Melt curve analysis was also completed by increasing the temperature in 1 °C increments from 72 °C to 95 °C. The cycle threshold (C_t) value for all qPCR reactions- defined by the cycle number at which the fluorescence signal of a sample becomes detectable above a threshold level- were generated on the Rotor-Gene Q Series Software 2.1.0. A standard curve was also generated by

plotting the known concentrations of DNA against its C_t value and using this, the DNA concentration of each DNA sample was determined.

2.7 Microbial community modelling set up

2.7.1 Mock community biofilm set up

Individual bacterial inocula (either at OD_{600} 1.0 or at a specified cell concentration) were created using liquid growth medium (provided in Appendix 8.2) to mimic gingival crevicular fluid. This growth medium comprised of either 0.01 mg/ml (0.001 % w/v) or 10 mg/ml (1 % w/v) bovine submaxillary gland mucin (BSM) (Sigma-Aldrich, USA), 30 % heat-inactivated human serum (Sigma-Aldrich, USA) and 50 % modified fluid universal medium (mFUM) (Gmür and Guggenheim, 1983). The bovine submaxillary mucin was either autoclaved or filter-sterilised using 45 µm filters. The human serum was not filtered because it was purchased already filter-sterilised, but it was inactivated by heating at 65 °C for 30 min. 1 ml of each individual inoculum of known concentration was combined to produce a mixed community inoculum. As shown in Figure 2.4, the hydroxyapatite-coated pegs attached to the lid of a Minimum Biofilm Eradication Concentration MBEC plate (previously known as a Calgary Biofilm Device (Innovotech, Canada) were suspended in in 200 µl of the mixed community inoculum and incubated at 37 °C under anaerobic conditions. For the mock community models iteration 2 and later, the pegs were first preconditioned overnight with 100 % heat-inactivated human serum. Throughout the duration of the biofilm experiment, the growth medium was replaced with fresh growth medium every 3.5 days. Pegs containing only the growth medium were also included which acted as negative controls.

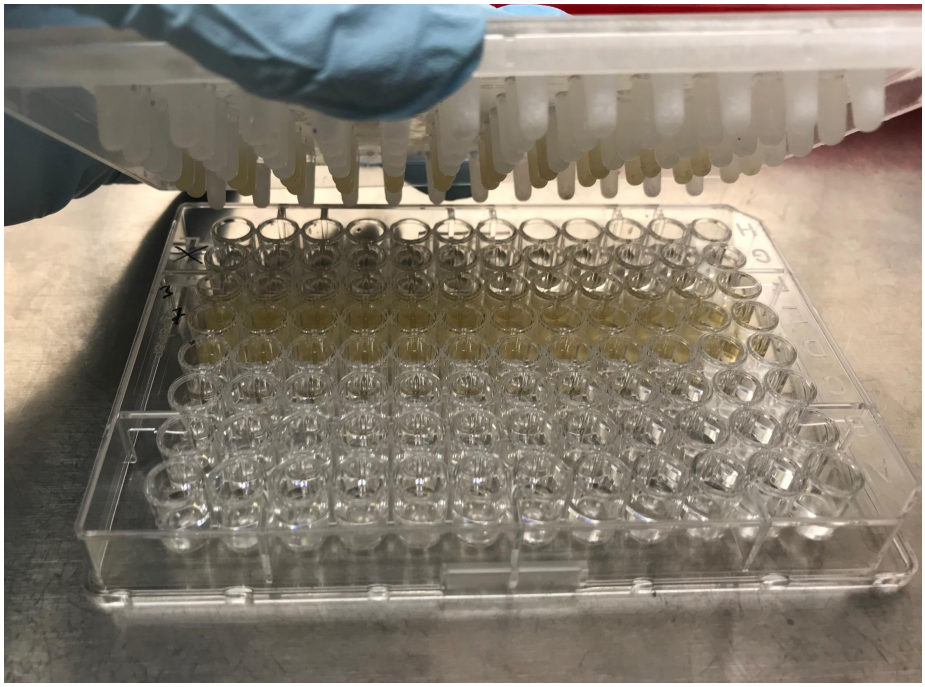

Figure 2.4 Use of MBEC plates in biofilm growth. Hydroxyapatite-coated pegs on a MBEC plate were suspended in 200 µl growth media containing either 0.001 % or 1 % mucin, 30 % heat-inactivated human serum and 50 % modified fluid universal medium (mFUM).

2.7.2 Periodontal plaque community biofilm set up

2.7.2.1 Saliva and subgingival plaque collection

Saliva and subgingival plaque samples were collected from periodontal patient volunteers who attended the Periodontology Clinic in the Charles Clifford Dental Hospital for use as inocula for the plaque community biofilm model. Ethical approval was given by the National Research Ethic Service Committee Yorkshire and Humberside (study number 18/WM/0068, IRAS Ref No: 240510, STF Ref No. STH20225). Criteria for volunteer recruitment were as follows:

Inclusion criteria:

- Healthy adult patients aged over 18 years
- Diagnosis of chronic periodontitis, which is characterised as a slowly progressive disease and may involve bone loss, pockets, abscesses and calculus (Armitage, 1999)

Exclusion criteria:

- Patients who do not have the capacity to consent for themselves

- Patients who received periodontal treatment and antibiotics during the previous 3 months
- Patients with diabetes, immunodeficiency, infectious diseases (such as HIV and hepatitis) or medication that may affect the periodontal condition including cyclosporine, calcium-channel blockers and anti-epileptic medications
- Non-English speaking participants who cannot provide consent themselves

Participants were asked to spit 1 ml of saliva into a sterile 30 ml universal tube. Subgingival plaque samples were scraped from the tooth surface with a fine periodontal curette and placed into sterile 2 ml Eppendorf tubes containing liquid growth medium comprising the complete modified fluid universal medium (mFUM) as previously described for the community modelling work. Samples were immediately stored at -80 °C until a later date when samples were pooled and used to inoculate a plaque biofilm community model.

2.7.2.2 Plaque biofilm set up

To prepare the plaque biofilm inoculum, subgingival plaque samples were pooled and centrifuged at 10,000 xg to obtain a cell pellet. The cell pellet was resuspended in mFUM growth medium. Preconditioned MBEC pegs were suspended in 200 µl of this plaque inoculum and incubated at 37 °C under anaerobic conditions. The plaque biofilm communities were grown for 21 days, and the growth medium was replaced with fresh growth medium every 3.5 days. Pegs containing only the growth medium were also included which acted as negative controls.

2.8 Biofilm community analyses

2.8.1 Harvesting the biofilms

Biofilm compositions for the initial set of mock biofilm communities were analysed 1, 3 and 7 days after biofilm incubation. The updated model iteration 2 communities were analysed at days 3, 7 and 14. The mock community model iterations 3 and later, as well as the plaque model were analysed at 14 and 21 days only.

On days of analysis, pegs on the MBEC plate were snapped off with sterile forceps, washed thrice in PBS and resuspended in 500 µl PBS. A hand-operated pestle motor mixer (VWR, USA) was used to carefully disrupt and harvest bacterial cells from the pegs for 2 min each.

2.8.2 Cultural analysis

Harvested cells from three replicate pegs were pooled, Gram-stained and plated onto Fastidious Anaerobe Agar supplemented with 5 % horse blood (neat, 1:10, 1:100, 1:1000 dilution) and incubated under anaerobic conditions at 37 °C for up to 12 days. Gram staining was performed on the colonies grown on the agar plates.

2.8.3 Scanning electron microscopy (SEM)

SEM analysis was performed on intact pegs by washing the pegs twice in PBS and fixing in 2.5 % glutaraldehyde in PBS buffer (Alfa Aesar, USA) for 1 h. After further washing with PBS, the samples were sequentially dehydrated in 35, 60, 80, 90 and 100 % ethanol for 15 min each. Samples were subsequently immersed in ethanol:hexamethyldisilazane (HMDS) solution for 1 h then twice in 100 % HMDS (Thermo Scientific, USA) for 5 min each before being air-dried for 1 h. After drying, the samples were mounted on aluminium stubs using adhesive carbon tabs and sputter-coated with gold (SC500, emscope) with a current of 15 mA for 2 min at 0.05 atm. The spatial organisation and structure of the biofilm communities were visualised using a scanning electron microscope (Philips/FEI XL30 ESEM) operating with an electron beam energy of 15.0 kV at various magnifications.

2.8.4 Extraction of biofilm community DNA

Harvested bacterial cells from three replicate MBEC pegs were pooled, centrifuged at 10,000 xg, the supernatant removed, and the cell pellet resuspended in 500 µl PBS. The harvested biofilm cells were then treated with PMA dye with a 10-min photo-exposure. DNA was then extracted using the QIAamp DNA Mini Kit (Qiagen, UK). Briefly, cells were initially pelleted by centrifugation at 10,000 xg and rehydrated in 300 µl PBS. This was performed twice. Bacterial cells were lysed by

37 °C incubation for 1 h with 90 µl lysozyme (10 mg/ml, prepared with Tris-EDTA buffer), 3.6 µl mutanolysin (25,000 U/ml in Tris-EDTA) and 1.8 µl lysostaphin (4000 U/ml in nuclease-free water). The cells were further incubated with 24 µl proteinase K, 4.8 µl RNAse A (100 mg/ml) and 300 µl kit Buffer AL at 56 °C for 30 min. After mixing and a brief centrifugation step, DNA was precipitated by adding 400 µl 100 % ethanol. Washing steps with kit Buffer AW1 and AW2 followed according to the kit manufacturer's guidelines, and DNA was finally eluted in 100 µl kit Buffer AE and stored at -20 °C until quantitative analysis.

2.8.5 qPCR Analysis on biofilm community DNA

The proportions of bacterial species among the total bacterial community DNA were determined by performing qPCR reactions and using the validated species-specific primers following the procedure mentioned previously. To measure the total bacterial community DNA, extracted DNA was measured by running qPCRs as described previously, but with universal 16S rRNA gene primers: forward primer 5'-CCATGAAGTCGGAATCGCTAG-3' and reverse primer 5'-GCTTGACGGGCGGTGT-3' at an annealing temperature 60 °C. A standard curve (range 10^{-1} to 10^{-6} ng/µl) for the total bacterial DNA concentration was generated by using DNA purified from a mixture of bacterial species.

2.8.6 16S rRNA gene community profiling using Illumina MiSeq

Following PMA treatment, the approximately 300 bp hypervariable regions V1-V2 of the 16S rRNA gene were PCR-amplified. This was performed using fusion primers comprising MiSeq adapter sequences (i5 and i7), an 8 nucleotide-long barcode sequencing to allow pooling of amplicons and following Illumina's recommendations: a 10 nucleotide-long primer pad sequence to raise the Tm of the primers to 60-65 °C and a 2 nucleotide-long linker sequence that is anti-complimentary to the first two bases of the 16S rRNA gene-specific sequence. 27FYM was used as the forward primer of the 16S rRNA gene-specific sequence (5'-AGAGTTTGATYMTGGCTCAG-3') and 338R-R was the reverse primer (5'-TGCTGCCTCCCGTAGRAGT-3'). A list of the barcoded fusion primers is available in Appendix 8.3. PCR reactions were performed in 25 µl final reaction volumes

comprising 12.5 µl 2X Thermo Scientific Phusion Green Hot Start II High-Fidelity PCR Master Mix (Thermo Fisher Scientific, USA), 9.5 µl nuclease-free water, 0.5 µl each of barcoded forward and reverse primers (10 µM each) and 2 µl template DNA. PCR amplification was performed under the conditions: initial denaturation at 98 °C for 3 min, followed by 25 cycles of denaturation at 98 °C for 10 s, annealing at 60 °C for 30 s and extension at 72 °C for 30 s. A final extension step of 72 °C for 5 min followed. PCR reactions for a negative no template control (NTC), a PMA-treated extraction negative control (reagents only), DNA extracted from a negative control peg (mFUM growth medium in place of mixed community inoculum during biofilm model set up) and a ZymoBIOMICS Microbial Community DNA Standard comprising defined proportions of genomic DNA from a mixed community of different bacteria and yeasts (Zymo Research, USA) were also performed as controls. Amplicons were then visualised under UV light on a 2 % agarose gel stained with ethidium bromide to check the amplicons were correctly sized at approximately 300 bp in length, and purified using Agencourt AMPure XP (Beckman Coulter, USA) at a ratio of 0.7 beads per 1 µl amplicon following manufacturer's instructions, with the purified PCR products resuspended in sterile PCR grade water. The size and quality of the amplicons were then assessed on an Agilent 2100 Bioanalyzer using the DNA 1000 kit at the Microarray and Next Generation Sequencing Facility at the University of Sheffield, and their DNA concentrations calculated on a Qubit™ 2 Fluorometer using a Qubit™ dsDNA HS Assay Kit (ThermoFisher, USA). Finally, the amplicons were pooled in equal concentrations and paired-end sequenced using the Illumina MiSeq Nano platform using a 500 cycle kit (2x250 bp) V2 chemistry. Sequencing was performed by the DNA Sequencing Facility at the Department of Biochemistry, University of Cambridge, UK.

2.8.7 16S rRNA gene community profiling using Nanopore

As an alternative to sequencing the V1-V2 hypervariable regions of the 16S rRNA gene on the Illumina MiSeq, the full ~1500 bp 16S rRNA gene was sequenced on either a MinION flow cell or a Flongle flow cell (Oxford Nanopore Technologies, UK). First, an amplicon library was prepared by amplification of PMA-treated DNA template using either the standard 27F/1492R primer set (27F: 5'-

AGAGTTTGATCCTGGCTCAG-3', 1492R: 5'-CGGTTACCTTGTTACGACTT-3') or using modified 27F-YM/1492R-D barcoded primers (27F-YM: 5'-AGAGTTTGATYMTGGCTCAG-5', 1492R-D: 5'- CGGDTACCTTGTTACGACTT-3'). The forward primer consisted of a unique barcode sequence attached to the primer sequence and the reverse primer also consisted of the same unique barcode sequence. A list of the barcoded primers is available in Appendix 8.4.

PCR reactions for amplifying mock community DNA were prepared in the same manner as previously described for preparing an amplicon library for Illumina MiSeq. This involved using the Thermo Scientific Phusion Green Hot Start II High-Fidelity PCR Master Mix (Thermo Fisher Scientific, USA). The alternative option LongAmp Taq 2X Master Mix (NEB, USA) was used to amplify plaque model DNA. PCR reactions performed on the plaque community DNA were run in 25 µl final reaction volumes comprising 12.5 µl LongAmp Taq 2X Master Mix, 5.5 µl nuclease-free water, 0.5 µl each of barcoded forward and reverse primers (10 µM each) and 6 µl template DNA. PCR amplification was performed under the conditions: initial denaturation at 95 °C for 1 min, followed by 25 cycles of denaturation at 95 °C for 20 s, annealing at 55 °C for 30 s and extension at 65 °C for 2 min. A final extension step of 72 °C for 5 min followed. Again, PCR reactions for a negative no template control (NTC), a PMA-treated extraction negative control (reagents only), DNA extracted from a negative control peg (mFUM growth medium in place of mixed community inoculum during biofilm model set up) and a ZymoBIOMICS Microbial Community DNA Standard comprising defined proportions of genomic DNA from a mixed community of different bacteria and yeasts (Zymo Research, USA) were also performed.

After PCR, the methodology for preparing amplicon libraries remained identical for both mock and plaque communities. The amplicons were checked by performing an agarose gel electrophoresis, cleaned by using Agencourt AMPure XP beads (Beckman Coulter, USA) at a ratio of 1.8 µl beads per 1 µl amplicon following manufacturer's instructions, quantitated on a Qubit™ 2 Fluorometer using a Qubit™ dsDNA HS Assay Kit (ThermoFisher, USA) and checked for amplicon sizing

and quality using the Agilent DNA 1000 Kit on an Agilent 2100 Bioanalyzer. This was performed at the Microarray and Next Generation Sequencing Facility at the University of Sheffield. The amplicons were then pooled together in equal concentrations equating to a final total of 50-100 fmol DNA when a Nanopore Flongle flow cell was later used. A total of 100-200 fmol amplicon DNA was pooled instead when a Nanopore MinION flow cell was later used. Next, the pooled DNA was end-repaired and end-prepared for adaptor ligation using the NEBNext Companion Module for Oxford Nanopore Technologies (New England Biolabs, USA) and cleaned up using the Agencourt AMPure XP beads according to the Nanopore Amplicons by Ligation Protocol (SQK-LSK109). MinION AMX adaptors were ligated using the Ligation Sequencing Kit (Oxford Nanopore Technologies, UK) and a further clean up step using the Agentcourt AMPure XP beads was performed prior to loading into either a Flongle flow cell or a MinION flow cell according to the manufacturer's instructions. MinION reads were basecalled in real-time using a MinIT device (Oxford Nanopore Technologies, UK), the FASTQ sequencing data acquired, and the barcode and adapter sequences trimmed and demultiplexed using Porechop (https://github.com/rrwick/Porechop/) and binned according to barcode sequence.

2.8.8 Microbiome sequence analysis

Fastq files were first checked for quality using the software FastQC v0.11.8 (https://www.bioinformatics.babraham.ac.uk/projects/fastqc/). Demultiplexed sequence reads obtained from Illumina MiSeq and Nanopore MinION were then both analysed using the mothur software suite v1.42.3 (https://mothur.org), following the MiSeq standard operating procedure as described by Kozich et al. (Schloss *et al.*, 2009; Kozich *et al.*, 2013). Fastq files were initially converted to fasta files and every fasta file was pooled to create a combined fasta file. For MiSeq sequence reads, sequences <300 bp and >350 bp in length were discarded, whereas for Nanopore sequence reads, sequences <1470 and >1540 bp were discarded. The remaining sequences were aligned to the SILVA 16S rRNA reference alignment (Quast *et al.*, 2012) and any base positions not aligned in the overlap region were removed. Sequences with homopolymers of >8 bases in length were

also discarded, as were duplicate sequences. The VSEARCH algorithm (Rognes *et al.*, 2016) was then used to identify chimeric sequences, which were consequently removed from the dataset. MiSeq sequences were further denoised by clustering sequences that had ≤3 base differences together, whereas Nanopore sequences were clustered for those with ≤15 differences. This allowed for 1 base difference per 100 bp of sequence. After denoising, the sequences were classified using a Naïve Bayesian classifier (Wang *et al.*, 2007) with the Human Oral Microbiome Database (HOMD) 16S rRNA reference dataset v.15.1 (Chen *et al.*, 2010). Relative abundance plots were visualised using the package ggplot2 in R studio v3.3.1 (http://www.rstudio.com/). The α-diversity of the communities was calculated using the Simpson's diversity index (Simpson, 1949) and the β-diversity was measured using the Jaccard index to calculate distance matrices (Jaccard, 1900), which were then visualised in principal coordinates analysis (PCoA) plots using the online tool MicrobiomeAnalyst (Dhariwal *et al.*, 2017).

2.9 Detection of sialidase activity

2.9.1 4-Methylumbelliferyl N-acetyl-a-D-neuraminic acid (MUNANA) assay for detecting bacterial sialidase activity

Sialidase activity was quantified using MUNANA assays by observing the cleavage of the substrate 4-Methylumbelliferyl N-acetyl-a-D-neuraminic acid (MUNANA) to produce Neu5Ac and the fluorochrome 4-Methylumbelliferone (4-MU) (Potier *et al.*, 1979). MUNANA assays were performed for each of the 18 bacteria present in the mock community model. Bacterial colonies were suspended in 1 ml PBS pH 7.4 at a final optical density OD_{600} = 0.5 and standard curves for 4-MU were created by 1:1 serial dilutions of 1 mM 4-MU (final concentrations 4-MU at 0.0014-0.0909 mM). In total reaction volumes of 110 µl in black flat-bottomed 96 well polystyrene plates (Greiner, UK), the following were then added: 10 µl 4-MU or bacterial suspension; 90 µl PBS and 10 µl 2mM MUNANA. A blank control was also included, and the reactions were incubated at 37 °C for 4 h. Reactions were then quenched by the addition of 50 µl 100 mM Na_2CO_3 buffer pH 10.5 and the fluorescence measured at excitation 355 nm and emission at 430 nm using a Tecan Infinite M200 microplate reader. Concentrations of 4-MU were then extrapolated using the 4-

MU standard curve.

2.9.2 Detection and inhibition of sialidase activity in biofilm whole cell and supernatant

Sialidase activity was quantified following the protocol described previously using the MUNANA assay, with the exception of resuspending the frozen biofilm whole cell pellets at an optical density OD_{600} = 0.5. In place of whole cell samples, supernatant (i.e. "spent" growth medium from biofilm models) collected were diluted 1 in 10 prior to use.

The sialidase inhibitors zanamivir (GlaxoSmithKline UK), oseltamivir (Carbosynth, UK), siastatin B (Carbosynth, UK) and N-Acetyl-2-3-dehydro-2-deoxyneuraminic acid DANA (Carbosynth, UK) at 10 mM were serially diluted 1:2 into reaction mixtures and tested in the MUNANA assays at final inhibitor concentrations of 0-0.909 mM. MUNANA reactions were stopped and read 4 h after incubation. Sialidase activity of the samples in reactions where an inhibitor was present was expressed as the percentage change in fluorescence, when compared to fluorescence in reactions where inhibitors were absent. This is denoted by the formula:

Change in fluorescence (%) = $\frac{fluorescence\ at\ 0.0005\ to\ 0.909\ mM\ inhibitor}{fluorescence\ at\ 0\ mM\ inhibitor}$

2.9.3 Disk diffusion assays using sialidase inhibitors

As DANA and oseltamivir were selected as the most effective sialidase inhibitors of those tested from IC_{50} estimates, these inhibitors were tested for their direct antimicrobial activity using disk diffusion assays. Suspensions at OD_{600} = 0.1 for *S. oralis* and *F. nucleatum* subsp. *nucleatum* and OD_{600} = 0.5 for *T. forsythia* were created and 100 µl spread onto Fastidious Anaerobe Blood agar plates. The optical density of these suspensions was selected for these three bacteria to ensure growth on the plates were not sparse yet also not overgrown, thus allowing any antimicrobial effect to still be observed. Blank diffusion plates impregnated with 20 µl of either 100 µM oseltamivir, 250 µM DANA, 100 µM oseltamivir + 250 µM DANA and placed onto the agar plates. Acting as an experimental negative control,

a blank disk containing 20 µl PBS was also included, as was a penicillin disk (Oxoid, UK) for the Gram-positive bacterium *S. oralis* and a metronidazole disk (Oxoid, UK) for the Gram-negative bacteria *F. nucleatum* subsp. *nucleatum* and *T. forsythia*. These antimicrobial disks acted as experimental positive controls as penicillin is highly active against *S. oralis* and metronidazole is highly active against Gram-negative anaerobic bacteria. The agar plates were incubated at 37 °C under anaerobic conditions until colonies and any zones of inhibition were observed on the plates.

2.9.4 Addition of sialidase inhibitors to the mock and plaque communities

Final concentrations of 250 µM DANA and 100 µM oseltamivir were added to mFUM growth medium from the day of biofilm set up. This was conducted in parallel to control biofilm communities grown in mFUM growth medium absent of DANA and oseltamivir. As described previously, growth medium (with and without the sialidase inhibitors as appropriate) was replaced with fresh equivalent every 3.5 days. Biofilm communities were grown for 21 days, with the communities harvested and analysed at days 14 and 21.

2.10 NanH and NanS protein purification

2.10.1 Protein synthesis

E. coli BL21 Origami strains expressing genes for either NanS or NanH were plated onto LB agar supplemented with 50 µg/ml ampicillin and incubated aerobically at 37 °C overnight. For each *E. coli* strain, 5-6 colonies were selected from the overnight culture and inoculated into 500 ml 2XYT broth supplemented with 50 µg/ml ampicillin. This was incubated at 25 °C, shaking at 150 rpm for ~5 h until OD_{600} = 0.6-0.8 was reached to indicate mid log phase. Protein synthesis was induced by further overnight incubation, but with the addition of a final concentration of 0.2 mM IPTG. Centrifugation at 10,000 xg followed to pellet *E. coli*, which was then resuspended in 50 mM sodium phosphate buffer with 500 mM NaCl (pH 7.4) and centrifuged again at 10,000 xg. The cell pellet was frozen at -20 °C until purification.

2.10.2 Sodium dodecyl sulphate-polyacrylamide gel electrophoresis (SDS-PAGE)

Two 1 mm-depth 12 % SDS-PAGE gels were prepared by pouring resolving gel (comprising of the following: 3 ml acrylamide; 2.5 ml lower tris pH 8.8 (18.17 g Tris Base, 0.4 g SDS in 100 ml distilled water); 4.3 ml distilled water; 5 µl TEMED; 350 µl 10 % ammonium persulphate) into BioRad-supplied glass plates and gel casting stations, leaving 1 cm room for stacking gel. Isopropanol was added above the resolving gel to level gel and prevent air bubbles. Once the resolving gel was set, the isopropanol was washed off with water and stacking gel (comprising of the following: 0.975 ml acrylamide; 2.1 ml upper tris pH 6.8 (6.06 g Tris Base, 0.4 g SDS in 100 ml distilled water); 17 µl TEMED; 100 µl 10 % ammonium persulphate) was then poured atop the resolving gel and a comb was placed to form wells. Set gels were then placed in an SDS-PAGE tank (mini PROTEAN Tetra System) and the tank filled with running buffer (comprising of the following: 12 g tris base; 4 g SDS; 57.5 g glycine dissolved in 1 L distilled water as stock, and 160 ml stock added to 840 ml distilled water prior to use).

Cell pellets of uninduced and induced sialidase gene expression (1 ml each) were boiled at 95 °C with SDS lysis buffer (comprising of the following: 40 ml 100 mM Tris-HCl; 10 ml glycerol; 1 g SDS; 0.1 g bromophenol blue; 200 mM DTT) for 10 min and ran on a 12 % SDS-PAGE gel at 150 V for 1 h, alongside a molecular weight marker (either using the EZ-run Prestained Protein Marker or the Prime-Step™ Prestained Broad Range Protein Ladder). The gel was then stained with InstantBlue™ (Expedeon) for 10 min at room temperature with agitation and washed twice with deionised water before visualisation under light.

2.10.3 NanH purification

Previously frozen induced cell pellet was resuspended in a purification buffer (50 mM sodium phosphate buffer plus 500 mM NaCl, pH 7.4) containing 10 µg/ml DNAse and one complete EDTA-free protease cocktail inhibitor tablet (Roche, Switzerland). Cells were lysed by French pressure cell press twice at 1000 psi and the lysate centrifuged at 10,000 xg for 30 min at 4 °C. The C-terminal histidine-tagged NanH protein of the cell-free lysate was purified by its binding to nickel-

nitrilotriacetic acid (Ni-NTA) agarose resin in an affinity column at a flow rate of 1 ml min^{-1}, whereby unbound proteins were removed in the flow-through and then by washing with 30-40 ml wash buffer (50 mM sodium phosphate buffer + 500 mM NaCl + 5 mM imidazole) also at a flow rate of 1 ml min^{-1}. As imidazole competitively binds to Ni, the addition of imidazole minimises the binding of non hist-tagged contaminating proteins to increase purity. After wash, the his-tagged protein was eluted from the column over 10 x 1 ml fractions using an elution buffer comprising 50 mM sodium phosphate buffer containing 500 mM NaCl and 300 mM imidazole (pH 7.4). Cell lysate, flow-through, wash and the initial 6 elution fractions were tested on a 12 % SDS-PAGE gel for the presence of pure NanH protein over-production. Eluted fractions containing pure proteins of expected molecular weight of ~60 kDa were pooled into a dialysis tubing with membrane pore molecular weight cut-off of 12-14 kDa (Medicell Membranes, UK), and dialysed overnight on a stirrer against a dialysis buffer (50 mM sodium phosphate plus 150 mM NaCl, pH 7.4). Dialysed, pure NanH proteins were stored at 4 °C until the protein concentration was determined by performing either a Pierce bicinchroninic (BCA) assay or by using a Qubit™ Protein Assay kit (ThermoFisher, USA) and measured on a Qubit™ 2 Fluorometer (Invitrogen, USA) following the manufacturer's guidelines.

2.10.4 Quantitation of protein concentration using Pierce bicinchroninic (BCA) assay

Pierce bicinchroninic (BCA) assay kit (ThermoFisher Scientific) was used to quantitate protein concentration, according to the manufacturer's instructions. Briefly, proteins were diluted 1:5, 1:10, 1:100 in 50 mM sodium phosphate buffer with 150 mM NaCl (pH 7.4). 10 µl of each were added into reaction wells containing 200 µl kit working solution, and incubated for 30 min at 37 °C, shaken at 150 rpm. Absorbance at 562 nm was measured and an albumin (BSA) standard curve was also generated (0-2000 µg/ml). Protein concentrations were extrapolated using the bovine serum albumin (BSA) standard curve.

2.10.5 Testing NanH enzyme activity

NanH activity was confirmed by using the 4-Methylumbelliferyl N-acetyl-a-D-neuraminic acid (MUNANA) assay as previously described, but with some

modifications. Briefly, 10 µl 50 nM NanH stock (intact and denatured) was incubated at room temperature with final concentrations of 0.1 mM MUNANA in 50 mM sodium-phosphate buffer plus 200 mM NaCl. Denaturation of NanH was completed by incubating NanH at 95 °C for 30 min. A standard curve with the final concentrations of 0-0.2 mM for the fluorochrome 4-Methylumbelliferone (4-MU) was also generated. Reactions were quenched after 2 min by the addition of 75 µl 100 mM Na_2CO_3 buffer pH 10.5 and the fluorescence measured at excitation 355 nm and emission at 430 nm using a Tecan Infinite M200 microplate reader. Concentrations of 4-MU were then extrapolated using the 4-MU standard curve.

2.10.6 GST-free NanS purification

Cell-free lysate of *E. coli* cell pellet post NanS synthesis was generated as previously described for NanH purification. The *N*-terminally glutathione-S-transferase (GST)-tagged protein of the cell-free lysate was purified by its binding to glutathione agarose resin in an affinity column at a flow rate of 1 ml min^{-1}, whereby unbound proteins were removed in the flow-through and then by washing with 30-40 ml purification buffer (50 mM sodium phosphate buffer plus 500 mM NaCl, pH 8) also at a flow rate of 1 ml min^{-1}. GST-tagged protein was eluted from the column over 10 x 1 ml fractions using an elution buffer comprising 50 mM reduced L-glutathione (Thermo Fisher Scientific, USA) dissolved in 50 mM sodium phosphate buffer plus 500 mM NaCl, pH 8. Cell lysate, flow-through, wash and the initial 5 elution fractions were tested on a 12 % SDS-PAGE gel for the presence of pure GST-tagged NanS protein over-production. Eluted fractions containing pure protein were expected to have a molecular weight of ~110 kDa. The GST-tag of NanS proteins were proteolytically removed from the eluted fractions by incubating the proteins with 1 unit/µl thrombin (Sigma Aldrich, USA) in the purification buffer, sealed and kept at room temperature for 5 h with mixing. After cleavage of GST tags from NanS, 50 µl p-aminobenzamidine-agarose (Sigma Aldrich, USA) pre-equilibrated with purification buffer was added to remove thrombin and incubated at 4 °C for 3 h with mixing prior elution. Eluted GST-free NanS proteins were stored at 4 °C until the concentration of protein was quantitated by performing either a Pierce bicinchroninic (BCA) assay or a Qubit™ Protein Assay as described earlier.

2.10.7 Testing NanS enzyme activity

NanS activity was confirmed by incubating intact and heat-denatured NanS enzyme (neat and 50 nM) at room temperature with final concentrations of the substrate 0.1 mM p-nitrophenyl acetate (pNP-Ac) in 50 mM sodium phosphate buffer plus 200 mM NaCl. Free p-nitrophenol (pNP) was released from pNP-Ac after substrate hydrolysis upon enzyme binding and the appearance of the colour yellow was observed in the reactions with neat intact proteins after 1 min. The release of pNP was recorded by measuring its absorbance (A_{405}) in a spectrophotometer (Tildon and Ogilvie, 1972) and compared against a pNP standard curve.

2.11 Deglycosylation of bovine submaxillary mucin (BSM) and human serum

2.11.1 Testing deglycosylation methodologies

To deglycosylate BSM, 10 mg/ml (20 µM or 1 % w/v) mucin was incubated at 37 °C overnight with varying final concentrations of NanH, NanS, or NanH and NanS combined in PBS, pH 7.4 (Sigma Aldrich). The concentrations of the enzymes tested were at 0.1 µM- 2 µM in total reaction volumes of 50 µl. 30 % human serum was also incubated at 37 °overnight with either 2 µM NanH, 2 µM NanS, or 2 µM NanH + 2 µM NanS. As an alternative method of deglycosylating mucin to using enzymes, 10 mg/ml mucin was also co-incubated with 1 M H_2SO_4 at 80 °C for 50 min, 4 h and overnight.

2.11.2 Thiobarbituric acid (TBA) assay to measure sialic acid release

A thiobarbituric acid (TBA) assay (Romero *et al.*, 1997) was conducted to measure the release of free sialic acids from these reactions. Here, 25 µl of 20 mM sodium periodate (Sigma Aldrich) in 60 mM H_2SO_4 were added to the reactions. This was incubated for 30 min at 37 °C to oxidise free sialic acids. Oxidation was then halted by the addition of 20 µl 2% (w/v) sodium arsenite (Sigma Aldrich) in 500 mM HCl. Red chromophore formation was enhanced by the addition of 100 µl of 100 mM TBA (Sigma Aldrich), pH 9, and incubation at 95 °C for 7.5 min. 100 µl of the reaction was then added to a clear 96-well plate (Greiner) and the absorbance at 549 nm was measured using a Tecan infinite M200 plate reader. Free sialic acid

(Carbosynth, UK) was used to generate a standard curve of 0-1250 µM.

2.11.3 Visualisation of deglycosylation using NU-PAGE™ 4-12 % Bis-Tris SDS-PAGE gels

Precast NU-PAGE™ 4-12 % Bis-Tris Gels (Thermo Fisher Scientific, USA) were used to analyse the structures of glycosylated and deglycosylated bovine submaxillary mucin and human serum. The gel was placed into a XCell SureLock Mini-Cell tank (Thermo Fisher Scientific, USA) filled with NU-PAGE™ 1x MOPS SDS Running buffer (Thermo Fisher Scientific, USA), and run at 100 V for 2 h to allow proteins to run slower and increase protein separation. The gel was then stained with InstantBlue™ (Expedeon) for 10 min at room temperature with agitation and washed twice with deionised water before visualisation under light. As an alternative to staining the gel with InstantBlue™, the gel was also stained using the Pro-Q Emerald 300 Glycoprotein Stain Kit (ThermoFisher, USA) to visualise only the glycoproteins. This was performed according to the manufacturer's instructions.

2.11.4 Removal of sialidase enzymes after deglycosylation

Following mucin and serum deglycosylation, they were put into 20 ml Vivaspin® ultrafiltration spin columns (Sartorius, Germany) which were fitted with 3000 molecular weight cut-off (MWCO) filters and centrifuged at 6000 xg until no more flow-through passed through the columns. The flow-through obtained from these columns was removed and stored at -20 °C. To replace the removed flow-through here, flow-through obtained from centrifuging glycosylated mucin and serum (without the presence of sialidase enzymes) were put back into the spin columns to replace the removed flow-through. The columns were centrifuged again at 6000 xg and the process was conducted a total of three times. Following this, the deglycosylated mucin and serum with as much of the sialidase enzymes removed were heated at 65 °C for 30 min to inactivate the enzymes. The reagents were then stored at -20 °C until ready for use in the biofilm growth medium.

Chapter 3 – Laying the foundation for biofilm experiments

3.1 Introduction

Most microorganisms that have been characterised in the oral microbiome belong to the *Bacteria* domain and up to approximately 300 oral bacterial species are present in a person's mouth at any one time (Griffen *et al.*, 2012). As of May 2022, 1009 16S rRNA gene reference sequences exist in the expanded Human Oral Microbiome Database (version 3) (Escapa *et al.*, 2018). The housekeeping 16S rRNA gene is frequently used in classifying bacteria as it is crucial in bacterial cell function and thus, it is highly conserved in all bacteria (Eisenberg and Levanon, 2013). By using the curated, oral-focused 16S rRNA gene eHOMD database (Chen *et al.*, 2010) in conjunction with 16S rRNA gene sequencing, researchers can analyse oral bacterial communities to high resolution. Even strain-level resolution has been achieved with the use of novel computational tools such as Minimum Entropy Decomposition (MED) (Eren *et al.*, 2015). MED is a user-independent tool that clusters sequences into defined high-resolution groups since sequence errors typically occur randomly along the sequence whereas phylogenetically important differences occur at specific points of the sequence.

To enable bacterial classification to species- and strain-level, metagenomics has been used to replace 16S rRNA gene community profiling, as it captures all of the DNA within a sample instead of only the 16S rRNA marker gene. A further advantage of metagenomics is the functional genes within a mixed microbial community sample can be investigated so that species-to-species interactions can be explored. However, as recently reviewed by Wade and Prosdocimi (2020), 16S rRNA gene community profiling is still considered a valuable method for characterising bacteria as well as being more cost-effective. The choice of laboratory procedures, bioinformatics pipeline and primer sets were reported to influence the results obtained from 16S rRNA gene community profiling (Rausch *et al.*, 2019). For example in this study, the choice of V3-V4 hypervariable region of the 16S rRNA gene over the V1-V2 region was shown to be the preferred primer set in profiling a commercially available non-oral bacterial and yeast DNA mixture from ZymoBIOMICS™. As compared to amplifying the V1-V2 region, the V3-V4 region demonstrated the closest matches between the observed and expected relative

abundances of taxa present in the ZymoBIOMICS™ DNA standard mixture. In contrast, the V1-V2 region is known to best discriminate between *Streptococcus* species, making this region a better choice for classifying sequences obtained from the oral microbiome, as *Streptococcus* is one of the most common genera in the mouth (Wade and Prosdocimi, 2020). These findings therefore highlight the importance in first reviewing and optimising the methodology for analysing mixed microbial communities and was therefore a focus in this chapter.

3.1.1 Aims

As mentioned in Chapter 1, a primary aim of this PhD project was to construct a novel *in vitro* mock biofilm community model to better represent the periodontal dysbiotic bacterial community than the previously reported models. This chapter focuses on optimising the methodology for developing and analysing a mock biofilm model.

3.2 Results

3.2.1 Selection of bacterial species from literature review

An initial literature search was completed to determine which oral bacteria are relevant to periodontitis development. A total of 73 studies were reviewed as well as a further 58 studies, which were focused on oral bacterial community modelling. From these publications, 18 bacterial species were deemed most relevant to representing the microbiota relating to periodontal disease. Table 3.1 presents a summary of the species selected for inclusion in the mock biofilm community model in this study, their inclusion in previous models as well as their association with periodontitis in the literature. As the oral microbiota is known to be complex, this study's approach to inoculating biofilm community models with a more complex composition of 18 bacterial species should better mimic the community found in periodontal subgingival plaque than many published models that often included 10 or fewer species. Of the bacterial taxa chosen, commensal bacteria acting as pioneer species from genera such as *Streptococcus, Actinomyces* and *Neisseria* were included. Bacteria which were described within the orange microbial complex (Socransky *et al.*, 1998) were also incorporated into the mock

community model: *P. intermedia; P. nigrescens; P. micra* (formerly known as *P. micros*); *F. nucleatum* spp.; *C. rectus.* and *C. showae*. Although more bacteria have been described by Socransky with associations to periodontal disease, only a selection of species from these were included in this study because of the already laborious work involved with maintaining cultures for 18 bacterial strains. Finally, the three red-complex pathobionts *Porphyromonas gingivalis, Tannerella forsythia* and *Treponema denticola* were also included in the mock community model. Two strains of *T. forsythia* were included in the model as the reference strain ATCC 43037 contains pseudaminic acid on its surface glycan chains, whereas the clinical isolate UB4 contains legionaminic acid. The strain numbers of all 18 bacteria used in this study were described in Chapter 2 (Table 2.1).

Table 3.1 Relevant oral bacterial species determined from literature and their inclusion in previous biofilm models. Summary of bacterial taxa selected for inclusion in the mock biofilm community model which were determined from previous biofilm models and their association with periodontitis in key literature. 'N/A' denotes the bacterial species has not been included in previous biofilm models.

Bacterial species	Inclusion in previous biofilm models	Likely role in oral microbiota from key literature
Actinomyces oris	Guggenheim *et al.*, 2001; Peyyala *et al.*, 2011; Sánchez *et al.*, 2011; Ammann *et al.*, 2012; Soares *et al.*, 2015; Thurnheer and Belibasakis, 2016; Bloch *et al.*, 2017; Kommerein *et al.*, 2017	Pioneer species (Cisar *et al.*, 1984)
Campylobacter rectus	Ammann *et al.*, 2012; Soares *et al.*, 2015; Thurnheer *et al.*, 2016; Bloch *et al.*, 2017	Periodontitis-associated (von Troil-Lindén *et al.*, 1995)
Campylobacter showae	Soares *et al.*, 2015	Periodontitis-associated (Socransky *et al.*, 1982)
Dialister invisus	N/A	Periodontitis-associated (Kistler *et al.*, 2013)
Filifactor alocis	N/A	Periodontitis-associated (Kumar *et al.*, 2005; Griffen *et al.*, 2012; Kistler *et al.*, 2013)
Fusobacterium nucleatum subsp. *nucleatum* and subsp. *polymorphum*	Bradshaw *et al.*, 1990; Kinniment *et al.*, 1996; Guggenheim *et al.*, 2001; Peyyala *et al.*, 2011; Sánchez *et al.*, 2011; Ammann *et al.*, 2012; Millhouse *et al.*, 2014; Park *et al.*, 2014; Soares *et al.*, 2015; Thurnheer *et al.*, 2016; Bloch *et al.*, 2017	'Bridging' organism between early and late oral colonisers (Socransky *et al.*, 1982; Moore *et al.*, 1983; Kistler *et al.*, 2013)
Neisseria subflava	Bradshaw *et al.*, 1990; Kinniment *et al.*, 1996	Pioneer species (Liu *et al.*, 2015)
Parvimonas micra	Soares *et al.*, 2015	Periodontitis-associated (Socransky *et al.*, 1982; von Troil-Lindén *et al.*, 1995; Kistler *et al.*, 2013)

Porphyromonas gingivalis	Kinniment *et al.*, 1996; Peyyala *et al.*, 2011; Sánchez *et al.*, 2011; Ammann *et al.*, 2012; Millhouse *et al.*, 2014; Park *et al.*, 2014; Soares *et al.*, 2015; Thurnheer *et al.*, 2016; Bloch *et al.*, 2017; Kommerein *et al.*, 2017	Periodontitis-associated (Socransky *et al.*, 1998; Hajishengallis, 2011; Griffen *et al.*, 2012; Kistler *et al.*, 2013)
Prevotella intermedia	Ammann *et al.*, 2012; Soares *et al.*, 2015; Thurnheer *et al.*, 2016; Bloch *et al.*, 2017	Periodontitis-associated (Socransky *et al.*, 1982; von Troil-Lindén *et al.*, 1995; Griffen *et al.*, 2012)
Prevotella nigrescens	Soares *et al.*, 2015	Periodontitis-associated (Socransky *et al.*, 1982)
Streptococcus gordonii	Kinniment *et al.*, 1996; Peyyala *et al.*, 2011; Park *et al.*, 2014	Pioneer species (Nyvad and Fejerskov, 1987)
Streptococcus oralis	Kinniment *et al.*, 1996; Guggenheim *et al.*, 2001; Sánchez *et al.*, 2011; Thurnheer *et al.*, 2016; Bloch *et al.*, 2017; Kommerein *et al.*, 2017	Pioneer species (Nyvad and Fejerskov, 1987)
Tannerella forsythia ATCC 43037	Ammann *et al.*, 2012; Soares *et al.*, 2015; Thurnheer *et al.*, 2016; Bloch *et al.*, 2017	Periodontitis-associated (Socransky *et al.*, 1998; Kistler *et al.*, 2013)
Tannerella forsythia UB4	Bloch *et al.*, 2017	
Treponema denticola	Ammann *et al.*, 2012; Thurnheer *et al.*, 2016; Bloch *et al.*, 2017	Periodontitis-associated (Socransky *et al.*, 1998; Griffen *et al.*, 2012)
Veillonella dispar	Bradshaw *et al.*, 1990; Kinniment *et al.*, 1996; Guggenheim *et al.*, 2001; Ammann *et al.*, 2012; Thurnheer *et al.*, 2016; Bloch *et al.*, 2017; Kommerein *et al.*, 2017	Early coloniser (Periasamy and Kolenbrander, 2010)

3.2.2 Design and validation of species-specific PCR primers

3.2.2.1 Primer search, design and specificity testing

Quantitative PCR assays can be used to quantitatively measure bacterial DNA concentrations in a community. A universal primer set amplifying a constant region of the 16S rRNA gene can be used to measure the DNA concentration of the total bacterial community. When species-specific (or strain-specific) PCR primers are used, the DNA concentration of only certain bacterial species or strains will be measured. It is therefore a technique that not only allows for the detection of bacteria, but also measures their abundance within a mixed community. In total, 18 primer sets were required at this stage of the project and these were tested for specificity in separate PCR reactions.

Wherever available in the literature, PCR oligonucleotide primer sequences specific for the 18 selected bacteria with an optimum product size 90-100 bp were chosen and ordered from Sigma-Aldrich, USA. This was because previous data have suggested SYBR green assays work optimally within this range of product size, as <80 bp can hinder differentiation between different sequences, produce primer-dimers and result in later cycle threshold readings due to its short length (Bustin and Huggett, 2017).

For the remaining bacteria requiring primer sequence design, the 16S rRNA gene sequence of the target species was aligned with sequences belonging to the same genus using BioEdit Sequence Alignment Editor (v7.2.5) (Hall, 1999). Sequences were downloaded from the Genbank nucleotide sequence database (Benson *et al.*, 2013). The alignment for a selection of streptococcal species to *S. gordonii* is shown as an example in Figure 3.1, where base conservation is viewed as dots and regions of high variability are highlighted in yellow. The 16S rRNA gene (Figure 3.1A) lacked any regions of yellow because its sequence is too highly conserved amongst the *Streptococcus* genus. The peptidoglycan biosynthesis gene D-alanine D-alanine ligase (*ddl*) in contrast contained regions of high variability (Figure 3.1B) and was thus chosen in place of the 16S rRNA gene for streptococcal species. From multiple sequence alignments for other genera, only 8 of the 18 bacterial strains had 16S

rRNA gene sequences that were sufficiently diverse to discriminate between bacterial species in a given genus. Alternative genes were also sought for the genera *Campylobacter* (*cpn60*), *Fusobacterium* (zinc protease gene), *Neisseria* (*rpoB*) and *Prevotella* (*rpoB*). To differentiate between the two *T. forsythia* strains, glycosylation genes coding for the synthesis of the terminal sugars found on the cell surface glycan. The gene *pseC* was used to detect pseudaminic acid found in the ATCC 43037 strain, whereas the gene *legC* was used to detect legionaminic acid in the UB4 clinical strain (Friedrich *et al.*, 2017), a strategy that made use of knowledge of the s-layer glycosylation biosynthetic gene clusters in this organism.

A) Alignment of 16S rRNA gene for selected streptococcal species

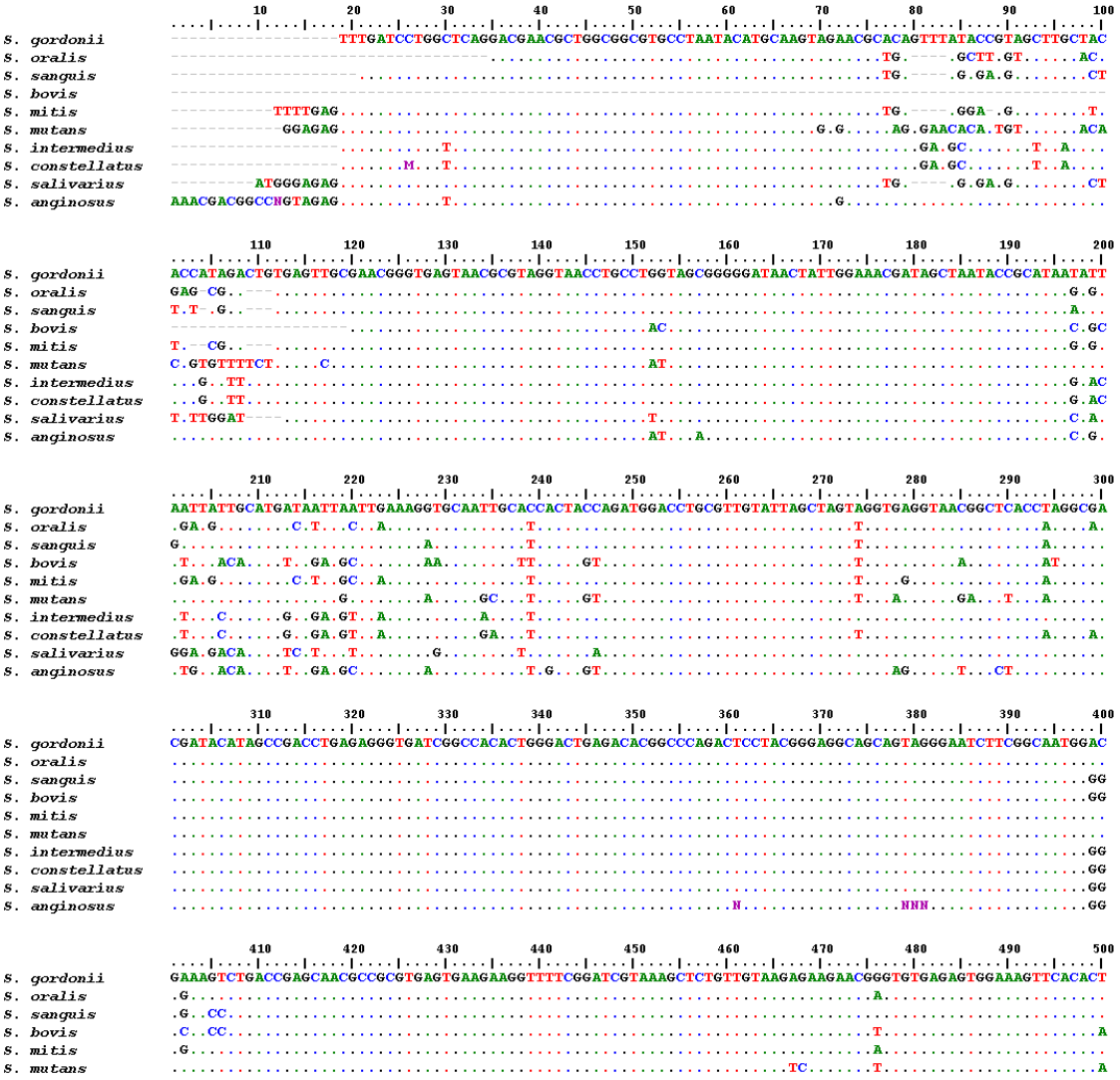

B) Alignment of *ddl* gene for selected streptococcal species

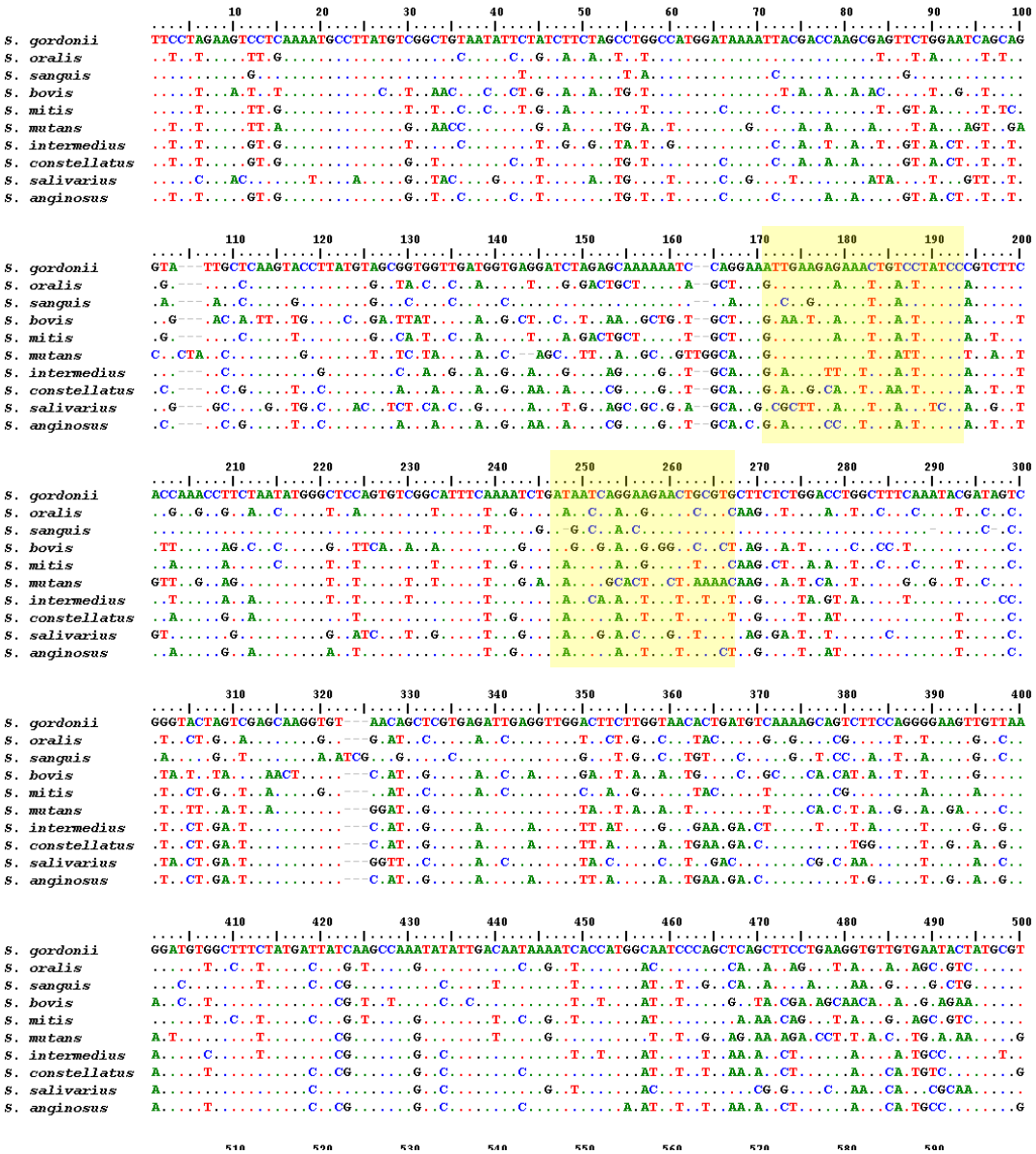

Figure 3.1 Alignments of both the (A) 16S rRNA and (B) ddl gene for some species within Streptococcus. In (A), the 16S rRNA gene was too highly conserved to be effective as primers to differentiate the selection of streptococcal species shown. Conversely in the ddl gene (B), regions of high sequence variability across species are highlighted in yellow and therefore used for designing the forward and reverse primers for S. gordonii. Sequences were aligned to S. gordonii using BioEdit Sequence Alignment Editor (v7.2.5) and conserved bases were plotted as dots whereas bases were written at positions which varied from S. gordonii. Regions of high base variability is highlighted in yellow.

Regions demonstrating high sequence variability were used to design potential primers using the PrimerQuest Tool (idtdna.com) and ordered from Sigma-Aldrich, USA. Each primer set was subsequently tested for specificity against DNA templates generated from all the other bacterial species in the model, in multiple end-point PCR reactions. The absence of non-specific bands on the agarose gel was suggestive that amplification specific to the intended bacterium successfully took place. In another words, bands only appeared for the specific species and were absent for all others. The optimum annealing temperature were also sought. Initial attempts at validating PCR primer sets also involved testing those reported in the literature. However, PCR oligonucleotide primers for *A. oris, C. rectus*, *D. invisus, F. alocis, F. nucleatum*, *P. micra, S. gordonii*, *S. oralis* and *V. dispar* were re-designed as their primers were shown to not be species-specific. This is demonstrated in the example of *V. dispar* in Figure 3.2 (highlighted with *), where a *V. dispar*-specific primer set was originally selected from a study by Ammann *et al.* (2012) but it needed re-design due to amplification taking place in PCR reactions where no *V. dispar* DNA was present (Figure 3.2A). Reactions using the redesigned *V. dispar* primers on the other hand produced amplification only where *V. dispar* was present (Figure 3.2B). The product size here was correct at 99 bp long.

A) Original *V. dispar* primers

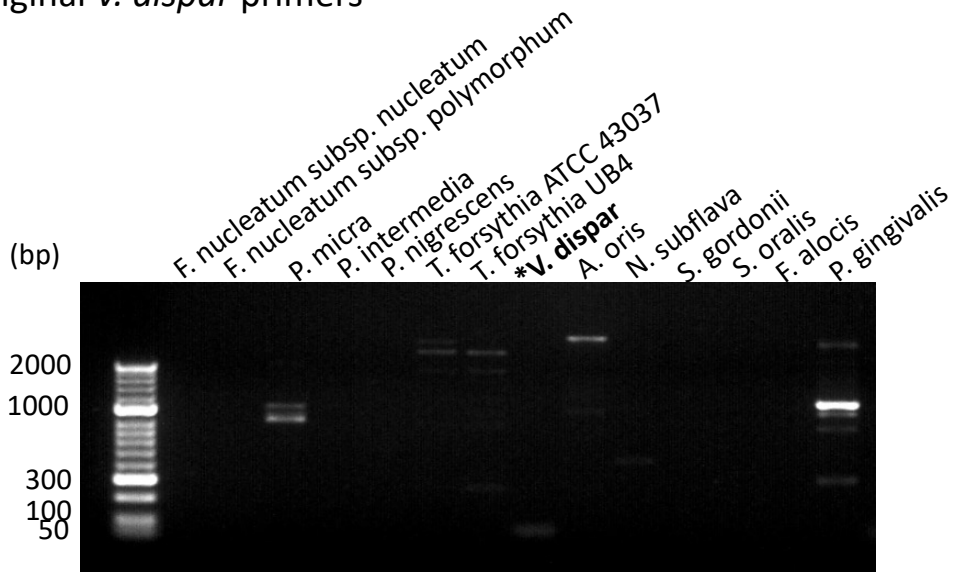

B) Redesigned *V. dispar* primers

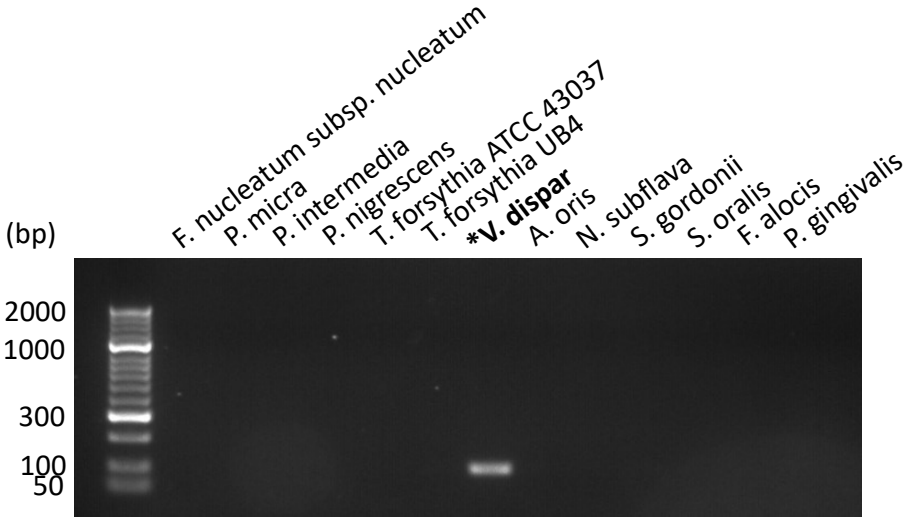

Figure 3.2 Agarose electrophoresis gel of PCR products for primer validation. An agarose electrophoresis gel of PCR products using DNA from species shown using A) initial primer set for *V. dispar obtained from study by Ammann et al. (2012) and B) redesigned PCR oligonucleotide primers specific only for *V. dispar DNA and at the correct molecular size of approximately 99 bp. There is also an absent of product in the no DNA template control reaction (not shown in gel). Both images are cropped for easier viewing.

Specific primer sets for 17 of the 18 bacterial strains were validated in this study, as shown in Table 3.2 and the DNA gels from this work are shown in Appendix 8.5. The exception was *F. nucleatum* for which the two subspecies *nucleatum* and *polymorphum* could not be distinguished despite multiple attempts at primer design using several different genes. Consequently, both subspecies are detected in this study using a single primer set that includes the forward primer sequence 5'-

GTCAGAACTAAGATATCCAGC-3’ and the reverse primer sequence 5’-ATAAACTGAATAAGCAAGTC-3’. A universal primer set targeting constant regions within the 16S rRNA gene was also obtained from the literature to amplify all species within the *Bacteria* domain (Ramseier *et al.*, 2009).

Table 3.2 Validated primer sets used in this study. Sequences of primers validated for species-specific (or strain-specific where applicable) bacteria selected for use in the mock bacterial community model and universal primers.

Bacterial Strain	Gene	Forward Primer	Reverse Primer	Product length (bp)	Annealing Temp (˚C)	Reference/Designed
A. oris MF1	16S rRNA	5'-GTAAACCTCTTTCGCCAGT-3'	5'-CTGCTGGCACGTAGTTAG-3'	94	60	Designed
C. rectus ATCC 33238	*cpn60*	5'-TGAGCTTCAAAGCCCATA-3'	5'-TAGCGGTTTGCCTGTTT-3'	103	60	Designed
C. showae ATCC 51146	*cpn60*	5'-GCCACTATCTCGGCAAATTC-3'	5'-ACGTTTAGCTCGTCGTGGAT-3'	125	60	Chaban *et al.* (2009)
D. invisus DSM 15470	16S rRNA	5'-ACCGAATAAGTTCCAAGAGC-3'	5'-AGCTAATCAGACGCAAACC-3'	95	60	Designed
F. alocis ATCC 35896	16S rRNA	5'-GTATAACATATTAATAGGGC-3'	5'-TCTCACCAACTAGCTAATCA-3'	86	50	Designed
F. nucleatum ATCC 25586 (subsp. *nucleatum*) and ATCC 10953 (subsp. *polymorphum*)	zinc protease	5'-GTCAGAACTAAGATATCCAGC-3'	5'-ATAAACTGAATAAGCAAGTC-3'	111	50	Designed
N. subflava ATCC 49275	*rpoB*	5'-TTGGCTCAATTGGCTGGAA -3'	5'-GTAATCGTCGTGTTCGTTCTGTG -3'	194	55	Park *et al.* (2013)
P. micra ATCC 33270	16S rRNA	5'-TTGTGGAAATTCTTTCGGGAAT-3'	5'-CCTGTGTAAGGTAGGTTGCT-3'	82	60	Designed
P. gingivalis NCTC 11834	16S rRNA	5'-GCGAGAGCCTGAACCAGCCA-3'	5'-ACTCGTATCGCCCGTTATTCCCGTA-3'	90	60	Ammann *et al.* (2012)
P. intermedia ATCC 25611	16S rRNA	5'-GCGTGCAGATTGACGGCCCTAT -3'	5'-GGCACACGTGCCCGCTTTACT -3'	68	60	Ammann *et al.* (2012)
P. nigrescens ATCC 25261	*rpoB*	5'-TTCCGTCGTACCAACCAAAAC -3'	5'-CTAAAAGATTTCGCCCAAGTGCT -3'	139	60	Park *et al.* (2013)
S. gordonii DL1	*ddl*	5'-ATTGAAGAGAAACTGTCCTATCC-3'	5'-CACGCAGTTCTTCCTGATTAT-3'	97	60	Designed
S. oralis C647	*ddl*	5'-TTCACGAAGCCGTCAAAC-3'	5'-TGGAAGGCAAGTTCCAAAG-3'	92	60	Designed
T. forsythia ATCC 43037	*pseC*	5'-GCCTGTCGACTTTGCTGGAT-3'	5'-TGGTGCATGACAAGCATCTTC-3'	100	55	Designed
T. forsythia UB4	*legC*	5'-TGCGGCTGTTTGTGAAGAGT-3'	5'-CCCGAAAAGTCCGGTATGCT-3'	97	60	Designed
T. denticola ATCC 35405	16S rRNA	5'-TAAGGGACAGCTTGCTCACCCCTA -3'	5'-CACCCACGCGTTACTCACCAGTC -3'	55	60	Ammann *et al.* (2012)
V. dispar WT	16S rRNA	5'-AGGCCTTCTTGCGAATAGTT-3'	5'-CGCTTGCCACCTACGTATTA-3'	99	60	Designed
Universal	16S rRNA	5’-CCATGAAGTCGGAATCGCTAG-3’	5’-GCTTGACGGGCGGTGT-3’	86	60	Ramseier *et al.* (2009)

3.2.3. Propidium monoazide (PMA) treatment validation

3.2.3.1 Validation on treated and untreated DNA

Biofilm matrix consists of a mixture of interbacterial substances such as salivary materials, bacterial surface structures and bacterial extracellular DNA (eDNA). The latter component eDNA from dead bacterial cells persists in biofilm communities and it is important to remove this during the community analysis because including eDNA can distort the analyses of community compositions. Coupling the addition of propidium monoazide (PMA) to cell samples prior to DNA extraction with qPCRs is a technique that permits the removal of eDNA or DNA from lysed bacterial cells, as the photo-reactive DNA-binding PMA dye cannot cross intact cellular membranes in viable cells.

To establish conditions for its use on plaque and 18-spp. biofilm samples, *F. nucleatum* DNA at different concentrations in solution was subjected to a PMA dye photo-activation step of varying lengths of time. These were compared to an identical untreated sample to confirm whether PMA treatment would decrease the amount of DNA detected and increase C_t values in qPCR assays. A box plot (Figure 3.3) was generated from the Ct values for each of the 6 experimental conditions (untreated DNA sample; PMA light exposure for 1 min; 3 min; 5 min; 10 min and 20 min), completed in triplicate. The mean Ct value for untreated DNA samples was statistically significantly lower than for all PMA-treated mean DNA samples ($P<0.05$, Tukey's Honest Significant Difference test). Furthermore, the mean Ct value for 20 min PMA light exposure condition was statistically significant to all mean PMA-treated DNA samples except those exposed to 10 min light samples ($P>0.05$, Tukey's Honest Significant Difference test). This therefore suggested that after 10 min, no more DNA was cross-linked in these samples and a 10 min light exposure step was sufficient to remove extracellular DNA from samples.

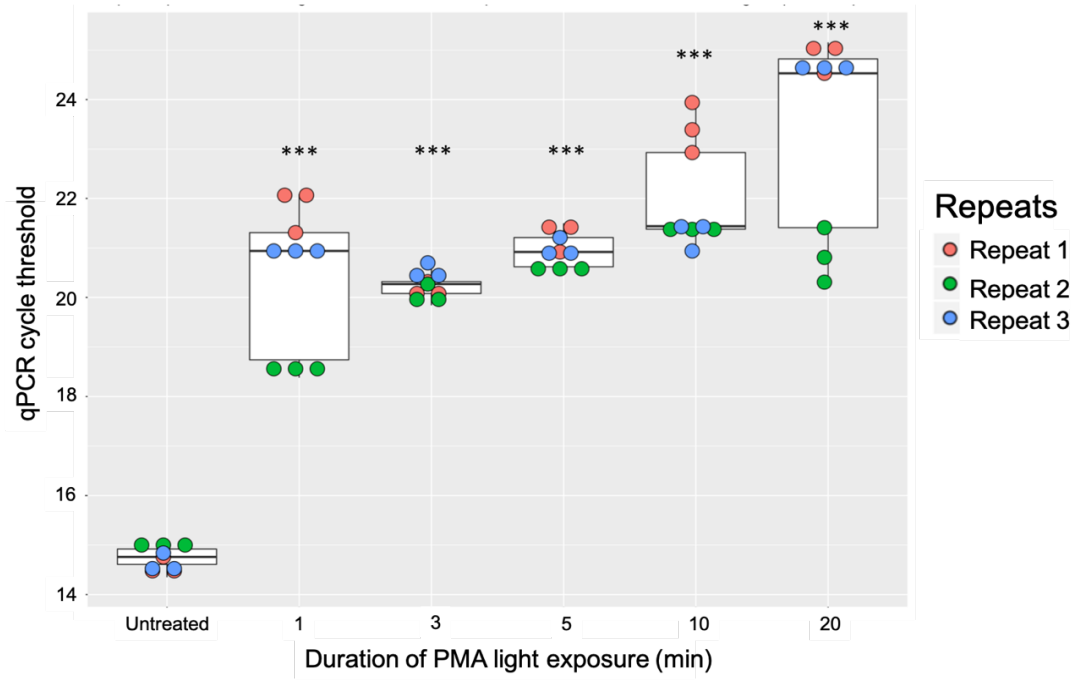

Figure 3.3 qPCR data for testing light exposure times in propidium monoazide (PMA) treatment. Box plots for cycle threshold (Ct) values generated from qPCR amplification of F. nucleatum subsp. nucleatum DNA using primers specific for F. nucleatum for six different experimental conditions (untreated; PMA light exposure time 1 min; 3 min; 5 min; 10 min; 20 min). Each condition was repeated in triplicate and statistical significance determined by Tukey's Honest Significance Difference Test p<0.001 ***.

3.2.3.2 Validation on PMA-treated and untreated biofilm samples

In addition to pure *F. nucleatum* subsp. *nucleatum* DNA, PMA treatment was also validated for cells harvested from mixed community samples. To investigate the effect of removing eDNA on total DNA concentration from bacterial cells harvested from 1-, 3- and 7-day mixed biofilm communities, each sample was split into two, with one half treated with 50 µM PMA dye and the second half remained untreated to act as a control prior to DNA extraction. The total DNA concentration for each sample was then measured by running qPCR assays using universal primers. The DNA concentration of all biofilm samples were <1 ng/µl, with higher DNA concentrations detected in untreated, more mature samples from 3- and 7-day growths. A reduction in total DNA concentration was seen in PMA-treated samples compared to control samples and this was significantly different in 1- and 7- day DNA biofilm samples ($p<0.001$ and $p=0.01$ respectively) as determined by multiple t-tests (Figure 3.4). The data also suggest 93.9 % and 96.8 % of total DNA in the 1- and 7-day DNA biofilm samples were in fact extracellular DNA and therefore removed by PMA treatment, suggesting the protocol for combining PMA treatment with qPCR was successful in removing eDNA from samples, to leave only

DNA measurements from viable bacterial cells. Lastly, a mean of 54.1 % eDNA was present in the 3-day DNA biofilm samples and the PMA-treated samples were not significantly different to equivalent untreated samples (p=0.137).

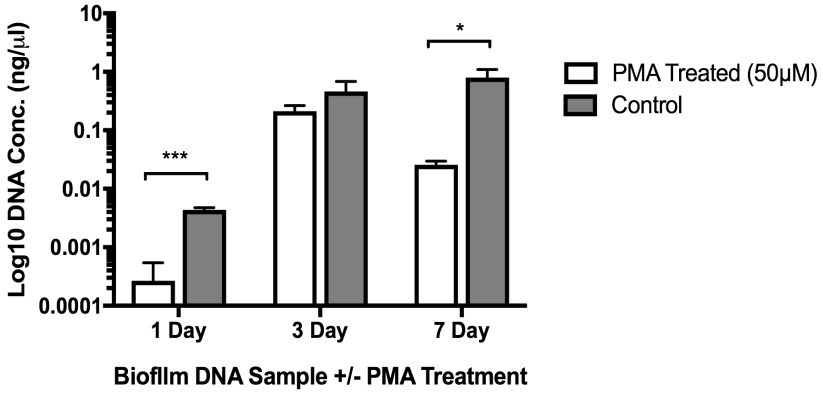

Figure 3.4 Effect of PMA treatment on total DNA concentration on biofilm cells. The biofilms were harvested after 1, 3- and 7-day growth. Data shown are averaged from n=3 independent experiments and statistical significance shown where 0.01<p<0.05 *, 0.01<p<0.001 **, p<0.001 *** as determined by multiple t-tests. Error bars determined by SD.

3.2.4. Comparison of bacterial DNA concentration quantitation techniques

A method to quantitatively determine levels of specific bacteria within mixed biofilm communities is to express it as a percentage of the total community. The total bacterial DNA concentration would therefore need to be measured first. Two methodologies for quantitating DNA concentration were assessed. These were the NanoDrop 1000 spectrophotometer which measures nucleic acids at a wavelength of 260 nm, and the Qubit dsDNA High Sensitivity (HS) kit with its DNA-binding dye-based chemistry.

Individual DNA concentrations extracted from 17 pure bacterial cultures were measured in parallel and compared between NanoDrop and Qubit assays (Figure 3.5). There was strong evidence that the Nanodrop over-inflated DNA concentrations as upon measuring DNA samples, nucleic acid concentrations varied widely between Nanodrop and Qubit readings (Figure 3.5A). For example, *P. gingivalis* DNA was measured at 213.3 ng/µl on the Nanodrop but 55.0 ng/µl on the Qubit. This was likely due to high levels of impurities such as RNA and extracellular DNA which could also have been absorbed at 260 nm on the Nanodrop. The Qubit assay was further validated by creating serial dilutions of the measured *P. gingivalis*

DNA sample (1:2, 1:5, 1:10, 1:50, 1:100 dilutions) which were measured against a standard curve and the expected versus observed Qubit readings were subsequently compared (Figure 3.5B). The expected readings for the serially diluted *P. gingivalis* DNA samples were calculated from the neat sample measured at 55 ng/µl. Except for 1:2 dilution, the measurements were comparable to what were expected.

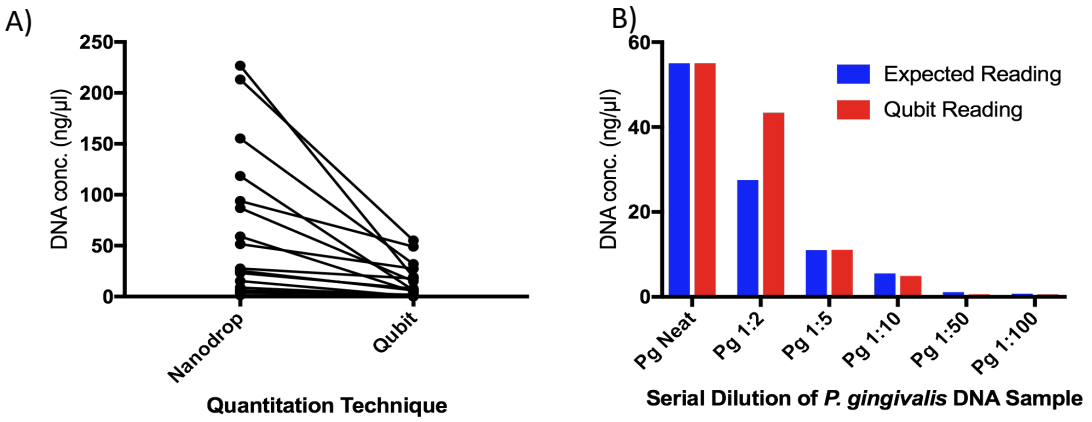

Figure 3.5 Comparison of DNA concentration measurements by Nanodrop and Qubit. (A) The DNA concentration readings from Nanopore and Qubit show a general trend of over-inflation by Nanodrop. (B) Serial dilutions of undiluted *P. gingivalis* DNA at 55 ng/µl plotted with the expected and observed readings.

Validations of the Qubit assay also found DNA concentrations <0.1 ng/µl could not be detected although the kit was advertised as being able to detect DNA concentrations as low as 10 pg/µl. Since initial data on biofilm DNA samples were determined to contain DNA concentrations below this, running universal qPCR assays was chosen as the preferred alternative to both the NanoDrop and Qubit for quantification of total biofilm DNA. The findings for using Qubit for DNA quantitation, however, would still be useful as the Qubit will be used to quantitate the DNA concentration of microbial community PCR products in generating DNA library preps for 16S rRNA gene community profiling.

3.2.5. 16S rRNA gene community profiling

3.2.5.1 Primer selection in 16S rRNA gene community profiling

To profile microbial communities using the 16S rRNA gene, the Illumina MiSeq sequencing platform was trialled. As the full 16S rRNA gene spans ~1500 bp but the Illumina MiSeq platform can only generate good quality reads of up to 300 bp in

length, primers that could detect bacteria relevant to the oral microbiome were required. Based on a literature review, the primer set 27F-YM/338R-R (27F-YM: 5'-AGAGTTTGATYMTGGCTCAG-3', and 338R-R: 5'-TGCTGCCTCCCGTAGRAGT-3') were selected to amplify the V1-V2 hypervariable region of the 16S rRNA gene over other regions of the gene. The V1-V2 region is approximately 311 bp long and the primer sequences contain wobble bases to ensure all bacterial sequences at highly variant base positions would still be amplified and thus not be missed or under-represented in the communities. In support of selecting the V1-V2 region, Zheng *et al.* (2015) demonstrated higher species-level OTU richness and evenness were achieved in subgingival plaque samples with V1-V3 region when compared to V3-V4.

3.2.5.2 Composition of pooled subgingival plaque samples obtained from Illumina MiSeq Sequencing

To provide a general guide on the proportions of different genera present in a dysbiotic subgingival plaque community, for which an *in vitro* mock community version could be based upon, subgingival plaque samples were collected from five volunteers (sample identities P011-P015 as given during recruitment for this study). The five plaque samples were pooled and the V1-V2 hypervariable region of the 16S rRNA gene were sequenced on the Illumina MiSeq platform. The pooled plaque community was classified to genus level (Figure 3.6). For ease of viewing due to the high number of genera classified in the pooled plaque, only the 13 genera selected for use in this project's *in vitro* mock biofilm model is coloured in the figure. *Porphyromonas, Prevotella* and *Selenomas* were found to be the most prevalent genera, with relative abundances of 21.8 %, 20.0 % and 17.0 % observed respectively. All genera previously chosen for inclusion in this study's mock community inoculum were also present in the pooled plaque community, with 10 of 13 also belonging to the plaque community's 20 most dominant genera. These 10 genera made up 63.5 % of the pooled plaque composition and included the following in order of highest relative abundance: *Porphyromonas; Prevotella; Fusobacterium; Treponema; Streptococcus; Neisseria; Dialister; Veillonella; Campylobacter* and *Tannerella.* As the sequences were classified to genus level,

species within the genera *Porphyromonas, Fusobacterium* and *Prevotella*, which each include multiple oral species, could not be distinguished. The results here suggest the oral bacteria previously selected for inclusion in the mock community model were appropriate.

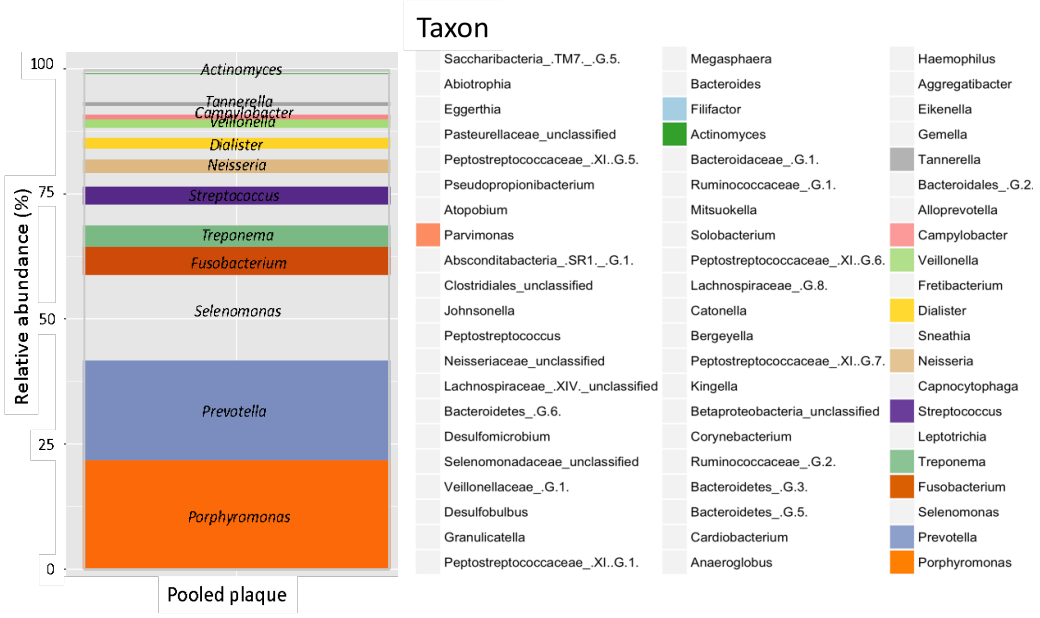

Figure 3.6 Relative abundance of genus-level taxa in pooled plaque. Five subgingival plaque samples collected from patients diagnosed with chronic periodontitis were pooled and profiled by sequencing the V1-V2 hypervariable region of the 16S rRNA gene on the Illumina MiSeq sequencing platform. The taxa are ordered by order of relative abundance (%), with the highest positioned at the bottom and the lowest at the top. For ease of viewing due to the high number of genera classified in the pooled plaque, only the 13 genera selected for use in this project's in vitro mock biofilm model is coloured.

3.2.6. Nanopore MinION sequencing as an alternative to Illumina MiSeq

3.2.6.1 Primer selection in Nanopore MinION sequencing

Some DNA sequencing platforms such as the Illumina MiSeq sequencing platform are costly and slow. Users typically wait days or even weeks before sequencing data are generated and received from genome centres. Such technology has improved rapidly in recent years and this is well illustrated by the Nanopore MinION device. This device is advantageous over the Illumina MiSeq platform because it produces data in real-time and in one's own laboratory. Another crucial benefit of the Nanopore MinION is it can also sequence much longer reads than the Illumina MiSeq. Nanopore MinION sequencing was therefore sought as an alternative to Illumina MiSeq in the 16S rRNA gene profiling of oral microbial communities. The MinION device however has its own limitations, such as using it

can produce sequences with > 1 % error rates and protocols for Nanopore sequence analysis are not readily available whereas protocols for setting up sequencing runs and preparing sequence libraries are. One such example is the protocol available from Oxford Nanopore for using its 16S Barcoding Kit.

The forward primer 27F (5'-AGAGTTTGAT**CC**TGGCTCAG-3') and the reverse primer 1492R (5'-CGG**T**TACCTTGTTACGACTT-3') are the default primers used in Nanopore's 16S Barcoding Kit. This is the standard kit available for genus-level bacterial identification. As the default 27F primer lacks the two wobble bases highlighted in bold that are present in the 27F-YM forward primer (5'-AGAGTTTGAT**YM**TGGCTCAG-3') previously described for Illumina MiSeq sequencing, the two different forward primers were compared by aligning multiple 16S rRNA gene sequences and highlighting where the primers sit. To do this, every 16S rRNA gene sequences present in HOMD v15.2 were aligned using BioEdit Alignment Editor (v7.2.5), and the alignment file is shown in Figure 3.7A although only a selection is shown for ease of readability. Here, the region where the primer sequences sat is highlighted in yellow and the two base positions where the two forward primer sequences differed were designated with an asterisk *. Conserved bases are plotted as dots whereas bases that differed from the *Abiotrophia* sequence (top of alignment) are written as letters. The figure below illustrates the two base positions, which differed between the 27F and 27F-YM. Primer sequences were highly variable amongst all the sequences extracted from HOMD. For example, as well as the nucleotide C in these two base positions, the nucleotides A and T were also present. The variability in these two base positions therefore suggested adding the wobble bases YM to the forward primer would be advantageous, i.e., the default 27F primer (5'-AGAGTTTGAT**CC**TGGCTCAG-3') to be modified to 27F-YM (5'-AGAGTTTGAT**YM**TGGCTCAG-3'). This would ensure bacterial sequences that contained C or T (using the Y wobble base) and A or C (using the M wobble base) at the two highly variant positions would be amplified and thus these bacteria would not be incorrectly under-represented in a community. An alignment was also performed for the 15 bacterial species (two subspecies present for *F. nucleatum*) selected for use in the mock community

model, although no base variants were observed in the same primer sequence region (Figure 3.7B). The results here highlight the importance of including the two degenerate bases in profiling a complex microbial community such as plaque but less so in the simpler 15-species mock community.

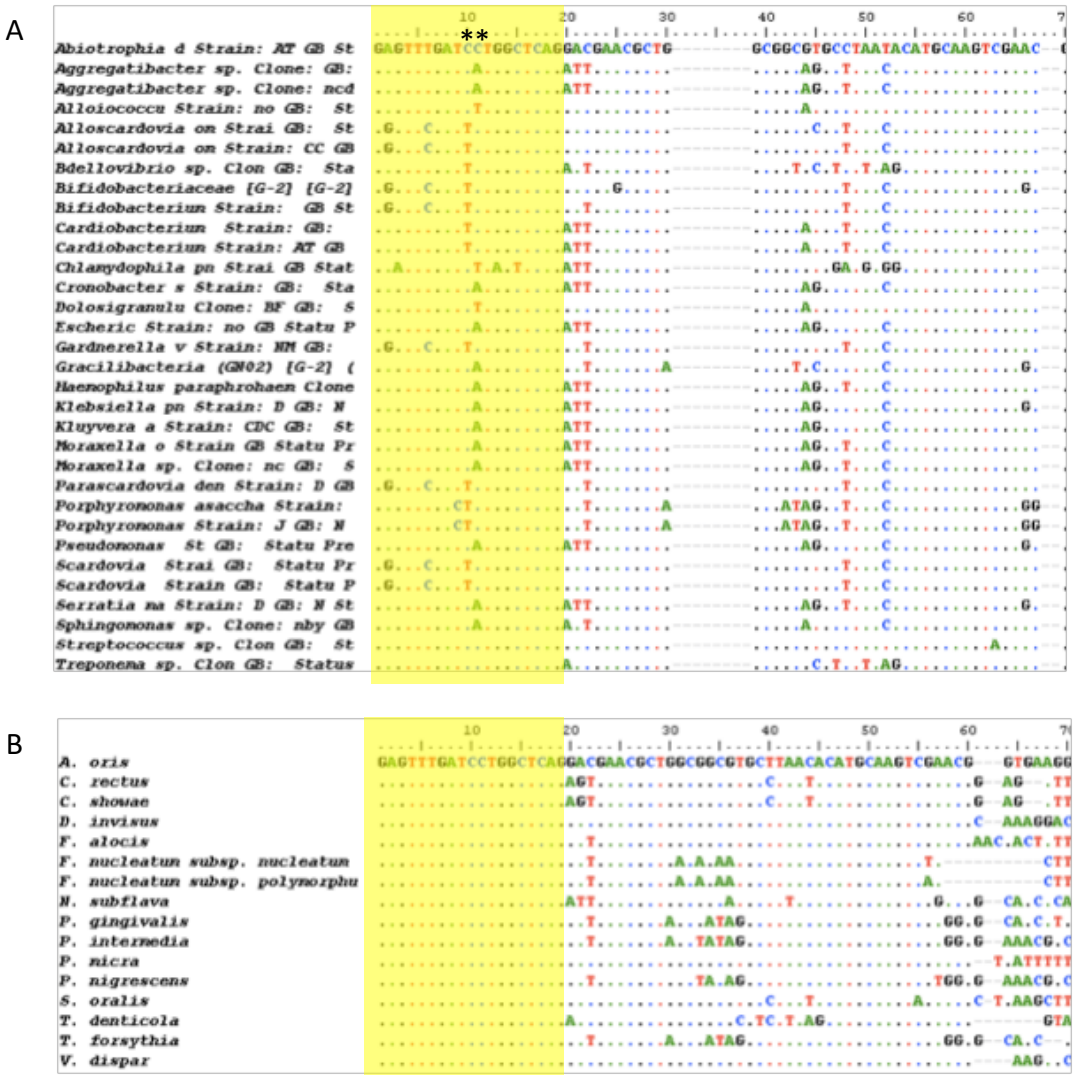

Figure 3.7 27F forward primer sequence highlighted in 16S rRNA gene sequence alignments of oral bacteria. The alignments of 16S rRNA gene sequences on a selection of oral bacteria obtained from HOMD v15.2 (A) and from the 15 bacterial species selected for inclusion in the mock community model (B). Sequences were aligned using BioEdit Alignment Editor (v7.2.5), the primer sequence highlighted in yellow and the highly variable base positions were designated with the asterisk *. Conserved bases were plotted as dots whereas bases were written at positions which differed from the top bacterial sequence.

The same practice was applied for investigating the reverse primer, as the default reverse primer used in Nanopore sequencing is the 1492R primer (5'-CGG**T**TACCTTGTTACGACTT-3'). Again, bacterial 16S rRNA gene sequences were obtained from HOMD v15.2 (Figure 3.8A) and for the 16 bacterial species (Figure

3.8B), aligned and the region where the primer sequence would anneal is highlighted in yellow. From both alignments, one highly variable base position was observed which is designated with an asterisk * in the two alignment plots. Taken together, the introduction of a wobble base 'D' to this base position in the 1492R primer sequence would be beneficial so that bacterial sequences containing the bases G, A or T at this position would all be amplified. The default standard 1492R primer (5'-CGG**T**TACCTTGTTACGACTT-3') was therefore modified to 1492R-D (5'-CGG**D**TACCTTGTTACGACTT-3').

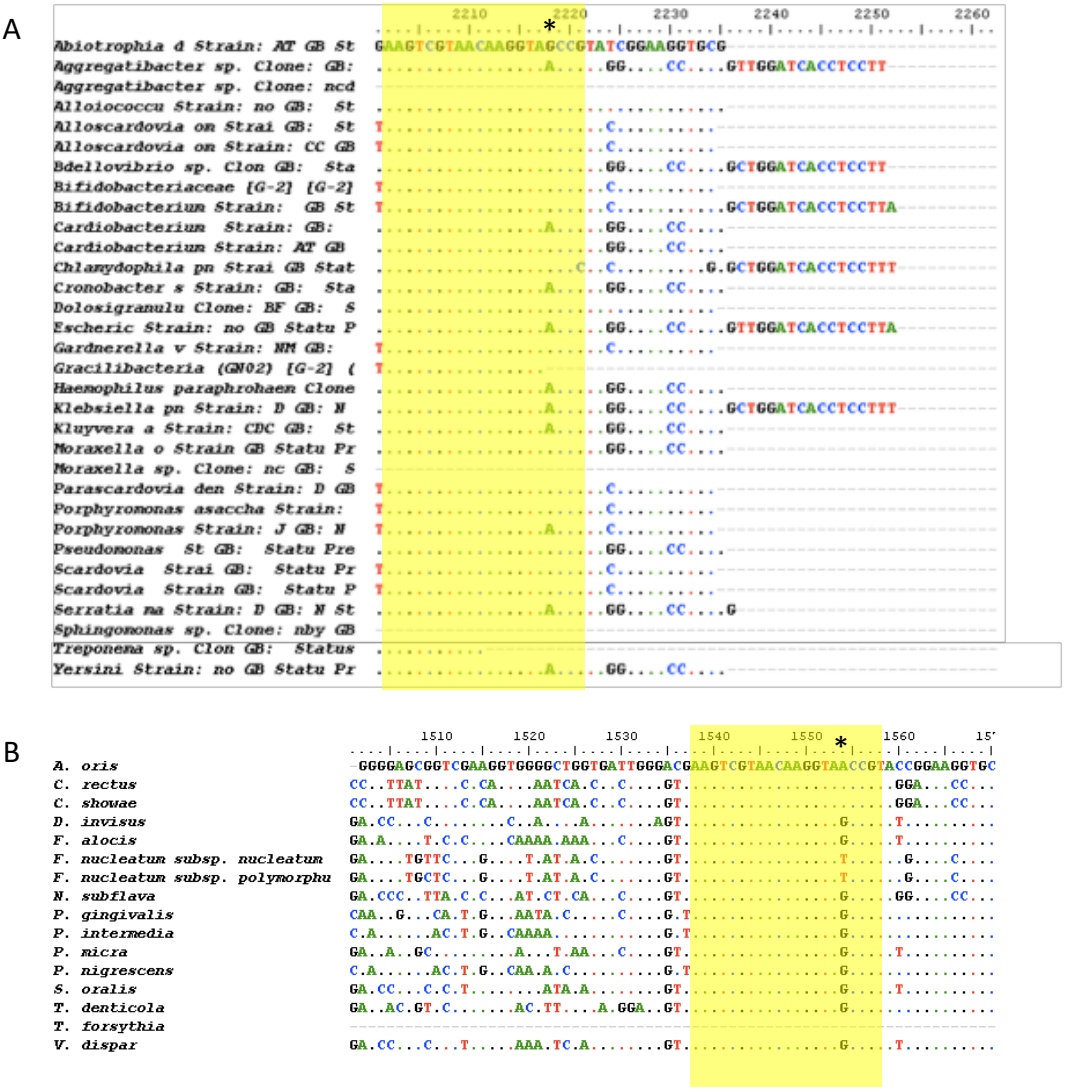

Figure 3.8 1492R reverse primer sequence highlighted in 16S rRNA gene sequence alignments of oral bacteria. The alignments of 16S rRNA gene sequences on a selection of oral bacteria obtained from HOMD v15.2 (A) and from the 16 bacterial species selected for inclusion in the mock community model (B). Sequences were aligned using BioEdit Alignment Editor (v7.2.5), the primer sequence highlighted in yellow and the highly variable base positions were designated with the asterisk *. Conserved bases were plotted as dots whereas bases were written at positions which differed from the top bacterial sequence.

Following on from this bioinformatics work, the default 27F/1492R and modified 27F-YM/1492R-D Nanopore primers were used on the same microbial community sample (multispecies inoculum used in June 2019 model) and sequenced using Nanopore MinION. DNA was first extracted from a mixture of live oral bacteria from 12 different genera using the QIAamp DNA Mini Kit. A third condition was also compared by sequencing the V1-V2 hypervariable region using 27F-YM/338R-R of the 16S rRNA gene of the same microbial community sample with Illumina MiSeq (Figure 3.9). What is striking about this figure is the composition of the single sample varied most when the default 27F/1492R primer set was used prior to sequencing with the Nanopore MinION sequencer. Here, the relative abundance of *Treponema* was reduced to 17.1 % and *Streptococcus* and *Veillonella* increased to 27.5 % and 35.9 % respectively. When compared against the two other techniques (Nanopore MinION 27F-YM/1492R-D and Illumina MiSeq 27F-YM/338R-R), which were more comparable to one another. The higher relative abundance of *Treponema* observed using Nanopore MinION 27F-YM/1492R-D might be explained by the degeneracy introduced to 1492R-D. Compared to the default 27F/1492R primer set, this could have allowed for the amplification of sequences such as *T. denticola* which contained a 'G' base instead of 'T' at the highly variable base position designated with an asterisk * as described in the previous section. Overall, this work together with the previous bioinformatics work suggested the modified 27F-YM/1492R-D primer set used with Nanopore MinION would produce a community composition more representative of the real community.

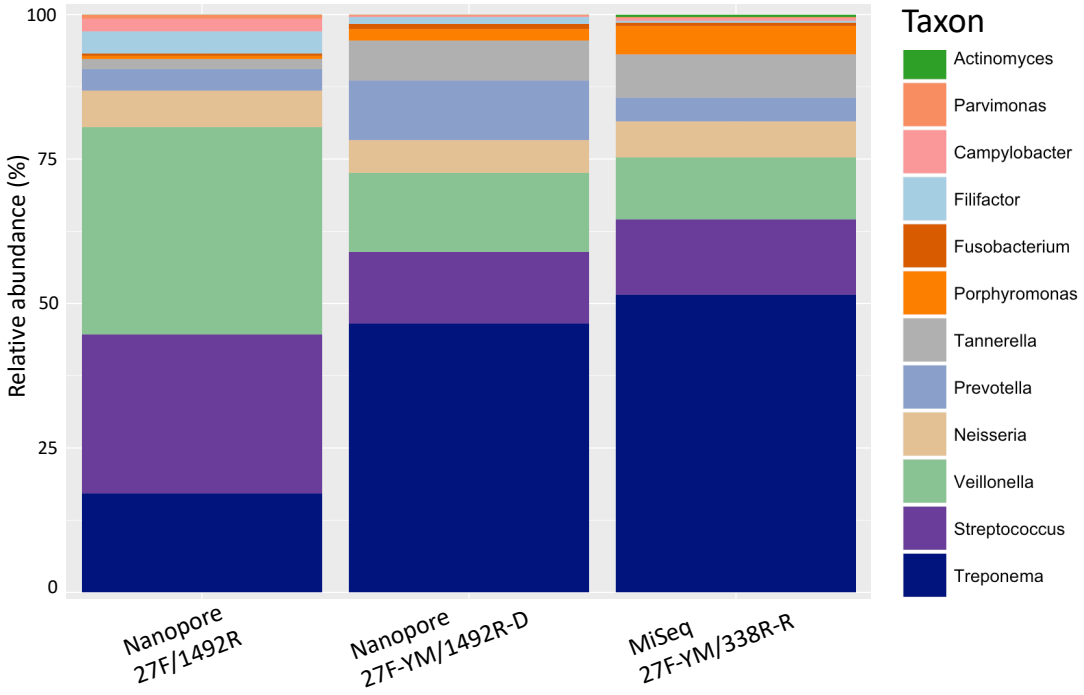

Figure 3.9 Comparison of amplicon library preparation and sequencing techniques. The relative abundances of genus-level taxa classified in the same microbial community sample (multispecies inoculum used in the June 2019 mock biofilm model) as sequenced by the Nanopore or MiSeq sequencing platforms. Also shown is the comparison between using the standard 27F/1492R or the modified 27F-YM/1492R-D PCR primer set prior to Nanopore sequencing. DNA was first extracted from a mixture containing live bacteria from 12 genera using the QIAamp DNA Mini Kit.

3.2.6.2 Improving the error rate associated with Nanopore sequencing

Errors can be introduced during sequencing that can lead to inaccurate sequence reads being produced. The resulting error rate of a sequencing run can be measured if a mock community sample with known proportions of different bacteria are included in the same sequencing run and their corresponding 16S rRNA gene sequences are also known. This sample acts as a reference sample whereby the error rate is calculated from the total sum of mismatches to the reference sequences divided by the sum of the total bases in the query sequences. Besides sequence read inaccuracy, it is important to calculate the error rate because if bacterial species-level OTUs are clustered at either 1.5 % or 3 % cut-off and the error rate is >3 %, it would mean the OTUs cannot be clustered to species level. As Nanopore sequencing is known to be associated with a higher error sequencing rate than Illumina MiSeq sequencing, the error rate of a Nanopore sequencing run was tested. To do this, a commercially available ZymoBIOMICS™

Microbial Community DNA Standard (Zymo Research, USA) was sequenced. This acted as a reference microbial community DNA sample as 16S rRNA gene abundance of eight bacterial and two fungal species were known (shown in Table 3.3 as supplied by the manufacturer). Attempts to improve the sequencing error rate were as follow.

Table 3.3 Theoretical composition of the ZymoBIOMICS Microbial Community DNA Standard. This is in terms of 16S rRNA gene abundance of eight bacterial species, as supplied by the manufacturer.

Microbial species	Theoretical composition (%)
Pseudomonas aeruginosa	4.2
Escherichia coli	10.1
Salmonella enterica	10.4
Lactobacillus fermentum	18.4
Enterococcus faecalis	9.9
Staphylococcus aureus	15.5
Listeria monocytogenes	14.1
Bacillus subtilis	17.4
Saccharomyces cerevisiae	NA (fungi)
Cryptococcus neoformans	NA (fungi)

Primer selection to improve the sequencing error rate

To test whether different 16S primers would help reduce the sequencing error rate, the default 27F/1492R and modified 27F-YM/1492R-D PCR primer sets were used prior to sequencing the ZymoBIOMICS^{TM} Microbial Community DNA Standard on the Nanopore MinION. Where the default 27F/1492R primer set was used, the sequencing error rate for the reference standard was calculated at 5.7 %. Consequently, for every 100 bp of the 16S rRNA gene sequenced, 5 bp of this were considered incorrect. The error rate was interestingly improved and lowered to 4.6 % when the modified 27F-YM/1492R-D primer set was used. It was likely the small reduction resulted from reducing the error rate during the PCR reaction within amplicon library preparation. The findings taken here together with that of section 3.2.6.1 indicate the modified 27F-YM/1492R-D primer set was recommended over the default Nanopore 27F/1492R primer set.

Basecalling software update to improve the sequencing error rate

As the improved 4.6 % error rate associated with Nanopore sequencing was still too close to the genus-level OTU clustering cut-off threshold of 5 % (Stackebrandt and Goebel, 1994), further work was completed to reduce the error rate. During the course of this studentship, the basecalling software Guppy (Oxford Nanopore Technology) that was used in Nanopore sequencing was progressively modified and improved. For example, updating the basecalling software Guppy from version 3.2.6 to version 4.3.4 and then re-basecalling the same sequence reads improved the error rate regardless of which PCR primer set was used. Table 3.4 shows the error rate reduction from 5.7 % to 3.8 % when the default 27F/1492R PCR primer set was used. Similarly, the error rate also declined when the modified 27F-YM/1492R-D PCR primer set was used- from 4.6 % to 3.4 %. It is important to note the Zymobiomics Microbial Community DNA standard sample using the different primer sets were amplified in the same PCR run and sequenced during the same Nanopore run.

Table 3.4 Error rate comparison between the use of different PCR primer sets as well as varying basecalling software versions. The error rate measured for the Zymobiomics Microbial Community DNA Standard sample after sequencing on the same Nanopore MinION flow cell, for when the basecalling software Guppy v3.2.6 was used versus the updated version 4.3.4.

Primer set type used in PCR	**Error rate for un-updated basecalling software Guppy v3.2.6**	**Error rate for updated basecalling software Guppy v4.3.4**
Standard 27F/1492R	5.7 %	3.8 %
Modified 27F-YM/1492R-D	4.6 %	3.4 %

Nanopore sequencing flow cell selection to improve the sequencing error rate

The previous Nanopore sequencing data were obtained on a Nanopore MinION flow cell. This type of flow cell was reusable but was costly to purchase so as a cheaper alternative to sequencing on the MinION flow cell, the newly available Nanopore Flongle flow cell was tested to see whether this could be used instead and whether the sequencing error rate would improve. A second benefit of using a Flongle flow cell in place of a MinION flow cell was its one-use capacity would

prevent the need for washing and storing the MinION flow cell between sequencing runs. This would also minimise the risk of leftover contaminating sequences leftover from a previous sequencing run.

Three different mock microbial communities were tested on a Nanopore MinION flow cell, a Nanopore Flongle flow cell, as well as in an Illumina MiSeq run for comparison. The three mock communities were as follow and labelled as communities 1-3 for clarity:

1. A multispecies whole bacterial cell inoculum used in the June 2019 mock biofilm model and described previously in section 3.2.6.1.
2. A mixture of DNA extracted from 13 oral bacteria each at 1 ng/µl.
3. ZymoBIOMICS^{TM} Microbial Community DNA Standard (with known concentrations for 8 bacteria and 2 yeasts as before).

As before, each of the three microbial communities were amplified in the same PCR run using two different 16S primer sets for each: the default Nanopore 27F/1492R and modified Nanopore 27F-YM/1492R-D primer sets. A DNA library constructed from the six amplicons was then sequenced first on a Nanopore MinION flow cell and then the same DNA library was loaded onto a Flongle flow cell. The microbial community composition for each of the three communities obtained from the Nanopore MinION flow cell are illustrated in Figure 3.10A and those obtained from the Nanopore Flongle flow cell are shown in Figure 3.10B. The composition of the same three samples resulting from an Illumina MiSeq was also artificially added into the plots for comparison. Overall, the community compositions were comparable between those that were obtained from a Nanopore MinION flow cell and those obtained from a Nanopore Flongle flow cell. This was regardless of which PCR primer set was used and from this work, indicated a Nanopore Flongle flow could replace the use of a Nanopore MinION flow cell when classifying the Nanopore sequence reads to genus level. Examining the diversity and overall shape of the communities revealed the communities were comparable when compared between using Illumina MiSeq and Nanopore's MinION and Flongle flow cells. This was indicated by using the Simpson's inverse index ($p=0.45$ as measured by ANOVA) to measure community richness and

evenness and visualised in a PCoA plot using distance matrices estimated by Jaccard index to measure community membership. The PCoA plot did not show distinct clusters based on the type of sequencing technique used but clustered based on sample (Figure 3.11).

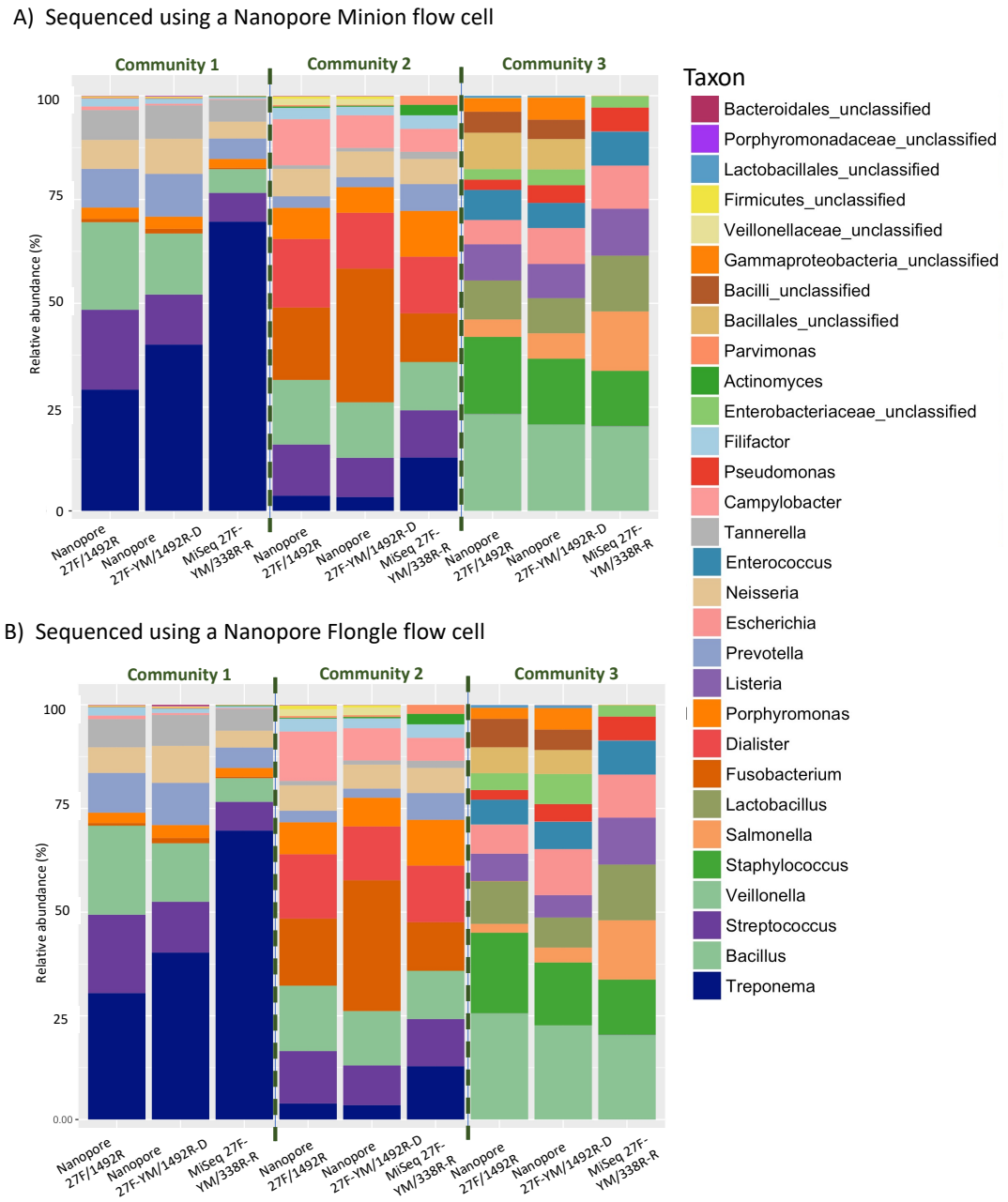

Figure 3.10. Comparison of community compositions between using Nanopore MinION and Flongle flow cells. The relative abundance of genus-level taxa in three 'mock' microbial community samples sequenced from the same DNA library but (A) loaded onto a Nanopore MinION flow cell and then (B) onto a Nanopore Flongle flow cell. Data from an Illumina MiSeq run was run separately but added into the plots for comparison.

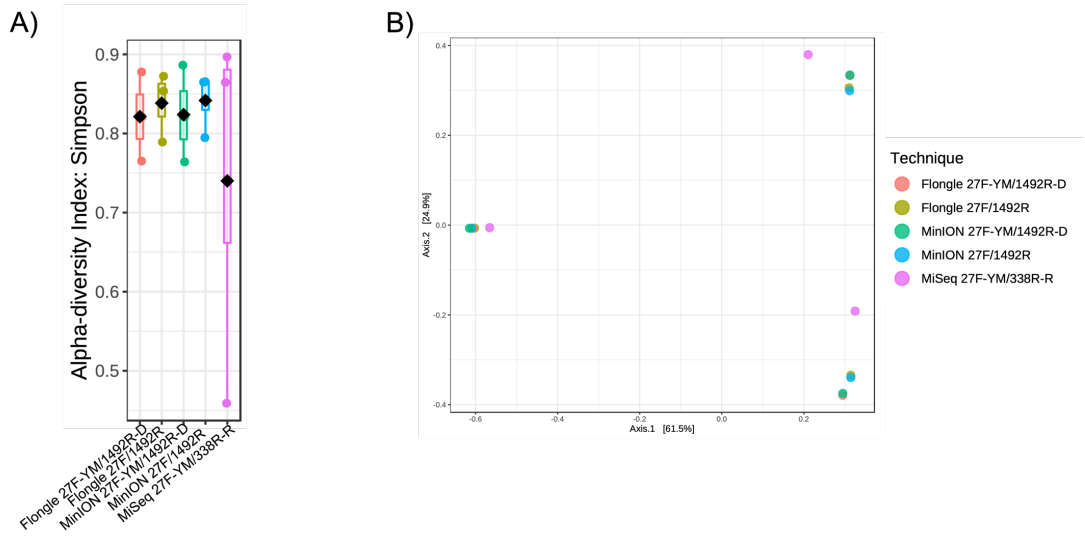

Figure 3.11 Diversity comparison for three community samples which were sequenced using various different techniques. The use of Nanopore's Flongle vs MinION flow cells were compared, as was the Illumina MiSeq sequencing platform. The use of 27F/1492 vs 27F-YM/1492R-D PCR primer sets were also compared. A) Boxplots depicting the Simpson's alpha-diversity index values B) Principal coordinates analysis plot based on community membership using the Jaccard index. An ANOVA test was performed for the Simpson's alpha-diversity indices, which generated a p-value of 0.45.

It was expected the sequencing error rate with using either the MinION or the Flongle flow cell would be alike. To assess the sequencing error rate associated with a Nanopore Flongle flow cell, the error rate of the Zymobiomics Microbial Community DNA Standard was calculated using the same methodology as before. As shown in Table 3.5, the sequencing error rate was once again improved when the modified 27F-YM/1492R-D primer set was used prior to sequencing compared to the default 27F/1492R primer set irrespective of which flow cell was used (3.4 % vs 3.8 % on the MinION flow cell respectively and 3.7 % vs 5.1 % on the Flongle flow cell respectively). There was, however, a strong indication that the error rate did not improve with using a Flongle flow cell and again, this was evident regardless of which PCR primer set was used.

Table 3.5 Error rate comparison between the use of different PCR primer sets as well as the use of the MinION or Flongle flow cell. The error rate measured for the Zymobiomics Microbial Community DNA Standard sample after sequencing on a Nanopore MinION flow cell and a Nanopore Flongle flow cell. The error rate was also compared between using the standard 27F/1492R primer set and using the modified 27F-YM/1492R-D primer set during PCR prior to sequencing.

Primer set type used in PCR	MinION flow cell	Flongle flow cell
Standard 27F/1492R	3.8 %	5.1 %
Modified 27F-YM/1492R-D	3.4 %	3.7 %

To further verify that using a Nanopore MinION flow cell instead of a Nanopore Flongle flow cell improved the sequencing error rate, a second sequencing run using a Flongle flow cell on the Zymobiomics Microbial Community DNA standard was performed. The 27F-YM/1492R-D primer set was used in the amplicon library preparation, and the use of the Flongle flow cell in sequencing produced an error rate of 6.0 % (Table 3.6). As this error rate was too high to classify the sequence reads to both genus and species levels, a new DNA library was created which used the same Zymobiomics Microbial Community DNA standard as before and sequenced on a MinION flow cell in place of a Flongle flow cell. This rationale was based on previous work described above that demonstrated a slightly higher error rate was associated with sequencing on a Flongle flow cell. Strikingly, the error rate measured from re-sequencing on a MinION flow cell did indeed reduce the error rate from 6.0 % to 2.2 %. The lower error rate was far closer to the speciation threshold of 1.5 % and thus a Nanopore MinION flow cell was recommended over the Flongle flow cell.

Table 3.6 Error rate comparison between the use of MinION and Flongle flow cells for sequencing the Zymobiomics Microbial Community DNA Standard. The error rate measured for the Zymobiomics Microbial Community DNA Standard sample after sequencing on a Nanopore MinION flow cell and a Nanopore Flongle flow cell. The modified 27F-YM/1492R-D primer set was used during PCR prior to sequencing.

Primer set type used in PCR	MinION flow cell	Flongle flow cell
Modified 27F-YM/1492R-D	2.2 %	6.0 %

3.2.7. Batch effect in microbiome research

To verify the microbiome data produced from comparing a mock microbial community sample (previously labelled June 2019 inoculum) between sequencing technologies in the previous section was reproducible, the extracted genomic DNA for the sample which was stored at -20 °C, was re-amplified and a new DNA library was sequenced on a new Nanopore MinION flow cell and on a new Illumina MiSeq sequencing run.

As demonstrated in Figure 3.12, re-amplifying and resequencing the same extracted genomic DNA samples produced markedly different compositions for the

sample microbial community between the first and second sequencing run. This was true whether the standard 27F/1492R primer set or its modified counterpart 27F-YM/1492R-D was used in PCR prior to sequencing on the Nanopore sequencing platform, but the variation observed was predominantly greater with the two MiSeq runs. Here, 7 of the 12 most abundant genus-level taxa were clearly observed for both MiSeq runs which sequenced the same sample. This included the following genera: *Neisseria; Porphyromonas; Prevotella; Streptococcus; Tannerella; Treponema* and *Veillonella*. The relative abundance of the most abundant genus for all compositions was *Treponema* but its relative abundance greatly increased from 51.5 % to 69.7 % on the second MiSeq run (shown as dark blue). The finding here suggested batch effect contributed to the variation observed between the first and second sequencing run regardless of sequencing technology. Although re-amplifying the extracted community DNA for this sample prior to re-sequencing produced changes to the relative abundance of certain bacteria, measuring the α-diversity (Figure 3.13A) revealed the community richness and evenness remained similar ($p=0.78$ as determined by conducting a t-test on the Simpson's diversity index values). However, β-diversity for the same samples varied as shown by the absence of clustering (Figure 3.13B) and was likely due to the variability introduced during amplicon preparation prior to sequencing.

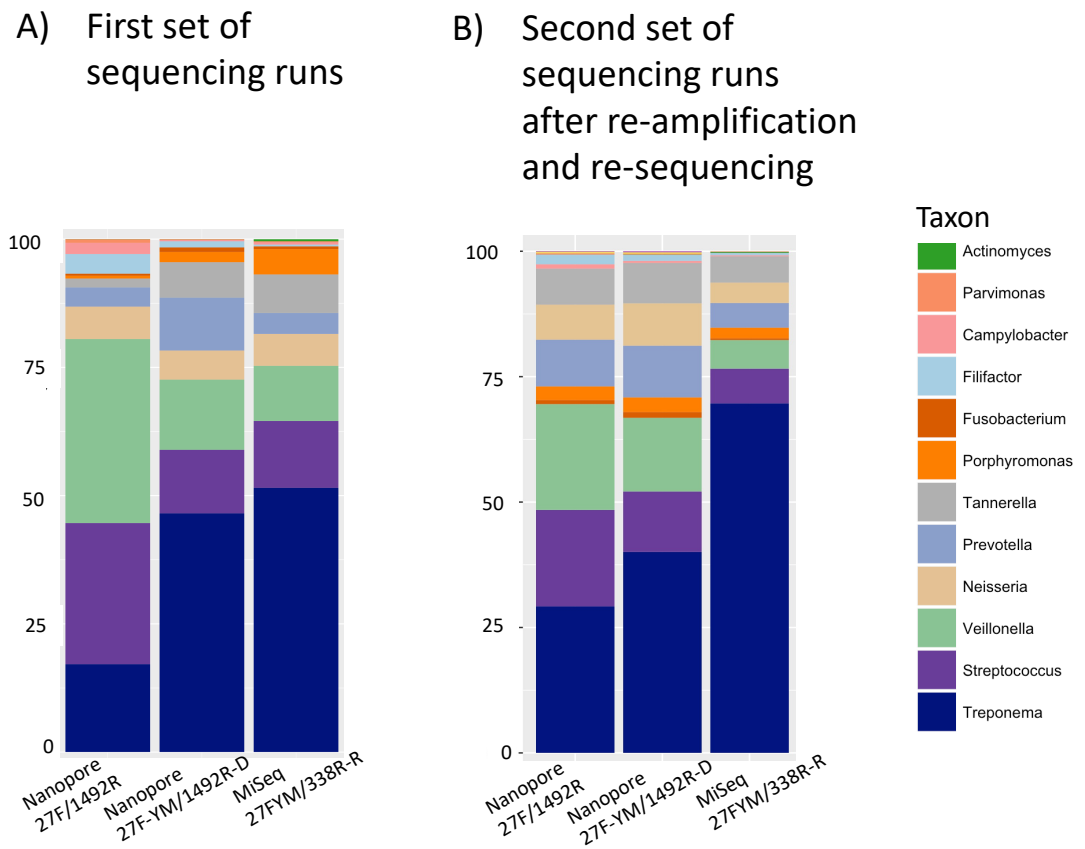

Figure 3.12 Comparison of microbial community compositions between different sequencing runs. The relative abundance of genera observed in a single microbial community sample after being sequenced using both Nanopore and MiSeq sequencing platforms. Unmodified standard 27F/1492R and modified 27F-YM/1492R-D primers were used in the PCR step prior to Nanopore sequencing. (B) In a second experiment to test for batch effect, the genomic DNA of the same single microbial community sample was re-amplified and re-sequenced following the same protocol.

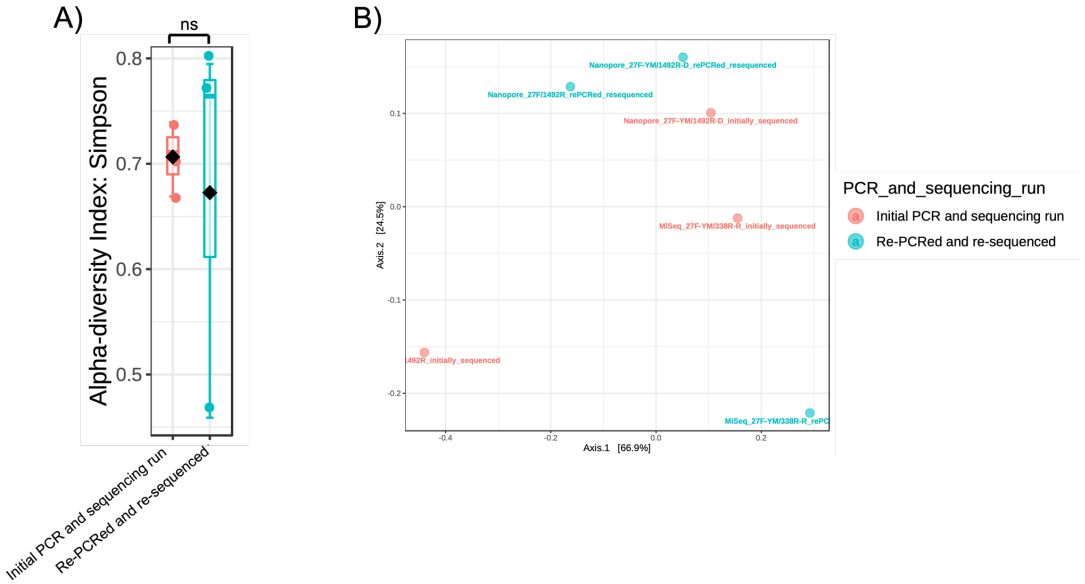

Figure 3.13 Diversity comparison for a microbial community sample which was re-PCRed and re-sequenced. The single community was initially sequenced using both Nanopore and MiSeq sequencing platforms, and then the extracted community DNA was re-amplified and re-sequenced. A) Boxplots depicting the Simpson's alpha-

diversity index values B) Principal coordinates analysis plot based on community membership using the Jaccard index. A t-test on the Simpson's alpha-diversity index values was performed, where 0.01<p<0.05 *, 0.01<p<0.001 **, p<0.001 *** and p<0.0001 ****.

To investigate whether re-amplifying the genomic DNA of microbial community samples contributed to the batch effect variation observed as before, or whether the variation was introduced downstream of the PCR step, three 'mock' microbial community samples were sequenced on a Nanopore MinION flow cell, and the same PCR products used in this first MinION sequencing run were then re-pooled to the same equimolar concentration and reloaded onto a new Nanopore MinION flow cell. The work differed to the previous section because DNA was not re-amplified here. The three 'mock' microbial community samples are as follows, but labelled as communities 1-3 for clarity:

1. A multispecies whole bacterial cell inoculum used in the June 2019 mock biofilm model and described previously in section 3.2.6.1.
2. A pool of DNA extracted from 13 oral bacteria each at 1 ng/µl.
3. ZymoBIOMICS™ Microbial Community DNA Standard (with known concentrations for 8 bacteria and 2 yeasts).

Each community sample was sequenced on a Nanopore MinION flow cell using PCR products amplified using the default standard 27F/1492R and the modified 27F-YM/1492R-D primers. Amplicons created for MiSeq sequencing however could not be re-sequenced in a second MiSeq run due to insufficient volumes of the amplicons. The results of the initial and then the repeated Nanopore sequencing run (DNA library created without a re-amplification step) for the three 'mock' community samples are shown in Figure 3.14. As demonstrated here, the microbial composition of all three mock community samples using both types of 16S rRNA gene PCR primers observed from the two plots were comparable. The marked variations observed in the previous section where genomic DNA was first re-amplified prior to re-sequencing were not seen here. Furthermore, comparison of the α-diversity using Simpson's diversity index revealed re-sequencing the same amplicons also produced similar communities (p=0.83) (Figure 3.15A). There was also overlap of the same communities when sequenced in two separate runs and visualised in a PCoA plot (Figure 3.15B). Therefore, the data here suggest re-sequencing on the same sequencing platform (in this case, Nanopore) using the

same amplicons produced comparative results. The overall shape of the communities remained comparable when sequencing was repeated even if the extracted community DNA was first re-amplified. However, any variability observed for bacterial abundance as a result of batch effect was reduced when the sample amplicons were sequenced during separate runs, compared to when the microbial community DNA was first re-amplified prior to re-sequencing.

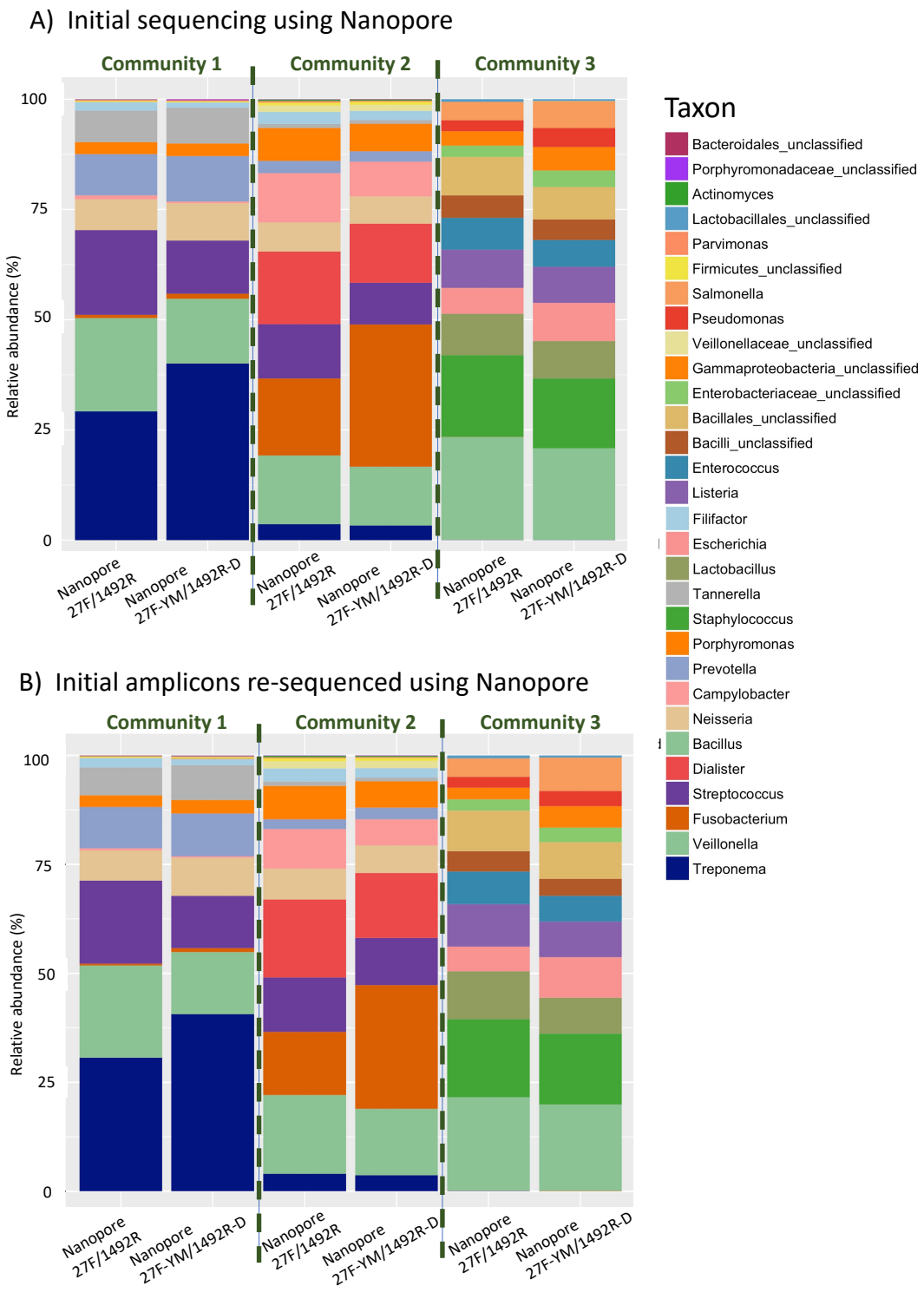

Figure 3.14. Effect of re-sequencing amplicons using Nanopore on microbial community compositions. DNA from three different 'mock' microbial community samples were amplified using unmodified standard 27F/1492R and modified 27F-YM/1492R-D primers. Amplicons created here were then (A) initially sequenced on a Nanopore MinION flow cell and then (B) re-sequenced using a new Nanopore MinION flow cell.

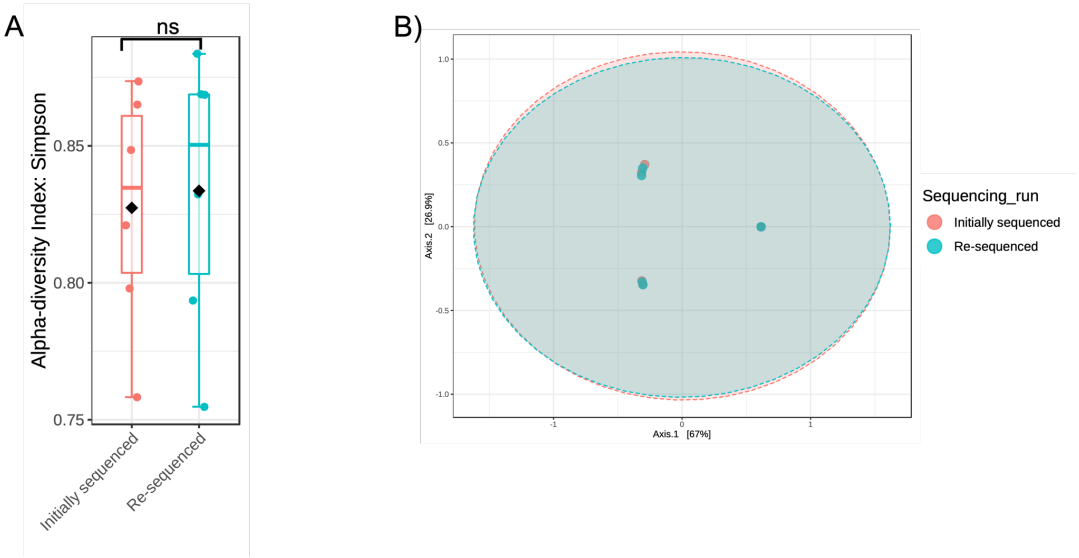

Figure 3.15 Diversity comparison for three microbial community samples which was re-sequenced using Nanopore without first repeating the PCR reactions. The three microbial community samples (labelled 1-3) were initially sequenced using Nanopore, and then the same amplicons were re-sequenced on a Nanopore MinION flow cell without first repeating the PCR reactions. A) Boxplots depicting the Simpson's alpha-diversity index values B) Principal coordinates analysis plot based on community membership using the Jaccard index. A t-test on the Simpson's alpha-diversity index values was performed, where 0.01<p<0.05 *, 0.01<p<0.001 **, p<0.001 *** and p<0.0001 ****.

3.3 Discussion

Since oral bacteria are known to aggregate as complex biofilm communities in nature, previous *in vitro* oral multispecies biofilm models have been reported that have helped to better understand periodontitis. To begin this study, a literature review was completed to determine how prior studies had established microbial community models which were associated with periodontal disease. From the initial works of Guggenheim *et al.* (2001), the Zürich biofilm model was frequently chosen as the model of choice and developed upon by other research groups. The following five species were included in the Zürich biofilm model: *A. oris; V. dispar; F. nucleatum; S. sobrinus* and *S. oralis*. By considering the bacterial species included in previously reported *in vitro* subgingival plaque models (Bradshaw *et al.,* 1990; Kinniment *et al.*, 1996; Peyyala *et al.*, 2011; Sánchez *et al.*, 2011; Ammann *et al.*, 2012; Park *et al.*, 2014; Soares *et al.*, 2015; Thurnheer *et al.*, 2016; Bloch *et al.*, 2017; Kommerein *et al.*, 2017), a total of 18 bacterial strains were selected for this study. This included both commensal bacteria such as Gram-positive aerobes and facultative anaerobes associated with health (such as the genera *Streptococcus, Actinomyces* and *Neisseria*) that would act as pioneer species and provide scaffolding for the growth of Gram-negative late colonisers which were frequently

associated with periodontitis. Oral *Streptococcus* species have also been demonstrated to bind to the sialic acids present on salivary mucins. *S. gordonii* DL1, one of the strains used in this study, expresses genes for a lectin-like adhesin factor called Hsa that binds sialic acids which is just one example of the many microbial protein adhesins *S. gordonii* holds and is part of the family of streptococcal serine-rich repeat (SRR) protein (Nyvad and Kilian, 1990; Takahashi *et al.*, 1997). Like streptococci, the oral bacterium *A. oris* is also one of the earliest oral colonisers and has been demonstrated to carry fimbrial adhesins for binding to salivary proteins and galactose-specific lectin which binds glycan receptors on streptococci to aid in the co-aggregation between *A. oris* and streptococci (Cross and Ruhl, 2018). For this reason, *A. oris* and the two *Streptococcus* spp. were included in this study, although a previously reported model suggested streptococci in fact impeded growth of *A. oris,* but promoted *P. gingivalis* growth (Ammann *et al.*, 2013). As the goal of this study was to mimic a periodontal community where *P. gingivalis* is thought to be a keystone pathogen, it was perhaps not detrimental if *A. oris* growth was consequently impeded. *V. dispar* was also included in this study's biofilm community because of its role as one of the earliest colonisers and its coaggregation properties with streptococci, as evidenced by Chalmers *et al.* (2008). An early dental plaque former, *N. subflava* was also included to help provide a foundation for microbial succession to take place.

It was concluded during the literature review process that a model which included more pathobionts (bacteria proposed as periodontitis-associated) than many of the previous models would be more representative of the periodontal microbial community, which is widely known to be characterised by the presence of these pathobionts although at low abundances for the Socransky's red microbial complex. One such pathobiont is the spirochaete *T. denticola*. However, this spirochaete was often absent in prior studies due to its fastidious nature, so the inclusion of *T. denticola* was deemed essential to provide a better representation of the periodontal plaque community. The remaining two members belonging to the microbial red complex *P. gingivalis* and *T. forsythia* were also included in this study, because of their strong associations with periodontitis (Socransky *et al.*,

1998) and were also frequently included in *in vitro* microbial community models. As discussed earlier in the literature review, it was hypothesised that microbial glycobiology may play an important role in periodontitis development. In this context, two separate *T. forsythia* strains with different surface glycan chains (pseudaminic acid in ATCC 43037 strain and legionaminic acid in UB4 clinical strain) which were previously demonstrated to interact differently in a mixed community (Bloch *et al.*, 2017) were included in the model to determine whether a specific glycan chain may better promote bacterial growth.

Other bacteria with close associations to periodontal disease are those within the orange microbial complex (Socransky *et al.*, 1998), which were described in the literature review and include the following: *P. intermedia; P. nigrescens; P. micra* (formerly known as *P. micros*); *F. nucleatum* spp.; *C. rectus.* and *C. showae* and these were therefore all included in this study. Although more bacteria have been described by Socransky with associations to periodontal disease, only a selection of species from these were included in this study because of the already labour-intensive work involved with maintaining cultures for 18 bacteria. Furthermore, *C. rectus* is also one of the most dominant species from deep periodontal sites and this was selected over *C. gracilis* because the latter species were typically isolated from shallow pockets instead (Macuch and Tanner, 2000). *F. alocis* and *D. invisus* were also included in the study due to their prevalence in chronic periodontitis (Hiranmayi *et al.*, 2017), although the two bacteria were often absent from previous models. Due to the complex nature of microbial communities, many of the chosen species are also found in close associations with others, such as *C. rectus* with *P. micra*, *P. gingivalis* with *P. micra, P. gingivalis* with *T. denticola,* plus *F. nucleatum* as a bridging microorganism to multiple species (Bradshaw *et al.*, 1998; Ammann, Gmür and Thurnheer, 2012; Neilands *et al.*, 2019). Lastly, both *F. nucleatum* subspecies *nucleatum* and *polymorphum* subspecies were included as the *nucleatum* subspecies is more associated with periodontitis, whereas *polymorphum* is considered more as a commensal microorganism, although it has also been correlated with a community shift towards a dysbiotic state (Kistler *et al.*, 2013). Sharma *et al.* (2005) have also reported on the synergy observed between *F.*

nucleatum and *T. forsythia* in biofilms which was dependent on cell-cell interaction. These were then taken as the basis for selecting the 18 strains in the mock community model. It would also have been useful to include oral fungi in the mock community model as *Candida* is frequently reported as present in the oral mycobiome, although this was beyond the scope of this study.

Following this work, it was key to establish a methodology for identifying different bacteria from mixed communities. There are several ways available in analysing a microbial community composition. Examples include the use of scanning electron microscopy, colony-forming unit counts and fluorescent *in situ* hybridisation following confocal laser scanning microscopy and shotgun metagenomics (Guggenheim *et al.*, 2001, 2009; Thurnheer, Gmür and Guggenheim, 2004; Sánchez *et al.*, 2011; Ammann, Gmür and Thurnheer, 2012; Song *et al.*, 2017; Naginyte *et al.*, 2019). Another way to analyse microbial communities would be to perform quantitative PCR assays on DNA extracted from mixed microbial communities which was the method chosen for this study. It would require the use of species-specific PCR primers and primers specific for each of the 18 bacterial strains were therefore assessed. Overall, it was possible to use species-specific qPCR primers available from the literature for 6 of the 18 bacterial strains (Chaban *et al.*, 2009; Ammann *et al.*, 2012; Park *et al.*, 2013). For the remaining 12 bacterial strains, primers specific for these bacteria were designed, although efforts to use primers already reported in the literature were tested for their specificity first by running multiplex end-point PCR reactions. This was found for the following bacteria: *A. oris; C. rectus; D. invisus; F. alocis; F. nucleatum; P. micra; S. gordonii; S. oralis* and *V. dispar*. Of these, the 16S rRNA gene sequence was initially tested for its conservation in multiple sequence alignments. This gene is widely used in classification as ribosomal RNA is ubiquitous in nature, functionally stable and the 16S rRNA gene is crucial in basic bacterial cell function (Eisenberg and Levanon, 2013), making this gene useful as a taxonomic target as it is highly conserved in all bacteria. Variable regions are also present in the 16S rRNA gene, which allows for the differentiation between different bacteria. However, based on multiple sequence alignments, the 16S rRNA gene was determined to be too highly

conserved to be able to differentiate between bacterial species in a particular genus such as *Streptococcus* for its use in classification and the literature was once again examined for alternative genes to the 16S rRNA gene. *Streptococcus* is an example of a genus that is widely known to have low variation in the 16S rRNA gene. Kawamura *et al.* (1995) have shown that the 16S rRNA gene sequences of *S. mitis, S. oralis* and *S. pneumoniae* had >99 % sequence homology to one another and so the discriminatory power of 16S rRNA gene sequencing would be limited here. Furthermore, streptococcal bacteria are highly competent which further complicates the species definition for this genus (Håvarstein, Hakenbeck and Gaustad, 1997). Garnier *et al.* (1997) have recognised the peptidoglycan biosynthesis gene D-alanine D-alanine ligase (*ddl*) was effective in differentiating between species in this genus and thus was tested in this study for the two *Streptococcus* species *S. oralis* and *S. gordonii*. The findings from Garnier *et al.* (1997) were consistent with what was found in this study by checking the multiple sequence alignment for the *ddl* gene for the *Streptococcus* genus. Secondly, primer sets based on the *ddl* gene which were only specific for either *S. oralis* or *S. gordonii* were verified to indeed be species-specific in multiplex end-point reactions. Yet, it is important to bear in mind that reference *ddl* gene sequences were only available from GenBank for 9 different *S. gordonii* strains and 123 different *S. oralis* strains. Multiple sequence alignments using these reference sequences revealed mismatches against the primer sets and thus the *ddl* sequence variation within the two species might not be fully captured. However, this would not be problematic in the mock model as it was inoculated with known strains (*S. gordonii* Challis strain and *S. oralis* C647 strain) and the primer sets were confirmed to be species-specific in the multiplex end-point PCR reactions. Conversely, there would be a possibility that not all strains of *S. gordonii* and *S. oralis* be captured in a more complex periodontal plaque community. Although specific primers for 16 of the 18 oral bacteria selected in this study were verified and this included the differentiation of two *T. forsythia* strains, it was not possible to find a gene sequence that could differentiate between the two *Fusobacterium* subspecies despite the same methodology being carried out. From this work, it was also concluded the use of species-specific primers would be too laborious for

investigating the composition of microbial communities and an alternative technique was pursued.

Next-generation sequencing was therefore tested as a means of analysing mixed microbial communities without the need for running 18 qPCR reactions, with each requiring a different species-specific primer set. The Illumina MiSeq platform was used but prior to beginning this work, it was important to first ensure any quantitation of bacteria in the communities were solely focused on viable cells. Any extracellular DNA (eDNA) or DNA that remained from bacterial cell lysis would need to be removed from analysis. Nocker *et al.* (2007) had reported the successful use of propidium monoazide (PMA) treatment on cell samples that allowed for the differentiation between intracellular DNA from viable bacteria and extracellular DNA. The principle behind this treatment was because when combined with qPCR, the photo-activating PMA dye would selectively bind only with extracellular DNA or DNA within membrane-compromised bacterial cells during a photoactivation step, whereby its covalent binding to the DNA would then block DNA amplification in downstream qPCR reactions. It was thought removing extracellular DNA prior to DNA extraction and PCR assays was important because including eDNA might give a false representation of the community composition. This was thought to be particularly important throughout biofilm development as dead bacterial cells would accumulate over time, lyse and eDNA could still be used as template in downstream PCR reactions to produce over-estimated abundance data. Within this study, it was demonstrated that as high as 96.8 % eDNA was detected in the biofilm communities where the total DNA content with and without eDNA removal were significantly different. This followed on from the completion of validating the PMA treatment-qPCR protocol, which was primarily due to ensuring the LED torch purchased for this protocol worked and that a 10-minute photoactivation step was optimal. To calculate the percentage of eDNA present in a sample, the DNA concentration measured for PMA-treated samples was taken as a percentage of the DNA concentration measured for untreated samples, which was then subtracted from 100. An unexpected outcome of this work, however, was the % eDNA values were higher than expected particularly at day 7, suggested either the

production of a lot of eDNA from these bacteria or significant bacterial cell lysis occurred prior to PMA treatment. Efforts to shorten the time between biofilms taken out of their optimum growth conditions and PMA treatment was thus attempted in all the biofilms that were grown following this work. The high eDNA percentage result was also in partial agreement to the comparison of total and viable DNA counts completed for plaque samples where PMA treatment reduced the DNA concentration of *S. mutans* DNA by 3-fold (Yasunaga *et al.*, 2013) and up to a 10-fold reduction on oral multispecies biofilm DNA (Alvarez *et al.*, 2013). Serrage *et al.* (2021) have also recently summarised the essential role eDNA plays in the formation of biofilm communities from its presence as part of the extracellular polymeric substance (EPS) that helps to encase bacteria together. Thus, it was proven the PMA-qPCR process was successful in removing eDNA and could therefore be integrated into the analyses of DNA harvested from biofilm community models. It was therefore decided only DNA from PMA-treated cells harvested from biofilm communities would be assessed in this study.

As well as the use of PMA treatment, another important step in preparing a DNA library intended for next-generation sequencing would be to first quantitate every amplicon sample and each would then be pooled together at the same equimolar concentration. This is a practice generally used in 16S rRNA gene community profiling as it ensures the equal representation of each sample in the DNA library pool. The NanoDrop 1000 spectrophotometer was readily available in our lab and this device was initially used to measure the total DNA concentration in the biofilm samples. Its principle is based on the absorption of all nucleic acid at wavelength 260 nm and any salt and protein contamination are highlighted by their absorbance at other wavelengths. Yet, because a particular drawback of using NanoDrop for DNA quantitation for this project was that even in biofilm DNA samples grown for up to 14 days where eDNA was not removed, the biofilm samples as previously described had DNA concentration <1 ng/µl. It was possible the use of the QIAmp DNA Mini Kit was insufficient for Gram-positive DNA extraction as it lacked a bead-beating step for breaking down Gram-positive bacterial cell walls. However, lysozyme, lysostaphin and mutanolysin were used in combination and in place of a

bead-beating step. The NanoDrop 1000 spectrophotometer is known to have low sensitivity compared to alternative quantitation methods, as the manufacturer advises only concentrations that are >2 ng/µl can be detected. An alternative method for quantitating DNA was therefore pursued. Qubit assays were trialled as a replacement for the Nanodrop as it has advantages over the NanoDrop, such as improved sensitivity and specificity due to its DNA-binding dye-based chemistry. For example, the Qubit dsDNA High Sensitivity (HS) kit uses a double-stranded DNA-binding fluorescent dye whereby the amount of fluorescence signal detected by a fluorometer means it only measures the concentration of DNA in samples, therefore producing accurate results. The Qubit dsDNA HS kit is also advertised as detecting DNA concentrations as low as 10 pg/µl although this study's DNA measurements obtained from pure bacterial cultures which were measured in both NanoDrop and Qubit assays found the Qubit produced error messages of "too low" when concentrations were below 0.1 ng/µl. To verify the two quantitation techniques, individual DNA concentrations extracted from 17 pure bacterial cultures were measured in parallel and compared between NanoDrop and Qubit assays. There was strong evidence that the Nanodrop over-inflated DNA concentrations as upon measuring DNA samples, nucleic acid concentrations varied widely between Nanodrop and Qubit readings. The reason for higher DNA concentration readings that were measured on the Nanodrop compared to the Qubit were likely due to high levels of impurities such as RNA which like DNA, could also have been absorbed at 260 nm on the Nanodrop. As the Qubit is a different technology to the Nanodrop, this effect was avoided and thus we would consider this a superior technique for quantitating DNA. It should be noted however that the presence of protein or salt contamination would not be observed in a Qubit assay and quality control by other means were necessary. The automated electrophoresis Agilent Bioanalyzer system (Agilent Technologies, USA) could be used for this means. As well as 16S rRNA gene community profiling, past studies (Thurnheer, Gmür and Guggenheim, 2004; Guggenheim *et al.*, 2009) focused on developing *in vitro* bacterial community models have also made use of the FISH technique to identify and visually and fluorescently label different bacteria within a multispecies community, but this technique is laborious due the necessity of

validating taxa-specific oligonucleotide probes so this technique was not used in this study. Until recently, FISH was also limited by the limited number of colours and hence, the number of bacteria that can be simultaneously visualised- a limitation similar to SEM imaging. An improved imaging technique called CLASI-FISH (combinatorial labelling and spectral imaging combined with FISH) is now available and uniquely allows up to 120 colours simultaneously, making it an effective technique for visualising the complexity present in oral samples (Valm, Mark Welch and Borisy, 2012). It was however decided that the time available in this PhD project proved too limited for the optimisation required to set up this technique in the current laboratory and although useful as a bacterial detection and visualisation tool, the focus of this project primarily remained on assessing the levels of different bacteria and how the models can be challenged and influenced over time.

The composition of a plaque sample pooled from 5 individuals diagnosed with periodontitis was assessed using the Illumina MiSeq sequencing platform as a means in verifying the bacteria selected for inclusion in the mock community model were true representatives of what would be found in plaque. As expected, the composition was far more complex than the 13 genera selected for the mock community model but as mentioned previously, it would be impractical to culture the 63 genera detected in the plaque sample in the laboratory, so a selection was initially chosen based on a review of the current literature. Nevertheless, compared to the simpler model seen here and in prior studies, Soares *et al.* (2015) successfully recovered 35 of the 40 species in their oral biofilms. Regarding the pooled plaque sample sequenced in this study, two of the three oral bacteria most highly associated with periodontitis (Socransky *et al.*, 1998) were the first and fourth highest in relative abundance. These were *Porphyromonas* and *Treponema* respectively, although the third red oral microbial complex bacterium *Tannerella* was the 17th most dominant genus in the plaque community. It was also promising to observe that 10 of the 13 genera which were selected for the mock community model did in fact belong to the pooled plaque community's 20 most dominant genera. The ten genera mentioned here included early colonisers such as *Streptococcus* and *Neisseria,* the bridging bacterium *Fusobacterium*, as well as

several strict anaerobes. An interesting finding was the high relative abundance of nearly 20 % found for bacteria belonging to the genus *Selenomonas*, which was the third most dominant genus after *Porphyromonas* and *Prevotella* in the pooled sample. There are several members of the genus *Selenomonas* and several reports have shown its association with periodontal disease (Dzink *et al.*, 1985; Ximénez-Fyvie *et al.*, 2000; Drescher *et al.*, 2010; Antezack *et al.*, 2021). The type species *S. sputigena* as an example, is reported to be significantly associated with chronic and aggressive periodontitis (Nagpal *et al.*, 2016). Although this genus is associated with periodontitis and is evidenced in this study's pooled plaque to be highly dominant, the work by Ximénez-Fyvie *et al.* (2000) suggested that compared to other bacteria such as those belonging to *Actinomyces* and *Fusobacterium*, *Selenomonas* was not found to be in high counts in subgingival plaque associated with periodontitis despite its reported ability to co-aggregate with fusobacteria and bacteria from *Actinomyces* (Kolenbrander *et al.*, 1989) and hence, was still not included in the mock community model. Following this work, it would be useful to investigate the variability present in microbial community composition between different pooled plaque samples and this will be described in chapter 5.

Although the Illumina MiSeq platform was successfully used to analyse the composition of a mixed spp. plaque sample, throughout this project, it took weeks to retrieve the sequencing data for the microbial communities as it was performed by an external DNA sequencing facility. To combat these time constraints, the use of the third-generation platform Nanopore sequencing was investigated as a replacement for MiSeq sequencing in the 16S rRNA gene community profiling of the microbial communities. Another major disadvantage of the Illumina MiSeq sequencing platform is that it can only generate good quality reads of up to 300 bp in length, resulting in low taxonomic resolution. Because of this, consideration must be taken in selecting a hypervariable region that would provide the best representation of a microbial community. Its site must be considered to ensure taxa of interest are not underrepresented which can directly over-estimate the abundance of other taxa. The V1-V2 hypervariable region of the 16S rRNA gene is ~311 bp and this was selected from the current literature as the region of choice

for profiling an oral microbial community. In support of selecting the V1-V2 region, Zheng *et al.* (2015) demonstrated higher species-level OTU richness and evenness were achieved in subgingival plaque samples with V1-V3 region when compared to V3-V4. Greater taxonomic resolution was also observed by Escapa *et al.* (2018) where for a set threshold of 100 % identity, only 14 species-level taxa present in the eHOMD v15.1 test dataset could not be classified to species level. This was compared to 63 taxa resulting from using the V3-V4 region. A pitfall of culture-independent analyses though is the risk of primer bias leading to the under- or over-reporting of members of a mixed bacterial community. Schulze-Schweifing *et al.* (2014) compared a variety of different primer sets on the characterisation of caries-associated dentine microbiome. The forward primer 27F-YM was included in the comparison study but alongside 27F-CM, 39F and 61F, all primers underestimated the levels *Actinobacteria* when compared to culture analysis that was performed in parallel. The authors were not able to improve the detection of high G+C sequences.

As culture-based analysis of complex multispecies communities has its own pitfalls, it was demonstrated that improving primer design was an alternative option to improve coverage. This was the reason why it was investigated whether the default 27F/1492R PCR primer set used in Nanopore 16S rRNA gene sequencing would indeed optimally detect each of the bacteria within a mixture. Firstly, multiple 16S rRNA gene sequence alignments for a selection of oral bacteria were obtained from HOMD v15.2 and observed whereupon the 27F/1492R primer set sat in the sequences. The same was performed for the 15 bacterial species selected for inclusion in this study's mock community model. The results showed adding wobble bases to the default 16S PCR primer set could ensure any base mismatches present in query bacterial sequences to the primer sequences would not be missed. This was confirmed particularly for the bacterium *Treponema denticola* when the two PCR primer sets used on a mock community sample prior to Nanopore sequencing were compared to sequencing on the arguably 'gold-standard' Illumina MiSeq platform. Using the modified 27F-YM/1492R-D primer set with Nanopore sequencing produced a community composition similar to the

results produced using Illumina MiSeq. The far lower relative abundance found for *Treponema* when the default 27F/1492R primer set was used compared to the two other techniques was a striking observation. This could have resulted from the reverse primer 1492R which lacked a degenerate base to detect any bacterial sequences that contained the nucleotide A or G at the variable base position highlighted in Figure 3.8. Therefore, the two experiments highlighted here showed the modified 27F-YM/1492R-D primer set was superior to the default 27F/1492R primer as it reduced the risk of potential primer bias.

The conclusion that the 27F-YM/1492R-D was the optimal 16S PCR primer set was further corroborated by the experiments involved with improving the known sequencing error rate associated with Nanopore sequencing. Updating the basecalling software Guppy and using the Nanopore MinION flow cell improved the sequencing error rate and for each of these, it was clear the use of the 27F-YM/1492R-D primer set consistently produced a lower sequencing error rate than when the default 27F/1492R primer set was used in the PCR reactions prior to creating a DNA library. It was possible to achieve a sequencing error rate at 2.2 % when all three improvements were used together. This was a marked reduction from the 6.0 % calculated when a Flongle flow cell with the same DNA library and the same Guppy software version was used instead. The reason why the focus on sequencing error rates was important here was because firstly, several reports have shown the error rate associated with Nanopore sequencing to be far higher than that with Illumina MiSeq (up to 15 % compared with 0.1 % respectively) and the aim of the work here was to investigate whether Nanopore sequencing could replace Illumina MiSeq sequencing in 16S rRNA gene sequencing (Winand *et al.*, 2019; Heikema *et al.*, 2020; Ciuffreda, Rodríguez-Pérez and Flores, 2021). Secondly, if bacterial species-level OTUs were clustered at either 3.0 % (Stackebrandt and Goebel, 1994) or even 1.5 % as later recommended by Stackebrandt and Ebers (2006), and the error rate was above these values, it would mean the OTUs could not be clustered to species level. The threshold of 5 % is generally accepted to discriminate between two genera (Stackebrandt and Goebel, 1994). While the thresholds described here should be taken with caution as it was previously

reported that many validly published named bacteria in fact do not respect the thresholds (Rossi-Tamisier *et al.*, 2015), the 6.0 % sequencing error rate mentioned earlier would void the ability to classify any sequence reads even to genus level and thus only family level classification would be achieved. As some of the oral bacteria selected for the mock community model belonged to the same family, for instance, *Tannerella* and *Porphyromonas* both belonged to the *Porphyromonadaceae* family, it would mean only low resolution could be achieved from any sequence reads obtained by Nanopore sequencing. It was therefore imperative that the sequencing error rate was lowered for the work involving Nanopore sequencing and this was achieved. Otherwise, the use of the Illumina MiSeq platform would remain instead. The issue with this would have been the long delays in obtaining the sequencing data back and any optimisation required for developing our the community model and creating later iterations of the model would thus also be delayed.

As reproducibility is important in research because it is imperative that the same data set and data analysis workflow can generate the same results at different times, it was investigated whether this was true for the microbiome experiments. However, data from microbiome studies are known to be affected by confounding factors such as batch effects which arise between independent runs of an experiment. This can introduce unwanted variation to the data and hence, can lead to data misinterpretation. It is known this can arise even when the methodology remains the same due to slight differences in sequencing depth, reagents, software and hardware, biological factors and personnel (Schloss, 2018). When dealing with large numbers of human or animal samples, it is also recommended that these will also need to be randomised across different sequencing runs. To test whether the same results could be achieved by performing a second set of sequencing runs, a mixed community sample was sequenced on a Nanopore MinION flow cell using both 27F/1492R and 27F-YM/1492R-D PCR primer sets and on Illumina MiSeq using the 27F-YM/338R-R PCR primer set. The genomic DNA that was already extracted which was kept at -20 °C was then re-amplified using the same batch of PCR primers and new DNA libraries were created and sequenced. Adopting the factors identified by Schloss (2018), effort was made to ensure the same batch of reagents

was used for both the first and second experiments. This included identical PCR primers and the reagents required for the creation of DNA libraries for the Nanopore and Illumina MiSeq sequencing runs. A new Nanopore MinION flow cell was used but the reagents used during the Nanopore sequencing runs and the software version remained identical. Unlike the Nanopore sequencing runs which were run in our laboratory, the two Illumina MiSeq runs were run externally by the University of Cambridge's DNA Sequencing Facility. As a result, it was not possible to guarantee the personnel, reagents and software used in the two MiSeq runs were identical. This might explain the variability observed in the community composition between the first and second MiSeq runs, where the relative abundance of *Treponema* increased by nearly 20 %. As the percentages of different genera were described in the analyses and not the absolute numbers of different bacteria, the reduction in the other genera might also have contributed to the higher relative abundance of *Treponema* in the second MiSeq run. It would be impossible to know whether this was true or whether the reverse was true. Although community diversity and membership remained comparable between Nanopore sequencing runs, variation in the relative abundances of genus-level taxa was observed between the first and second set of Nanopore sequencing runs after community genomic DNA was re-amplified. However, this was strikingly not observed when the same amplicons were directly re-sequenced (without an initial re-amplification step). The two experiments described together here suggested that variation was introduced during the re-amplification step and could be minimised if the PCR reactions were not repeated. This was verified for three different mixed community samples which were sequenced on two separate Nanopore sequencing runs.

3.4 Summary

The results in this chapter indicate that in summary, Nanopore sequencing could be used in place of the Illumina MiSeq platform for 16S rRNA gene profiling of microbial communities, but this work evidenced there were several ways to minimise any sequencing error risk. Firstly, the modified 27F-YM/1492R-D 16S PCR primer set containing wobble bases should be used. Secondly, the newest version

of the basecalling software Guppy should be used and finally, a Nanopore MinION flow cell instead of a Flongle flow cell should be used for a sequencing run. Though not related to sequencing error, the risk of batch effects in microbiome research should also be considered and thus all comparison samples should ideally be sequenced together. Where this is not possible, variability in composition arisen from batch effects could be reduced if the same amplicons are re-sequenced without first re-amplifying the community DNA. The next chapter moves on to using these techniques to analyse microbial community compositions in the development of a dysbiotic mock oral microbial community model.

Chapter 4 - Development of an *in vitro* periodontal biofilm community model

4.1 Introduction

It is widely understood that in nature, microorganisms grow and aggregate as complex biofilm communities rather than as individual planktonic cells. *In vitro* biofilm community models offer a way of understanding the complexity of biofilms by mimicking naturally occurring biofilms within the human body, under controlled, laboratory conditions.

There are several ways of modelling biofilm communities, where continuous culture involves the constant replenishment of growth medium and the removal of waste. Batch cultures in contrast are simpler to set up, whereby throughout the duration of an experiment, nutrients in the system are not replenished and the waste is not removed. Here, population growth is not maintained, and this can result in the eventual end of population growth. However, the concern for microbial population death in batch culture systems can be minimised by manually replenishing the growth medium and removing waste on a regular basis.

Historical laboratory models aimed at simulating periodontal diseases have involved growing biofilms on extracted teeth placed on agar plates (Magitot, 1878; Miller, 1890; Dietz, 1943; Pigman, Elliott and Laffre, 1952). However, replenishing the nutrients with this method was not possible. Fortunately, tools for studying microbial communities have since improved and the minimum biofilm eradication concentration (MBEC) assay biofilm inoculator (formerly known as Calgary Biofilm Device) available from Innovotech, Canada allows the user to do this with ease. Developed by Ceri *et al.* (1999), it is convenient and easy to set up as biofilms are established on hydroxyapatite-coated pegs which are suspended in growth medium sat within the individual wells of a 96-well plate. The pegs containing the established biofilms can then be transferred to a new 96-well plate containing fresh growth medium. The MBEC assay has been successfully used in several studies to model oral biofilms (Kistler, Pesaro and Wade, 2015; Soares *et al.*, 2015; Naginyte *et al.*, 2019; Baraniya *et al.*, 2020). As a result, the MBEC assay biofilm inoculator was chosen as the optimum tool for modelling oral mock and plaque biofilm communities in this PhD project.

4.1.1 Aims

The experiments described in this chapter aimed to develop a mock community model using the MBEC assay biofilm inoculator. The model would need to be fully supportive of multi-species growth and be representative of the dysbiotic bacterial communities occurring naturally in periodontitis.

4.2 Results

4.2.1 First iteration of an *in vitro* mock community biofilm

4.2.1.1 Cultural analyses of 7-day mock biofilms (iteration 1)

To check whether the 18 different bacteria selected in the previous chapter could grow under laboratory conditions, mock biofilm communities were set up and inoculated with the 18 bacterial species. The protocol for setting up this biofilm model is described in section 2.7 but briefly, an inoculum comprising 18 strains each at OD_{600} of 1 was created in growth medium containing 0.001 % mucin, 30 % heat-inactivated human serum (Sigma-Aldrich, USA) and 50 % modified fluid universal medium (mFUM). The inoculum was added to the individual wells of a MBEC plate. The plate was then incubated at 37 °C under anaerobic conditions for 7 days. The inoculum was replaced with fresh growth medium on day 1 and fresh growth medium was again provided on day 3.5.

To check whether the 18 different strains successfully grew in the biofilm model, bacterial cells were harvested from the mock communities on days 1, 3 and 7 and these were checked by culture analysis. This was done by Gram-staining and visualising the harvested bacterial cells by light microscopy (Figure 4.1). 1-day old biofilm cells comprised primarily of Gram-positive cocci but by day 3, multiple bacterial types were seen. Here, Gram-negative short rods and coccobacilli were observed alongside Gram-positive cocci. Longer Gram-negative rods also appeared in the biofilm communities by day 7. These Gram-negative rods could be *T. forsythia* or *F. nucleatum* although culture-independent methods would be required for their accurate identification.

The same harvested cells were also serially diluted up to 1 in 1000 and plated out onto Fastidious Anaerobe Blood agar plates and incubated anaerobically for up to 12 days. An assortment of different bacterial colony morphologies from the agar plates are also shown and labelled. Several colonies were selected from the agar plates and Gram-stained. The presence of *Fusobacterium* and *Streptococcus* species were observed on the agar plates which were inoculated with 1-day biofilm cells. For agar plates cultured from 3- and 7-day biofilms, the addition of black-pigmenting colonies (likely *P. gingivalis* and/or *Prevotella* spp.) and mixed species types were also seen. More diverse communities were also seen in the more mature biofilms. For example, very long Gram-negative rods were seen at day 7 biofilms which were absent from 1-day biofilms and were likely *Fusobacterium* spp. or the late colonisers *Tannerella* spp (which can also appear as fusiform cells). The cultural analyses described here suggested the biofilm models supported the growth of an array of different bacterial species. Molecular methods such as qPCR assays and microbiome analysis would however be required for definitive bacterial identification.

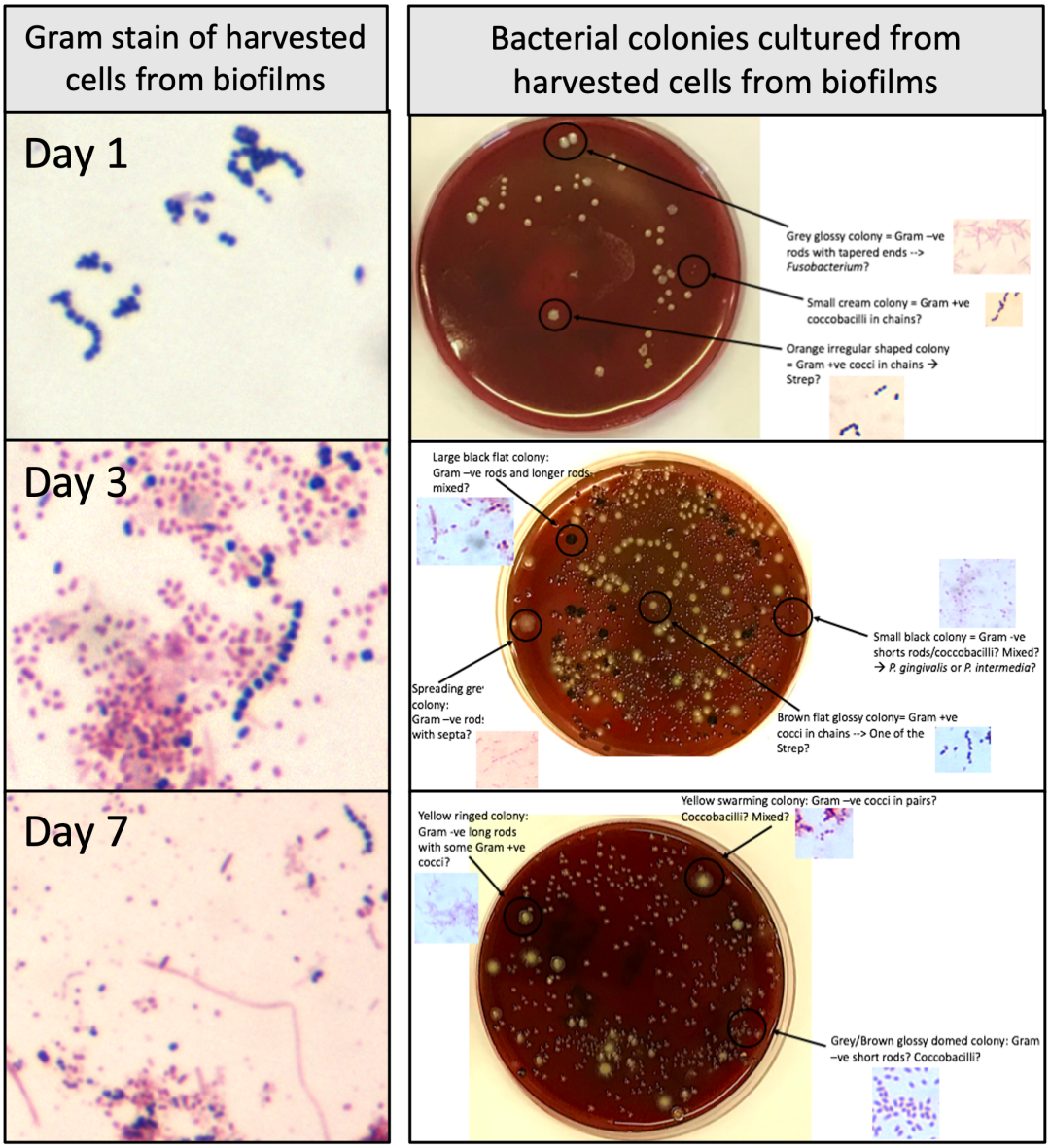

Figure 4.1 Cultural analyses of initial mock biofilms. Bacterial cells harvested from initial mock communities grown for 1, 3 and 7 days were analysed by Grain stain and by their colony morphologies. More diversely mixed bacterial communities were observed in the more mature biofilm communities.

4.2.1.2 Quantitation of specific bacteria in communities using qPCR

As qPCR assays using biofilm community DNA can definitively detect the levels of specific bacteria in the communities at different growth timepoints, qPCR reactions for several of the 18 bacteria were also run in parallel to the previously described cultural analyses. To ensure only DNA from viable bacterial cells would be assessed, each biofilm sample was first treated with propidium monoazide (PMA) prior to the qPCR reactions. The percentage of key bacteria (*F. nucleatum, P. gingivalis, P. intermedia* and *P. nigrescens*) in biofilm DNA samples harvested after 1-, 3- and 7-days growth were determined by PMA-qPCR and shown in Figure 4.2. Percentage

means were calculated from triplicate technical repeats and error bars were determined from SD. *F. nucleatum* was calculated as >100 % in 2 of 3 repeat 1-day biofilm communities, thus rendering the data invalid. This likely occurred because at 1-day biofilm growth, the total and *F. nucleatum*-specific DNA concentrations were all $<10^{-4}$ ng/µl so a small difference in concentration could lead to a large percentage change, thereby giving percentages >100. Means of 31.6 % and 30.3 % *F. nucleatum* were detected from 3- and 7- day biofilm communities respectively. These data suggested that DNA concentrations from 1-day biofilm communities could be too low to produce accurate and reliable results. The next important step would be to incubate the biofilms beyond 7 days in the future models, although the preliminary data here were encouraging that multiple species were present in the model even at low concentrations.

For the late colonisers *P. gingivalis, P. intermedia, P. nigrescens, T. denticola* and *T. forsythia* a general trend was observed whereby the DNA concentration extracted from viable cells reduced after 1 day of biofilm growth. The reference strain ATCC 43037 for *T. forsythia* was tested here and not the clinical *T. forsythia* strain UB4. Except for *P. intermedia* which was measured at a mean of 63.3 % for the 1-day biofilm communities, the remaining late colonisers that were assessed for their abundance were measured at percentages <20 %. By day 7 of biofilm growth, each of the five late colonisers which were tested had relative abundances <1 %. The data obtained here suggested that viable *Fusobacterium* spp. cells dominated in the communities throughout the biofilm development compared to the late colonisers *P. gingivalis, P. intermedia, P. nigrescens, T. forsythia* and *T. denticola*. For these late colonisers, their levels reduced over time to <1 % which could possibly be due to the model environment not being able to support their growth beyond day 1. As a result, further optimisation experiments were performed to improve the mock community model.

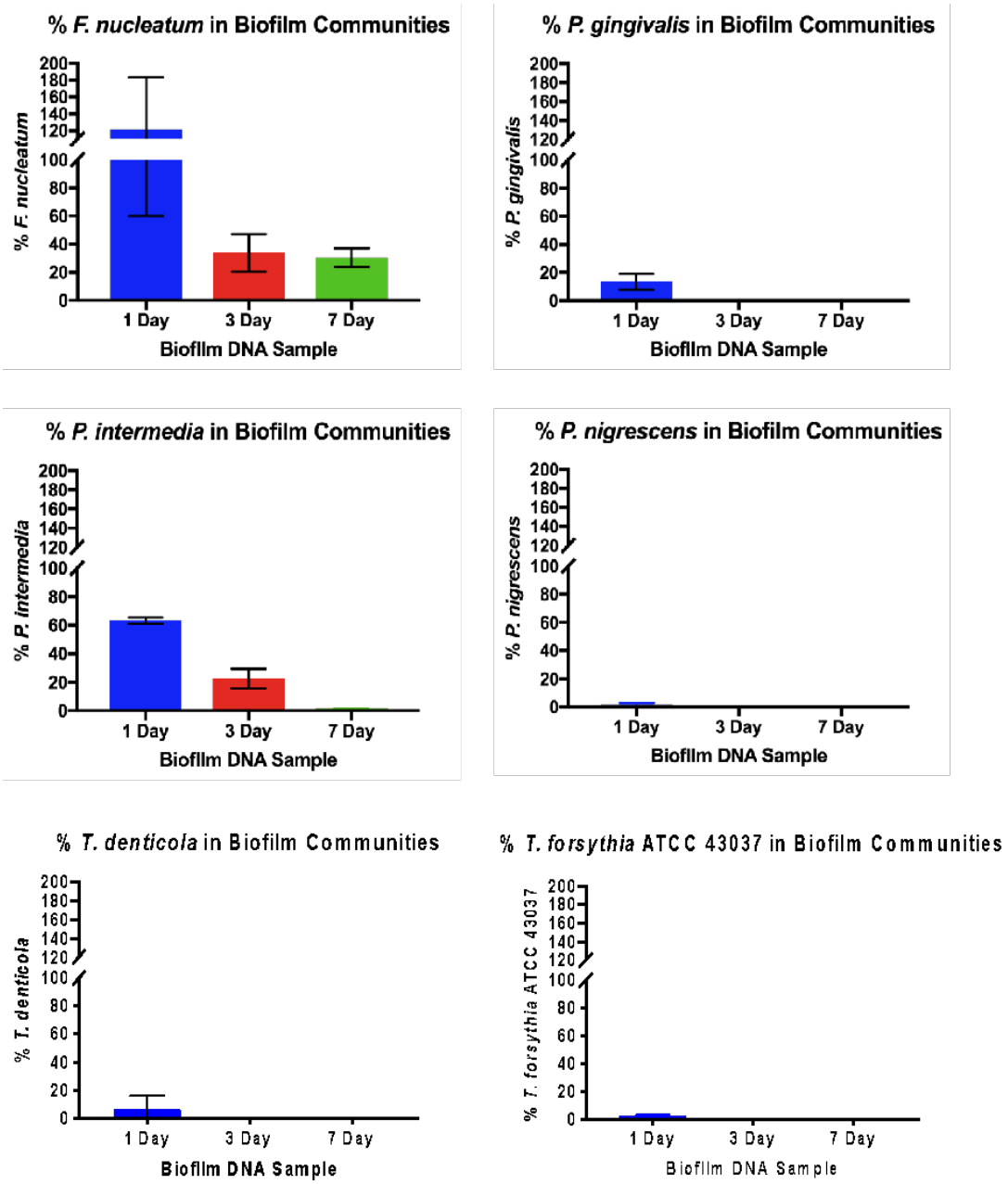

Figure 4.2 qPCR analysis of initial mock biofilms. The percentage of specific bacteria (*F. nucleatum, P. gingivalis, P. intermedia, P. nigrescens, T. denticola*, *T. forsythia* ATCC 43037) harvested from mock biofilm community models grown for 1, 3 and 7 days. Each biofilm sample was treated with propidium monoazide (PMA) to remove extracellular DNA. Means were calculated from n=3 and error bars = SD.

4.2.2 Normalisation of bacterial cell abundances in mock community inoculum

To normalise the bacterial cell concentrations across all 18 bacteria in a simple manner, the initial model described for the previous trial run was inoculated with OD_{600} = 1.0 suspensions for each bacterium. However, optical densities which measure the amount of light absorbed from cell suspensions are in fact influenced by cell size and shape. Larger bacterial cells at the same optical density as smaller bacterial cells would have fewer cells in the suspension. Therefore, creating optical

densities of 1 at a wavelength of 600 nm for each of the 18 bacterial strains would not ensure consistent cell densities across all the strains. As such low levels of *P. gingivalis* and *P. nigrescens* were detected in the model from the qPCR assays, it was important to check whether their low levels in the community were as a direct result of their lower cell abundances in the mixed inoculum compared to the other species. One might theoretically expect the presence of 5.6 % each species in the 18-multispecies inoculum if all OD 1.0 suspensions contained the same number of cells. To assess the number of viable bacterial cells in an OD_{600} 1.0 suspension, the colony-forming units (CFUs) representing the clonal expansion of a single viable bacterial cell was measured for each of the bacterial strain. Cell abundances at OD_{600} 1.0 for each of the 18 bacterial strains are shown in Figure 4.3. Measurements were taken from two independent experiments although those with highly variable readings were repeated once more and highlighted in colour.

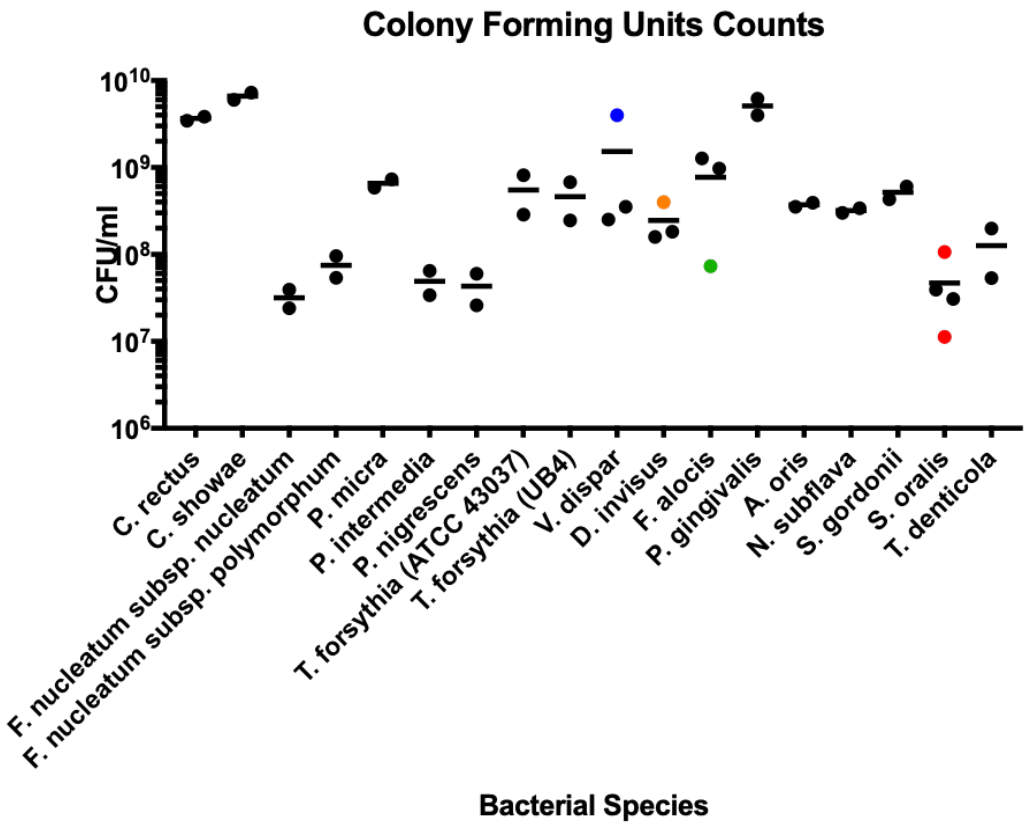

Figure 4.3 Bacterial cell abundance as determined by measuring colony-forming (CFU) units. Each point represents an average reading of CFU/ml for three technical repeats from two independent experiments, with exception of those with highly variable measurements. For these, additional biological repeats were completed, and significantly different readings are coloured in the plot for clarity.

Table 4.1 summarises the mean viable cell abundance (CFU/ml) from the two closest readings. From this work, it was evident that certain bacteria such as *C. showae* and *P. gingivalis* in 1-ml suspensions contained as many as 100-fold more cells than *S. oralis, T. denticola* and species belonging to the genera *Fusobacterium* and *Prevotella*. This therefore highlighted the discrepancy in the cell abundance between optical density readings and those measured from viable cell counts. It demonstrated the need to normalise this parameter in the future model. As 3.17 x 10^7 CFU/ml was the lowest cell abundance found for the 18 bacteria measured, the cell abundance of 10^7 cells/ml was chosen as the cell abundance parameter. Consequently, the next iteration of the mock community model would be inoculated with 10^7 cells/ml of each of the 18 different bacteria. This would ensure all 18 bacterial cell abundances are equalised, and any differences observed would be a direct result of changes occurring during biofilm community growth.

Table 4.1 Mean of bacterial cell abundance (CFU/ml) for each bacterial strain. The mean CFU/ml was calculated from the two closest repeats.

Bacterial Strain	OD	CFU/ml Closest Repeat 1	CFU/ml Closest Repeat 2	CFU/ml Mean of Closest Repeats
C. rectus	1	3.46E+09	3.86E+09	3.66E+09
C. showae	1	6.00E+09	7.27E+09	6.63E+09
F. nucleatum subsp. *nucleatum*	1	3.93E+07	2.40E+07	3.17E+07
F. nucleatum subsp. *polymorphum*	1	9.60E+07	5.40E+07	7.50E+07
P. micra	1	7.34E+08	5.86E+08	6.60E+08
P. intermedia	1	3.40E+07	6.47E+07	4.93E+07
P. nigrescens	1	2.60E+07	6.00E+07	4.30E+07
T. forsythia (ATCC 43037)	1	2.87E+08	8.13E+08	5.50E+08
T. forsythia (UB4)	1	6.80E+08	2.47E+08	4.63E+08
V. dispar	1	2.53E+08	3.53E+08	3.03E+08
D. invisus	1	1.83E+08	1.59E+08	1.71E+08
F. alocis	1	9.70E+08	1.27E+09	1.12E+09
P. gingivalis	1	6.20E+09	4.00E+09	5.10E+09

A. oris	1	3.93E+08	3.53E+08	3.73E+08
N. subflava	1	3.40E+08	3.00E+08	3.20E+08
S. gordonii	1	6.07E+08	4.33E+08	5.20E+08
S. oralis	1	3.93E+07	3.07E+07	3.50E+07
T. denticola	1	1.99E+08	5.35E+07	1.26E+08

4.2.3 Optimising the mock community biofilm model (iteration 2)

4.2.3.1 Molecular-based analysis of the biofilm compositions from optimised model iteration 2

As a result of the findings described earlier for the initial mock community modelling trial run (such as the low total DNA concentration detected in the younger biofilms and low *P. gingivalis* abundance in 3- and 7-day biofilms), a new set of mock biofilm communities was grown with some modifications. This included growing the biofilm communities for longer and harvesting the biofilms at days 3, 7 and 14 of growth instead. To assist the growth of *P. gingivalis* and *T. denticola*, the pegs on the MBEC plates were also suspended in 100 % inactivated human serum for 24 h before inoculation. Lastly, each individual bacterial suspension was adjusted to a cell concentration of $1x10^7$ cells/ml prior to creating a mixed community inoculum during the model set up. The normalisation of bacterial cell concentration across all bacterial strains was possible because of the colony-forming units (CFUs) data described previously.

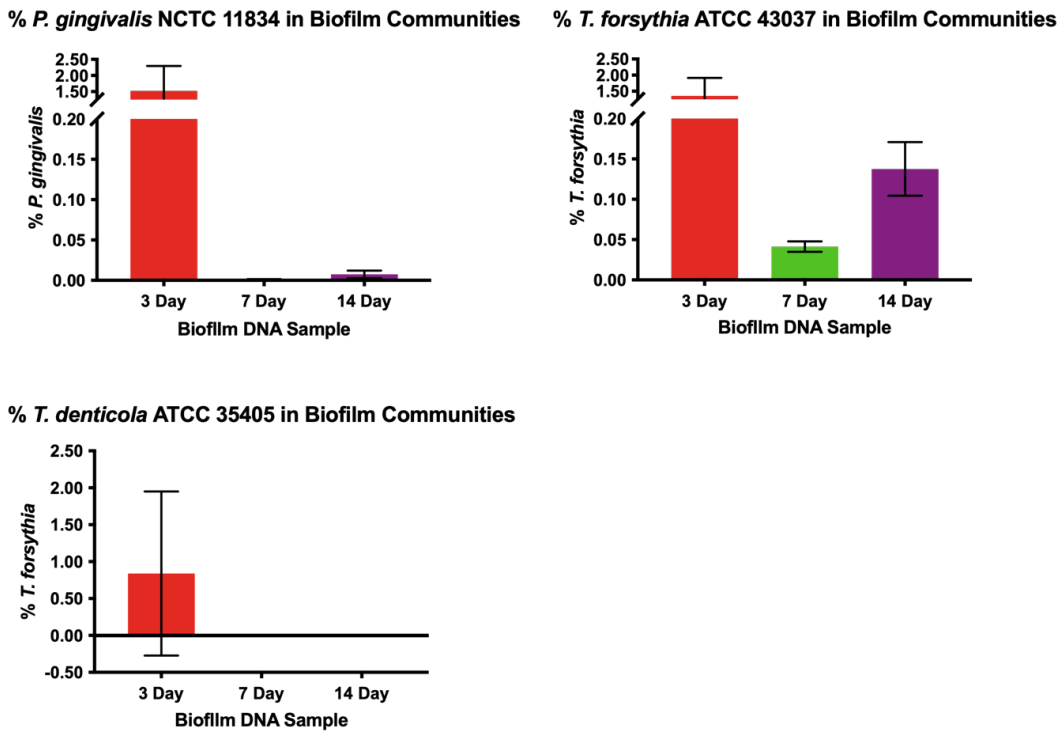

Figure 4.4 Percentages of red microbial complex bacteria in mock model iteration 2 communities. The percentages of *P. gingivalis* NCTC 11834, *T. forsythia* ATCC 43037 and *T. denticola* ATCC 35405 were harvested from mock biofilm communities grown for 3, 7 and 14 days. Protocol optimisation occurred by longer biofilm growth, normalisation of bacterial cell abundance during biofilm model set up, and the use of serum in preconditioning of a MBEC plate. Each biofilm sample was treated with propidium monoazide (PMA) to remove extracellular DNA. Means were calculated from n=3 and error bars = SD.

Figure 4.4 shows the percentages of the three bacterial species classed within the red microbial complex that were harvested from the mock model iteration 2. An increase in the percentage of *P. gingivalis* was seen in the optimised 3-day mock biofilm community compared to the initial iteration prior to optimisation. A mean of 1.5 % *P. gingivalis* vs 0.005 % was found respectively. In a similar manner to the pre-optimised mock model communities, the levels of the three bacterial species were also reduced after day 3 of biofilm growth to relative abundances <0.05 %. Only *T. forsythia* appeared to increase to >0.1 % by day 14 of biofilm growth. *P. gingivalis* and *T. denticola* however remained at almost undetectable levels, with the means for these two bacteria measured at <0.01 % in the biofilm communities.

To compare between using species-specific qPCR to 16S rRNA gene community profiling in assessing the composition of the biofilm communities described above, the 7- and 14-day communities were also sequenced using the Illumina MiSeq

platform. The methodology used to perform this is described in section 2.8.6. In brief, the V1-V2 hypervariable regions of the 16S rRNA gene were sequenced and the Human Oral Microbiome Database was used to classify the sequence reads to genus level. The relative abundances of *Tannerella* and *Treponema* were generally comparable between the two methods, with no sequenced reads detected for either genus. As illustrated in Figure 4.5A and Figure 4.6A , the genus *Porphyromonas* on the other hand dominated in all triplicate communities at both days 7 and 14 of growth. A relative abundance of >75 % was measured for *Porphyromonas* here, which contrasted with the 0.005 % observed with the qPCR data described previously. Upon further investigation, it became clear there was a contaminant present in the inoculum used in setting up the biofilm communities. Genome sequencing of this contaminant then revealed that a *Porphyromonas* spp. was growing in a mixed culture with *Campylobacter rectus*. This was not detected in the qPCR data as PCR primers specific to only *P. gingivalis* was used. The contaminant was subsequently removed from future experiments and for clarity, the genus *Porphyromonas* is removed in Figure 4.5B and Figure 4.6B. Here, the highest non-contaminating genera present in the 7-day mock biofilm communities are clearly shown as *Streptococcus* (mean of 18.7 % relative abundance across three replicate communities), *Campylobacter* (mean of 1.1 %), *Dialister* (mean of 0.8 %) and *Fusobacterium* (mean of 0.3 %). For the same communities grown for a further 7 days, a similar picture was observed for the mean relative abundance of *Streptococcus* (19.3 %), *Fusobacterium* (0.5 %) and *Dialister* (1.0 %), although there were lower levels of *Campylobacter* (0.2 %) compared to the 7-day old biofilms. The data described here have also suggested that the replicate communities which were grown in parallel were consistent with each other.

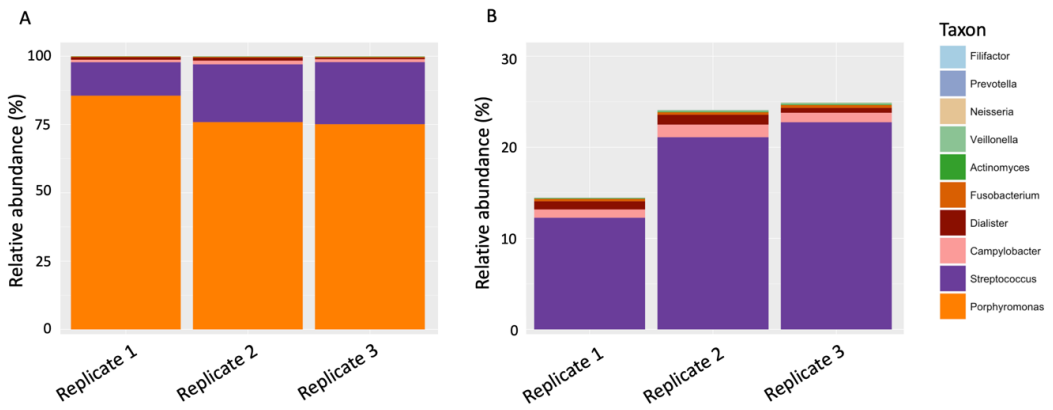

Figure 4.5 Genus-level relative abundance plots of 7-day iteration 2 mock communities. Relative abundances calculated for communities plotted with (A) and without (B) the genus *Porphyromonas* for clarity. The taxa are ordered by abundance from bottom (highest) to top (lowest).

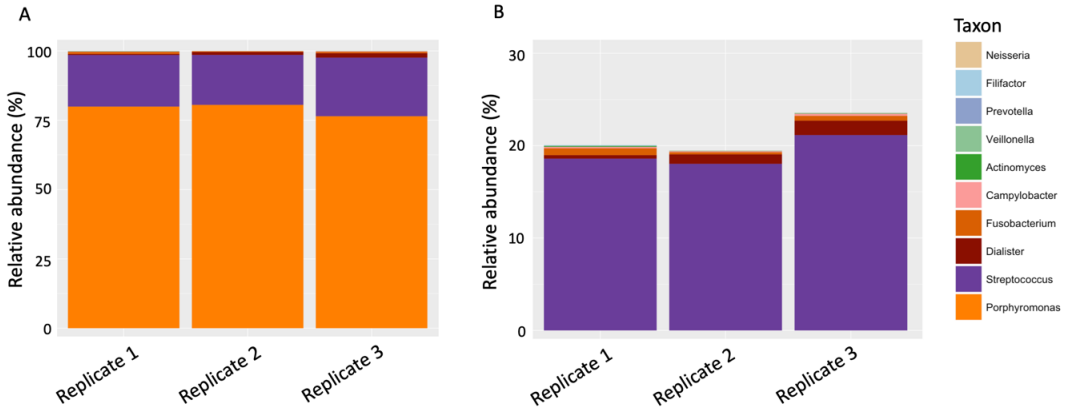

Figure 4.6 Genus-level relative abundance plots of 14-day iteration 2 mock communities. Relative abundances calculated for communities plotted with (A) and without (B) the genus *Porphyromonas* for clarity. The taxa are ordered by abundance from bottom (highest) to top (lowest).

4.2.3.2 Scanning electron microscopy as a tool for analysing the composition of an optimised mock community biofilm model (model iteration 2)

To enable the imaging of the biofilm communities at high resolution, scanning electron microscopy (SEM) on the same biofilm samples was also performed. Here, the biofilm sample pegs remained intact for direct visualisation but were fixed, dehydrated, and dried before visualisation. This was conducted for the mock biofilm communities grown for 3, 7 and 14 days (Figure 4.7). This revealed the more mature biofilm communities at days 7 and 14 were denser than an equivalent community grown for only 3 days. Although some very long rods were present, coccal-shaped, and coccobacilli-shaped bacteria dominated the 3-day old biofilm community (shown by asterisk). Arguably, there was however a more even

distribution in the older biofilm communities which could support the molecular-based data described previously. It was also clear that across all the biofilm communities, the aggregation of different bacterial types and the connecting extracellular matrix (ECM) were seen though this was better visualised at a higher magnification (40,000x, labelled red arrows). This work has therefore shown that it was possible to obtain high-magnification and high-resolution images of the biofilm communities grown on the hydroxyapatite-coated pegs. This has allowed us to observe not only different bacterial morphotypes, but also their distribution, how they were spatially organised with one another, and their embedment onto the peg substratum over time.

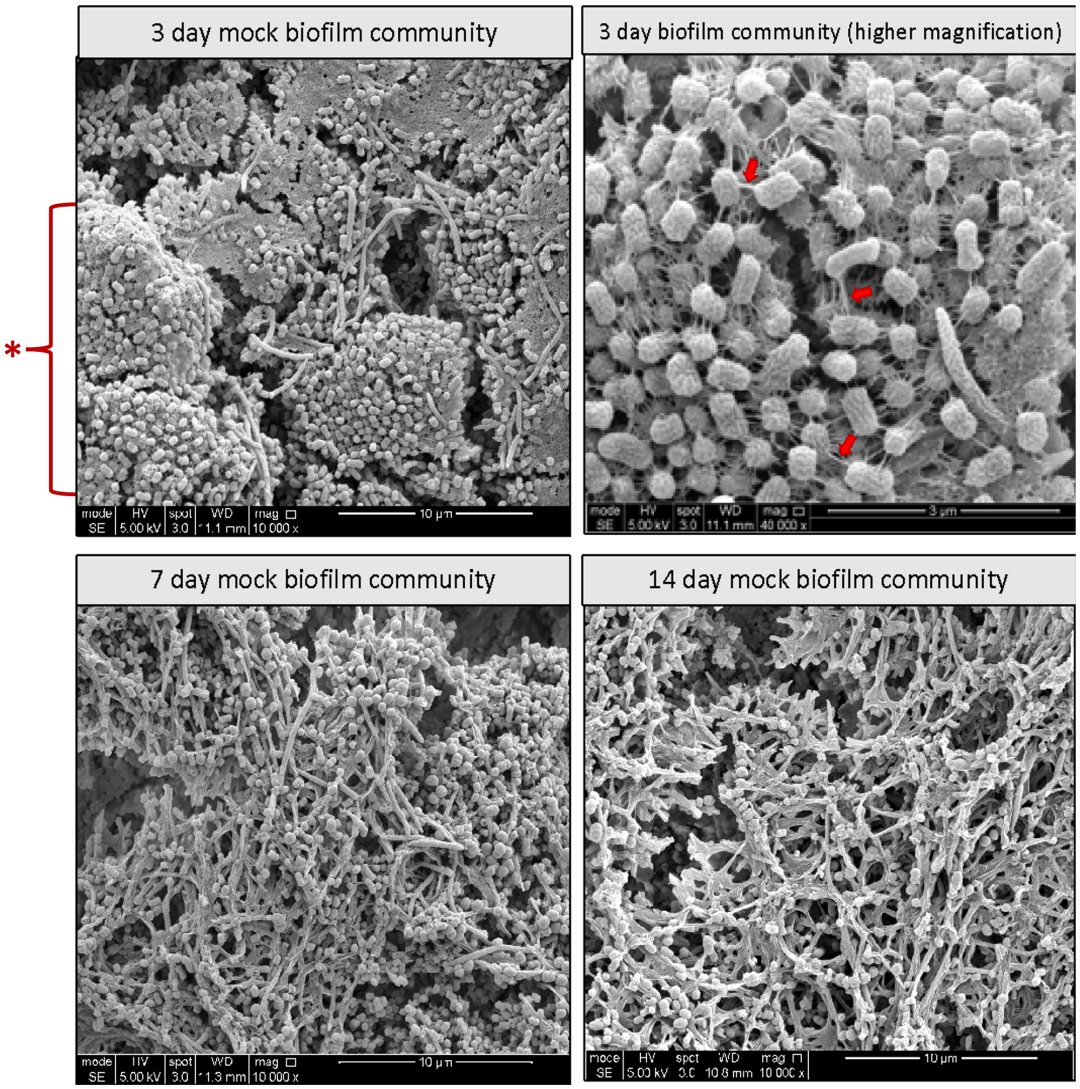

Figure 4.7 Scanning electron microscopy (SEM) images of iteration 2 mock biofilm communities. The biofilms were grown for 3, 7 and 14 days, demonstrating the spatial organisation of different bacterial types and extracellular matrix (shown by red arrows in higher magnification) within the multispecies communities. Aggregation of different cell types can also be observed but coccal-shaped bacteria clearly dominate (shown by asterisk).

4.2.4 Analysis of the community composition of model iteration 3 mock using Nanopore MinION sequencing

Previous iterations of the mock biofilm model suggested a dominance of *Fusobacterium* and *Streptococcus* in the biofilm communities. To further encourage the growth of the red microbial complex bacteria in the multispecies communities for the mock model iteration 3, *S. gordonii* was removed from the inoculum and the bacterial cell abundance of *F. nucleatum* in the multispecies inoculum was reduced 10-fold from $1x10^7$ cells/ml to $1x10^6$ cells/ml. The bacterial cell abundances of *P. gingivalis*, *T. forsythia* and *T. denticola* as well as *P. intermedia* and *P. nigrescens* were also increased to $2.5x10^7$ cells/ml. This value was selected because as previously shown, a *T. denticola* suspension at an optical density of 1 contained the fewest number of bacterial cells. This was measured at a cell abundance of $2.5x10^7$ cells/ml. The contaminating *Porphyromonas* spp. detected in the previous model iteration was also removed and was therefore not present in the inoculum.

As already discussed in Chapter 3, there are several benefits to sequencing and analysing microbial community compositions with the Nanopore MinION device in place of the Illumina MiSeq platform. Together with the speed and lower cost involved with Nanpore MinION sequencing, this study's previous data have also demonstrated that the sequencing data obtained from the two sequencing techniques were comparable. As such, using the Nanopore MinION device for profiling the mock communities was another adjustment that was made in setting up and in analysing a third iteration set of mock biofilm communities. Despite being able to sequence the full 16S rRNA gene with the use of the Nanopore MinION device, this study previously measured the sequencing error rates as >2 %. Speciation from the 16S rRNA gene using this technique could therefore not be achieved. For this reason, only one species per genus was included in the multispecies inoculum of model iteration 3. There were 13 genera present and those species most highly associated with periodontitis were selected and included *C. rectus* and *P. intermedia*. The bacterium *F. nucleatum* subsp. *polymorphum* was

also selected due to its synergistic relationship with *T. forsythia* and it is ubiquitous in oral samples. These bacteria were inoculated alongside reference strains belonging to *A. oris, D. invisus, F. alocis, N. subflava, P. gingivalis, P. micra, S. oralis, T. forsythia, T. denticola* and *V. dispar*, and grown for up to 21 days. As a comparator community, a simple biofilm model was also set up. This included only 6 bacteria: *D. invisus; F. nucleatum* subsp. *polymorphum; P. gingivalis; P. intermedia; T. forsythia* and *T. denticola.* The genus *Campylobacter* dominated in the 13-genera mixed communities (Figure 4.8A), whereas *Fusobacterium* dominated in the simpler 6-genera mixed communities (Figure 4.8B). For both models, the relative abundances of the three red microbial complex bacteria remained at <0.0001 % in 21-day old biofilms and thus it was not possible to improve their growth in the biofilm communities. The genera *Prevotella* and *Dialister* were detected in both models.

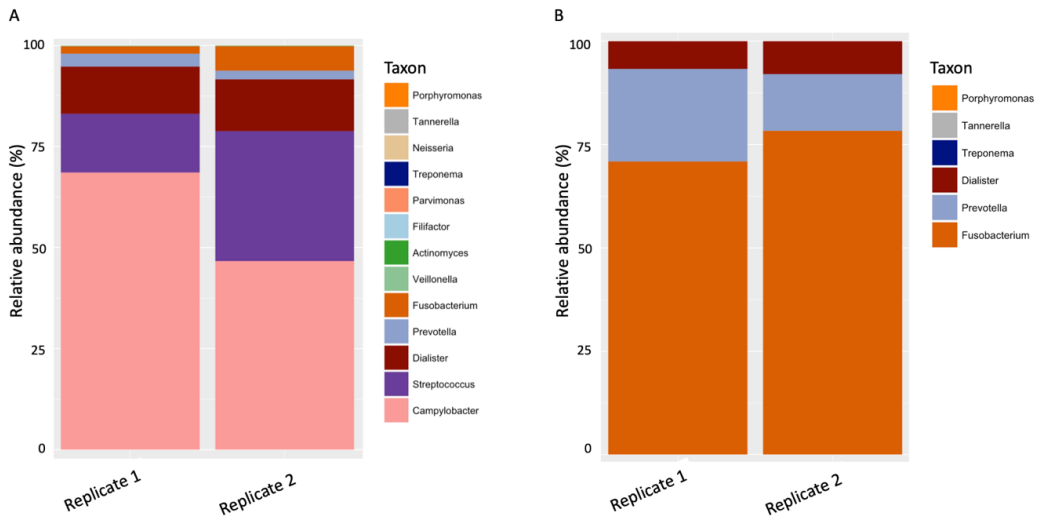

Figure 4.8 Relative abundance of genus-level taxa in iteration 3 mock communities profiled using Nanopore MinION. The communities were grown for 21 days and inoculated from using A) one species per genus and B) 6 species.

4.2.5 Effect of mucin concentration and inoculum replacement day on community composition

The previous data have generally shown the three red microbial complex bacteria were unable to grow in the *in vitro* mock biofilm model. It was theorised that replacing the mixed microbial community inoculum at day 1 with fresh growth medium was not allowing any slow growing bacteria such as *P. gingivalis, T.*

forsythia or *P. gingivalis* (all typically take >3 days to grow) to attach to the substratum or to other colonising bacteria such as *F. nucleatum.* This latter bacterium typically takes 2 days to grow on agar plates. To test this and to see if increasing the concentration of mucin from 0.001 % to 1% would improve *T. forsythia* biofilm attachment and growth on the MBEC plates, *T. forsythia* was inoculated onto MBEC plates at a concentration of $2.5x10^7$ cells/ml in mFUM growth medium containing 0.001 % mucin and 1 % mucin. The MBEC plates were incubated under anaerobic conditions for 7 days, with the inoculum being replaced with fresh mFUM growth medium on either day 1 or day 3. The biofilms were then harvested by vibration on day 7 and neat bacterial suspensions were plated out in triplicate onto FAB-NAM plates. These agar plates were incubated for 9 days under anaerobic conditions until colonies could be clearly observed and counted. Aside from the concentration of mucin and the inoculum replacement day, all other experimental conditions remained the same for all the biofilms.

As shown in Figure 4.9, for the biofilms which had the inoculum replaced on day 1, only one *T. forsythia* colony-forming unit (CFU) was observed on the FAB-NAM plates after the cells were harvested from the MBEC pegs. For biofilms whereby the inoculum was replaced on day 3, *T. forsythia* growth was clearly observed on the FAB-NAM plates. This was true for both mucin concentrations used in the biofilm growth medium, where a mean of 27.7 CFUs was measured from plating out 10 μl of the harvested *T. forsythia* single species biofilms when grown in 0.001 % (w/v) bovine submaxillary mucin. This was compared to a mean of 14.3 CFUs which was measured when 1 % (w/v) bovine submaxillary mucin was used. This equated to the recovery of $2.8x10^3$ and $1.4x10^3$ viable *T. forsythia* cells/ml respectively. The methodology for setting up an *in vitro* mock biofilm model was therefore altered so that the mock community inoculum was replaced with fresh growth medium 3 days after setting up to allow slow-growing bacteria to become established prior to medium replacement. The concentration of bovine submaxillary mucin was also increased from 0.001 % to 1 % mucin to increase the chance of red microbial complex growth.

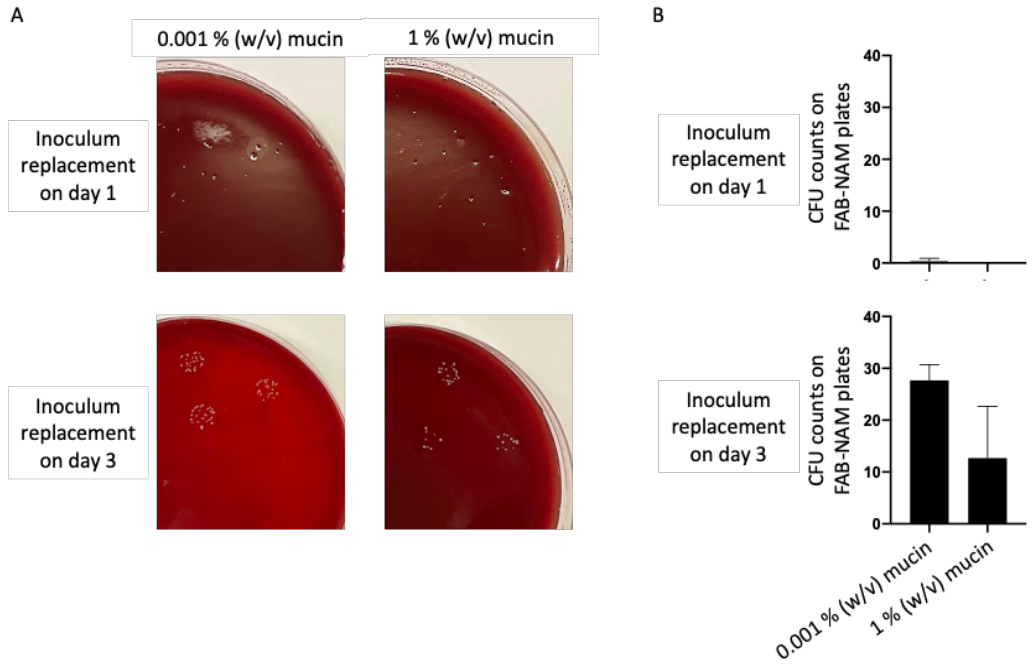

Figure 4.9 CFU counts of harvested *T. forsythia* biofilms grown under different conditions. Here, 10 µl of the harvested 7-day *T. forsythia* biofilm cells was plated neat onto FAB-NAM plates and incubated under anaerobic conditions for 9 days. Colony forming units (CFUs) was clearly seen (A) and were counted (B) where the mixed microbial community inoculum was replaced on day 3 compared to when the inoculum was replaced on day 1.

4.2.6 Effect of different mucin sterilisation techniques on a mock biofilm model

4.2.6.1 Investigating the potential effect of mucin degradation from autoclaving

The previous biofilm communities described in this chapter were grown in growth medium containing autoclaved bovine submaxillary mucin (BSM). One of the aims of this project was to not only develop a mock community model, but to also investigate the importance of glycosylation on oral bacterial growth. As mucin and human serum contain glycosylated sugars, it was therefore essential to test whether the proteins were at risk of denaturation due to the high temperature and pressure associated with autoclaving. Unlike human serum, the BSM that is commercially available (Sigma) is not sterile so as an alternative to autoclaving, BSM at 10 mg/ml were filter-sterilised using 0.45 µm filters. BSM at this concentration which was either non-sterile, autoclaved or filter-sterilised was run on SDS-PAGE protein gels and the proteins were visualised by staining the gel with Instant Blue as well as with the Pro-Q Emerald 300 Glycoprotein Stain Kit (Figure 4.10). When compared to the non-sterilised mucin, the autoclaved equivalent suggested a loss of the larger molecular weight proteins (proteins with approximate weight of 62-240 kDa), whereby its denaturation likely resulted in an

increase of smaller molecular weight proteins (<27 kDa). The filter-sterilised mucin in contrast looked comparable to the non-sterilised mucin, as evidenced by the protein gels when stained with both Instant Blue and with the Glycoprotein Stain. This finding led to the use of filter-sterilisation in place of the autoclave for sterilising mucin in future work.

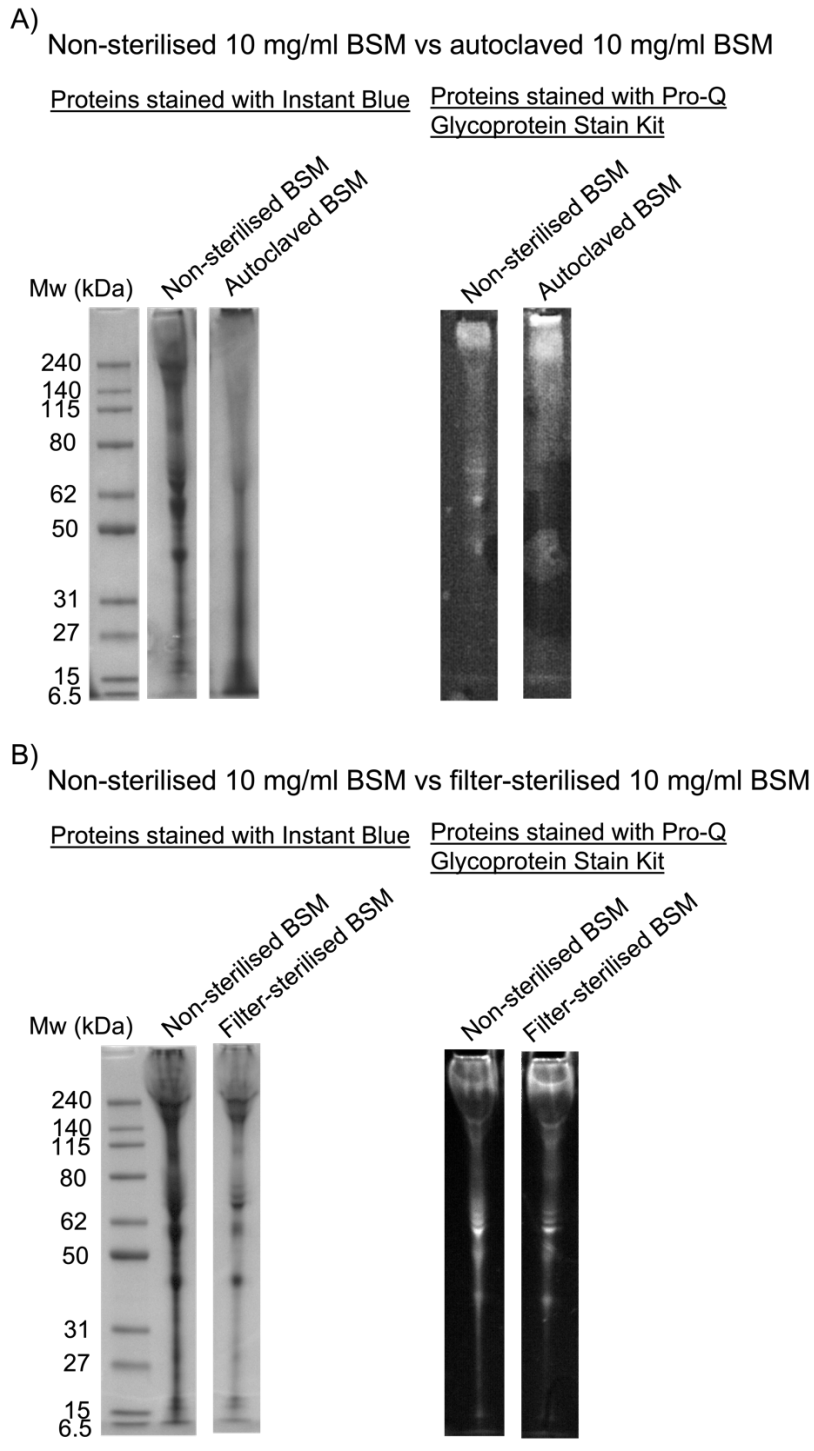

Figure 4.10 Testing bovine submaxillary mucin (BSM) sterilisation techniques. BSM at 10 mg/ml was either left unsterilised, (A) autoclaved or (B) filter-sterilised using 45 μm filters. The proteins from each condition

were then ran on a 5-12 % Bis-Tris gradient SDS-PAGE gel and stained with Instant Blue (left. The Pro-Q Emerald 300 Glycoprotein Stain Kit (right) was also used to visualise glycoproteins.

4.2.6.2 Investigating the potential effect of autoclaved versus filter-sterilised mucin in the mock biofilm model

To further investigate the potential effect of using filter-sterilised mucin in place of the autoclaved mucin used in the previous mock biofilm experiments, mucin that was sterilised from both sterilisation techniques was added to the growth medium during the set-up of a mock biofilm model. In biofilms grown using autoclaved mucin (Figure 4.11A) and filter-sterilised mucin (Figure 4.11B), streptococcal bacteria dominated. Each biofilm community was represented by >85 % *Streptoccocus*, with anaerobes such as *Dialister* and *Veillonella* forming much of the remaining percentage. Differences between the two types of mucin sterilisation techniques were also detected. The most obvious difference was that for mock biofilms using autoclaved mucin, a mean of 5.9 % of the 14-day old communities were found to belong to the genus *Veillonella* and a mean of 4.6 % of the 21-day old communities also belonged to *Veillonella*. In contrast, for biofilms using filter-sterilised mucin, a mean of 3.0 % and 8.4 % of the 14- and 21-day communities belonged to the genus *Dialister.* It can also be seen from the relative abundance plots that the percentage of *Dialister* increased as the microbial communities matured from day 14 to day 21 for both types of mucin sterilisation techniques that were used. The α-diversity of the communities did not significantly differ ($p=0.77$), although PCoA clustering comparisons based on the Jaccard index indicated there were differences in the community memberships (Figure 4.12). From this work, the data suggested that using filter-sterilised mucin in place of autoclaved mucin produced generally similar microbial communities. For experiments thereafter, filter-sterilised mucin was used.

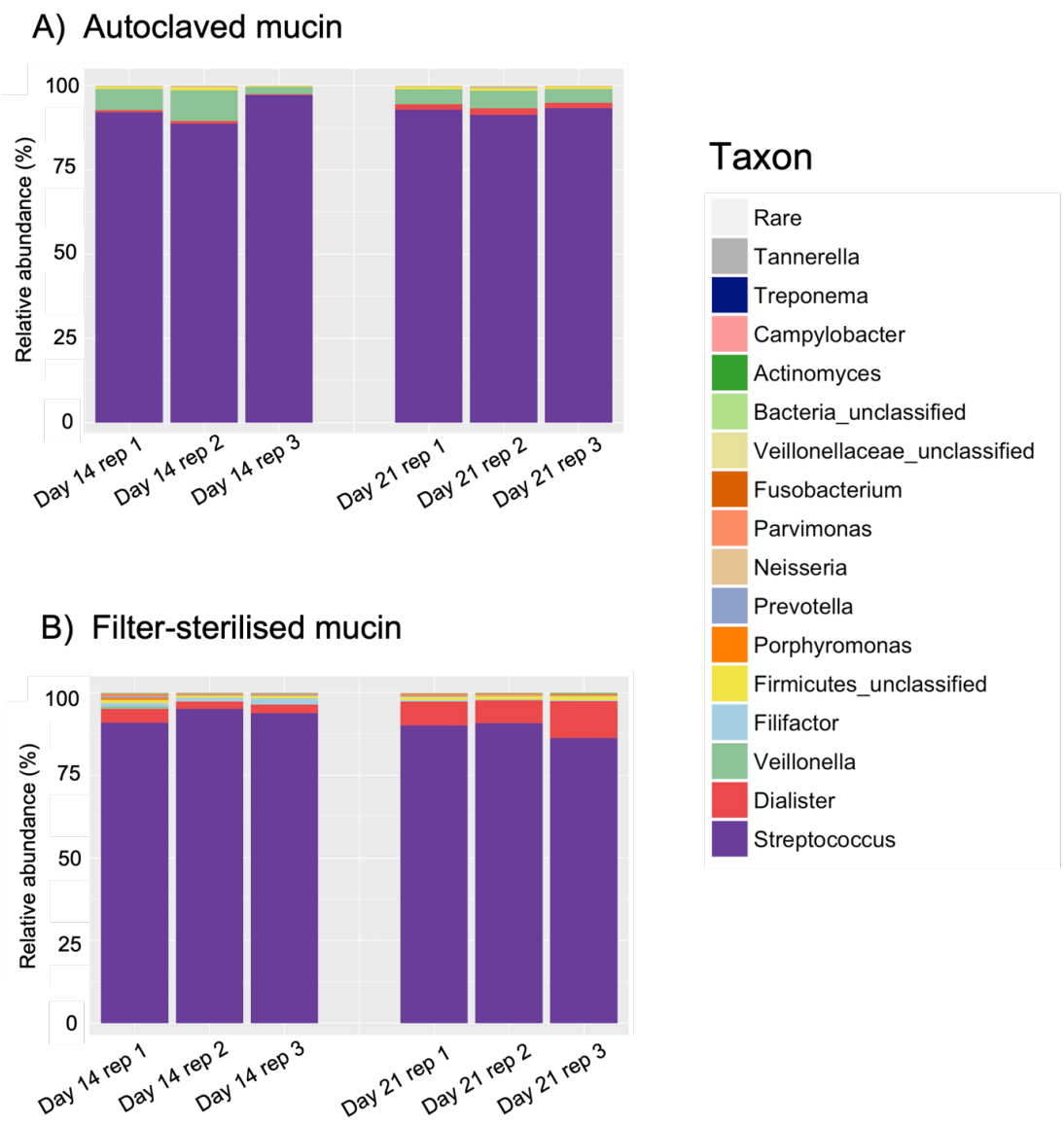

Figure 4.11 Testing the effect of mucin sterilisation techniques on mock community compositions. The relative abundance plots of genus-level taxa detected in 14- and 21-day old mock biofilms using autoclaved mucin (A) and filter-sterilised mucin (B) in the growth medium. Each biofilm was replicated three times and grown for up to 21 days. The group labelled "Rare" is comprised of the combination of all genera that did not have >0.1 % in at least one microbial community.

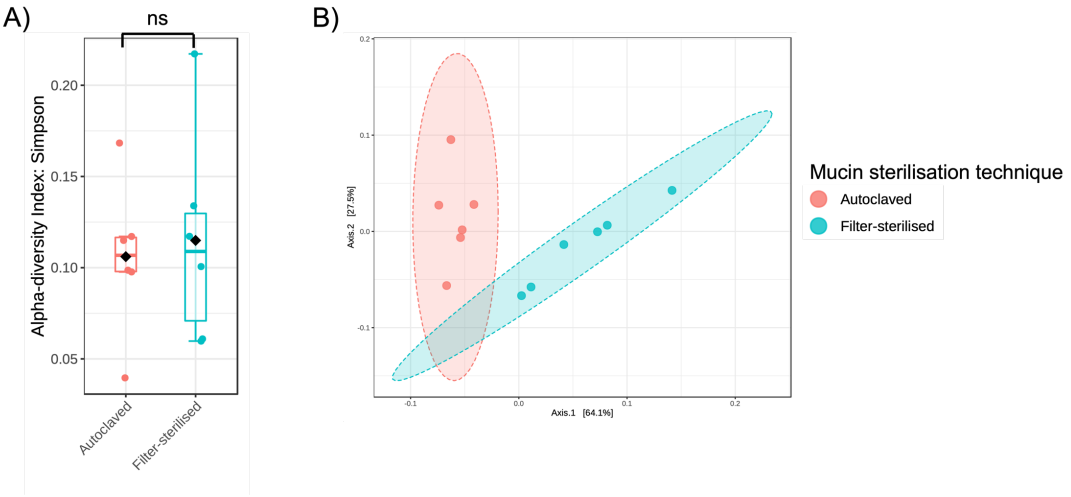

Figure 4.12 Diversity comparison between mock biofilm communities grown using autoclaved and filter-sterilised mucin in the growth medium. A) Boxplots depicting the Simpson's alpha-diversity index values B) Principal coordinates analysis plots based on community membership using the Jaccard index. A t--test was performed for Simpson's alpha diversity index values, where ns is non-significant, 0.01<p<0.05 *, 0.01<p<0.001 **, p<0.001 *** and p<0.0001 ****.

4.3 Discussion

An initial trial run of the mock biofilm community modelling was completed to primarily see whether the model supported multispecies growth. Cultural and qPCR analyses were principally used to analyse this. Mixed bacterial colonies and cellular morphotypes were observed from the cells harvested from the biofilms, although cultural analysis was insufficient in assessing the relative abundance of all 18 bacteria. As a result, alongside cultural work which suggested the presence of anaerobes such as *Prevotella* and *Fusobacterium* spp., a few key bacteria from the trial mock biofilm communities grown for up to 7 days were quantitatively assessed by qPCR. This included *F. nucleatum* and three black-pigmented anaerobes (*P. gingivalis, P. intermedia* and *P. nigrescens)* which were of particular interest. The percentage of the reference strain *T. forsythia* ATCC 43037 in the biofilm communities was also assessed but not the clinical strain UB4 of *T. forsythia*. The data from this work indicated the total DNA concentration obtained from 1-day biofilms using the universal PCR primers was too low to produce reliable results, leading to percentages >100 % which were seen for *F. nucleatum*. It would therefore be advantageous to only analyse biofilms grown for longer than 3 days, although it was striking to see the low levels of the remaining anaerobes detected on day 1 which was reduced further by day 3. It was possible that on day 1, the

anaerobes were viable but became less so as the biofilms matured. This could suggest the model itself was not sustaining multispecies bacterial growth beyond day 1, so attempts at optimising the model would be essential. An alternative explanation might be that the individual slow-growing bacteria such as *P. gingivalis* and *T. forsythia* were perhaps dormant or still attempting to gain a foothold amongst the other bacteria within the complex mixed community throughout the first few days of incubation. Thus, 7 days might not be sufficiently long enough for some bacteria to grow to detectable levels (Cheng *et al.*, 1985; Tanner *et al.*, 1986; Shah and Collins, 1988).

Similar to the strict anaerobes mentioned previously, low levels from qPCR assays were also observed for *T. denticola.* This bacterium is understood to have a synergistic relationship with *P. gingivalis* and preliminary understanding might still be possible from the qPCR data gathered for *P. gingivalis*. Here, a mean of 13.5 % *P. gingivalis* DNA was found in the communities, which reduced by day 3 but increased again to an eventual 0.036 % by day 7 of biofilm growth. This was in keeping with current understanding that as a keystone pathogen, *P. gingivalis* is found at very low concentrations in mixed communities. Hajishengallis *et al.* (2011) had estimated the abundance of *P. gingivalis* as low as <0.01 %. Like *P. gingivalis*, it is likely the *T. denticola* abundance would also be low because co-aggregation between the two bacteria was previously established by Ammann *et al.* (2012). The co-aggregation occurring between *T. denticola* and *P. gingivalis* can perhaps be explained by the expression of genes coding for the key surface adhesion factors Hgp44 by *P. gingivalis,* which resulted in the reduced coaggregation with *T. denticola* when expression was lost (Ito *et al.*, 2010). Moreover, the synergistic relationship between the two anaerobes also involves the exchange of the fatty acid succinic acid from *T. denticola* to *P. gingivalis,* and the transfer of isobutyric acid from *P. gingivalis* to *T. denticola* (Grenier, 1992). It is likely these fatty acids provide a carbon source and are incorporated into amino acids and lipids during their biosynthesis. Ng *et al.* (2019) have also recently described the synergistic relationship between *T. denticola* and *P. gingivalis*. The authors showed that co-culturing the two bacteria produced biofilms with a two-fold higher mass than

when single-species biofilms were grown. More importantly, inactivation of the flagella-associated genes *motB* and *flgE* in *T. denticola* reduced growth in the dual-species biofilms. This suggested the importance of *T. denticola*'s motility in its synergistic relationship with *P. gingivalis* in their biofilm formation.

Although it is important to understand the mutualistic relationships existing between different bacteria based on their individual metabolic activities and requirements, understanding antagonistic relationships is also essential. The antimicrobial bacteriocins produced by the *S. salivarius* K12 strain to inhibit the growth of Gram-negative bacteria is one such example (Wescombe *et al.*, 2009). The strain *P. nigrescens* ATCC 25261 is similarly thought to produce bacteriocins, which are active against *P. intermedia, P. gingivalis, T. forsythia* and some *Actinoymces* spp. (Kaewsrichan, Douglas and Teanpaisan, 2005). As the same strain of *P. nigrescens* was used in this study, it is possible the low levels of *P. gingivalis* and *T. forsythia* that were observed were due to the antimicrobial compound exhibited by *P. nigrescens*. However, because *P. nigrescens* abundance was very low (0.0007 % at day 7) in the mixed biofilm communities obtained in the initial trial run, it was likely this was not a contributing factor in the model.

With the primary aim of increasing bacterial cell numbers and thus also increasing species-specific DNA concentrations, modifications were made to the protocol for setting up the mock community model. Biofilm communities were grown for 14 days instead of 7, and the cell abundance for each of the 18 individual bacteria were normalised based on colony-forming units prior to inoculating the MBEC plate. Lastly, pegs on the MBEC plates were also suspended in 100 % inactivated human serum for 1 day prior to inoculation. This was conducted to assist the growth of *P. gingivalis* and *T. denticola* as high serum content in the growth medium would mimic the gingival crevicular fluid present in the mouth. The serum could also promote higher *T. denticola* cell numbers in oral communities, although *P. gingivalis* growth was found to remain unchanged at varying serum concentrations in several previous studies (Ammann *et al.* 2012; Fernandez y Mostajo *et al.*, 2017). Therefore, preconditioning the substrata before any biofilm

growth might allow these bacteria to gain a foothold in the community. From the qPCR data obtained from this experiment, which was labelled model iteration 2, they were indicative that the modifications had increased *P. gingivalis, T. forsythia* and *T. denticola* abundance in the early growth when compared to data from the initial trial run. It was also interesting to see the levels of the three bacteria reduced on day 7 but increased again on day 14. This might be indicating that these slow-growing anaerobes required 14 days to gain a foothold amongst the other bacteria within the complex mixed community. As the duration of growth was extended to 14 days in the updated model, only analyses at days 3 and 7 could be directly compared between the two model iterations. The comparison between the two iterations was further limited because only the abundance of three bacteria were measured for both iterations, thus highlighting the usefulness of performing further qPCR assays on additional species if time permitted. However, the reason why only *P. gingivalis, T. forsythia* and *T. denticola* were analysed here was because an immediate goal of this study was to set up and optimise microbiome sequencing for the biofilm communities, so this took priority. As already described in Chapter 3, it was thought microbiome analysis would be a useful tool in establishing a snapshot of which bacteria were present in the communities, without the need of designing and validating multiple species-specific primers. The need to run subsequent multiple PCR reactions was therefore considered impractical and laborious.

Microbial communities are complex and highly organised and as scanning electron microscopy (SEM) allow us to visualise the community structure, SEM images were also taken of the mock communities obtained from the model iteration 2. It was possible to view how different bacterial types were spatially organised and that the interactions were much looser during early biofilm development. By day 7 of biofilm growth, it was clear that the coccal-shaped bacteria were spatially very close and the majority of these were adhered to both short and long rods. However, their identities remained undetermined because of the complex nature of these mixed communities. As different bacterial species shared similar morphotypes under SEM, it was challenging to identify between bacterial species.

This could only be understood by SEM imaging if the communities were simple and contained only a few different bacterial morphotypes, such is the case in dual-species biofilm models. Past studies (Thurnheer, Gmür and Guggenheim, 2004; Guggenheim *et al.*, 2009) which focused on developing *in vitro* bacterial community models have already made use of the FISH technique to identify and visualise fluorescently labelled different bacteria within a multispecies community. Like qPCR, this technique is laborious due the necessity of validating taxa-specific oligonucleotide probes. Until recently, FISH was also limited by the limited number of colours and hence, the number of bacteria that are simultaneously visualised. An improved imaging technique that combats this limitation is called CLASI-FISH (combinatorial labelling and spectral imaging combined with FISH) and it uniquely labels up to 120 colours simultaneously, making it an effective technique for visualising the complexity present in oral samples (Valm, Mark Welch and Borisy, 2012). It was however decided that the time available in this PhD project proved too limited for the optimisation necessary in setting up this technique in the laboratory. Although it would be useful as a bacterial detection and visualisation tool, the focus of this project primarily remained on assessing the levels of different bacteria by qPCR and microbiome sequencing, and how the model could be challenged and influenced over time.

A third iteration of the mock community model was subsequently developed. The duration that the communities were grown was extended further and now up to 21 days. An additional improvement was also made, which was the use of Nanopore sequencing in the 16S rRNA gene community profiling of the biofilm communities to help with the time constraints. As only genus-level classification could be derived from the Nanopore sequence reads, the mock model was inoculated with one species per genus and a total of 13 genera were included. Another drawback to microbiome sequencing is the risk that contaminants present in the multispecies communities could be missed, such as the contaminant found in the model iteration 2. As previous experiments had suggested the dominance of *Streptococcus* and *F. nucleatum* species, the biofilm experiments conducted for the third iteration were inoculated with a 10-fold lower level of *F. nucleatum* subsp.

polymorphum. The species *S. gordonii* was also removed from the mixed community inoculum so that only *S. oralis* from the *Streptococcus* genus remained. The reason why *S. oralis* was selected over *S. gordonii* in this study was because *S. oralis* was frequently selected in previously published mock oral community models such as the Zürich biofilm model. Furthermore, Singh *et al.* (2017) and Byers *et al.* (2000) have demonstrated the presence of neuraminidase in *S. oralis*. It has not been found in *S. gordonii* and as the another aim of this PhD project was to ascertain the role of these enzymes in the development of periodontal disease, the mock model continued to be inoculated with *S. oralis*. The experiments involving the investigation of neuraminidases were not the focus of this chapter and thus will be described in Chapter 5. From analysing the composition of duplicate microbial communities at day 21, *Streptococcus* and several strict anaerobes belonging to genera such as *Campylobacter, Dialister* and *Fusobacterium* were present. This was an improvement to the previous iterations whereby a *Porphyromonas* spp. (not *P. gingivalis)* contaminant dominated the mixed microbial communities. Interestingly, these were the four non-contaminating bacteria with the highest relative abundances detected in both iterations of the mock community model. The three genera *Porphyromonas, Tannerella* and *Treponema* were once again not detected in this model. It is possible that antagonistic interactions occurred in the more complex 13-species model as it was previously found that including the *S. oralis* in a 5-species biofilm model led to the absence of *P. gingivalis* growth (Naginyte, 2018). Upon replacing *S. oralis* with *S. salivarius*, the author found that *P. gingivalis* was able to grow in the model. This was due to the high production of hydrogen peroxide by *S. oralis* compared to *S. salivarius,* which was known to be inhibitory to anaerobes (Kreth *et al.*, 2005b; Jakubovics *et al.*, 2008). As the complexity of the 13-species model meant it was not possible to fully understand the interactions occurring between each of the bacteria, this highlighted the advantage of a simpler model. A simple 6-species biofilm model which was inoculated with only *Porphyromonas, Tannerella, Treponema, Dialister, Prevotella* and *Fusobacterium* was thus trialled. Streptococcal bacteria were removed based on the work mentioned previously but in the simpler 6-species model, the absence of *Porphyromonas, Tannerella* and *Treponema* remained.

Salivary mucin is a source of carbohydrates for oral bacteria. To increase the chance of growth for the red microbial complex, a higher concentration of 10 mg/ml (1 % w/v) bovine submaxillary mucin in the growth medium was tested alongside the lower concentration of 0.01 mg/ml (0.001 % w/v) that was previously used. The higher concentration was selected to replicate the conditions of other published subgingival plaque models where 1-10 mg/ml was used (Van der Hoeven and Camp, 1991; Bradshaw *et al.*, 1994; Kistler, Pesaro and Wade, 2015; Naginyte *et al.*, 2019). *T. forsythia* grown on the MBEC plates for 7 days under these two conditions were harvested and plated onto agar plates so that their colony-forming units could be measured. In parallel, the replacement of the mixed community inoculum with fresh growth medium on day 3 instead of day 1 was also tested. It was theorised the delayed inoculum replacement might allow the slow-growing bacteria such as *P. gingivalis*, *T. forsythia* and *T. denticola* to attach to the substratum or to the other bacteria within the mixed inoculum before the inoculum was removed. It was clear from this experiment that replacing the inoculum on day 3 improved the survival of *T. forsythia* grown as biofilms on the MBEC pegs. Increasing the concentration of mucin did not. Though *T. forsythia* was selected for testing in this experiment due to the challenging nature of growing and counting *T. denticola* CFUs, Lamont *et al.* (2021) similarly showed the largest factor in encouraging the presence of *T. denticola* in their subgingival plaque model at 48 h was not increasing mucin concentration to 8 mg/ml (equivalent to 0.8 % w/v) but due to increasing the sucrose concentration in their growth medium. The growth medium contained no sucrose but did contain 3 mg/ml glucose. As increasing the mucin concentration did not hinder *T. denticola* growth, the higher concentration of mucin would be used. The eventual choice of the growth medium for the model comprised of 50 % mFUM (modified fluid universal medium) (Gmür and Guggenheim, 1983), supplemented with 1 % bovine submaxillary mucin and 30 % heat-inactivated human serum. The mFUM medium is a well-established tryptone-based medium used in microbial community models and it contains haemin and menadione which have for example, been reported as growth co-factors for *Prevotella* and *Porphyromonas* spp. (Gibbons and Macdonald, 1960). The rationale for this composition was also because of the work by Ammann, Gmür and

Thurnheer (2012) who achieved greater *T. denticola* abundance and denser biofilms with human serum content of 50 %.

Although the mucin concentration was finalised, it was essential to test whether filter-sterilising mucin in place of autoclaving it could alter the biofilm community compositions. The work that was previously described in this chapter involved autoclaving the mucin as this technique has been used to sterilise mucin in several studies focused on developing multispecies community models (Kistler, Pesaro and Wade, 2015; Naginyte *et al.*, 2019). However, as the focus of the next chapter was to investigate the importance of glycosylation in the growth of a multispecies community, it was important the mucin remained intact. Autoclaving the mucin would subject it to high temperature and pressure and could lead to denaturation. As filter-sterilisation using a 0.45 μm filter was an alternative method for sterilising mucin without heat and pressure, experiments were conducted to test whether filter-sterilisation could produce mucin that was identical to non-sterilised mucin. This was essential to test as the filters could be blocked by the thick consistency of mucin. However, no noticeable differences were observed between the two when the proteins were separated on SDS-PAGE gels and visualised by using both Instant Blue and the Pro-Q Emerald 300 Glycoprotein Stain. In contrast, large molecular weight proteins were lost with autoclaving the mucin, suggesting this technique did cause protein denaturation and thus was not suitable for work in the next chapter. A further experiment was conducted to assess whether using the filter-sterilised mucin in place of autoclaved mucin in the growth medium of mock communities would produce comparable 14- and 21-day communities. The dominance of streptococcal bacteria was seen in the mixed communities under both conditions, though bacteria belonging to *Veillonella* were at higher levels in the autoclaved growth medium. In contrast, *Dialister* was observed at higher levels in the communities using filter-sterilised mucin. It was however challenging to see the proportions of the remaining genera in the communities as *Streptococcus* levels were over 85 %. Through using Simpson's diversity, it was shown the microbial community diversity was not influenced by replacing autoclaved mucin with filter-sterilised mucin. However, the communities clustered based on mucin sterilisation techniques using distance matrix values calculated with the Jaccard index,

indicating some differences occurred and were likely due the higher relative abundance of *Dialister* in the communities grown using filter-sterilised mucin.

4.4 Summary

Although it was not possible to consistently grow the red microbial complex bacteria in the mock community model despite developing several iterations, the mock model did support the growth of mixed oral anaerobes. This has included the growth of both facultative and strict oral anaerobes. The next chapter makes use of this model to investigate the role of glycans in oral bacterial growth.

Chapter 5 - Role of siallo-glycoproteins and oral bacterial sialidases in periodontal biofilm communities

5.1 Introduction

As described in Chapter 1, sialic acids are a family of anionic 9-carbon polyhydroxyaminoketoacid (also known as nonulosonic acids) sugars found as terminal monosaccharides on eukaryotic and bacterial surface-bound glycans and secreted glycoproteins and glycolipids (Varki and Diaz, 1983; Varki, 1992). Sialic acids are important to the human mouth because saliva and gingival crevicular fluid (GCF) are rich in sialic acid containing glycans. As described in chapter 4, the growth medium mFUM used in the biofilm model of this project therefore contained both mucin and human serum, to better mimic the conditions found in a periodontal pocket.

Mucin is found in mucus secretions and it makes up approximately 16 % protein content in saliva (Payment *et al.*, 2000). Salivary mucin is heavily glycosylated due to their O-glycosylated sugar chains, which are attached to the protein backbone by serine/threonine linkages and encompass 40-80 % of their mass (Levine *et al.*, 1987; Zalewska *et al.*, 2000). Sialic acids present in the mouth can be harvested by oral bacteria via the enzyme sialidase, which cleave the α2,3- or the α2,6-glycosidic linkages to expose the sialic acids (Corfield, 1992). It is widely understood sialidases act as virulence factors to help promote bacterial growth through a wide variety of means for both resident and pathogenic bacteria. Many commensal oral bacteria such as *S. oralis* and *S. intermedius* (Beighton and Whiley, 1990) and those associated with periodontal disease such as *P. gingivalis, T. forsythia* and *T. denticola* from the red microbial complex can secrete sialidases to access this additional energy source and aid their adhesion. The role of bacterial sialidases in biofilm formation was highlighted by a sialidase-lacking *P. gingivalis* mutant which consequently prevented capsule synthesis and reduced biofilm formation (Li *et al.*, 2012). Likewise, a *T. forsythia* mutant with *nanH* sialidase deletion reduced biofilm growth and adhesion to glycoprotein-coated surfaces (Roy *et al.*, 2011). The importance of oral sialidases in periodontitis was further highlighted by Gul *et al.*, (2016), who demonstrated significantly higher levels of sialidases present in the sites associated with periodontitis than in the healthy sites.

Anti-influenza drugs such as zanamivir and oseltamivir block the action of influenza neuraminidases. They are structural analogues of the transition molecule of sialic acid DANA (McKimm-Breschkin, 2013) that is present during the cleavage of glycosidic linkages by sialidases. As DANA and oseltamivir have been shown to reduce the adhesion of *T. forsythia* to mucin and epithelial cells (Roy *et al.*, 2011; Kurniyati *et al.*, 2013), inhibiting the function of the sialidases might mediate bacterial virulence and act as a potential therapy for periodontal disease.

5.1.1 Aim of Chapter

An aim of this project was to ascertain the potential role sialidase inhibitors might have on the growth of a periodontal bacterial community. This chapter therefore aims to address this and how sialidase activity function could be prevented.

5.2 Results

5.2.1 Oral sialidases in bacteria selected for mock community inoculum

5.2.1.1 Screening for production of sialidases

While sialidases have been isolated from many oral bacteria as summarised in Chapter 1, to gain a wider picture for this project, sialidase activity was screened across all 18 bacteria used in the mock community model. 2'-(4-methylumbelliferyl)-α-D-N-acetylneuraminic acid (MUNANA) sialidase assays were therefore performed on whole cells obtained from each bacterial culture. The detection of sialidase activity was consistent with those previously described in the literature (Table 5.1). For example, the following strains possessed sialidase activity: *A. oris* MF1, *P. gingivalis* NCTC 11834, *S. oralis* C647, *T. denticola* ATCC 35405, *T. forsythia* ATCC 43037 and *T. forsythia* UB4. The remaining bacteria which were tested did not demonstrate sialidase activity. *T. serpentiformis*, a second species within the *Tannerella* genus also did not exhibit sialidase activity.

Table 5.1 Sialidase activity in oral bacteria selected for mock model inclusion. Summary of the presence and absence of sialidase activity in the 18 oral bacterial species used in the mock community model.

Sialidase-positive bacteria	Sialidase-negative bacteria
A. oris MF1	*C. showae* ATCC 51146

P. gingivalis NCTC 11834	*C. rectus* ATCC 33238
S. oralis C647	*D. invisus* DSM 15470
T. denticola ATCC 35405	*F. alocis* ATCC 35896
T. forsythia ATCC 43037	*F. nucleatum* subsp. nucleatum ATCC 22586
T. forsythia UB4	*F. nucleatum* subsp. polymorphum ATCC 10953
	N. subflava ATCC 49275
	P. intermedia ATCC 25611
	P. micra ATCC 32370
	P. nigrescens ATCC 25261
	S. gordonii DL1 (Challis)
	V. dispar WT
	T. serpentiformis DSM 102894

5.2.1.2 Screening for sialidase genes in whole genome sequences

To verify the results from the MUNANA assays, the presence of the glycoside hydrolase family 33 (GH33) in whole genome sequences of each bacterial species was screened using the Carbohydrate-Active Enzyme Database (CAZy.org). The GH33 is a family of enzymes that includes bacterial sialidases. As shown in Table 5.2, all of the bacteria which showed sialidase activity in the MUNANA assay possessed a gene from the GH33 family. According to the publications, NanH was found in *A. oris,* SiaPG (PG0352) in *P. gingivalis*, NanA in *S. oralis*, a putative Td_{neu} (TDE471) in *T. denticola,* and both NanH and NanS were found in *T. forsythia*. The MUNANA assay data for the bacterial species shown to not exhibit sialidase activity also corroborated with the absence of the GH33 family in the whole genome sequences of these bacteria.

Table 5.2 GH33 family in the whole genome sequences of oral bacteria selected for mock model inclusion. Summary of the presence of absence of the GH33 glycoside hydrolase family in whole genome sequences according to Carbohydrate-Active Enzymes Database (CAZy.org).

Bacterial species	**Presence of GH33 in genome sequence**	**Evidence for sialidase in bacteria species found in publication**
Bacteria previously confirmed by MUNANA to exhibit sialidase activity		

A. oris	+	NanH (Do *et al.*, 2008)
P. gingivalis	+	PG0352 SiaPG (Nelson et al. (2003)
S. oralis	+	NanA (Singh *et al.*, 2017)
T. denticola	+	TDE0471, putative Td_{neu} (Kurniyati *et al.*, 2013)
T. forsythia	+	NanH, NanS (Thompson *et al.*, 2009; Phansopa *et al.*, 2015)

Bacteria previously confirmed by MUNANA to *not* exhibit sialidase activity

C. showae	-
C. rectus	-
D. invisus	-
F. alocis	-
F. nucleatum	-
N. subflava	-
P. intermedia	-
P. micra	-
P. nigrescens	-
S. gordonii	-
V. dispar	-
T. serpentiformis	-

5.2.2 Detection of sialidase activity in multispecies community supernatant

To avoid enzyme-substrate saturation during MUNANA assay reactions, an initial study revealed the optimum incubation period for performing MUNANA assays on a representative multispecies community supernatant sample was 1-4.5 h as this period existed within the linear phase in Figure 5.1. This supernatant was a sample of “spent” growth medium collected from mock biofilms.

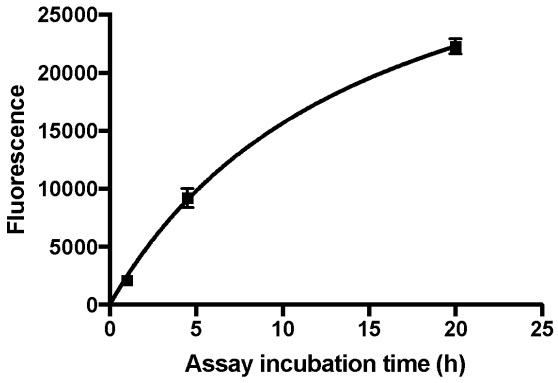

Figure 5.1 Enzyme-substrate saturation in MUNANA assay reactions. The MUNANA assay was performed on a representative multispecies community supernatant sample for 1 h, 4.5 h and 20 h before quenching. The optimum assay incubation time was determined as between 1-4.5 h. Data shown are the mean of two repeats.

5.2.3 Sialidase inhibition

5.2.3.1 IC50 assay on 4 sialidase inhibitors

To investigate which commercially available sialidase inhibitors were effective in reducing sialidase activity in the biofilm supernatant samples, four inhibitors were tested, and their half-maximal inhibitory concentration (IC_{50}) values calculated. Sialidase inhibitors at concentrations 0-0.909 mM were tested: zanamivir (GlaxoSmithKline), oseltamivir (Carbosynth), N-Acetyl-2,3-dehydro-2-deoxyneuraminic acid (DANA, Carbosynth) and siastatin B (Carbosynth). As shown in Figure 5.2, zanamivir and oseltamivir are structural derivatives of DANA. The structures of siastatin B and N-acetylneuraminic acid are also shown.

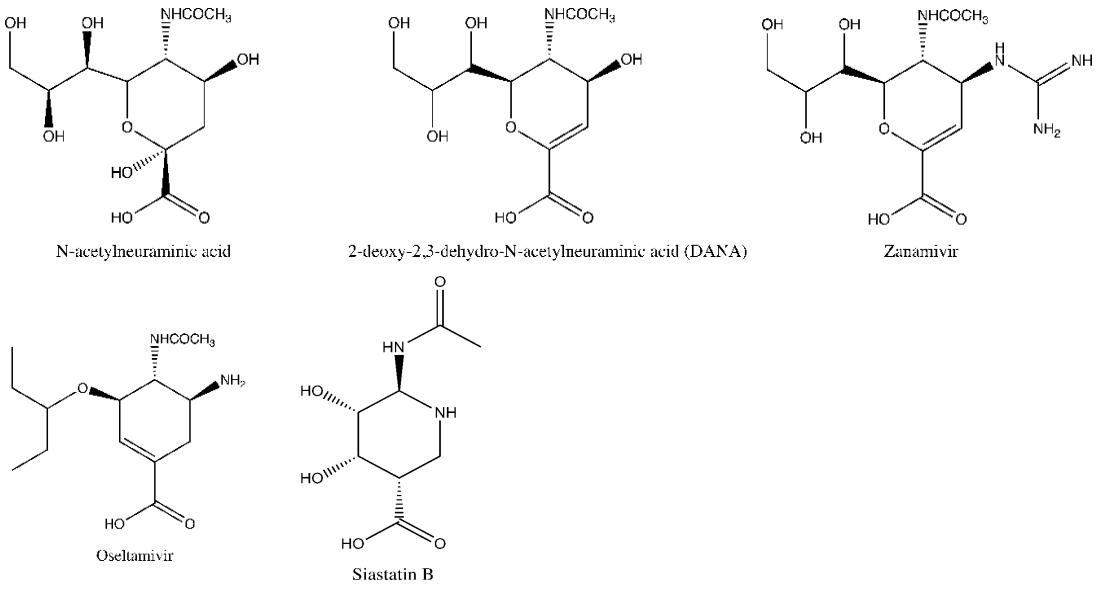

Figure 5.2 Chemical structures of N-acetylneuraminic acid (Neu5Ac) and the neuraminidase inhibitors DANA, zanamivir, oseltamivir and siastatin B.

As a measure of inhibitor efficacy, obtaining IC_{50} values provided the inhibitor concentration at which 50 % sialidase inhibition was reached. Supernatant collected from a biofilm model was diluted 1:10 and incubated for 4 h in the presence of 0.18 mM MUNANA. To mimic host physiological conditions, 50 mM sodium phosphate buffer with 200 mM NaCl at pH7.4 instead of pH 5-6 was used as this was reported as the optimal pH for sialidases (Frey *et al.*, 2018). Inhibition of secreted sialidase activity by the addition of each of the 4 sialidase inhibitors at concentrations 0-0.909 mM was then expressed as a percentage in relation to the reaction wells absent of an inhibitor (Figure 5.3). In order of efficacy, the IC_{50} of oseltamivir was found at 0.78 µM, for DANA 2.06 µM, siastatin B at 11.40 µM and zanamivir at 1611.00 µM (1.611 mM). This therefore suggested of the four inhibitors tested, oseltamivir and DANA were the most efficacious at inhibiting secreted sialidase activity in the biofilm supernatant. Following this finding, only the effect of adding oseltamivir and DANA on biofilm communities were investigated further.

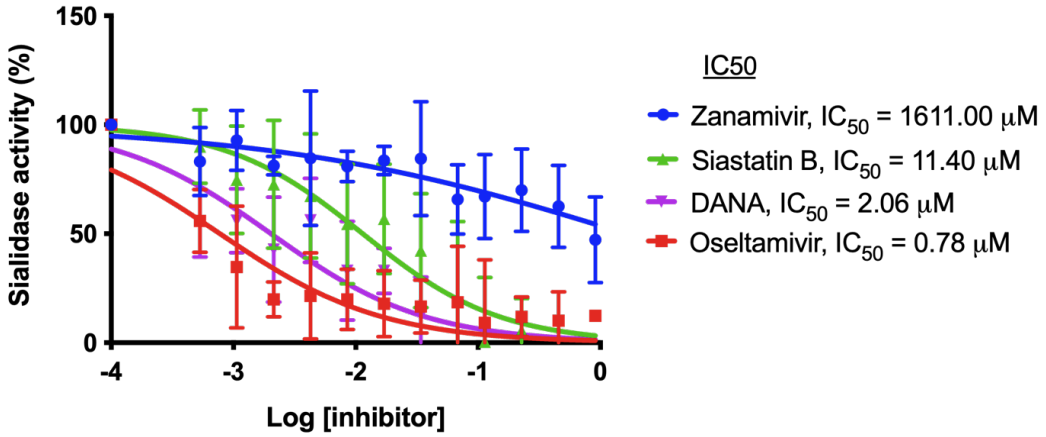

Figure 5.3 Half-maximal inhibitory concentration (IC_{50}) values measured for four sialidase inhibitors. IC50 curve depicting the Log[inhibitor] against percentage of sialidase activity (%) relative to absent of each of the inhibitors: zanamivir, siastatin B, N-Acetyl-2,3-dehydro-2-deoxyneuraminic acid (DANA) and oseltamivir. IC50 values were expressed as µM whereby a 50 % reduction in fluorescence was measured for reactions where an inhibitor was present when compared to reactions in the absence of an inhibitor. Data represent the mean of three biological repeats and error bars calculated from standard error of mean (SEM).

5.2.4 Use of sialidase inhibitors in the mock and plaque biofilm models

5.2.4.1 Pooled plaque community composition under control and oseltamivir test conditions

A pool of 10 subgingival plaque samples collected from patients with periodontitis was used to inoculate a MBEC plate and the plaque model was grown under two different conditions for 21 days. Duplicate plaque biofilms were grown in growth medium containing 100 µM oseltamivir and without oseltamivir which acted as a control comparator. As shown in Figure 5.4, the predominant genus-level taxa detected in the 7-, 14- and 21-day plaque biofilm communities were *Veillonella* and *Streptococcus.* This was comparable to the results of the literature review carried out in this study that determined which oral bacteria typically associated with periodontal disease and was irrespective of the age of the biofilms and whether oseltamivir was added to the growth medium. Furthermore, as the plaque biofilms matured, the mean relative abundance of *Enterococcus* of duplicate biofilms increased from 1.26 % to 19.67 % in control communities and from 0.02 % to 4.71 % in the communities that contained 100 µM oseltamivir in the growth medium. Comparison of the mean relative abundances of *Campylobacter* (1.06 % vs 0.00 % at day 7, 1.24 % vs 0.35 % at day 21)*, Capnocytophaga* (4.37 % vs 0.16 % at day 7, 3.04 % vs 0.01 % at day 21) and *Veillonella* (84.11 % vs 33.19 % at day 7, 28.09 % vs 17.76 % at day 21) compared to those where 100 µM oseltamivir was included. In contrast, the relative abundance of *Streptococcus* was higher in the communities treated with 100 µM oseltamivir (3.10 % vs 51.77 % at day 7, 26.66 % vs 67.72 % at day 21). Furthermore, *Granulicatella* was also higher in the day 7 inhibitor-treated communities compared to the control communities (5.25 % vs 12.40 %), although the percentages were comparable between the two conditions at days 14 and 21 (3.09 % vs 4.04 % and 4.21 % vs 3.72 % respectively).

The α-diversity of the plaque biofilm communities was also assessed using the Simpson's diversity index which considers both richness and evenness (Figure 5.5A). The Simpson's diversity index was selected over alternative diversity indices as it provides more weight to the dominant taxa and thus is not influenced by the few rare species, which was seen in the biofilm communities. This revealed there

was no significant difference in the α-diversity of the biofilms grown with and without 100 μM oseltamivir (p=0.73). In contrast, comparison of the community membership using the distance matrices measured by the Jaccard index showed distinct clustering based on whether the plaque biofilms were treated with 100 μM oseltamivir (Figure 5.5B). Unfortunately, as only duplicate biofilm samples were grown, it was not possible to also test for any significant changes in the relative abundance of individual genera. Despite this, the data taken together suggested the presence of 100 μM oseltamivir did cause an overall change in the composition of the plaque communities. Figure 5.6 revealed the α-diversity (Simpson's diversity index) of plaque communities increased with time but this increase was not statistically significant (p=0.34). This was likely due to the small sample size (n=2). Principal coordinates analysis based on distance matrices calculated by using the Jaccard index also showed clustering of communities based on the duration of biofilm growth.

A) All genus-level taxa >0.1 % relative abundance

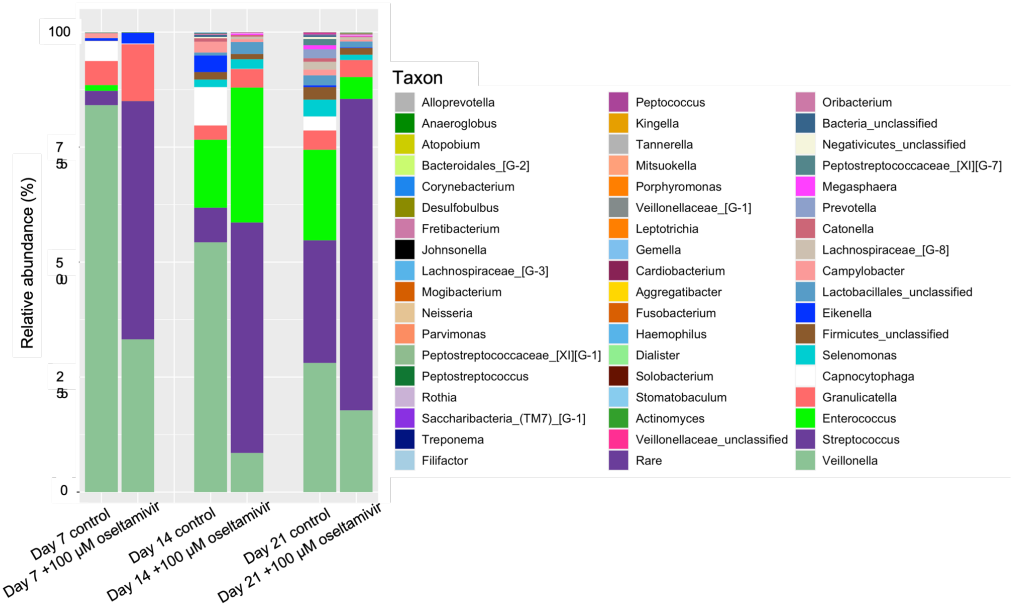

B) Ten most abundant genera

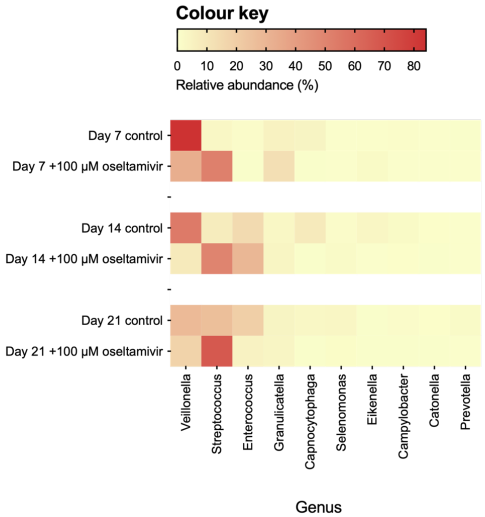

Figure 5.4 Community composition of plaque biofilms growth with and without 100 µM oseltamivir. The relative abundances of A) all genus-level taxa that were >0.1 % in at least one sample and B) ten most abundant named genera in plaque biofilm communities grown for 21 days with and without 100 µM oseltamivir. The group labelled "Rare" was comprised of a combination of all genera that did not have >0.1 % relative abundance in at least one plaque community. The taxa in the legend are ordered by the level of relative abundance, with *Veillonella* highest at the bottom and far-right and *Alloprevotella* lowest at the top and far-left.

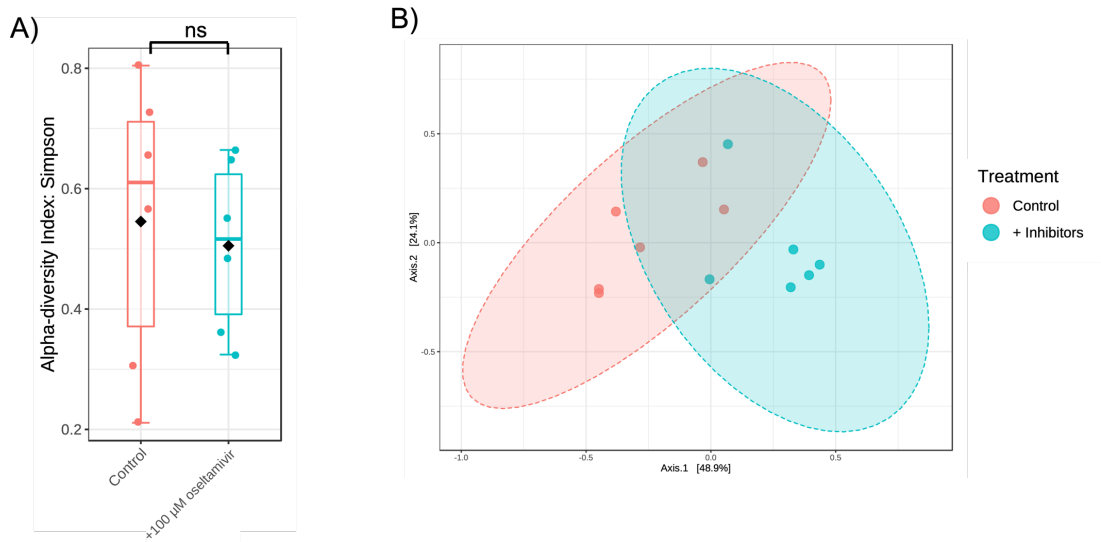

Figure 5.5 Diversity for plaque biofilms compared between control and the addition of 100 µM inhibitors. A) Boxplots depicting the Simpson's alpha-diversity index values B) Principal coordinates analysis plots based on community membership using the Jaccard index. T-test was performed on the alpha-diversity values, where ns is non-significant, 0.01<p<0.05 *, 0.01<p<0.001 **, p<0.001 *** and p<0.0001 ****.

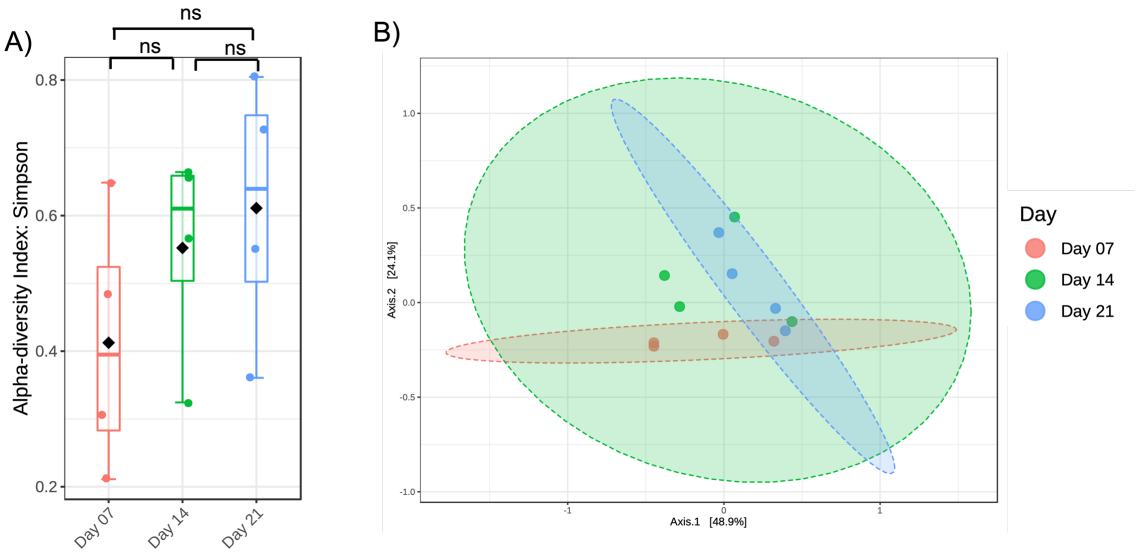

Figure 5.6 Diversity for plaque biofilms compared between biofilm growth periods. Comparison between days 7, 14 and 21 of biofilm growth for A) Boxplots depicting the Simpson's alpha-diversity index values B) Principal coordinates analysis plots based on community membership using the Jaccard index. ANOVA was performed on the alpha-diversity index values, where ns is non-significant, 0.01<p<0.05 *, 0.01<p<0.001 **, p<0.001 *** and p<0.0001 ****.

5.2.4.2 Inhibition of sialidase in sialidase-secreting oral bacteria with oseltamivir and DANA

As the addition of 100 µM oseltamivir to the growth medium of the plaque model showed small changes to the microbial community composition, it was theorised that perhaps the addition of DANA (the second most efficacious sialidase inhibitor that was tested) could cause a similar effect at reducing sialidase activity. To assess

this, DANA and oseltamivir were incubated with sialidase-positive bacteria and the sialidase activity was quantified by the release of 4-MU in a MUNANA assay.

Using the IC_{50} values confirmed for the four sialidase inhibitors mentioned previously, the addition of DANA and oseltamivir were tested at 100x the IC_{50} concentration (rounded up to 250 µM and 100 µM for DANA and oseltamivir respectively) in a whole cell MUNANA assay. Here, triplicate reactions were performed separately for three different test conditions: control (i.e., without the addition of inhibitors); 250 µM DANA and 100 µM oseltamivir. Alongside *C. rectus* acting as a negative control due to its confirmed absence of sialidase activity, only the bacterial species mentioned previously in section 5.2.1 which possessed sialidase activity were tested. These were the five species *A. oris, P. gingivalis, S. oralis, T. denticola* and *T. forsythia*, with a final OD_{600} of 0.05 used.

As shown in Figure 5.7, the fluorescence for the reactions was read with the averages blank-subtracted and expressed as a percentage in relation to the reaction wells absent of an inhibitor (control reactions). The reactions were also visualised under UV light, where higher fluorescence was associated with higher sialidase activity. *A. oris*, *T. denticola* and *T. forsythia* demonstrated the greatest sialidase activity of the bacteria tested, as shown by the average blank-subtracted fluorescence units of between 10,000-14,000 for the control reactions. This was also in line with the brighter control wells observed under UV light compared to *P. gingivalis, S. oralis* as well as the negative control *C. rectus*. The addition of 250 µM DANA to the MUNANA assay also clearly reduced the sialidase activity of *A. oris, T. denticola* and *T. forsythia* compared to the control reaction. The presence of 100 µM oseltamivir on the other hand, also reduced the % sialidase activity for these bacteria but to a lesser effect. This was evidenced by normalising the % sialidase activity to the control reactions, where sialidase activity was reduced from 100 % to as low as 1.6 % in the presence of 250 µM DANA, and from 100 % to 73.5 % in the presence of 100 µM oseltamivir. The bacteria *P. gingivalis* and *S. oralis* exhibited lower sialidase activity than the three aforementioned bacteria but the data here

also suggested a concentration of 250 µM DANA was more effective at reducing sialidase activity than 100 µM oseltamivir.

***A. oris* averaged blanked**

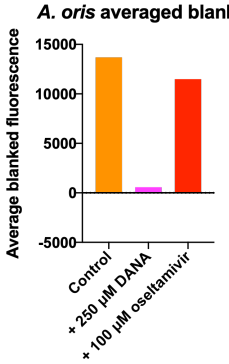

***A. oris* normalised to control**

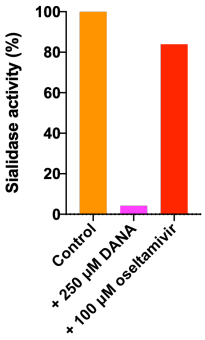

***A. oris* MUNANA reactions read under UV**

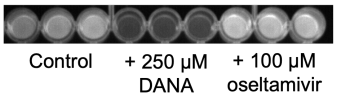

***P. gingivalis* average blanked**

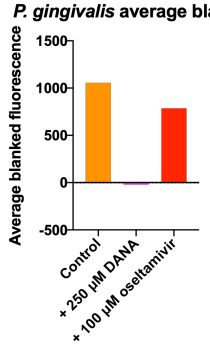

***P. gingivalis* normalised to control**

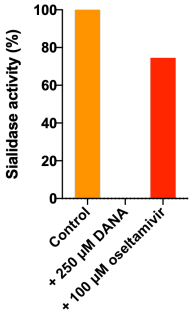

***P. gingivalis* MUNANA reactions read under UV**

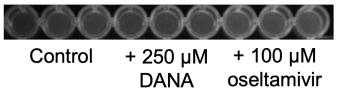

***S. oralis* average blanked**

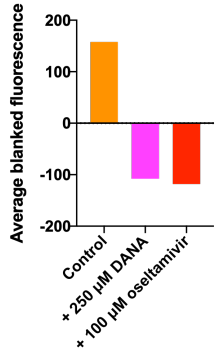

***S. oralis* normalised to control**

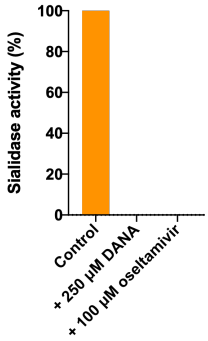

***S. oralis* MUNANA reactions read under UV**

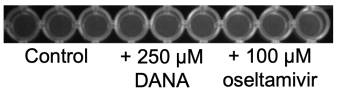

***T. denticola* average blanked**

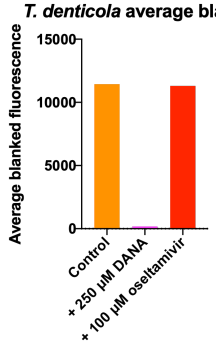

***T. denticola* normalised to control**

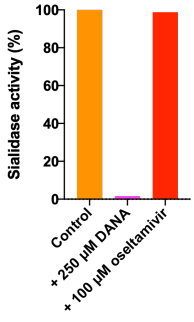

***T. denticola* MUNANA reactions read under UV**

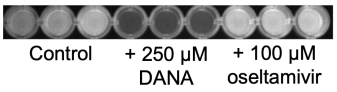

***T. forsythia* average blanked**

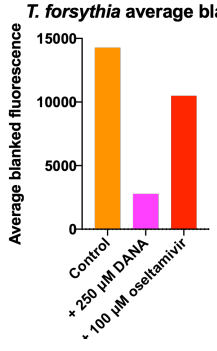

***T. forsythia* normalised to control**

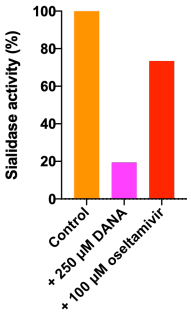

***T. forsythia* MUNANA reactions read under UV**

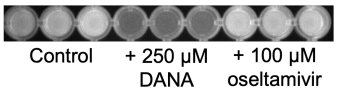

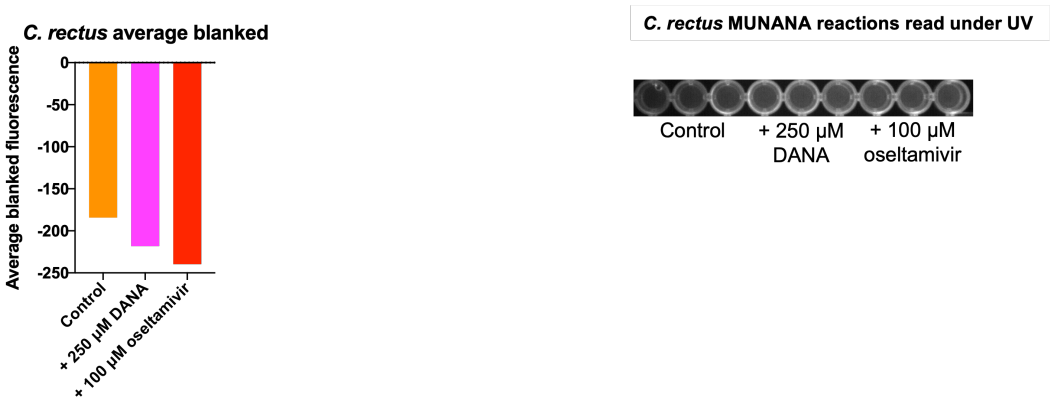

Figure 5.7 MUNANA assay measurements on sialidase-positive bacteria treated with sialidase inhibitors. Bacterial species which were previously confirmed to exhibit sialidase activity were tested separately in a MUNANA assay without the presence of any inhibitors (control), with the addition of 250 µM DANA and with the addition of 100 µM oseltamivir. Fluorescence was most measured for the bacterial species *A. oris, T. denticola* and *T. forsythia* and this was also confirmed by visualising the reactions under UV light as depicted by the brightness of the control wells when compared to the control wells of *P. gingivalis* and *S. oralis*. The addition of 250 µM DANA also caused the greatest reduction in fluorescence and in sialidase activity, with 100 µM oseltamivir demonstrating partial effect. *C. rectus* was included to act as a negative control and therefore its sialidase activity for the addition of inhibitors was not compared against the control reactions.

5.2.4.3 Verifying the non-antimicrobial effect of oseltamivir and DANA

To check that the sialidase inhibitors oseltamivir and DANA at these concentrations were not antimicrobial but instead functioned to only inhibit sialidase activity, disk diffusion assays were performed on a selection of oral bacteria using disks impregnated with 100 µM oseltamivir, 250 µM DANA, and 100 µM oseltamivir + 250 µM DANA. Antibiotic disks acted as positive controls and PBS acted as a negative control. The bacteria tested included *S. oralis, F. nucleatum* subsp. *nucleatum* and *T. forsythia*. As shown in Figure 5.8, bacterial growth was observed across the agar plate for each of the three bacteria, except in the surrounding area around the antimicrobial disks. This therefore suggested oseltamivir at 100 µM and DANA at 250 µM were not directly antimicrobial and any changes arising in future biofilm community compositions upon the addition of the sialidase inhibitors at these concentrations would be due to their effect on sialidase activity.

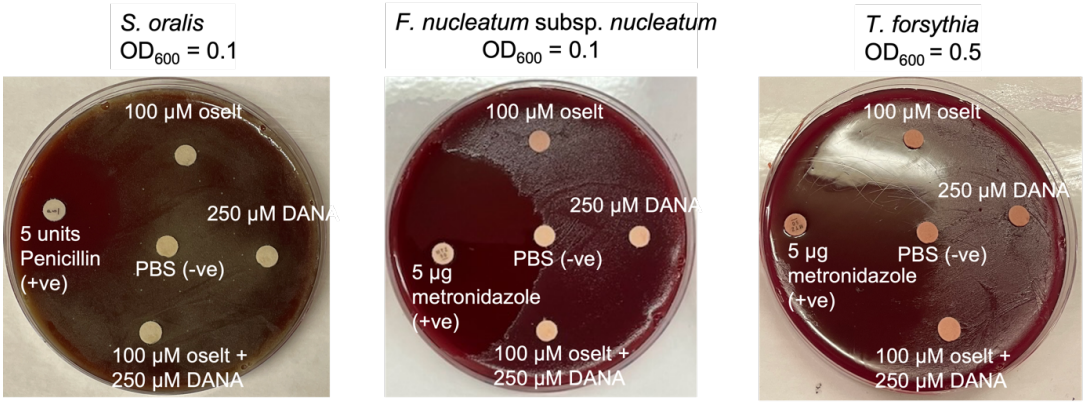

Figure 5.8 Disk diffusion assay to test for antimicrobial activity from sialidase inhibitors. Blank diffusion disks impregnated with 20 µl of either 100 µM oseltamivir, 250 µM DANA, 100 µM oseltamivir + 250 µM DANA, or PBS were placed onto fastidious anaerobe blood agar plates spread with either *S. oralis, F. nucleatum* subsp. nucleatum or *T. forsythia*. Bacterial growth was observed around the disks under these conditions thus suggesting the oseltamivir and DANA at these concentrations were not antimicrobial. Acting as experimental positive controls, a penicillin disk (Oxoid, UK) was added to the plate containing *S. oralis* and metronidazole disks (Oxoid, UK) were added to the plates containing *F. nucleatum* subsp. *nucleatum* and *T. forsythia*. Bacterial growth was inhibited around the antimicrobial disks as expected.

5.2.4.4 Potential synergy effect from combining oseltamivir with DANA

As shown in the previous sections, DANA at 250 µM was the most effective at reducing sialidase activity in mock biofilm supernatant. It was also previously shown that small microbial community composition changes occurred upon the addition of a final concentration of 100 µM oseltamivir to the plaque biofilm growth medium. It was therefore investigated whether these microbial community composition changes could be amplified by combining oseltamivir and DANA.

Supernatant collected from a previous mock biofilm model was diluted 1 in 10 and its secreted sialidase activity was measured after the addition of 0-0.909 mM oseltamivir, and 0-0.909 mM oseltamivir in combination with DANA. Sialidase activity was expressed as a percentage in relation to the reaction wells absent of an inhibitor. Figure 5.9 suggests the addition of DANA in combination with oseltamivir at equal concentrations was more effective at reducing sialidase activity in the biofilm supernatant than the addition of oseltamivir alone. This was shown by the IC_{50} of "oseltamivir + DANA" measured at 0.93 µM whereas a higher concentration of oseltamivir only was required to reduce sialidase activity by 50 % (as demonstrated by the 2.26 µM which was measured for oseltamivir only). Following

this finding, the effects of oseltamivir only and in combination with DANA were tested on purified NanH enzymes against the substrate MUNANA.

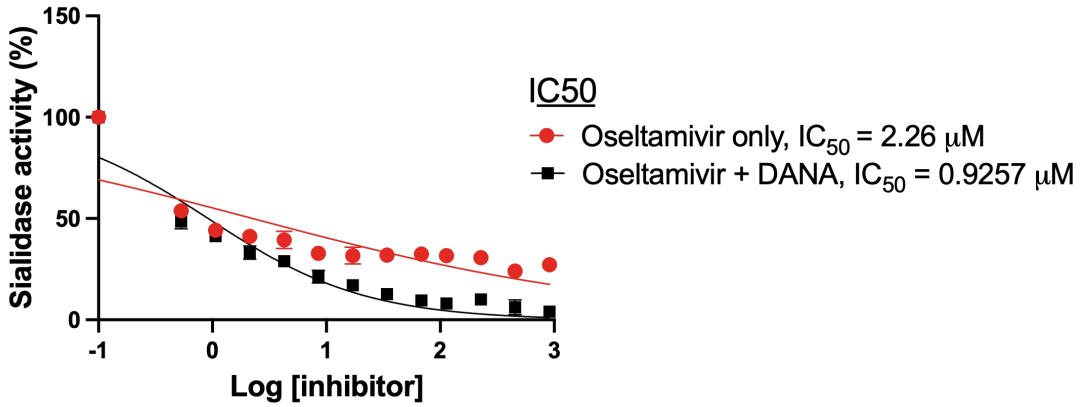

Figure 5.9 Half-maximal inhibitory concentration (IC_{50}) values measured for oseltamivir and oseltamivir combined with DANA. IC50 curve depicting the Log[inhibitor] against percentage of sialidase activity (%) relative to absent of either oseltamivir only, or oseltamivir in combination with N-Acetyl-2,3-dehydro-2-deoxyneuraminic acid (DANA) in biofilm supernatant collected during multispecies biofilm growth. IC50 values are expressed as mM whereby a 50 % reduction in fluorescence is measured for reactions where an inhibitor is present when compared to reactions with absence of inhibitor. Data represent the mean of three biological repeats and error bars calculated from standard error of mean (SEM).

A MUNANA assay was therefore performed to observe whether the 4-MU concentration was reduced when DANA was co-present with oseltamivir at various concentrations, compared to when sialidase inhibitors were absent and when either oseltamivir or DANA was solely present. Under these conditions, 2.5 nM purified NanH was incubated with 100 µM MUNANA substrate at 37 °C for 2 min. As shown in Figure 5.10A, from 4 independent repeats a mean of 8.3 µM 4-MU was released from the MUNANA substrate present in the assay when no inhibitors were present. This was not significantly different to when 100 µM oseltamivir was solely added to the reactions. Interestingly, the mean 4-MU concentration was significantly reduced to 0 µM when only 100 µM DANA was added, and the same observation was seen when varying concentrations of both oseltamivir and DANA were added to the reactions. The varying concentrations tested were as follow: the addition of 100 µM oseltamivir + 250 µM DANA based on the previous IC_{50} data; proportionate concentrations of 28.6 µM oseltamivir + 71.4 µM DANA to total 100 µM, and 100 µM oseltamivir and 100 µM DANA so that the concentration of each inhibitor was equal.

The loss of fluorescence in these reactions was also clearly visualised when under UV light (Figure 5.10B). These data suggest the addition of 100 µM oseltamivir did not affect NanH activity. DANA on the other hand, even on its own, did impact NanH activity, but this effect was as significant when oseltamivir was additionally added to the MUNANA reactions. Based on this finding, it was decided that both oseltamivir and DANA would be introduced to future biofilm communities to increase the likelihood that the composition of these communities would be impacted by the loss of sialidase activity.

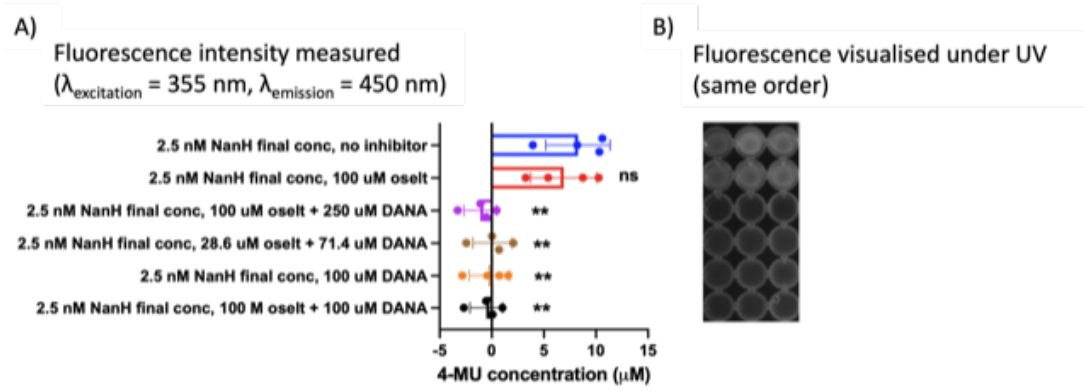

Figure 5.10 MUNANA assay to test for NanH enzyme activity in combination with sialidase oseltamivir and DANA. A MUNANA assay was performed where 2.5 nM purified NanH was incubated at 37 C for 2 minutes with 100 µM MUNANA substrate with and without the presence of sialidase inhibitors. (A) The concentration of 4-MU released from MUNANA in each of the six experimental conditions was measured at the excitation wavelength 355 nm and emission wavelength 450 nm. This showed the addition of 100 µM oseltamivir was not significantly different to when no inhibitor was present. The addition of DANA (at various concentrations with or without oseltamivir present) however did significantly reduce the concentration of 4-MU when compared to the no inhibitor control. (B) The reduced fluorescence in these reactions was also visualised under UV light. Data from the MUNANA assay were obtained from four independent repeats and error bars calculated from standard error of mean (SEM). Multiple paired t-tests were performed, where ns is non-significant, $0.01<p<0.05$ *, $0.01<p<0.001$ **, $p<0.001$ *** and $p<0.0001$ ****.

5.2.4.5 Effect of adding 100 µM oseltamivir and 250 µM DANA to the mock community model

To trial the effect of adding both 100 µM oseltamivir and 250 µM DANA on microbial communities, the inhibitors at these concentrations were added to the growth medium of mock communities which were grown for up to 21 days. As previously mentioned in Chapter 4, mucin that was sterilised by autoclaving and by filter-sterilising prior to use was also tested separately. As shown in Figure 5.11A and Figure 5.11B, the addition of inhibitors compared to the absence of inhibitors caused a reduction in the relative abundance of streptococci. The genus *Dialister*

also increased in its relative abundance for both 14-day and 21-day old biofilms. This was seen from an increase of a mean of 1.3 % to 7.2 % for the triplicate communities at day 14 and an increase from a mean of 1.7 % to 14.7 % at day 21. Compared to the biofilms absent of inhibitors, bacteria from genera such as *Actinomyces, Prevotella, Parvimonas, Filifactor* and *Fusobacterium* were also in higher abundance although this was more pronounced at day 14 than at day 21. These observations were also seen in the microbial communities where filter-sterilised mucin was used (Figure 5.11C and Figure 5.11D). As before, the relative abundance of *Streptococcus* reduced whereas *Dialister* increased but with greater effect than previously observed when autoclaved mucin was used. The genus *Porphyromonas* was also detected at 18.7 % in one 14-day old biofilm community that had inhibitors added in (Day 14 rep 1) although this was not found in the two other replicate communities. The data shown here suggest the addition of 100 µM oseltamivir alongside 250 µM DANA reduced streptococcal growth and increased the abundance of strict anaerobes in the communities. The dominant 5 named genera were tested for their significance using paired t-tests as demonstrated in Figure 5.12. However, it should be highlighted that the changes observed for individual genera from the addition of inhibitors were not statistically significant and it was likely a result of the caveat of small sample size (n=3).

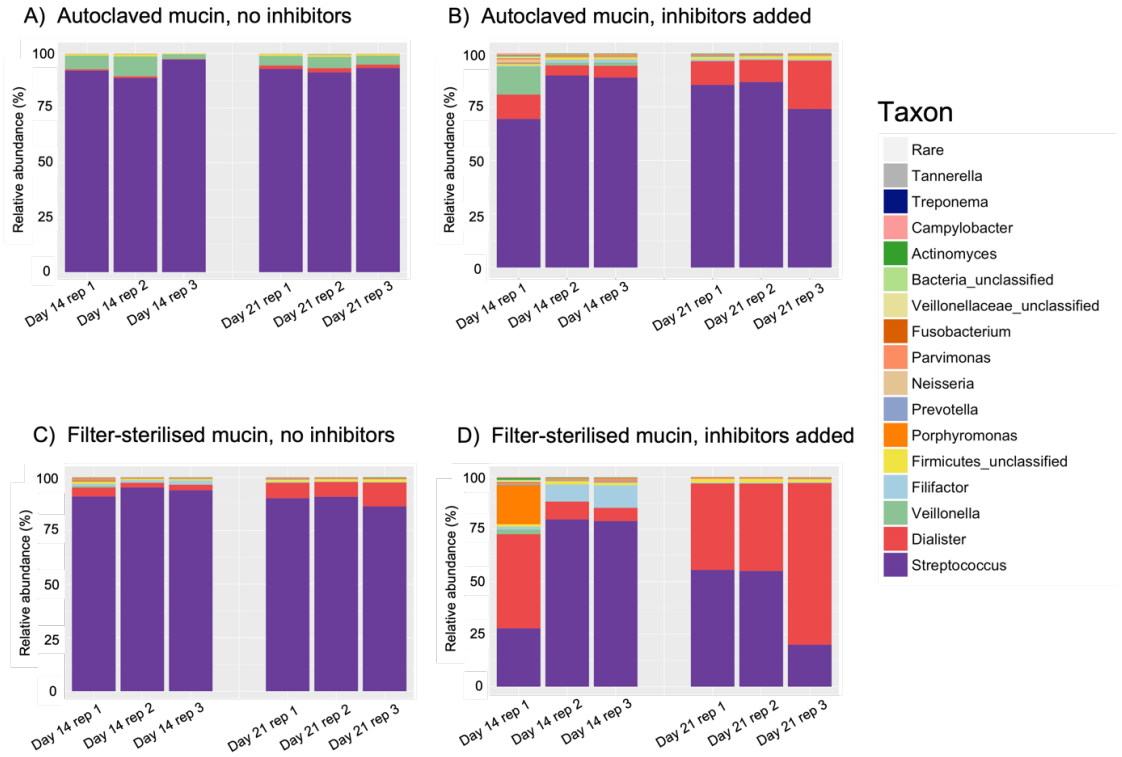

Figure 5.11 Relative abundance plots of genus-level taxa in autoclaved vs filter-sterilised mucin, with and without the addition of 100 µM oseltamivir and 250 µM DANA. The group labelled "Rare" was comprised of a combination of all genera that did not have >0.1 % relative abundance in at least one microbial community. The taxa in the legend were ordered by the level of relative abundance, with *Streptococcus* highest at the bottom and the group "Rare" lowest on the top.

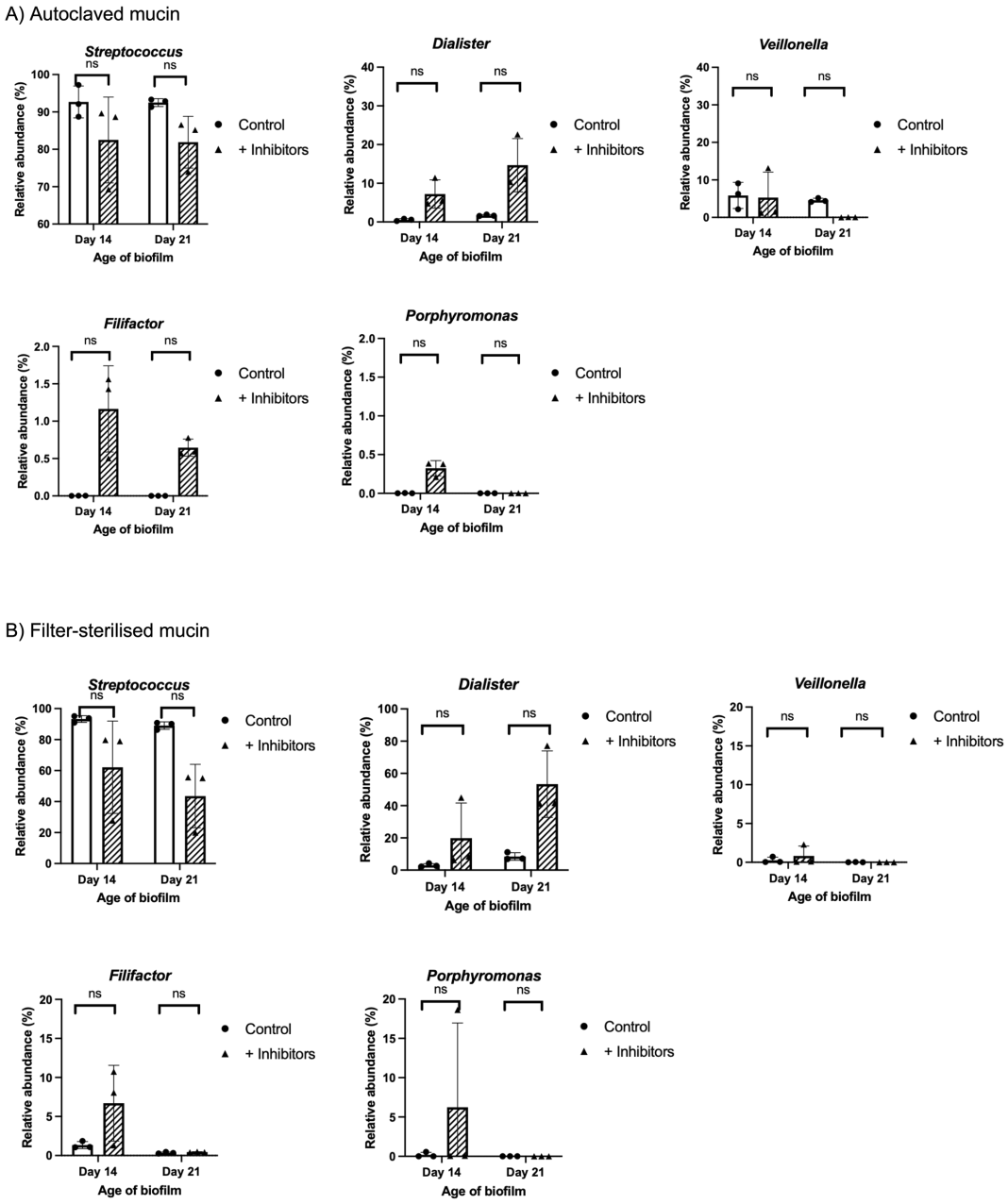

Figure 5.12 Relative abundances of 5 most dominant genera compared between use of autoclaved vs filter-sterilised mucin and treatment with 100 µM oseltamivir and 250 µM. The top 5 named genera are in order of abundance for when A) autoclaved mucin and B) filter-sterilised mucin was used in the biofilm growth medium. Multiple paired t-tests conducted for comparison between the absence (control) and presence of 100 µM oseltamivir and 250 µM, where ns is non-significant, 0.01<p<0.05 *, 0.01<p<0.001 **, p<0.001 *** and p<0.0001 ****.

The overall shape of the communities was consistent between triplicate mock community samples although this effect was clearer in the control biofilms. As shown in Figure 5.13A, Figure 5.14A and Figure 5.15A, there was a significant difference in α-diversity (Simpson's diversity index) between the presence and absence of inhibitors (p=0.0002) but not between using autoclaved and filter-sterilised mucin (p=0.15) and day of biofilm harvest (p=0.66). Principal coordinates

analysis based on distance matrices calculated by using the Jaccard index in Figure 5.13B, Figure 5.14B and Figure 5.15B demonstrated that the clustering of communities was independent on day of biofilm harvest and dependent on whether inhibitors were present as well as the mucin sterilisation technique used.

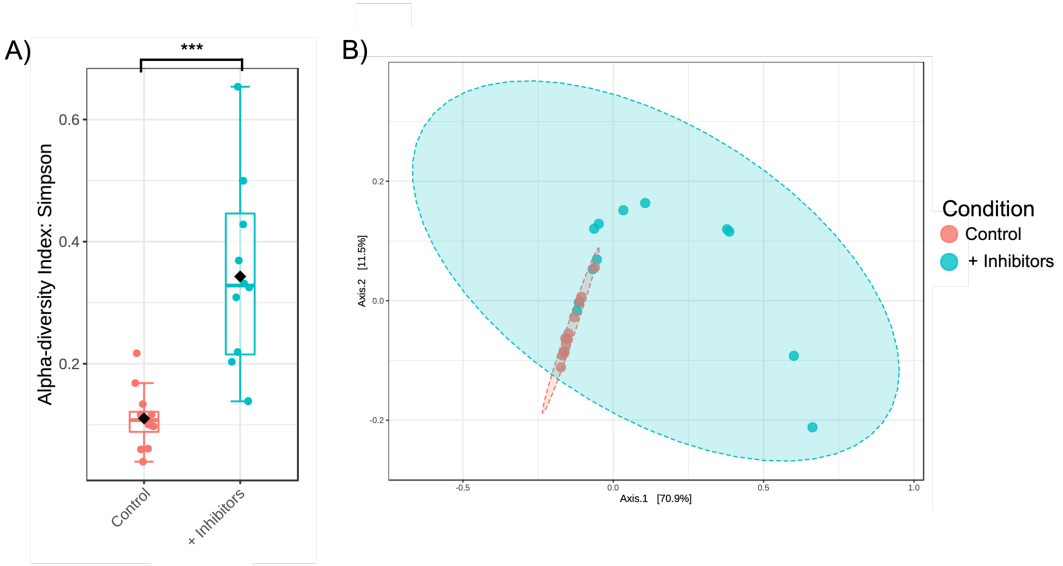

Figure 5.13 Diversity comparison between mock biofilm communities grown without (control) and with 100 µM oseltamivir and 250 µM DANA. A) Boxplots depicting the Simpson's alpha-diversity index values B) Principal coordinates analysis plots based on community membership using the Jaccard index. A t-test was performed on the alpha-diversity index values, where ns is non-significant, 0.01<p<0.05 *, 0.01<p<0.001 **, p<0.001 *** and p<0.0001 ****.

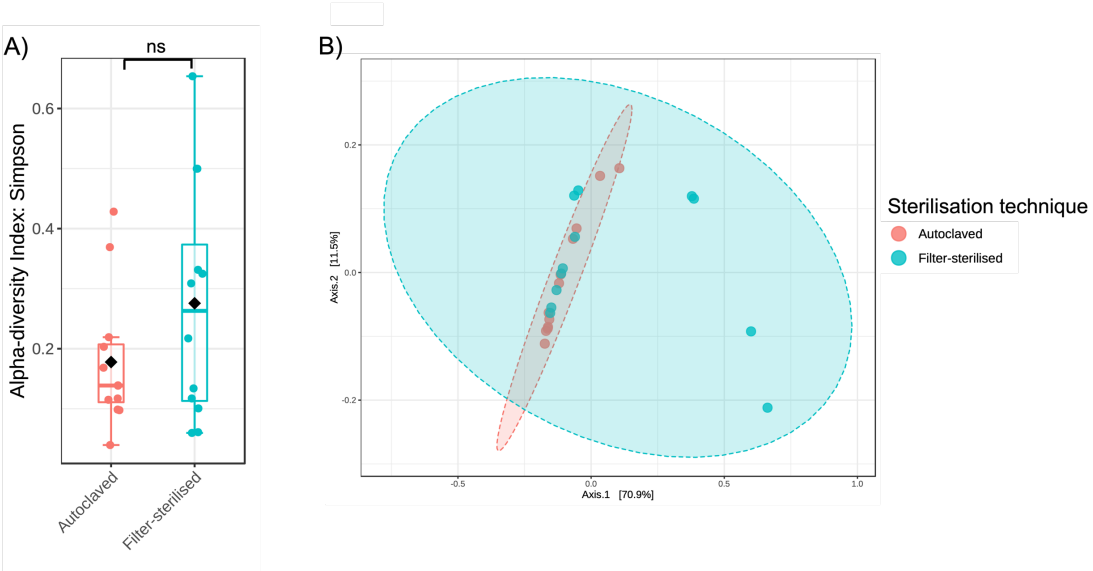

Figure 5.14 Diversity comparison between mock biofilm communities grown in growth medium containing autoclaved and filter-sterilised mucin. A) Boxplots depicting the Simpson's alpha-diversity index values B) Principal coordinates analysis plots based on community membership using the Jaccard index. A t-test was performed on the alpha-diversity index values, where ns is non-significant, 0.01<p<0.05 *, 0.01<p<0.001 **, p<0.001 *** and p<0.0001 ****.

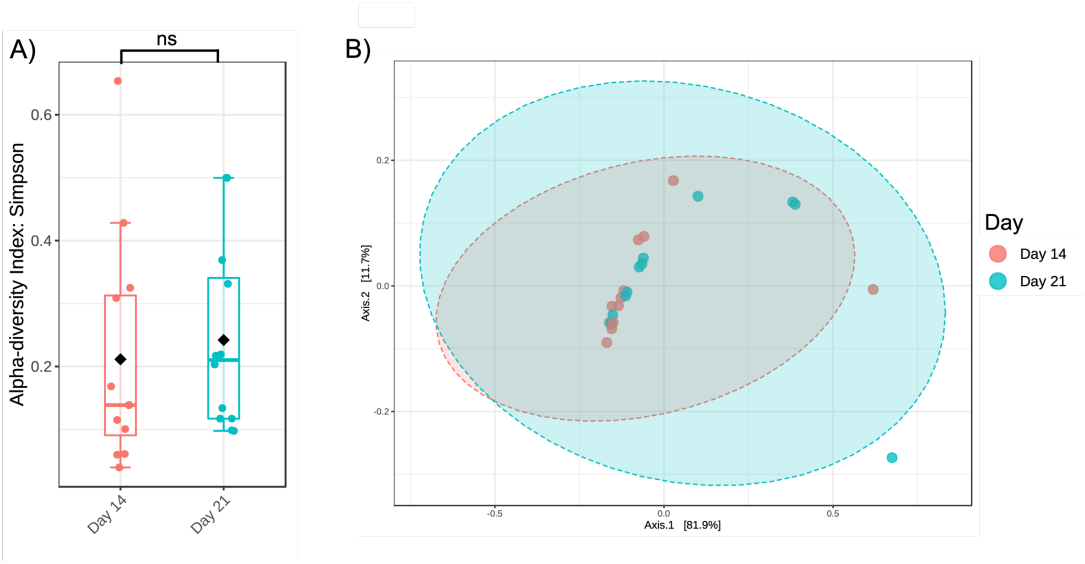

Figure 5.15 Diversity comparison between mock biofilm communities harvested at days 14 and 21. A) Boxplots depicting the Simpson's alpha-diversity index values B) Principal coordinates analysis plots based on community membership using the Jaccard index. A t-test was performed on the alpha-diversity index values, where ns is non-significant, 0.01<p<0.05 *, 0.01<p<0.001 **, p<0.001 *** and p<0.0001 ****.

5.2.4.6 Effect of oseltamivir and DANA on plaque biofilm communities

To establish whether the effect observed in section 5.2.4.5 with adding 100 µM oseltamivir and 250 µM DANA to the mock community model could also be replicated in the plaque biofilm model, the same conditions were used to grow plaque biofilms which were inoculated from each of three different subgingival plaque pools collected from 10 volunteers each. Biofilms from three MBEC pegs were pooled to create one plaque biofilm sample and three plaque biofilm samples were created for each condition. Only filter-sterilised mucin was used in these experiments.

<u>Influence of different pooled plaque samples to inoculate plaque biofilms</u>

To assess the variability in the composition of subgingival plaque, three pools of subgingival plaque were first profiled by sequencing the 16S rRNA gene using the Nanopore MinION flow cell. Each pool comprised of ten plaque samples per 8 ml to obtain the sufficient volumes required for inoculating plaque biofilms on the MBEC plates. However, as DNA could not be amplified from each of the plaque communities using the Thermo Scientific Phusion Green Hot Start II High-Fidelity PCR Master Mix (Thermo Fisher Scientific, USA), this master mix which was used in all previous work was replaced with the LongAmp Taq 2X Master Mix (NEB, USA).

As shown in Figure 5.16 (labelled 'Inoculum' on top row), the community compositions of the three inocula were consistent across all three pools. Additionally, across the pools, the predominant genus-level taxa in order of relative abundance were *Streptococcus* (32.4-53.0 %), *Veillonella* (19.3-39.1 %), *Selenomonas* (4.8-15.4 %), *Dialister* (3.0-4.9 %), *Gemella* (1.3-4.1 %), *Granulicatella* (1.2-2.9 %), *Prevotella* (0.7-3.1 %), *Fusobacterium* (0.5-2.2 %), *Capnocytophaga* (0.8-1.5 %) and *Anaeroglobus* (0.4-2.2 %).

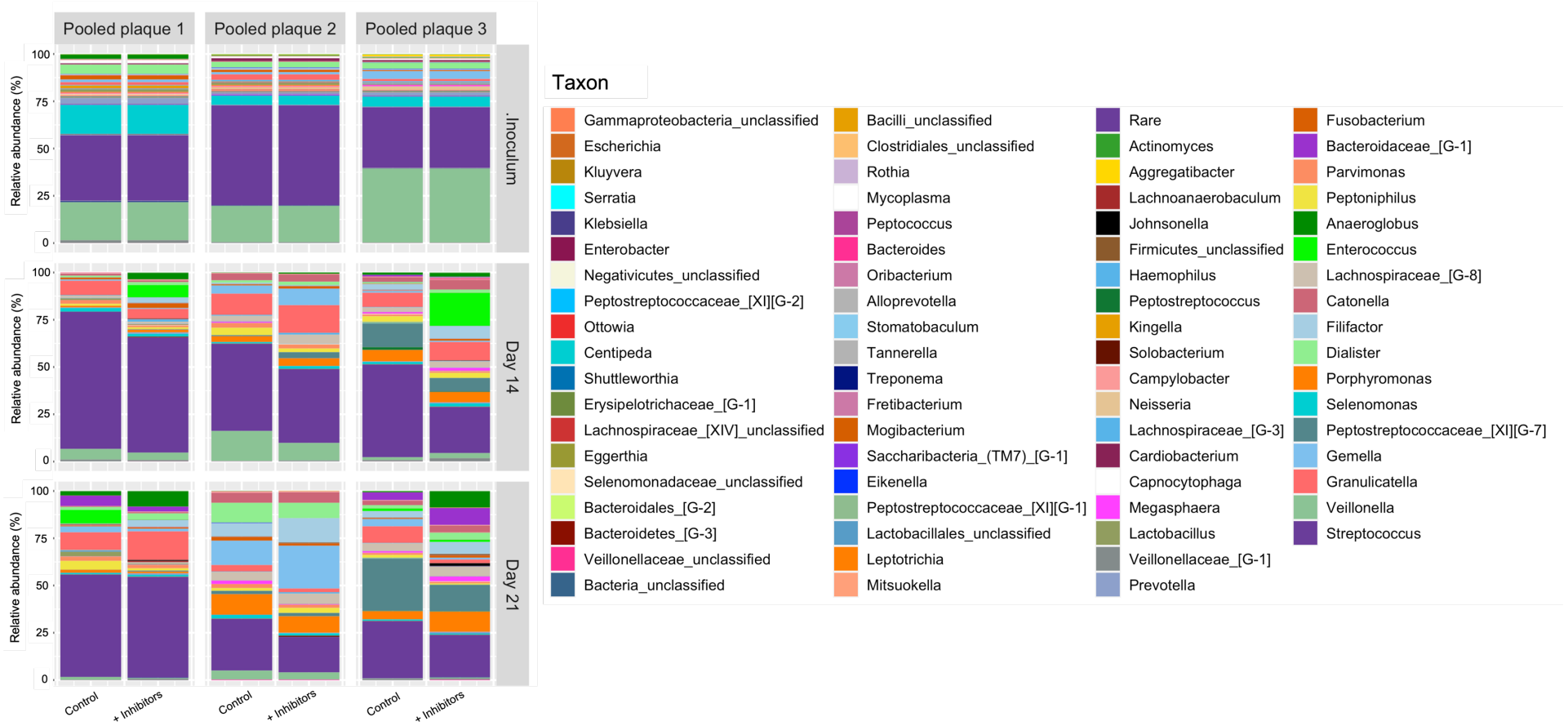

Figure 5.16 Relative abundance plots of the three pooled plaque inocula used to inoculate plaque biofilms and the plaque biofilms grown with and without treatment of 100 µM oseltamivir and 250 µM DANA. The data are separated by inoculum, whether is inoculum or biofilm grown for 14 or 21 days, and with and without the addition of 100 µM oseltamivir and 250 µM DANA to the growth medium. The group labelled "Rare" is comprised of a combination of all genera that did not have >0.1 % relative abundance in at least one plaque community. The taxa in the legend are ordered by the level of relative abundance, with *Streptococcus* highest at the bottom and far-right and *Gammaproteobacteria_unclassified* lowest on the top and far-left.

The plaque biofilm samples were analysed for their compositions using Nanopore sequencing on days 14 and 21 and the mean relative abundance of genus-level taxa were also plotted in Figure 5.16 (labelled 'Day 14' and 'Day 21' on middle and bottom rows respectively). Across all the biofilm communities irrespective of the age of the biofilms, whether the inhibitors were added, or which pooled plaque inoculum was used, *Streptococcus* dominated with mean relative abundances of 18.7-72.4 % measured. Like the three inocula profiled, all the biofilms were dominated by anaerobes. Generally, across the biofilms grown from different inocula, the other 6 most dominant genus-level taxa were *Granulicatella, Veillonella, Porphyromonas, Enterococcus, Dialister,* and *Filifactor.*

Influence of age of plaque biofilm communities

Comparison between the biofilms grown for 14 and 21 days again irrespective of the presence of absence of inhibitors showed an overall reduction in the relative abundances of the taxa *Streptococcus* and *Veillonella,* and an increase in *Porphyromonas, Peptostreptococcaceae_[XI][G-7], Gemella, Filifactor* and *Dialister*. This indicated the age of the biofilms appeared to influence the plaque community compositions and this was further supported by diversity data shown Figure 5.17. Here, α-diversity analysis of the samples by Simpson's diversity index demonstrated it significantly increased with biofilm age (p=0.03) and PCoA analysis of plaque biofilm samples also indicated distinct clusters which was driven by the age of the communities.

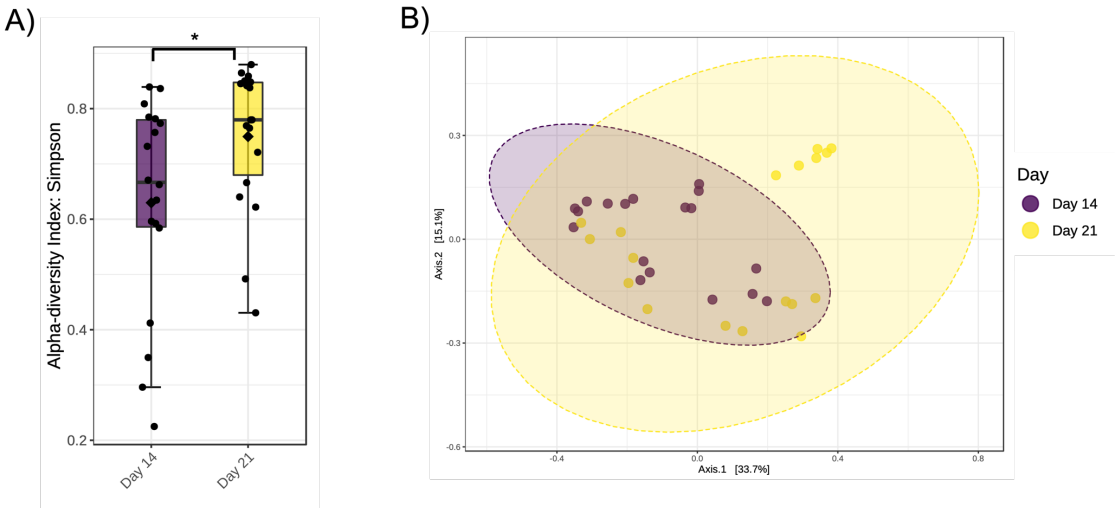

Figure 5.17 Diversity for plaque biofilms compared between days 14 and 21. A) Boxplots depicting the Simpson's alpha-diversity index values B) Principal coordinates analysis plots based on community membership

using the Jaccard index. T-test was performed, where ns is non-significant, 0.01<p<0.05 *, 0.01<p<0.001 **, p<0.001 *** and p<0.0001 ****.

Influence of sialidase inhibitors on plaque biofilm communities

As Figure 5.16 previously showed clear differences in the community compositions between plaque biofilms grown with and without sialidase inhibitors, more detailed analysis was conducted to measure these differences. Figure 5.18 compares the relative abundances of the 20 predominant genus-level taxa between control biofilms and the biofilms treated with 100 µM oseltamivir and 250 µM DANA. Here, the mean relative abundances of *Streptococcus* and *Veillonella* were significantly reduced in the treated biofilms compared to control ($p<0.05$ and $p<0.01$ respectively). This was observed for both growth periods. In contrast, the genera *Filifactor, Dialister* and *Fusobacterium* had higher mean relative abundances in the biofilms that grew in medium containing the sialidase inhibitors ($p<0.05$ on at least one day). Interestingly, the mean relative abundance of *Capnocytophaga* in the plaque biofilms appeared to decrease in the presence of 100 µM oseltamivir and 250 µM DANA but this reduction was not statistically significant ($p>0.05$). This observation also emerged when 100 µM oseltamivir was added to the earlier plaque biofilm communities, as described in section 5.2.4.1 above. As shown in Figure 5.19, there was a small increase in the overall α-diversity (Simpson's diversity index, $p=0.18$) when inhibitors were added to the plaque biofilm model, although this change was not significant. Furthermore, no distinct clusters were observed in the PCoA plot between the presence and absence of inhibitors. Taken together, the data indicated treating the biofilms with inhibitors caused changes to the relative abundance of individual genera but not to the overall shape of the communities.

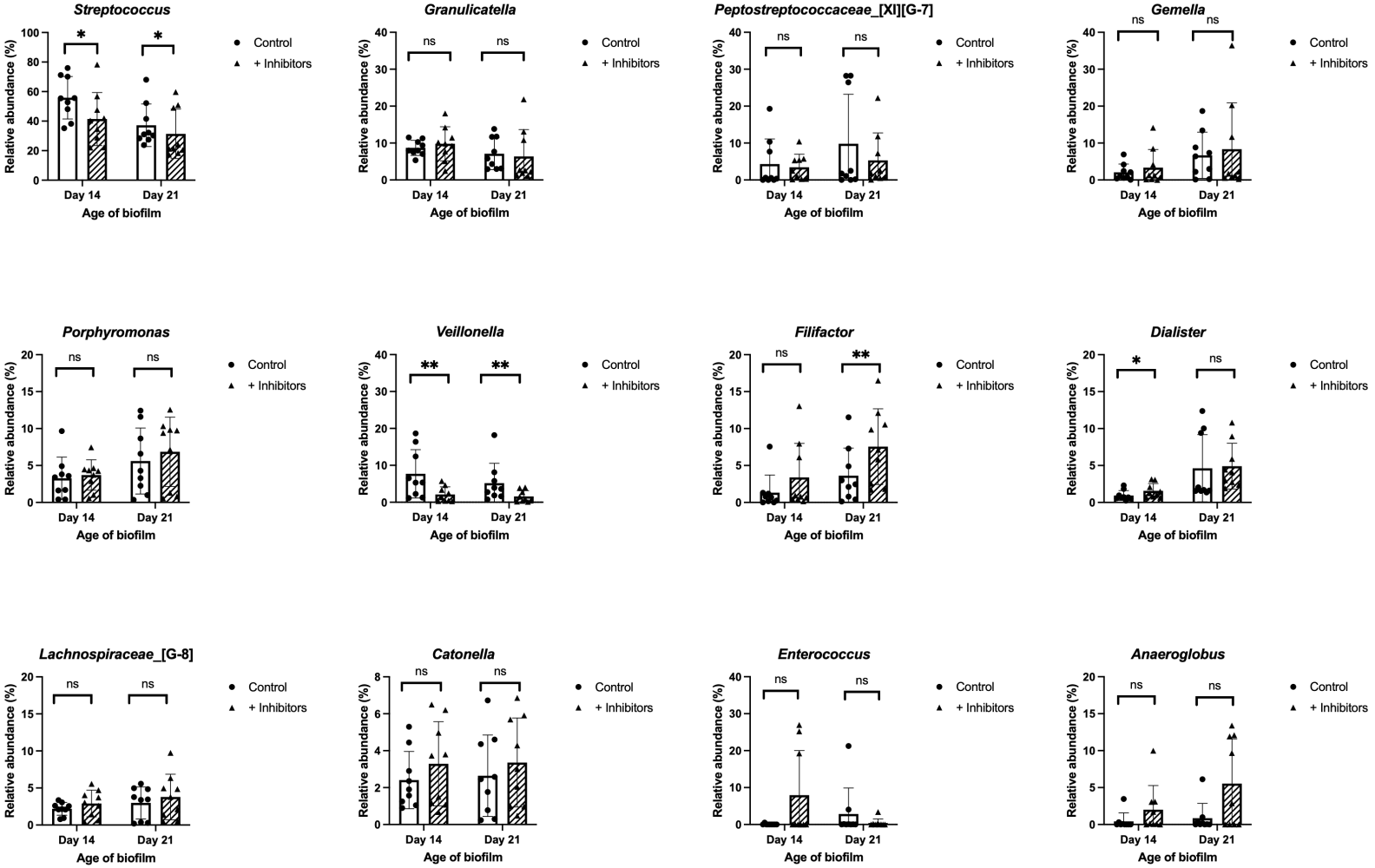
Streptococcus
Granulicatella
Peptostreptococcaceae_[XI][G-7]
Gemella
Porphyromonas
Veillonella
Filifactor
Dialister
Lachnospiraceae_[G-8]
Catonella
Enterococcus
Anaeroglobus
Relative abundance (%)
Age of biofilm
Day 14
Day 21
Control
+ Inhibitors
ns
*
**

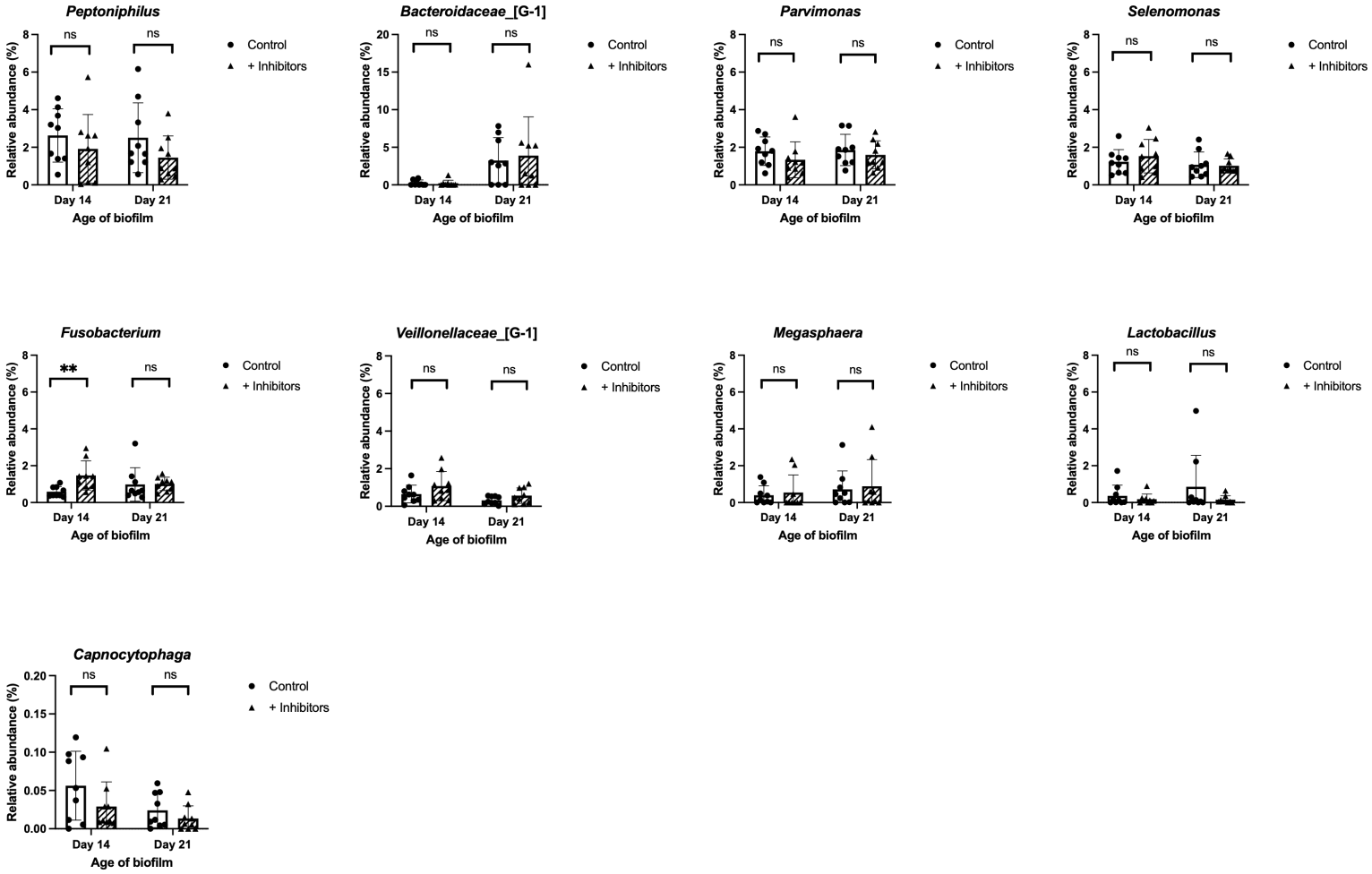

Figure 5.18 Relative abundances of 20 most dominant genus-level taxa in order of abundance, when comparing between control and inhibitor-treated plaque biofilms. The biofilms were also analysed at day 14 and 21 of growth and the genus Capnocytophaga was also included due to the results described in section 5.2.4.1 above. Multiple paired t-tests were performed, where ns is non-significant, 0.01<p<0.05 *, 0.01<p<0.001 **, p<0.001 *** and p<0.0001 ****.

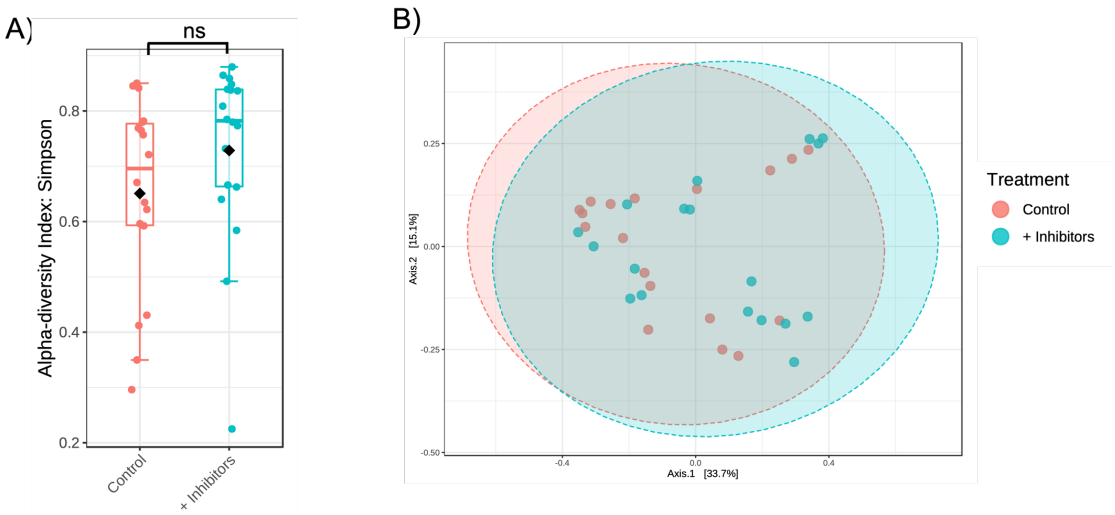

Figure 5.19 Diversity for plaque biofilms compared between the absence (control) and presence of inhibitors. A) Boxplots depicting the Simpson's alpha-diversity index values B) Principal coordinates analysis plots based on community membership using the Jaccard index. T-test was performed, where ns is non-significant, 0.01<p<0.05 *, 0.01<p<0.001 **, p<0.001 *** and p<0.0001 ****.

5.2.5 Use of deglycosylated growth medium in the plaque biofilm model

5.2.5.1 NanH and NanS gene expression and protein purification

An aim of this project was to investigate the impact of using deglycosylated growth medium on the development of a plaque biofilm community. This was an important consideration as the mFUM growth medium used in growing *in vitro* biofilm communities in this study comprised of 10 µM bovine submaxillary mucin and 30 % human serum. Both components naturally contain sialic acids on the termini of their glycoproteins and the sialidases NanH and NanS could be used to deglycosylate the mucin and serum. The two enzymes were therefore initially purified before using them in the deglycosylation process.

Both NanH and NanS genes were expressed in *E. coli* BL21 Origami having been previously established in the laboratory and the purification of NanH enzyme was completed using nickel-affinity chromatography. In contrast, the purification of NanS enzyme involved using glutathione-affinity chromatography combined with the thrombin cleavage of the GST-NanS domains to release free NanS. As shown by the SDS-PAGE gel in Figure 5.20A, purified NanH (containing His-tag) at the correct approximate molecular weight of 57.4 kDa was eluted in the elution fractions 1-6, with over 95 % purity observed. GST-free NanS was also purified but only following thrombin cleavage first to remove the GST-tag and similar to NanH, the protein was

also confirmed at >95 % purity at the correct molecular weight of approximately 76 kDa (Figure 5.20B).

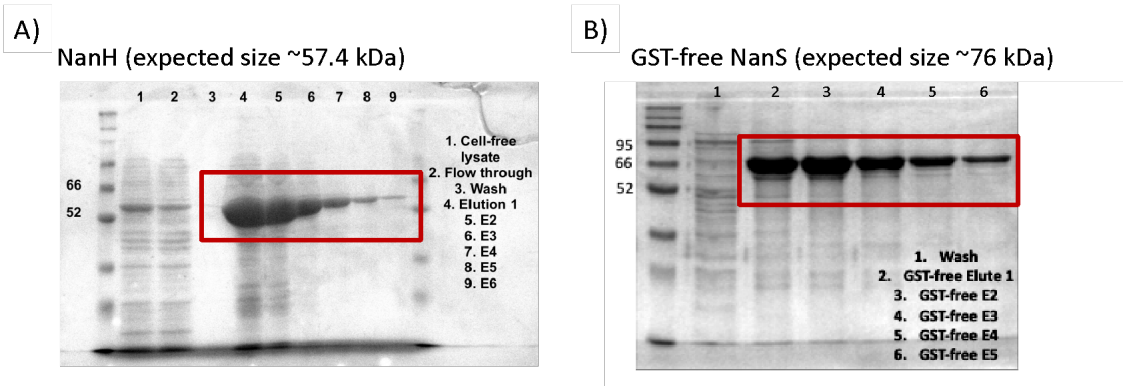

Figure 5.20 Elution profiles to confirm purification of NanH and NanS. SDS-PAGE gels of A) NanH at correct approximate size of 57.4 kDa and B) GST-free NanS at correct approximate size of 76 kDa. Elution fractions (E1-E6 for NanH and E1-E5 for GST-free NanS) are highlighted in red.

The concentration of purified NanH was quantitated to 1.92 mg/ml and the concentration of purified NanS to 0.51 mg/ml by performing a Pierce BCA assay. The activity of both enzymes (each at concentrations of 2.5 nM) was then confirmed. NanH activity was confirmed quantitatively after 2 min incubation (Figure 5.21A) by using the MUNANA assay to check for NanH enzymatic cleavage of the MUNANA substrate against a 4-MU standard curve. NanS activity was also confirmed (Figure 5.21B) but with the p-Nitrophenol Acetate (pNP-Ac) assay via the cleavage of the substrate pNP-Ac and comparing against a p-Nitrophenol (pNP) standard curve. Heat-denatured NanH and NanS that were incubated at 95 °C for 30 min acted as negative controls. After testing, the purified intact enzymes were then used to carry out deglycosylation of bovine submaxillary mucin and human serum as outlined below.

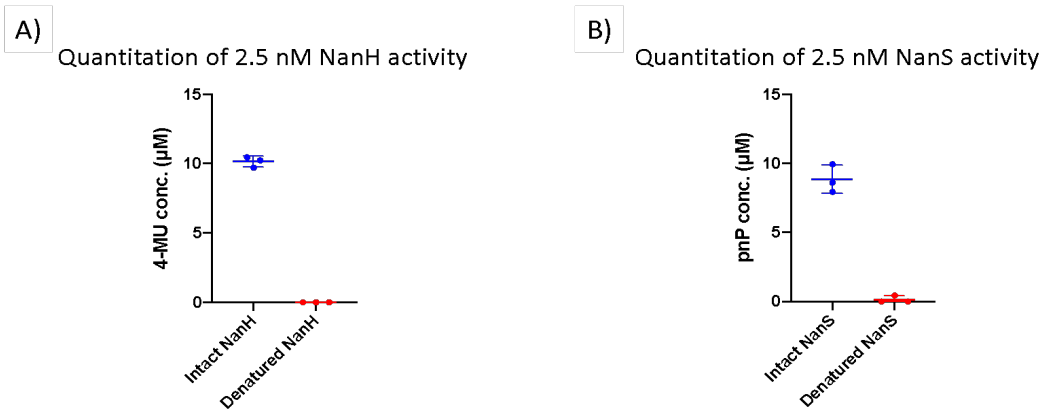

Figure 5.21 Quantitation of purified intact and denatured enzyme activity. A) 2.5 nM NanH activity was measured against a 4-MU standard curve when MUNANA was cleaved by NanH. B) 2.5 nM NanS was measured against a pNP standard curve when pNP-Ac was cleaved by NanS.

5.2.5.2 Deglycosylation of bovine submaxillary mucin and human serum

In line with an aim of this project, work was then set out to test whether the two enzymes NanH and NanS which were previously purified, could release sialic acids from bovine submaxillary mucin and human serum. The process for deglycosylating mucin was previously described by Phansopa *et al.* (2015) but optimisation was required for this project as here, the deglycosylated mucin and serum would consequently be used as components of the biofilm growth medium. To do this, 30 % heat-inactivated human serum was first incubated at 37 °C overnight with sialidase enzymes. As illustrated in Figure 5.22A and measured by the thiobarbituric (TBA) assay, 93.3 nmoles sialic acids were released from serum upon overnight incubation with 2 µM NanH and 2 µM NanS. This was an almost 3-fold increase from the 31.6 nmoles sialic acids released from serum when incubated solely with 2 µM NanH. NanS alone released a lesser number of sialic acids (10.9 nmoles), which was similar to the findings already evidenced in the study by Phansopa *et al.* (2015). The authors here have previously revealed the increased accessibility to sialic acid for cleavage by the presence of NanS together with NanH. This finding was also observed here. However, it was not possible to replicate this experiment as the turbidity observed for 30 % human serum affected the colorimetric readings in the TBA assay. As indicated by "<" in Figure 5.22B, the loss of high molecular weight proteins was also seen when the reactions were run on 4-12 % Bis-Tris gradient SDS-PAGE gels and visualised with Instant Blue.

30 % heat-inactivated human serum

A) Quantitation of released sialic acids

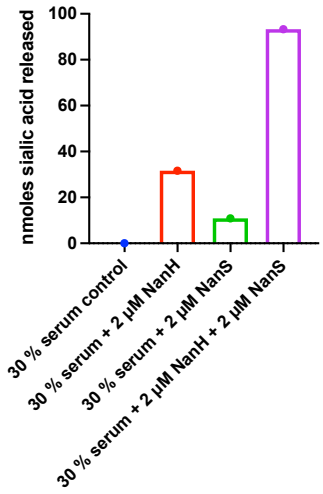

B) Visualisation of proteins stained with Instant Blue

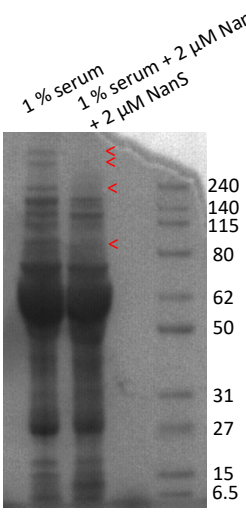

Figure 5.22 Quantitation of free sialic acids released from serum after overnight co-incubation with sialidases. The incubation of 30 % heat-inactivated human serum, with and without 2 µM NanH and/or 2 µM NanS are as indicated. Reactions were incubated overnight at 37 °C before released free sialic acids were quantitated with the TBA assay and visualised on a 4-12 % Bis-Tris gradient SDS-PAGE gel. "<" indicates loss of protein bands in the reaction where NanH and NanS were added. The presence of NanH and NanS cannot be seen on the protein gel in the reaction containing human serum (likely due to being obstructed by high amounts of proteins present in human serum). Data from the TBA assay were from one independent testing.

Given the growth medium also contained bovine submaxillary mucin, the cleavage of sialic acids from mucin under these conditions were also tested. This was illustrated after the removal of sialic acids from 1 % bovine submaxillary mucin (Figure 5.23A). Here, the incubation of mucin with 2 µM NanH resulted in the release of a mean of 50.5 nmoles sialic acids but an approximately 1.5X increase (77.6 nmoles) of sialic acids were released from mucin with the addition of both enzyme types. NanH alone and NanH combined with NanS released amounts of sialic acids that were statistically significantly different to the mucin only control. NanS alone however did not. As observed with human serum, a small number of sialic acids (mean of 6.5 nmoles) was seen when mucin was incubated solely with 2 µM NanS. These data were again in agreement with those findings from Phansopa *et al.* (2015).

As these sialidase enzymes would need to be either removed or deactivated from the deglycosylated mucin and human serum at a later stage before the deglycosylated glycoproteins could be used as components of growth medium used

in the biofilm model, it was likely useful to reduce the enzyme concentration used in the deglycosylation process. Serially diluted enzyme concentrations of 0.1 µM to 2 µM for each enzyme were therefore tested and co-incubated with 1 % bovine submaxillary mucin. Figure 5.23B suggests it might be advantageous to reduce the concentrations of enzymes from 2 µM to 0.1 µM (the lowest concentration of enzymes tested here). This was evidenced by a mean of 83.5 nmoles free sialic acids being released from the mucin when 0.1 µM NanH and 0.1 µM NanS were added, compared to a mean of 103.3 nmoles released when 2 µM NanH and 2 µM NanS were added. It was shown the two conditions produced non-statistically significant results to one another (p-value = 0.1916). At each varying concentration of enzymes, the nmoles of free sialic acids that were released were statistically significantly different to the 1% mucin control. In order of increasing enzyme concentrations compared to the mucin control, the p-values were as follow: p-value = 0.0059 for 0.1 µM; p-value <0.0001 for 0.25 µM; p-value = 0.003 for 0.5 µM; p-value = 0.0043 for 1 µM and p-value = 0.0019 for 2 µM each enzyme. Because of these data, the lowest and highest concentrations of enzymes (0.1 µM and 2 µM) alongside the mucin control were run on 5-12 % Bis-Tris gradient SDS-PAGE gels (Figure 5.23C and Figure 5.23D), with one stained with Instant Blue to visualise all of the proteins, and a second stained with Pro-Q Emerald 300 Glycoprotein Stain Kit in order to visualise only the glycoproteins. These gels showed the loss of molecular weight proteins >115 kDa in mucin incubated with both concentrations of enzymes (as indicated by “<”) when compared to the mucin control. The increase in protein band intensity (as indicated by “>”) was also observed for molecular weight proteins <115 kDa which was likely due to the cleavage of the higher molecular weight proteins into smaller proteins. The presence of both enzymes NanH and NanS (molecular weights of approximately 57.4 kDa and 76 kDa respectively) were also highlighted with “*” at the correct molecular weights on the SDS-PAGE gel stained with Instant Blue.

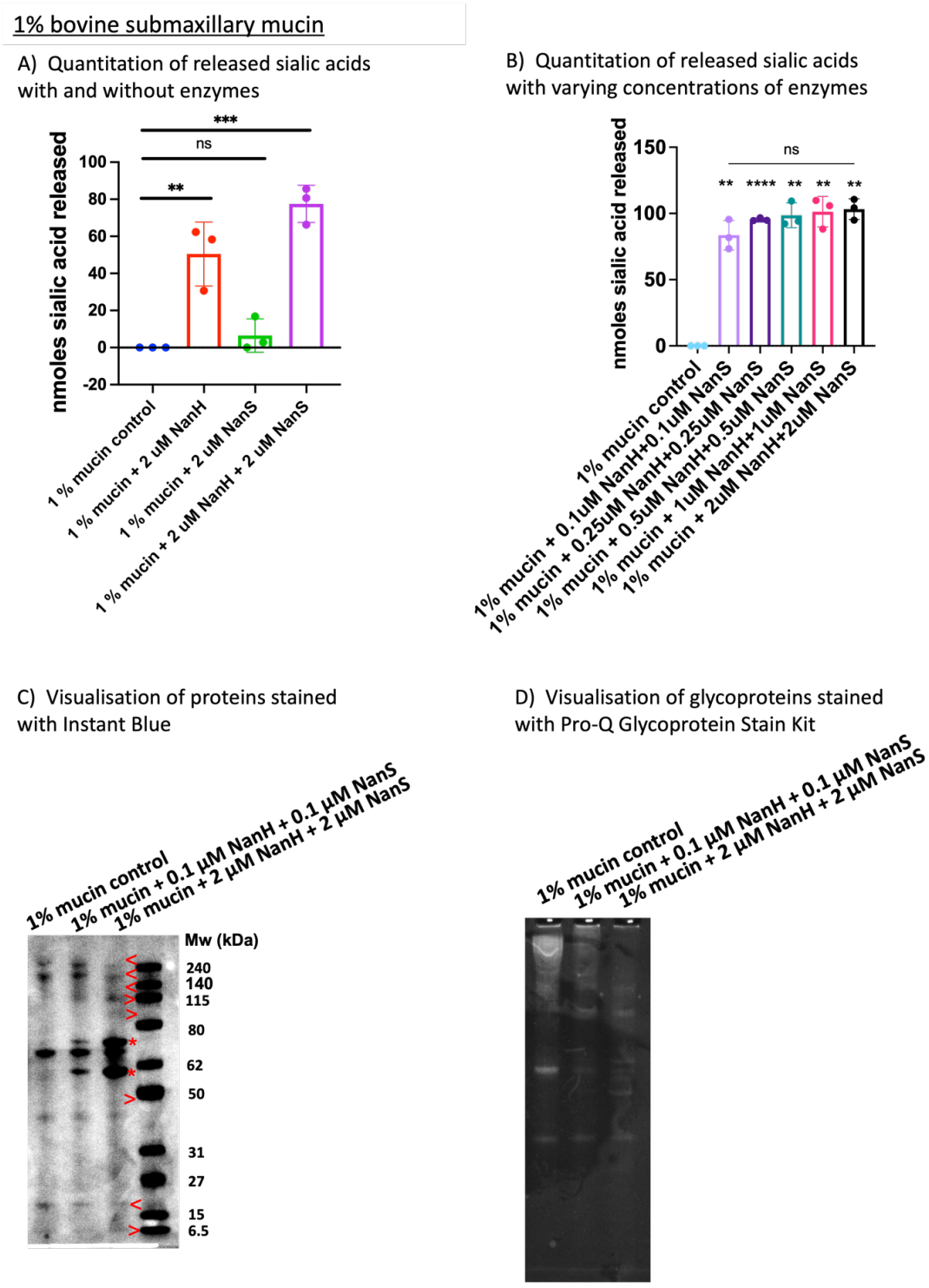

Figure 5.23 Quantitation of free sialic acids released from mucin after overnight co-incubation with sialidases. Shown are incubation of 1 % (20 µM) bovine submaxillary mucin, (A) with and without NanH and/or NanS present and (B) at with and without varying concentrations of enzymes as indicated. Reactions were incubated overnight at 37 °C before released free sialic acids were quantitated with the TBA assay and C) visualised on a 5-12 % Bis-Tris gradient SDS-PAGE gel stained with Instant Blue. "<" indicates loss of protein bands and ">" indicates increase in protein band intensity in the reaction where NanH and NanS were added and * indicates the presence of NanH and NanS. D) The Pro-Q Emerald 300 Glycoprotein Stain Kit was used to visualise glycoproteins that was first run on a 5-12 % Bis-Tris gradient SDS-PAGE gel. Data from the TBA assay from three independent repeats and error bars calculated from standard error of mean (SEM). Multiple paired t-tests were performed, where ns is non-significant, $0.01<p<0.05$ *, $0.01<p<0.001$ **, $p<0.001$ *** and $p<0.0001$ ****.

In addition to these data, acid hydrolysis was also considered as an alternative method to using purified sialidases in the deglycosylation process as this would not require a method of removing or deactivating the sialidase enzymes prior to their use in the biofilm model. To release sialic acids from mucin, incubation of 1 % bovine submaxillary mucin with 0.1 M H_2SO_4 was tested under varying incubation conditions as similarly described in studies by Pearce and Major (1978) and Schauer (1982). 87.1 nmoles sialic acids were released from mucin when co-incubated with 0.1 M H_2SO_4 at 80 °C for 50 min as shown in Figure 5.24. This was more similar to the 83.5 nmoles free sialic acids being released from the mucin when 0.1 µM NanH and 0.1 µM NanS were added, compared to a mean of 103.3 nmoles released when 2 µM NanH and 2 µM NanS were added, although it was previously shown the released sialic acids to not be statistically significantly different to each other. Increasing incubation duration with H_2SO_4 however did not aid with increasing sialic acid release. In fact, increasing the duration of 80 °C incubation to 4 h and to overnight hindered sialic acid release. This was shown by the lower levels of sialic acid released (46.3 nmoles and 23.0 nmoles respectively). Incubation at 4 °C released the least sialic acids (3.8 nmoles only). This therefore suggested that the use of purified sialidase enzymes released slightly more sialic acid than the use of acid hydrolysis.

Acid hydrolysis for deglycosylating mucin

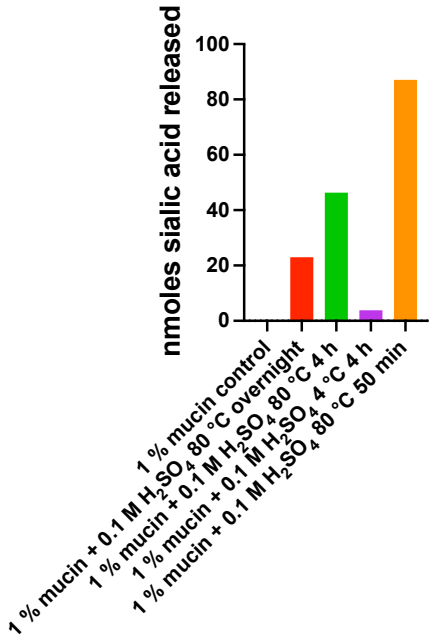

Figure 5.24 Quantitation of free sialic acids released from mucin after acid hydrolysis. Shown are measurements from a TBA assay depicting free sialic released from 1 % (20 µM) bovine submaxillary mucin by 0.1 M H2SO4 acid hydrolysis under different incubation conditions.

5.2.5.3 Removal of sialidase enzymes after mucin and serum deglycosylation

As shown previously, deglycosylating mucin and serum led to the release of sialic acids so it was imperative that these free sialic acids were removed from the growth medium before the medium was then used in biofilm modelling.

Vivaspin® ultrafiltration spin columns (Sartorius, Germany) fitted with 3000 molecular weight cut-off (MWCO) filters were used to remove any compounds with MWCO <3000 from deglycosylated bovine submaxillary mucin and human serum. For example, mucin and serum which were first incubated with 0.1 µM NanH and 0.1 µM NanS at 37 °C for 24 h. As free sialic acids were <3000 MWCO (MWCO = 309.27), they would pass through the Vivaspin® ultrafiltration spin filters and be discarded and therefore removed from the deglycosylated mucin and human serum. Both the mucin and human serum were spun thrice using the Vivaspin® ultrafiltration spin columns, where after three centrifugal spin cycles mucin contained a theoretical 64-fold reduction in free sialic acids and human serum a 216-fold reduction (Table 5.3).

Table 5.3 Theoretical x fold reduction in released free sialic acids from deglycosylated mucin and serum. Calculations based on fold reduction in released sialic acids during and after three centrifugal spin cycles using Vivaspin® ultrafiltration spin columns on deglycosylated mucin and human serum.

	Post first centrifugal spin (fold reduction in free sialic acids)	Post second centrifugal spin (cumulative fold reduction in free sialic acids)	Post third centrifugal spin (cumulative fold reduction in free sialic acids)	**Total reduction in free sialic acids after three centrifugal spins**
Mucin	4-fold	16-fold	64-fold	**64-fold**
Human serum	6-fold	36-fold	216-fold	**216-fold**

The latter step of using the Vivaspin® ultrafiltration spin columns were also used on non-deglycosylated mucin and serum (i.e. which had been incubated with heat-inactivated NanH and NanS for 24 h) which acted as controls as the mucin and serum would still contain sialo-glycoproteins. An additional step of denaturing NanH and NanS enzymes prior to setting up any biofilms was therefore required to prevent further unwanted deglycosylation occurring during biofilm growth. To verify at which temperature and the duration exposing the enzymes to would lead to their loss of function activity, a MUNANA assay was performed for 50 nM NanH that was incubated under a variety of conditions: unheated; 60 °C for 30 min; 60 °C for 60 min; 65 °C for 30 min and 65 °C for 60 min. Under the same variety of conditions, a PnPA assay was also performed on 50 nM NanS to check for its enzyme activity. As shown in

Figure 5.25, all four heat conditions led to the complete loss of activity for both NanH and NanS so treating the two enzymes at 65 °C for 30 min was selected. This condition was chosen to optimise enzyme activity loss but for the shortest duration tested.

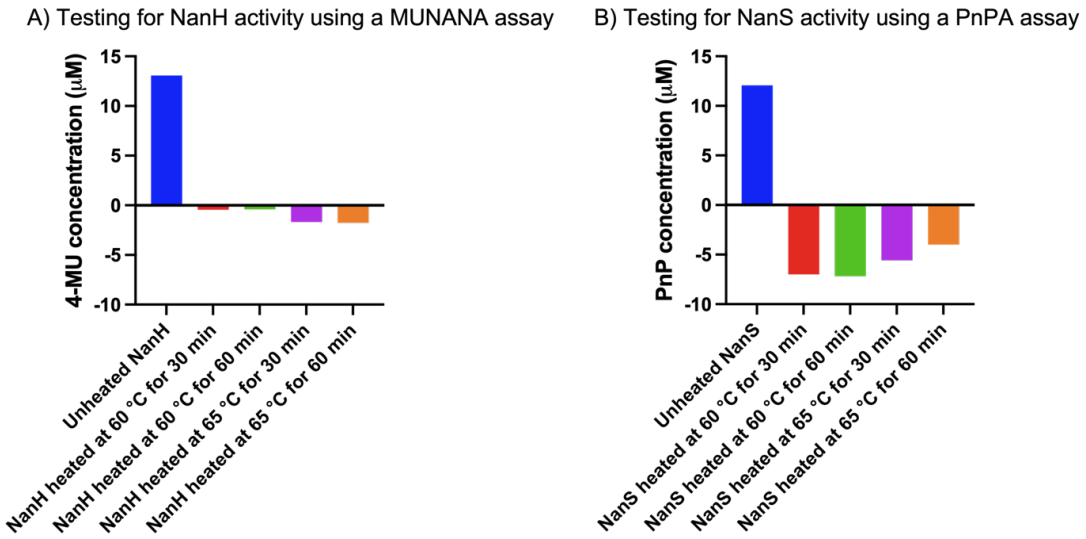

Figure 5.25 Assessment of NanH and NanS activity after heat treatment. After NanH and NanS were incubated under a variety of heat conditions (including unheated as a control), MUNANA and PnPA assays were performed to test for NanH and NanS activity respectively. The loss of enzyme activity function was evident for all four of the heat conditions and for both NanH and NanS.

A TBA assay was performed on the human serum that was either incubated with denatured or intact enzymes and had been centrifuged thrice in the Vivaspin® ultrafiltration spin columns. This was conducted to quantitate the amount of released free sialic acids that remained in the spin columns. Furthermore, a TBA assay was also conducted on the flow-through of the deglycosylated serum as it should contain any discarded free sialic acids. Time did not permit the same assessment for the deglycosylated mucin samples. As shown in Figure 5.26, comparable concentrations of free sialic acid were detected in the human serum that was first incubated with denatured and intact enzymes prior to being centrifuged thrice in the Vivaspin® ultrafiltration spin columns. No free sialic acids were detected in the flow-through sample, which was an unexpected outcome as it was theorised that free sialic acids would pass through the column and thus be collected in the flow-through.

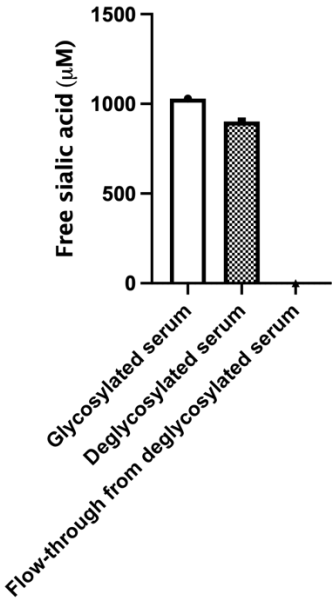

Figure 5.26 Quantitation of free sialic acids from deglycosylated serum released after removal from Vivaspin® ultrafiltration spin columns. TBA assay measurements of free sialic acids released from glycosylated serum, deglycosylated serum and flow-through from deglycosylation after centrifugation thrice in Vivaspin® ultrafiltration spin columns.

5.2.5.4 Effect of deglycosylated growth medium on the plaque biofilm communities

To investigate the role of sialo-glycoproteins in the growth of plaque biofilm communities, the compositions of the communities were also compared between using glycosylated and deglycosylated growth medium. Figure 5.27 provides an overview of the relative abundances of the genus-level taxa detected in plaque biofilms and compares the communities between using glycosylated and deglycosylated growth medium. The communities grown for this experiment were separate from the previous experiments, although they were also inoculated from pooled plaque 3. The genus *Veillonella* dominated (40.4-65.2 %) across the plaque biofilms irrespective of the age of the biofilms and whether the growth medium contained sialo-glycoproteins, followed by *Streptococcus* (16.7-38.0 %). When deglycosylated growth medium was used, there was a higher relative abundance of *Megasphaera* (means of 0.6 % vs 3.3 % for Day 14 biofilms and 0.5 % vs 10.8 % for Day 21 biofilms), and a reduction in *Selenomonas* (means of 4.1 % vs 1.3 % for Day 14 biofilms and 5.3 % vs 1.3 % for Day 21 biofilms). However as shown in Figure 5.28, these two differences were not statistically significant. Overall, multiple paired t-tests did not reveal any significant differences between plaque biofilms grown in glycosylated and deglycosylated growth medium and α-diversity

measured by using the Simpson's diversity index was also not significantly different between the two conditions (p=0.19). In contrast, distinct clusters were formed after PCoA analysis of the plaque biofilm samples using distance matrices measured by the Jaccard index. This showed that clustering of biofilms was driven by the use of glycosylated and deglycosylated growth medium (Figure 5.29). The data taken together indicated the use of deglycosylated growth medium altered the community membership but richness, evenness and the abundance of individual genera remained comparable to using glycosylated growth medium. The biofilm growth periods were also analysed to see if this influenced the general shape of the plaque communities. As shown in Figure 5.30, α-diversity did not differ between harvesting the plaque biofilms on days 14 and 21, yet there was clustering of samples based on the biofilm growth periods on the PCoA plot. This suggested that like the use of deglycosylated growth medium, growing the communities for longer altered the community membership but not the richness and evenness of the plaque communities.

Figure 5.27 Community compositions of plaque biofilms grown using glycosylated and deglycosylated growth medium. Shown are relative abundance plots depicting the genus-level taxa present in plaque biofilms inoculated from pooled plaque 3 and using glycosylated and deglycosylated growth medium. The group labelled "Rare" is comprised of a combination of all genera that did not have >0.1 % relative abundance in at least one plaque community. The taxa in the legend are ordered by the level of relative abundance, with *Veillonella* highest at the bottom and far-right and the group *Bacilli*_unclassified lowest on the top and far-left.

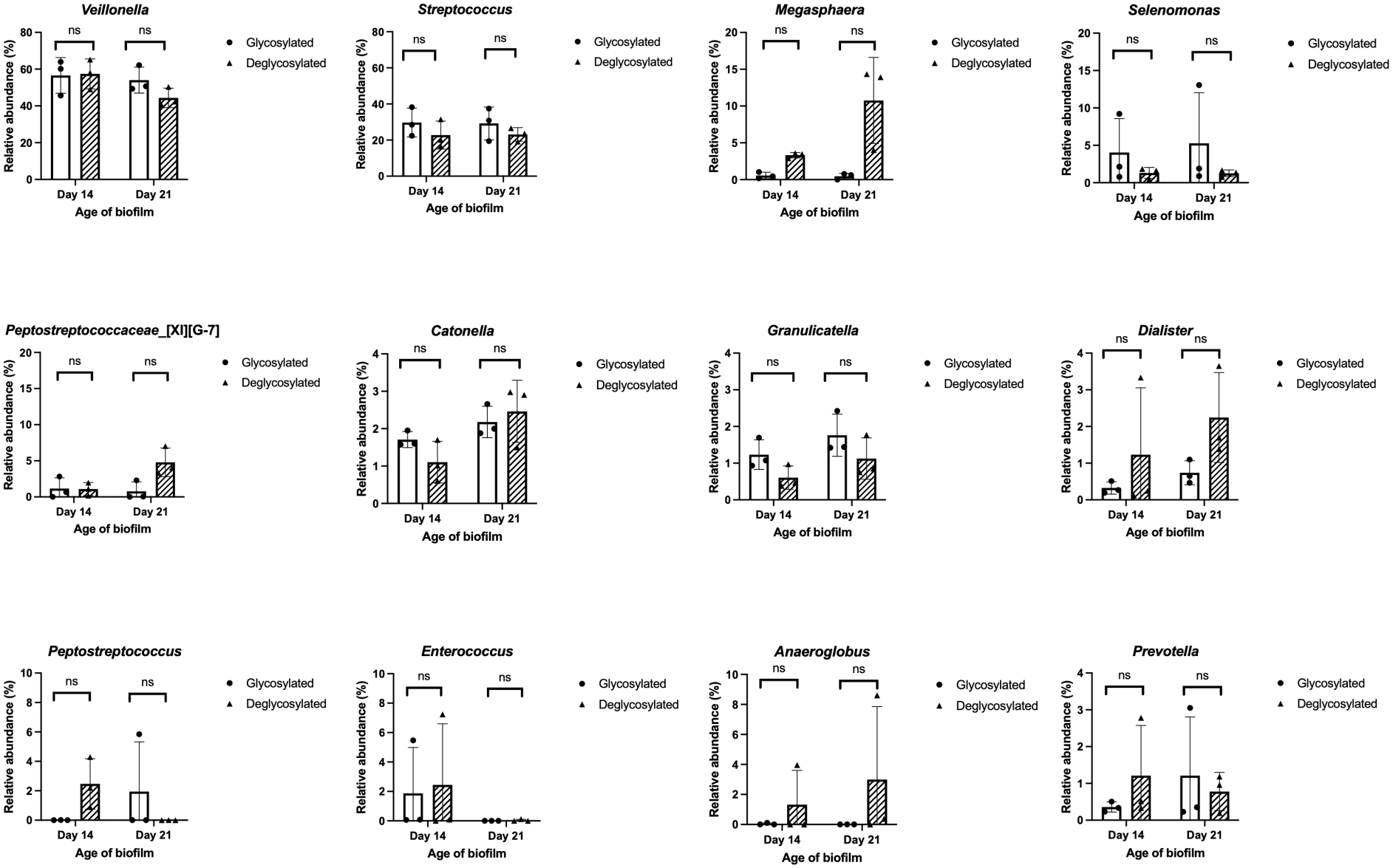
Veillonella
Streptococcus
Megasphaera
Selenomonas
Peptostreptococcaceae_[XI][G-7]
Catonella
Granulicatella
Dialister
Peptostreptococcus
Enterococcus
Anaeroglobus
Prevotella
Relative abundance (%)
Age of biofilm
Day 14
Day 21
ns
Glycosylated
Deglycosylated

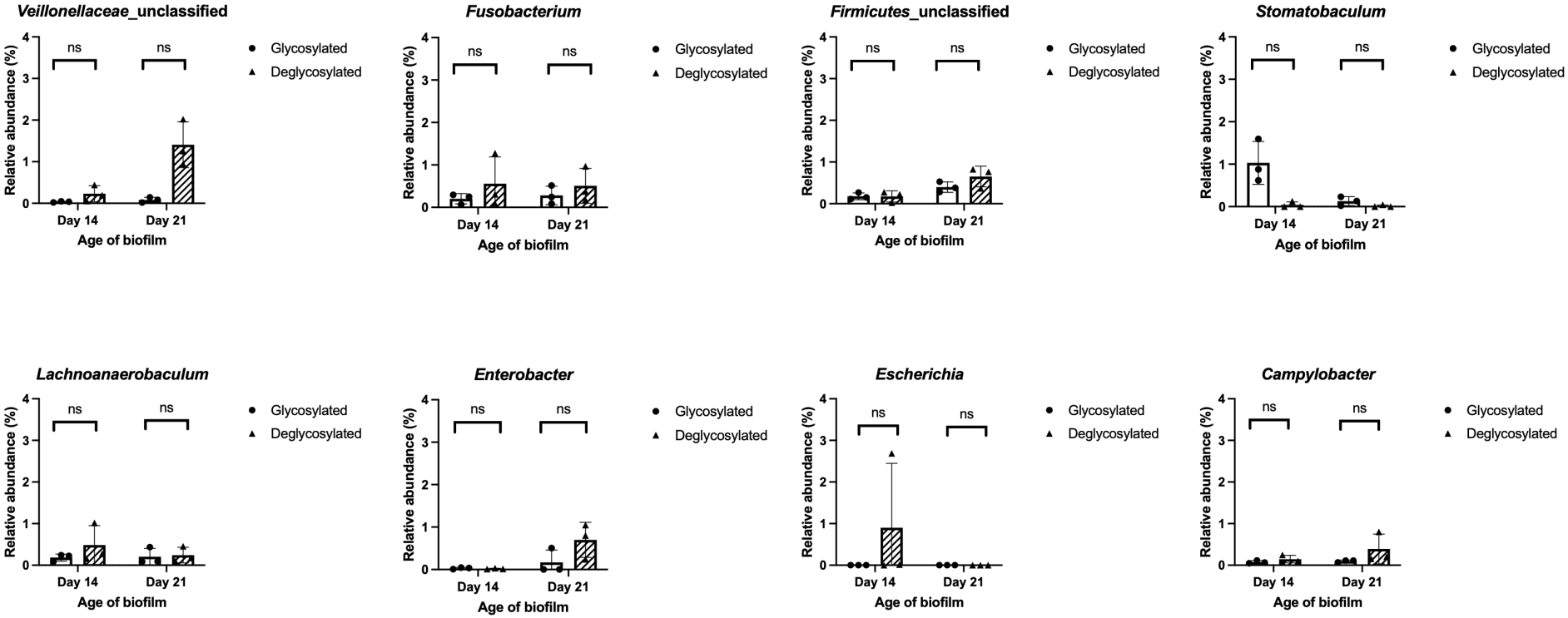

Figure 5.28 Relative abundances of 20 most dominant genus-level taxa in plaque biofilms grown using glycosylated and deglycosylated growth medium. The plots are in order of abundance and compare between the use of glycosylated and deglycosylated growth medium in growing 14- and 21-day plaque biofilms. Multiple paired t-tests were performed, where ns is non-significant, 0.01<p<0.05 *, 0.01<p<0.001 **, p<0.001 *** and p<0.0001 ****.

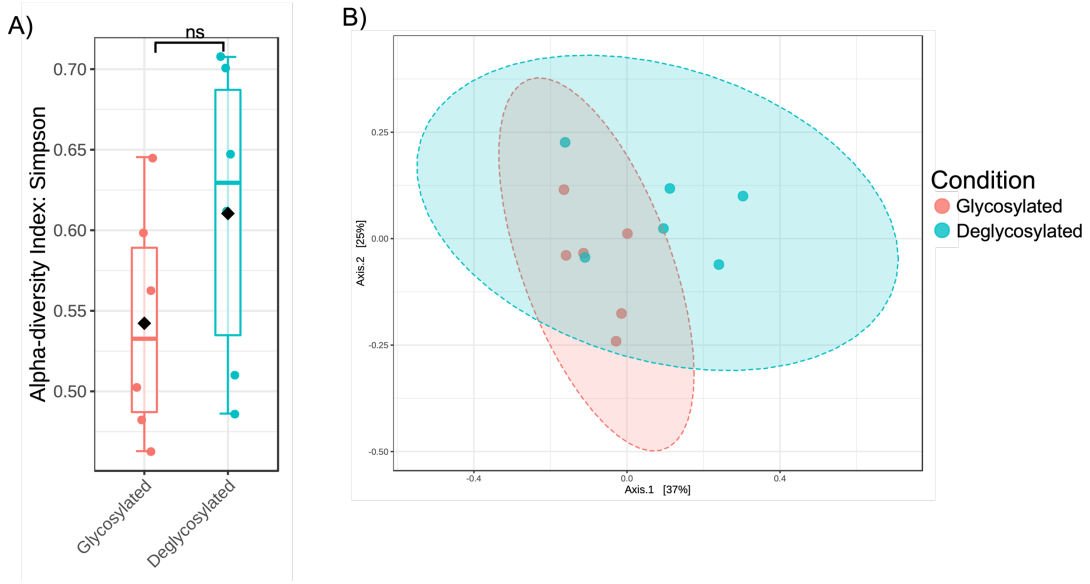

Figure 5.29 Plaque community diversity comparisons between the use of glycosylated and deglycosylated growth medium. The plaque biofilms were inoculated from pooled plaque 3 and analysed at day 14 and 21 of growth. A) Boxplots depicting the Simpson's alpha-diversity index values B) Principal coordinates analysis plots based on community membership using the Jaccard index. A t-test was performed on the Simpson's diversity index values, where ns is non-significant, 0.01<p<0.05 *, 0.01<p<0.001 **, p<0.001 *** and p<0.0001 ****.

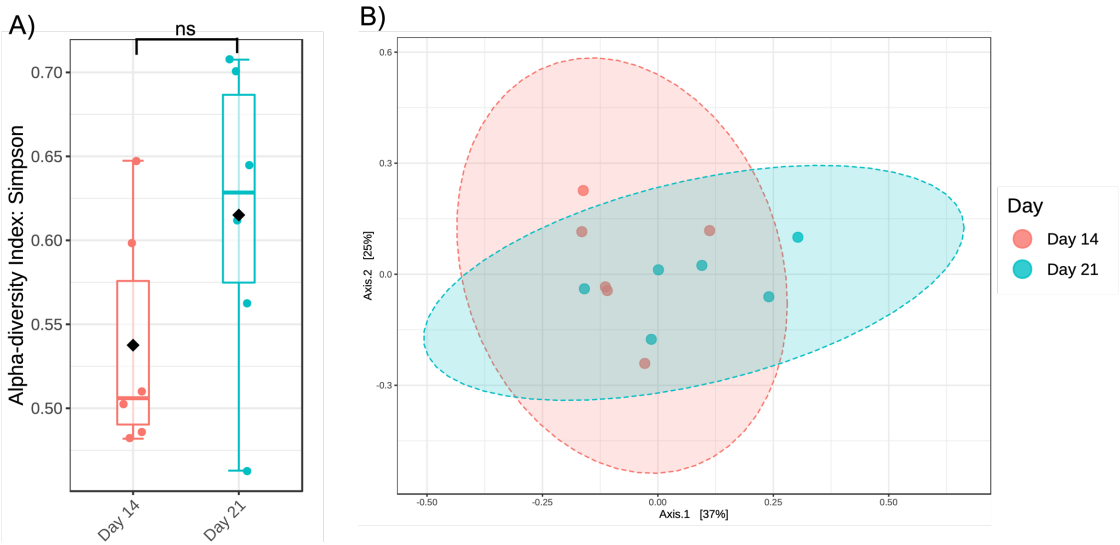

Figure 5.30 Plaque community diversity comparisons between Days 14 and 21 of biofilm growth. The plaque biofilms were inoculated from pooled plaque 3 and analysed at day 14 and 21 of growth. A) Boxplots depicting the Simpson's alpha-diversity index values B) Principal coordinates analysis plots based on community membership using the Jaccard index. A t-test was performed on the Simpson's diversity index values, where ns is non-significant, 0.01<p<0.05 *, 0.01<p<0.001 **, p<0.001 *** and p<0.0001 ****.

5.3 Discussion

As mentioned in the literature review, several reports have shown that sialidases were previously isolated from a range of oral bacteria such as *Streptococcus* spp., *Actinomyces* spp., *P. gingivalis, T. forsythia* and *T. denticola*. In this study, this was further expanded to include assessment for all 18 bacteria which were selected for use in the mock community inoculum. MUNANA assays were conducted on whole

bacterial cells to detect whether sialidases were present in the assay reactions. Of the 18 bacterial strains, 6 produced sialidases and these were *S. oralis, A. oris, P. gingivalis, T. denticola* and the two *T. forsythia* strains. These findings were consistent with the literature and this work was additionally verified by screening for sialidase genes in the whole genome sequences of all 18 bacteria. As sialidases belong to the glycoside hydrolase family 33 (GH33) of enzymes, the presence of GH33 in the genome would indicate a bacterium exhibiting sialidase activity. The GH33 is a family of enzymes that can hydrolyse the glycosidic bond between carbohydrates and this family includes bacterial sialidases, trans-sialidases, anhydrosialidases, Kdo hydrolyases and KDNases. In contrast to Aruni *et al.* (2011) who used the Amplex Red neuraminidase assay kit (Molecular Probes, USA) to detect sialidases in *F. alocis*, no evidence of sialidase activity was found in its genome sequence and in the MUNANA assay. It was possible the use of different assays contributed to the contrasting findings. For example, the Amplex Red neuraminidase assay kit relies on the generation of hydrogen peroxide by galactose oxidase after sialic acids are removed by sialidases. However, unlike the MUNANA assay, the presence of hydrogen peroxide or galactose oxidase in the Amplex Red neuraminidase assay reactions can generate false positive results.

As it was thought targeting sialidases with more potent sialidase inhibitors could hinder periodontal biofilm formation, it was important that sialidase inhibitors were assessed in their efficacy for inhibiting sialidase activity. Four commercially available sialidase inhibitors were selected and these were zanamivir, oseltamivir, DANA and siastatin B. Zanamivir and oseltamivir were selected for initial testing as they are FDA-approved drugs for treating influenza and are structural derivatives of the transition state analogues of sialic acids DANA. Furthermore, as mentioned earlier, studies have demonstrated their inhibitory effect on sialidase activity and bacterial growth (Roy *et al.*, 2011; Kurniyati *et al.*, 2013; Frey *et al.*, 2019; Yu *et al.*, 2021). The binding of sialic acid with oseltamivir has also recently been investigated by Satur *et al.* (2022). The authors revealed through structural modelling of the active site in NanH, the negatively charged carboxyl groups of oseltamivir interacted with the highly conserved arginine triad of the sialidase, bound by

hydrogen bonds to the cyclohexene ring, and its N-acetyl tail sat within a conserved hydrophobic pocket. Siastatin B was selected because it is commercially available and has been shown to be an inhibitor of neuraminidase, β-glucuronidase and N-acetyl-β-D-glucosaminidase (Nishimura *et al.*, 1988; Rahman *et al.*, 2015). Plant-based sialidase inhibitors such as berberine, palmatine and the catechin epigallocatechin gallate (EGCg) which is found in green tea extract, have also been shown to exhibit inhibitory activity against influenza neuraminidase (Song, Lee and Seong, 2005; Wu *et al.*, 2011; Kim *et al.*, 2014; Enkhtaivan *et al.*, 2017). Although it would also have been useful to assess the efficacy of these plant-based sialidase inhibitors, it was beyond the scope of this project to test them at this stage. This project was focused on developing an *in vitro* biofilm model and using this model as a proof of concept first.

Through MUNANA assays, it was discovered oseltamivir and DANA were the two most efficacious in inhibiting the activity of sialidases secreted from biofilm supernatant, with IC_{50} values measured at 0.78 μM and 2.06 μM respectively. Zanamivir in contrast was measured in the millimolar range instead of the micromolar and nanomolar ranges observed for oseltamivir, DANA and siastatin B. These results differed to those by Holzer *et al.* (1993), who found the inhibition constant K_i of DANA on influenza virus neuraminidases was in the micromolar range instead of the nanomolar range observed for zanamivir and oseltamivir. It is possible this was the reason why DANA is not an FDA-approved anti-influenza drug. However, the differing results might partly be explained by the varying levels of inhibitory effect that different sialidase inhibitors can have on different microorganisms. As an example, both DANA and oseltamivir were demonstrated to require concentrations in the micromolar range for inhibiting *T. forsythia* NanH activity by 50 %, compared to requiring zanamivir concentrations in the millimolar range under the same scenario (Satur, 2019). Of those tested, DANA was therefore the most potent inhibitor of NanH activity. In contrast, zanamivir more efficiently inhibited the sialidase activity (SiaPG) of *P. gingivalis* than the NanH sialidase activity of *T. forsythia* (Frey *et al.*, 2019). In addition, a nearly 20-fold difference in the zanamivir concentration was required to inhibit *T. forsythia* NanH activity by 50

% when compared to inhibiting the activity of *P. gingivalis* SiaPG by 50 %. This observation could be particularly relevant in a multispecies community whereby the addition of *T. forsythia* NanS has been shown to enhance the removal of sialic acids from mucin by *P. gingivalis* SiaPG sialidase (Frey *et al.*, 2019). As bacteria are known to act in synergy, the authors here have also tested and revealed a significant reduction of attachment and invasion of oral epithelial cells during a co-infection by *T. forsythia, P. gingivalis* and *F. nucleatum*. The high IC_{50} value observed for zanamivir in the MUNANA assay could also be explained by a possible lack of *P. gingivalis* growth in the biofilms and thus, a low concentration of SiaPG would also have been present in the biofilm supernatant sample which was tested.

An implication of the varying levels of inhibition associated with different sialidase inhibitors on different bacteria was the possibility that compared to control plaque biofilms, the addition of 100 µM oseltamivir caused a small change in the communities as shown in section 5.2.4.1. For example, clustering of the community samples was dependent on whether the biofilms were treated with oseltamivir. Although bacteria from the genera *Veillonella* and *Streptococcus* dominated in all plaque biofilms irrespective of treatment, in the presence of 100 µM oseltamivir, the relative abundances of *Veillonella* and *Capnocytophaga* decreased. Although *Veillonella* does not exhibit sialidase activity, the genome sequences of various species from the genus *Capnocytophaga* contain the GH33 family although the sialidase activity have yet to be directly tested. This includes the oral bacteria genus *C. haemolytica, C. leadbetteri, C. ochraceae,* and *C. sputigena*. It might be the case that the presence of oseltamivir inhibited the sialidases secreted by these bacteria and thus, hindered their growth in the plaque biofilms. It would have been worthwhile if time permitted, that follow-up experiments were conducted to measure the inhibition of sialidase activity using MUNANA assays on the whole cells of these *Capnyocytohaga* species to confirm their sialidase-positive statuses.

In contrast, the relative abundance of *Streptococcus* spp. increased to >50 % across all days of analysis in the presence of oseltamivir. This was an unexpected finding as the work in section 5.2.4.2 showed the reduction of sialidase activity in *S. oralis*

whole cells in the MUNANA assay reactions containing 100 µM oseltamivir. As sialidases are considered to be bacterial virulence factors (Corfield, 1992), it might have been expected that the inhibition of sialidases would impede *S. oralis* growth in the oseltamivir-treated plaque communities. The contradictory result seen here could be due to several reasons. Firstly, the plaque communities are complex and likely comprised of different *Streptococcus* spp.. Although sialidases have been isolated from *S. oralis, S. mitis* and *S. intermedius* (Beighton and Whiley, 1990; Byers *et al.*, 2000), there are also many *Streptococcus* spp. found in the human mouth that do not exhibit sialidase activity. According CAZy.org as examples, the genomes of the oral species *S. anginosus, S. cristatus, S. gordonii, S. pyogenes* and *S. salivarius* do not contain the GH33 family. The species *S. gordonii* was also confirmed by a MUNANA assay to not exhibit sialidase activity in Table 5.1. It was therefore possible that although these species could have used the harvested sialic acids, that the inhibitory effect of oseltamivir was to a lesser extent. Another possible explanation might be oseltamivir at 100 µM was insufficient to cause a large shift in the plaque biofilm compositions.

As DANA was the second most effective sialidase inhibitor tested in this project, it was investigated whether the aforementioned community composition changes could be amplified by the addition of DANA. It was clear after adding 250 µM DANA, as well as adding the combination of 100 µM oseltamivir + 250 µM DANA, that the fluorescence from MUNANA experiments conducted on whole bacteria and on NanH enzymes reduced in Figure 5.7 and Figure 5.10. This was in comparison to the control reactions and reactions containing only 100 µM oseltamivir. The findings here suggested the combination of oseltamivir and DANA produced the largest inhibitory effect. It was also possible that compared to oseltamivir, DANA was less selective in inhibiting different sialidases so had a broader range of effect. Still, it could be argued that the sialidase inhibitors were directly causing an anti-microbial effect on the tested micro-organisms, but this was disproved by conducting disk diffusion assays on several bacteria in section 5.2.4.3.

The effect of adding 100 µM oseltamivir and 250 µM DANA together to biofilm growth medium was investigated for both mock and subgingival plaque biofilms. Firstly, the overall community compositions changed upon the addition of the sialidase inhibitors on the mock biofilms. This was evidenced by the significant increase in diversity (as measured by Simpson's diversity index) and the distinct clustering of communities based on community membership, which indicated that differences arose due to the presence of the sialidase inhibitors. The results also suggested that even by day 14 of biofilm growth, it was clear a more even distribution of bacterial genera started to appear in the communities and was likely due to the reduction of streptococci which dominated in the control biofilms (Figure 5.11 and Figure 5.13). A similar picture was seen when plaque biofilms were also treated with 100 µM oseltamivir and 250 µM DANA together. Here, three sets of plaque biofilms were grown separately and inoculated from different pools of subgingival plaque samples. The most obvious finding to emerge from the Nanopore sequencing analysis of all the plaque biofilm communities was that like the findings from the mock biofilms, the relative abundance of *Streptococcus* in the plaque biofilms also reduced in the presence of the sialidase inhibitors. This reduction was statistically significant, as revealed by conducting paired t-tests on the percentages of *Streptococcus* measured in the plaque communities (Figure 5.18). This outcome was somewhat surprising as the opposite effect was observed when only 100 µM oseltamivir was added to previous plaque communities so the observed fall in *Streptococcus* growth could be attributed to solely the presence of 250 µM DANA. To develop a full picture of this effect, it would be interesting to detect any changes to individual *Streptococcus* spp. growth when plaque biofilms are grown in the presence and absence of only 250 µM DANA.

Also, in contrast to earlier findings, no change in the relative abundance of *Capnocytophaga* was detected in the plaque communities although this was likely due to the low relative abundances (<0.0015 %) detected for *Capnocytophaga* even in the control biofilms and in the three pooled plaque inocula (<1.5 %). The low abundance of this genus in the inocula is contrary to that of Zaura *et al.* (2009) who found *Capnocytophaga* to be dominant in samples obtained from patients with

periodontal disease. Furthermore, this genus was also considered to be part of the core oral microbiome (Bik *et al.*, 2010). The presence of 100 µM oseltamivir and 250 µM DANA also reduced the relative abundance of *Veillonella* significantly. This matched the observation found in the earlier plaque biofilms and could perhaps be explained by the widely reported co-aggregation between *Streptococcus* and *Veillonella* (Hughes et al. 1988, Chalmers et al. 208, Zhou et al., 2015, Zhou et al., 2021), where poorer streptococci growth could have resulted in the reduced growth of *Veillonella* species. Bacteria from both genera are thought to be key initial colonisers of the mouth. In relation to the red microbial complex (Socransky et al. 1998), *Tannerella* and *Treponema* spp. were not detected in any of the plaque biofilm communities, although *Porphyromonas* was found at low levels (<0.15 %) across the plaque biofilms. Although *P. gingivalis* was reported to exhibit sialidase activity (Moncla, Braham and Hillier 1990) and this was also confirmed in this study, there was no evidence of a reduction in *Porphyromonas* spp. growth due to the presence of sialidase inhibitors in the plaque biofilms. According to these data, it was possible a shift in the composition of the plaque communities occurred upon the presence of the sialidase inhibitors, although the complexity of the plaque communities hindered the ability to infer any direct changes to specific bacteria from the sialidase inhibition.

From a broader perspective, comparison between control and inhibitor-treated communities based on the Simpson's diversity index and on membership did not show any significant differences. In fact, the data suggested these overall community measures were more influenced by the age of the biofilms. Increases in α-diversity were observed with increasing biofilm growth periods for Figure 5.6, Figure 5.15, Figure 5.17 and Figure 5.30, although this increase was not always statistically significant and was likely due to small sample size. The significant shift in the communities observed in Figure 5.17 due to the age of the biofilms could be affected by the reduction of the dominant genus *Streptococcus* over time in both the mock and plaque communities, resulting in a significantly more even distribution in the communities irrespective of sialidase inhibitor treatment. This observation supported previous reports of dysbiosis in periodontitis progression,

where the relative abundance of Gram-positive aerobes such as *Streptococcus* would reduce, and higher levels of anaerobes would appear in the transition from health to diseased state (Kistler et al. 2013, Zaura et al. 2009). This study's oral biofilm models therefore simulated periodontitis progression over time and were useful as tools in studying the development of disease.

An important research question also remained, which was whether the addition of the sialidase inhibitors after the plaque biofilms become established instead of being added from the start would produce comparable results. Like the addition of antimicrobials to established biofilm communities, the effect of sialidase inhibition may be hindered compared to developing communities. As periodontal disease is a progressive disease where the oral microbial composition shifts over time, growing plaque biofilms under the two different conditions might help in the understanding of whether the sialidase inhibitors at these concentrations could suppress the growth of oral bacteria once they become established in the plaque communities.

As this study also set out to assess the role glycoproteins play in the growth of plaque biofilm communities, along with the inhibition of sialidases, this study sought to determine whether deglycosylated growth medium could also alter the microbial community compositions. The mFUM growth medium used in this study contained bovine submaxillary mucin (BSM) and human serum, both known to contain sialo-glycoproteins (Blix 1936, Lundblad et al., 2015). As reviewed by Sillanaukee et al. (1999), an estimated 80 % of the sialic acids present in human serum is 5-*N*-acetylneuraminic acid (Neu5Ac) and approximately 20 % is N-acetyl-9-O-L-lactylneuraminic acid (Neu5Ac9Lt). Furthermore, a low amount of the diacetylated sialic acid Neu5,9Ac_2 is found in serum. As mentioned in the literature review, this is thought to hamper access and the harvesting of the diacetylated sialic acids by bacteria and thus plays a protective role in humans. Bacteria in the human mouth therefore requires an additional enzyme such as NanS which is secreted by *T. forsythia* (Douglas et al. 2014, Phansopa et al. 2015), to first remove the O-acetyl group at the C9 position of Neu5,9Ac_2. Sialidases such as NanH can

then access and cleave the mono-N-acetylated sialic acids (Neu5Ac) (Douglas et al. 2014).

Phansopa et al. (2015) have previously reported the successful release of free sialic acids from mucin and oral epithelial glycans through the use of NanH and NanS. As mucin- and human serum-based sialic acids comprise of mono- and di-acetylated versions, this study made use of both NanH and NanS to deglycosylate the mucin and serum. The deglycosylated biofilm growth medium could then be used in growing plaque biofilms and assessed against growing the biofilms in glycosylated medium. The process of deglycosylating mucin and serum first involved the purification of these enzymes. These enzymes were incubated at various concentrations with mucin and serum overnight, and then any released and free sialic acids were quantitated by conducting a thiobarbituric (TBA) assay and visualised on an SDS-PAGE gel. It was found that as the TBA assay used was a colorimetric assay, the turbidity seen in the reactions containing 30 % human serum affected the reading of the pink colour that was associated with the presence of sialic acid. To combat this technical issue, an alternative method of detecting sialic acids could have been used. This would involve first performing a Western Blot on the deglycosylated and glycosylated proteins, and to then detect any sialic acid present with stains such as the Sambucus Nigra (SNA) Lectin stain. Lectins are proteins that preferentially bind to specific carbohydrate complexes and the SNA lectin for example, recognises the terminal sialic acids that are attached to α-2,6-galactose and α-2,6-galactosamine in sialo-glycoproteins (Shibuya et al. 1987).

This study confirmed with the findings by Phansopa et al. (2015), that the combination of NanH and NanS released higher levels of sialic acids from mucin. This was likely attributed to the cleavage of both mono- and diacetylated sialic acids in the mucin and the effect was also observed with human serum. Given the deglycosylated mucin and serum would be used as components of the biofilm growth medium, it was essential that the sialidases be removed or deactivated prior to their use. On this basis, it was thought lower concentrations of the

enzymes would be easier to remove or deactivate and it was found using 0.1 µM for each enzyme released comparable amounts of sialic acids to the highest examined concentration of 2 µM. Acid hydrolysis of mucin was also tested as it was a common technique for mucin deglycosylation (Pearce and Major 1978, Schauer 1982). Although this released similar levels of sialic acids to the combined use of 0.1 µM NanH and 0.1 µM NanS (87.1 moles vs 83.5 moles respectively), the use of sialidases was selected in place of using acid to reduce the risk of protein denaturation caused by incubating the mucin with 0.1 M sulphuric acid.

It was hypothesised that a shift in the plaque biofilm compositions might occur between growing plaque biofilms in glycosylated and deglycosylated growth medium, similar to the changes resulting from the inhibition of sialidases by oseltamivir and DANA. The PCoA plot (Figure 5.29) revealed a shift in community membership as well as a small non-significant increase in α-diversity upon the use of deglycosylated growth medium. However, no significant difference in the relative abundances of genus-level taxa in the plaque biofilm compositions were observed between the two conditions (Figure 5.27 and Figure 5.28). This finding might be due to some oral bacteria such as *Streptococcus agalactiae* being able to synthesise sialic acids de novo (Chaffin et al. 2005), and the readily available sialic acids that decorated the surfaces of bacteria in the plaque biofilms (Severi et al. 2007), so that bacteria were still able to acquire sialic acids, albeit not from the growth medium. As a result, the lower amounts of sialo-glycoproteins in the growth medium might not have significantly influenced or driven the microbial communities. Another likely explanation for the similar plaque compositions observed might be due to an inadequate removal of the free sialic acids after the deglycosylation process so that some cleaved sialic acids remained in the growth medium. The use of the Vivaspin® ultrafiltration spin columns during three centrifugal spins was likely insufficient as only total reductions of 64-fold and 216-fold in the released free sialic acids from mucin and serum were estimated respectively. However, this experiment was only performed once and due to time constraints, it was not possible to optimise the methodology further. Furthermore, free sialic acids remained in the deglycosylated serum as evidenced by the TBA

assay conducted after the Vivaspin® ultrafiltration spin columns were used. This result was somewhat unexpected as any sialic acids that were cleaved due to the presence of intact sialidase enzymes should have passed through the ultrafiltration spin columns and not be detected in the deglycosylated sample by the TBA assay. Furthermore, one might have expected the detection of released sialic acids in the flow-through collected during the Vivaspin® ultrafiltration of deglycosylated human serum, yet no free sialic acids were detected here. This suggested that although NanH and NanS released free sialic acids, the released sialic acids were not removed. As a result, free sialic acids likely remained in the deglycosylated mucin and serum, either due to insufficient Vivaspin® centrifugal spins or the free sialic acids did not pass through the Vivaspin® column membranes. The outcome of this was that the effect of using deglycosylated growth medium was insufficient to cause a shift in the plaque community compositions.

5.4 Summary

The results in this chapter describe the work related to experiments conducted to investigate the secondary aim of this study, which was whether microbial glycobiology influences microbial community structure. It was found that the diversity and community membership of the mock biofilms were significantly influenced by the presence of the sialidase inhibitors 100 µM oseltamivir and 250 µM DANA. In addition, the relative abundances of genus-level taxa such as *Streptococcus* and several strict anaerobes were significantly altered in the inhibitor-treated plaque biofilms. There was also evidence that the composition of the microbial communities was significantly influenced by the age of the biofilms, although not by replacing the glycosylated growth medium with a deglycosylated version. The latter finding might however be somewhat limited by the possibility that some free sialic acids cleaved by the action of NanH and NanS remained in the deglycosylated growth medium. This experiment was only performed once and would need further optimisation.

Chapter 6 – Summary and concluding discussion

The main aims of this project were to develop mock and subgingival plaque models that were representative of the microbial communities found in a periodontal pocket in the progression of oral dysbiosis. These models could then be used to test the potential effect of sialidase inhibitors and deglycosylated growth medium on community growth. This chapter has therefore summarised the findings from the previous chapters and concluded the work involved in this project with a general discussion.

6.1 Summary of findings by chapter

6.1.1 Chapter 3 – Laying the foundation for biofilm experiments

This chapter aimed to optimise the methodology for developing and analysing microbial communities.

- From reviewing the literature, 18 oral bacterial species were determined as relevant in the progression of periodontitis and were therefore used to inoculate the mock community model.
- Through multiplex PCR and agarose gel electrophoresis, 16S rRNA gene primer sets specific to each of the 17 of the 18 bacteria were determined. However, even with multiple attempts by targeting different genes, a 16S rRNA gene primer set to differentiate between the *Fusobacterium* subspecies *nucleatum* and *polymorphum* could not be validated. The primers validated in this study could be used in assessing the abundance of specific bacteria in mixed communities.
- Nanopore sequencing was shown to be successful at 16S rRNA gene profiling of mixed microbial communities. Work involving sequencing mock microbial communities using the Illumina MiSeq and the Nanopore sequencing platforms demonstrated comparable community compositions between the two techniques. The Nanopore sequencing error rate reduced from >5 % to 2 %, and this work also highlighted the importance of using 27F-YM/1492R-D primer set in sequence library preparation, the MinION flow cell for sequencing, and the newest version of the software Guppy for read basecalling.

6.1.2 Chapter 4 – Development of an *in vitro* periodontal biofilm community model

This chapter described the process involved in developing an *in vitro* mock community model using the MBEC assay biofilm inoculator.

- Cultural analysis of mock community biofilms (model iteration 1) inoculated with an equal mix of OD_{600} of 1 suspensions of each of the 18 bacterial species and grown anaerobically for 7 days revealed mixed species types.
- Viable bacterial cells harvested from mock biofilms were analysed using a combination of species-specific and universal 16S rRNA gene PCR primers and PMA-qPCR. Separate qPCR reactions were run using each individual species-specific PCR primer set. The data here highlighted a technical problem with using qPCR for compositional analysis on 7-day old biofilms due to the low DNA concentrations measured for viable cells, which produced unreliable results. As a consequence, microbiome analysis using Nanopore sequencing became the technique of choice thereafter.
- Several iterations of the mock community model were trialled to encourage the growth of *P. gingivalis, T. forsythia* and *T. denticola* to better mimic periodontitis-associated biofilms as not all 18 bacteria were present after 21 days of growth. Examples of modifications included the MBEC plate which was used in biofilm growth was suspended in inactivated human serum for 24 h prior to inoculation to mimic GCF, and the biofilms were grown for longer and thus up to 21 days. In addition, the work on assessing the CFUs/ml for each bacterial suspensions at OD_{600} 1.0 allowed for more accurate bacterial cell concentrations to be used in the mixed community inoculum. Lastly, the growth medium was changed every 3.5 days throughout biofilm growth.
- The final iteration of the mock community included one species from each of the 13 genera: *Actinomyces; Campylobacter; Dialister; Filifactor; Fusobacterium; Neisseria; Parvimonas; Porphyromonas; Prevotella; Streptococcus; Tannerella; Treponema* and *Veillonella*. Although the red microbial complex was not consistently recovered, profiling these mock communities using Nanopore sequencing revealed the model supported the growth of both facultative and strict oral anaerobes. This work

demonstrated the multi-species model could be used as a tool to assess changes to the community compositions over time or upon the addition of specific factors.

- SDS-PAGE gels in combination with the Instant Blue Stain as well as the Glycoprotein Stain Kit revealed the denaturation of proteins and glycoproteins in autoclaving bovine submaxillary mucin, yet this did not occur with filter-sterilisation. Although the filters were often blocked by the high viscosity of mucin and therefore required filter replacement, the SDS-PAGE gels revealed comparable proteins were observed between non-sterilised mucin and filter-sterilised mucin. Mucin sterilised with both techniques were also used in the growth medium of 14- and 21- day old mock biofilms inoculated from 13 species (one species per genus). The compositions of the communities were compared using Nanopore sequencing, which revealed using either sterilisation techniques produced generally similar microbial communities. This has implications for any work involving the investigation of intact proteins in biofilms yet without the risk of mucin denaturation.

6.1.3 Chapter 5 – Role of siallo-glycoproteins and oral bacterial sialidases in periodontal biofilm communities

This chapter set out to assess the role sialo-glycoproteins play in the development of plaque biofilm communities. To address this aim, the inhibition of sialidases and the removal of sialo-glycoproteins from the nutrients provided to the plaque communities were investigated.

- Of the 18 bacterial species selected for inclusion in this study, *A. oris, P. gingivalis, S. oralis, T. denticola* and *T. forsythia* were determined as producers of sialidase from the literature although their levels of gene expression remain unknown, from conducting MUNANA assays and screening for the GH33 family (of which sialidases belong in) in genome sequences.
- The sialidase inhibitors oseltamivir and DANA were more efficient at inhibiting sialidase activity secreted in mock biofilm supernatant than zanamivir and siastatin B. The IC_{50} of oseltamivir was in the nanomolar

range (780 nM), DANA (2.06 µM) and siastatin B (11.40 µM) in the micromolar range and zanamivir in the millimolar range (1.611 mM).

- Through MUNANA assays, the presence of 100 µM oseltamivir and 250 µM DANA together reduced NanH activity greater than when only 100 µM oseltamivir was present or when sialidase inhibitors were absent. This effect was also observed for sialidase activity measured in mock biofilm supernatant.
- Compared to communities absent of inhibitors, the addition of 100 µM oseltamivir and 250 µM DANA to mock and plaque biofilms resulted in an increase in diversity (Simpson's inverse diversity index), as well as significantly different proportions of *Streptococcus, Veillonella* and *Dialister.* A principal coordinates' analysis using the Jaccard index also indicated significant clustering of samples between the presence and absence of inhibitors in the mock communities though this effect was less significant in the plaque communities. This suggested the microbial communities were influenced by the addition of sialidase inhibitors and highlighted the important role sialidases played in the growth of the microbial communities. The implications of these changes as well as the potential for oral health benefits remain to be seen and warrant further investigation.
- As measured by the Simpson's diversity index, increases in community richness and evenness were observed with growing mock and plaque communities for 21 days compared to 7 and 14 days. This finding was however not always statistically significant and was likely due to small sample sizes. In addition, clustering of the communities in PCoA plots were also observed with an increase in biofilm growth duration.
- The sialidase enzymes NanH and NanS were successfully purified and as revealed by TBA assays, the incubation of 0.1 µM NanH and 0.1 µM NanS released comparable amounts of free sialic acids from mucin compared to acid hydrolysis (83.5 nmoles vs 87.1 nmoles respectively). This highlighted the successful release of free sialic acids without the risk of denaturing mucin.

- Vivaspin® ultrafiltration spin columns were used to remove any free sialic acids released from deglycosylated mucin and serum. The use of deglycosylated growth medium did not appear to affect plaque biofilm growth, but this was difficult to confirm since a TBA assay revealed the likelihood that some free sialic acids remained in the deglycosylated mucin and serum. More investigation into the complete removal of free sialic acids would be required to determine the effect of asialoglycans on developing microbial communities.

6.2 The potential of Nanopore sequencing in profiling microbial communities

This study has demonstrated the capability of using Nanopore sequencing to 16S rRNA gene profile mock community samples that were limited to bacteria from 13 genera, as well as complex plaque communities that comprised >60 genera. In addition, its applicability to oral and non-oral communities were investigated in this study. As the current literature pertaining to the use of Nanopore sequencing in microbiome analysis is limited, this study has contributed to the work by others who have previously used Nanopore sequencing to profile the human nasal, gut, skin, and vaginal microbiome, using the full-length 16S rRNA gene (Matsuo et al. 2020, Komiya et al. 2022, Rozas et al. 2022, Heikema et al. 2020). As previously mentioned in Chapter 1, a pitfall of culture-independent analyses is the risk of primer bias, which can lead to the inaccurate estimation of relative abundances in mixed bacterial communities. Prior studies have also noted this, and a relevant example is the study by Kai et al. (2019) who noted the use of the standard 27F forward primer prior to Nanopore sequencing under-estimated *Bifidobacterium* sequences which was likely due to mismatches in the sequences. To overcome primer bias, the standard protocol for preparing DNA libraries for Nanopore sequencing was modified and replaced the 27F forward primer used in the Oxford Nanopore Technologies' 16S Barcoding Kit with a modified 27F-YM forward primer. By conducting multiple 16S rRNA gene sequence alignments for oral bacteria, it was clear the additional wobble bases in the forward and reverse 16S primers would reduce the risk that bacteria containing mismatches in their sequences such as *Treponema* would be missed. This was further corroborated by the far lower

abundance of *Treponema* measured in the sample community sample when the default 27F-1492R primer set was used. Furthermore, the community composition using these default primers was markedly different to when the community was sequenced with Illumina MiSeq and when the 27F-YM/1492R-D primer set was used with Nanopore sequencing. Further data from Chapter 3 have also provided strong evidence to suggest the use of the modified 27F-YM/1492R-D PCR primer set contributed to reducing the Nanopore sequencing error rate. This adjustment was used for all sequencing data obtained by Nanopore sequencing in Chapters 4 and 5. As such, it was found sequencing the 16S rRNA gene with Nanopore MinION offered a reliable method for characterising even complex microbial communities to genus level, provided the 27F-YM/1492R-D PCR primer set was used, the MinION flow cell was used in place of the Flongle flow cell, and the basecalling software Guppy was up-to-date.

In addition to sequencing the 16S rRNA gene, it is now possible to sequence the entire metagenome, and this could also be performed with the Oxford Nanopore MinION. Metagenomic sequencing overcomes many of the limitations associated with 16S rRNA gene sequencing, such as the low taxonomic resolution of 16S rRNA gene sequence reads at genus level, as well as the potential skew of bacterial abundances in communities due to the varying 16S rRNA gene copy numbers in different bacteria and the bias introduced during the PCR amplification of 16S rRNA gene hypervariable regions. Furthermore, taxonomic identification within mixed microbial communities is limited to only bacteria due to the sole use of the 16S rRNA gene. As a result, fungi such as *Candida* spp. which are known to be present in oral communities are overlooked. In contrast, the metagenome comprises of the genomes of every organism within mixed communities (Kilian et al. 2016). This could be particularly advantageous in studies such as this, as metagenomic sequencing is unbiased and untargeted so it can identify microorganisms from all taxonomic domains. Yet, taxonomic assignment of bacteria within a complex community could also be retrieved from the 16S rRNA gene data. Moreover, metagenomics would likely improve community abundance and to a lesser effect, functional genes in the genomes of the mock and plaque communities could also

be sequenced and this could predict the functional potential of proteins that are encoded in the genomes of these communities (Bikel *et al.*, 2015). For example, this could provide information on the putative functional pathways associated with the metabolism of glycans. Challenges associated with metagenomics, however, involve the dominance of host DNA in clinical samples so that only a small percentage of sequence reads might be derived from microbial genomes. For example, it was found >99 % of the DNA found in sputum collected from patients with cystic fibrosis was host-derived (Lethem *et al.*, 1990). This challenge of contaminating host-derived DNA in metagenomics however would be minimal in this study's plaque biofilm communities as plaque samples contain little host-derived DNA. Furthermore, recent advances in the improvement of sensitivity in sequencing technologies have also resolved a previous issue of requiring high DNA quantities for metagenomic sequencing (Quince *et al.*, 2017). For example, only 1 ng and 1 μg input DNA are required for metagenome sequencing according to the protocols by Illumina and Oxford Nanopore Technologies respectively. Furthermore, Sun *et al.* (2022) recently showed 1 pg total input DNA was sufficient for generating species-level profiles for stool and skin using shotgun metagenome sequencing.

Although there was insufficient time during this project, it would also be beneficial to investigate the use of metatranscriptomic analysis. This is the analysis of the active genes within a community (Kilian *et al.*, 2016), which would enable us to determine the levels of certain gene expression under certain environmental conditions. For example, it could provide information on the active metabolism of specific bacteria within this study's mock and plaque communities after the addition of sialidase inhibitors. It would be interesting to observe any unexpected metabolism pathway changes, whether proteins associated with sialic acid metabolism (such as the *nan* operon) (Stafford *et al.*, 2012) would be downregulated upon the addition of sialidase inhibitors. Similarly, the reduction of free sialic acids released into the community environment by sialidase inhibitors might also result in the downregulation of the *nan* operon in *F. nucleatum* subsp. *nucleatum*, where its genome is known to contain genes for sialic acid uptake and

catabolism (Kapatral *et al.*, 2002). However, the challenge of obtaining sufficient concentrations of RNA and to preserve its quality remains a problem. Despite this, future work derived from this study could be to use the Nanopore MinION sequencer to investigate the metagenome and metatranscriptome of plaque biofilms in response to interventions. Although there is currently a limited number of studies where Nanopore sequencing was applied to investigating the metagenomics and transcriptomics of microbial communities, the long sequence read benefit of the Nanopore sequencing platform has meant it has been used to characterise the adult stool and the preterm infant gut microbiome to high resolution (Leggett *et al.*, 2020; Moss, Maghini and Bhatt, 2020; Maghini *et al.*, 2021). Furthermore, using metagenomics has also enabled Leggett *et al.* (2020) to identify antimicrobial resistance genes present in the preterm gut microbiome, which would have useful implications for treatment and is a benefit that 16S rRNA gene profiling cannot offer.

6.3 The development of mock and plaque community models

Both *in vitro* mock and plaque biofilm models were developed using the MBEC assay biofilm inoculator (Innovotech, CA). This assay has been successfully used in several studies to model oral biofilms (Kistler, Pesaro and Wade, 2015; Soares *et al.*, 2015; Naginyte *et al.*, 2019; Baraniya *et al.*, 2020). This, plus the advantage of this assay to encourage tight bacterial attachments and avoid sedimentation, were the reasons why the MBEC assay was selected to model oral bacterial communities.

Initially, a mock community model comprising 13 bacterial species was developed where after 21 days of anaerobic incubation, it was clear that the model supported a variety of facultative and strict oral anaerobes. Data from Chapters 4 and 5 revealed that streptococci consistently dominated the mock biofilm communities, although its relative abundance appeared to reduce over time. This finding likened previous reports of dysbiosis occurring in the progression of periodontal disease. More specifically, the reduction of Gram-positive facultative anaerobes such as *Streptococcus* was observed in the transition from health to gingivitis (Kistler *et al.*, 2013). Furthermore, the oral community was shown by Zaura *et al.* (2009) to also

shift from a dominance of *Streptococcus* to one comprising fewer streptococci and richer in anaerobes such as *Campylobacter, Eikenella, Fusobacterium* and *Prevotella*. Similarly in this study, high levels of bacteria from the genera *Fusobacterium, Campylobacter, Prevotella* and *Dialister* were also consistently detected. As a result, the mock biofilm model partially reflected that of the natural environment found in periodontal disease due to the lower abundance of Gram-positive streptococci and the higher abundance of a variety of strict anaerobes over time. However, though several iterations of model development were conducted, the absence of the red microbial complex bacteria *Porphyromonas, Tannerella* and *Treponema* remained undetected in the mock biofilm model.

In contrast, the growth of *Porphyromonas* was achieved in the plaque biofilm model (Chapter 5), suggesting the environmental conditions of both the mock and plaque biofilm models were sufficient to support fastidious anaerobes, although the complexity of plaque likely aided *Porphyromonas* spp. growth. It is possible the models however did not fully provide the nutrients required for *Tannerella* and *Treponema* spp. to grow. The environmental conditions present in the growth of mock and plaque biofilms include the use of MBEC assay plate that was precoated with human serum for 24 h, the use of anaerobic conditions at 37 °C and the choice of growth medium which comprised of 50 % mFUM (Gmür and Guggenheim, 1983) supplemented with 1 % bovine submaxillary mucin and 30 % heat-inactivated human serum. From 16S rRNA gene profiling several pools of subgingival plaque samples using Nanopore sequencing (Chapters 3 and 5), it was observed that a diverse range of bacteria was detected in both the pools and in the plaque biofilms grown for up to 21 days. This primarily included bacteria from the genera *Veillonella, Streptococcus, Dialister, Granulicatella, Capnocytophaga, Selenomonas* and *Prevotella*. Many of these bacteria were previously linked to periodontitis (Socransky *et al.*, 1998; Kumar *et al.*, 2005; Griffen *et al.*, 2012; Kistler *et al.*, 2013; Hong *et al.*, 2015). Although compared to the plaque biofilm model, the mock biofilm model was not as representative of the dysbiotic community, it remained useful as a tool for testing proof-of-concept although there were also limitations. For example, such system cannot mimic the full complexity of the natural plaque

habitat which includes bacteria, viruses, fungi, and archaea as described in Chapter 1. Furthermore, the presence of tissue structures, vasculature and host immune components are also lacking. These cell types can be more accurately represented in 3D tissue-engineered models and have been demonstrated in the context of periodontal disease by Belibasakis, Thurnheer and Bostanci (2013), Bao *et al.* (2015) and Brown *et al.* (2019). Despite these limitations, the use of the mock biofilm model was particularly beneficial in testing the addition of sialidase inhibitors as it did not require the additional processes of obtaining ethical approval and collecting plaque samples from volunteers.

6.4 The potential for sialidase inhibitors as a treatment for periodontitis

The work described in this thesis built on previous work that have shown sialidase inhibitors such as DANA, oseltamivir and zanamivir reduced sialidase activity, biofilm formation and bacterial attachment to mucin and epithelial cells (Roy *et al.*, 2011; Kurniyati *et al.*, 2013; Frey *et al.*, 2019; Yu *et al.*, 2021). Through MUNANA assays, compared to the absence of sialidase inhibitors, oseltamivir was capable of inhibiting both the activities of purified NanH and other secreted sialidases by sialidase-positive oral bacteria. This effect was greater when a combination of oseltamivir and DANA was used. In addition, it was identified that the presence of oseltamivir and DANA in unison also significantly increased diversity in the mock biofilm communities and additionally significantly reducing the levels of *Streptococcus* and *Veillonella,* and increasing the levels of *Fusobacterium, FIlifactor* and *Dialister* spp.. Taken together, this suggested the microbial mock and plaque communities were influenced by sialidase inhibitors although the implications of this would need further investigation particularly as the species remained unknown. This was the first study to examine the effect of sialidase inhibitors on the growth of multi-species communities and it highlighted the important role bacterial sialidases play in the development of complex microbial communities. As the findings contributed to the investigation of the use of sialidase inhibitors as a novel treatment for periodontitis, further research could explore how to overcome the complex challenge associated with developing consumer products where sialidase inhibitors or any other novel targeted approaches are active ingredients.

Although this project set out to investigate the role bacterial sialidases played in driving microbial communities, further experiments focusing on targeting a broader range of enzymes could shed more light on the importance of microbial glycobiology in the human mouth. As a prime example, Roy *et al.* (2012) demonstrated the important role of β-hexosaminidase for *T. forsythia* to remove β-linked sugar residues in mucin that became exposed after the terminal sialic acids were first removed by sialidases. It would also be interesting to observe the effect of inhibiting important sialic acid metabolism pathways. Examples include targeting the TonB-dependent NanO transporter in *T. forsythia* which is part of the sialic acid uptake and harvesting system to help transport sialic acid to the inner membrane prior to peptidoglycan synthesis (Douglas *et al.*, 2014) or targeting the enzyme acetylneuraminate pyruvate lyase that is responsible for catabolising sialic acids into N-acetylmannosamine (again, a precursor for peptidoglycan synthesis) after transport into bacterial cells (Corfield, 1992). Other targets in the sequential removal of sugar residues in the degradation of glycans worth investigation include glycosidases such as β-D-galactosidase, α-L-fucosidase, N-acetyl-β-D-glucosaminidase, α-D- mannosidases and β-D-mannosidases which were shown to promote *S. oralis* growth by Byers *et al.* (1999). Given the complexity of sialic acid metabolism, it would be interesting to explore alternative ways of inhibiting biofilm growth in the treatment of periodontitis.

6.5 Conclusion

The work conducted for this thesis demonstrated the usefulness of Nanopore sequencing as a suitable tool for the taxonomic profiling of both simple mock communities and the more complex subgingival plaque biofilm communities. Ultimately, the findings from this project have expanded the currently available toolset in the investigation of the mechanisms underlying the progression. Lastly, this study has also shown the use of the sialidase inhibitors oseltamivir and DANA can influence the development of multispecies oral microbial communities.

Chapter 7 – References

Aas, J. A. *et al.* (2005) 'Defining the normal bacterial flora of the oral cavity.', *Journal of clinical microbiology*, 43(11), pp. 5721–32. doi: 10.1128/JCM.43.11.5721-5732.2005.

Aas, J. A. *et al.* (2007) 'Subgingival plaque microbiota in HIV positive patients.', *Journal of clinical periodontology*, 34(3), pp. 189–95. doi: 10.1111/j.1600-051X.2006.01034.x.

Aas, J. A. *et al.* (2008) 'Bacteria of dental caries in primary and permanent teeth in children and young adults', *Journal of clinical microbiology*. doi: 10.1128/JCM.01410-07.

Abe, T. and Hajishengallis, G. (2013) 'Optimization of the ligature-induced periodontitis model in mice.', *Journal of immunological methods*, 394(1–2), pp. 49–54. doi: 10.1016/j.jim.2013.05.002.

Abeles, S. R. *et al.* (2014) 'Human oral viruses are personal, persistent and gender-consistent.', *The ISME journal*. Nature Publishing Group, 8(9), pp. 1753–67. doi: 10.1038/ismej.2014.31.

Ai, D. *et al.* (2017) 'Integrated metagenomic data analysis demonstrates that a loss of diversity in oral microbiota is associated with periodontitis.', *BMC genomics*, 18, p. 1041. doi: 10.1186/s12864-016-3254-5.

Albers, M. *et al.* (2021) 'The sialyl-O-acetylesterase NanS of Tannerella forsythia encompasses two catalytic modules with different regiospecificity for O7 and O9 of sialic acid.', *Glycobiology*, 31(9), pp. 1176–1191. doi: 10.1093/glycob/cwab034.

Almeida, V. de S. M. *et al.* (2020) 'Bacterial diversity and prevalence of antibiotic resistance genes in the oral microbiome.', *PloS one*, 15(9), p. e0239664. doi: 10.1371/journal.pone.0239664.

Alvarez, G. *et al.* (2013) 'Method to quantify live and dead cells in multi-species oral biofilm by real-time PCR with propidium monoazide.', *AMB express*, 3(1), p. 1. doi: 10.1186/2191-0855-3-1.

Ammann, T. W. *et al.* (2013) 'Validation of a quantitative real-time PCR assay and comparison with fluorescence microscopy and selective agar plate counting for species-specific quantification of an in vitro subgingival biofilm model.', *Journal of periodontal research*, 48(4), pp. 517–26. doi: 10.1111/jre.12034.

Ammann, T. W., Belibasakis, G. N. and Thurnheer, T. (2013) 'Impact of early colonizers on in vitro subgingival biofilm formation.', *PloS one*, 8(12), p. e83090. doi: 10.1371/journal.pone.0083090.

Ammann, T. W., Gmür, R. and Thurnheer, T. (2012) 'Advancement of the 10-species subgingival Zurich biofilm model by examining different nutritional conditions and defining the structure of the in vitro biofilms.', *BMC microbiology*, 12(1), p. 227. doi: 10.1186/1471-2180-12-227.

An, S. Q. *et al.* (2022) 'An in vitro biofilm model system to facilitate study of microbial communities of the human oral cavity.', *Letters in applied microbiology*. John Wiley & Sons, Ltd, 74(3), pp. 302–310. doi: 10.1111/lam.13618.

Ansbro, K., Wade, W. G. and Stafford, G. P. (2020) 'Tannerella serpentiformis sp. nov., isolated from the human mouth.', *International journal of systematic and*

evolutionary microbiology, 70(6), pp. 3749–3754. doi: 10.1099/ijsem.0.004229.

Antezack, A. *et al.* (2021) 'Isolation and description of Selenomonas timonae sp. nov., a novel Selenomonas species detected in a gingivitis patient.', *International journal of systematic and evolutionary microbiology*, 71(10). doi: 10.1099/ijsem.0.005040.

Arias-Moliz, M. T. *et al.* (2010) 'Eradication of Enterococcus faecalis biofilms by cetrimide and chlorhexidine.', *Journal of endodontics*, 36(1), pp. 87–90. doi: 10.1016/j.joen.2009.10.013.

Armitage, G. C. (1999) 'Development of a classification system for periodontal diseases and conditions.', *Annals of periodontology*, 4(1), pp. 1–6. doi: 10.1902/annals.1999.4.1.1.

Aruni, A. W., Roy, F. and Fletcher, H. M. (2011) 'Filifactor alocis has virulence attributes that can enhance its persistence under oxidative stress conditions and mediate invasion of epithelial cells by porphyromonas gingivalis.', *Infection and immunity*, 79(10), pp. 3872–86. doi: 10.1128/IAI.05631-11.

Babu, Y. S. *et al.* (2000) 'Discovery of a novel, highly potent, orally active, and selective influenza neuraminidase inhibitor through structure-based drug design', *Journal of medicinal chemistry*, 43(19), pp. 3482–3486. doi: 10.1021/jm0002679.

Baker, J. L. *et al.* (2017) 'Ecology of the Oral Microbiome: Beyond Bacteria.', *Trends in microbiology*, 25(5), pp. 362–374. doi: 10.1016/j.tim.2016.12.012.

Baker, P. J., Evans, R. T. and Roopenian, D. C. (1994) 'Oral infection with Porphyromonas gingivalis and induced alveolar bone loss in immunocompetent and severe combined immunodeficient mice.', *Archives of oral biology*, 39(12), pp. 1035–40. doi: 10.1016/0003-9969(94)90055-8.

Balakrishnan, M., Simmonds, R. S. and Tagg, J. R. (2000) 'Dental caries is a preventable infectious disease.', *Australian dental journal*, 45(4), pp. 235–45. doi: 10.1111/j.1834-7819.2000.tb00257.x.

Bao, K. *et al.* (2015) 'Proteomic profiling of host-biofilm interactions in an oral infection model resembling the periodontal pocket.', *Scientific reports*, 5, p. 15999. doi: 10.1038/srep15999.

Baraniya, D. *et al.* (2020) 'Modeling Normal and Dysbiotic Subgingival Microbiomes: Effect of Nutrients.', *Journal of dental research*, 99(6), pp. 695–702. doi: 10.1177/0022034520902452.

Bardouniotis, E. *et al.* (2001) 'Characterization of biofilm growth and biocide susceptibility testing of Mycobacterium phlei using the MBEC assay system.', *FEMS microbiology letters*, 203(2), pp. 263–7. doi: 10.1111/j.1574-6968.2001.tb10851.x.

Beall, C. J. *et al.* (2014) 'Single cell genomics of uncultured, health-associated Tannerella BU063 (Oral Taxon 286) and comparison to the closely related pathogen Tannerella forsythia.', *PloS one*, 9(2), p. e89398. doi: 10.1371/journal.pone.0089398.

Beighton, D. and Whiley, R. A. (1990) 'Sialidase activity of the "Streptococcus milleri group" and other viridans group streptococci.', *Journal of clinical microbiology*, 28(6), pp. 1431–3. doi: 10.1128/jcm.28.6.1431-1433.1990.

Belay, N. *et al.* (1988) 'Methanogenic bacteria from human dental plaque.', *Applied and environmental microbiology*, 54(2), pp. 600–3. doi: 10.1128/aem.54.2.600-603.1988.

Belibasakis, G. N. and Thurnheer, T. (2014) 'Validation of antibiotic efficacy on in vitro subgingival biofilms.', *Journal of periodontology*, 85(2), pp. 343–8. doi: 10.1902/jop.2013.130167.

Belibasakis, G. N., Thurnheer, T. and Bostanci, N. (2013) 'Interleukin-8 responses of multi-layer gingival epithelia to subgingival biofilms: role of the "red complex" species.', *PloS one*, 8(12), p. e81581. doi: 10.1371/journal.pone.0081581.

Belkacemi, S. *et al.* (2018) 'Peri-implantitis-associated methanogens: a preliminary report.', *Scientific reports*, 8(1), p. 9447. doi: 10.1038/s41598-018-27862-8.

Bender, G. R., Sutton, S. V and Marquis, R. E. (1986) 'Acid tolerance, proton permeabilities, and membrane ATPases of oral streptococci.', *Infection and immunity*, 53(2), pp. 331–8. doi: 10.1128/iai.53.2.331-338.1986.

Bennick, A. *et al.* (1983) 'The role of human salivary acidic proline-rich proteins in the formation of acquired dental pellicle in vivo and their fate after adsorption to the human enamel surface.', *Archives of oral biology*, 28(1), pp. 19–27. doi: 10.1016/0003-9969(83)90022-5.

Bensing, B. A., López, J. A. and Sullam, P. M. (2004) 'The Streptococcus gordonii surface proteins GspB and Hsa mediate binding to sialylated carbohydrate epitopes on the platelet membrane glycoprotein Ibalpha.', *Infection and immunity*, 72(11), pp. 6528–37. doi: 10.1128/IAI.72.11.6528-6537.2004.

Benson, D. A. *et al.* (2013) 'GenBank.', *Nucleic acids research*, 41(Database issue), pp. D36-42. doi: 10.1093/nar/gks1195.

Bik, E. M. *et al.* (2010) 'Bacterial diversity in the oral cavity of ten healthy individuals.', *The ISME journal*, 4(8), pp. 962–74. doi: 10.1038/ismej.2010.30.

Bikel, S. *et al.* (2015) 'Combining metagenomics, metatranscriptomics and viromics to explore novel microbial interactions: towards a systems-level understanding of human microbiome.', *Computational and structural biotechnology journal*, 13, pp. 390–401. doi: 10.1016/j.csbj.2015.06.001.

Blix G (1936) 'Über die Kohlenhydratgruppen des Submaxillaris mucins', *Z physiol chem*, 240, pp. 43–54.

Bloch, S. *et al.* (2017) 'Behavior of two Tannerella forsythia strains and their cell surface mutants in multispecies oral biofilms.', *Molecular oral microbiology*, 32(5), pp. 404–418. doi: 10.1111/omi.12182.

Bouchet, V. *et al.* (2003) 'Host-derived sialic acid is incorporated into Haemophilus influenzae lipopolysaccharide and is a major virulence factor in experimental otitis media.', *Proceedings of the national academy of sciences of the United States of America*, 100(15), pp. 8898–903. doi: 10.1073/pnas.1432026100.

Bradshaw, D. J. *et al.* (1994) 'Metabolic cooperation in oral microbial communities during growth on mucin.', *Microbiology*, 140(12), pp. 3407–12. doi: 10.1099/13500872-140-12-3407.

Bradshaw, D. J. *et al.* (1998) 'Role of Fusobacterium nucleatum and coaggregation

in anaerobe survival in planktonic and biofilm oral microbial communities during aeration.', *Infection and immunity*, 66(10), pp. 4729–32. doi: 10.1128/IAI.66.10.4729-4732.1998.

Bradshaw, D. J., McKee, A. S. and Marsh, P. D. (1989) 'Effects of carbohydrate pulses and pH on population shifts within oral microbial communities in vitro.', *Journal of dental research*, 68(9), pp. 1298–302. doi: 10.1177/00220345890680090101.

Brinig, M. M. *et al.* (2003) 'Prevalence of bacteria of division TM7 in human subgingival plaque and their association with disease.', *Applied and environmental microbiology*, 69(3), pp. 1687–94. doi: 10.1128/AEM.69.3.1687-1694.2003.

Brockhausen, I., Schachter, H. and Stanley, P. (2009) *O-GalNAc Glycans*. 2nd edn, *Essentials of Glycobiology*. 2nd edn. Edited by A. Varki, R. D. Cummings, and J. D. Esko. Cold Spring Harbor (NY): Cold Spring Harbor Laboratory Press. Available at: http://www.ncbi.nlm.nih.gov/pubmed/20301232.

Brown, J. L. *et al.* (2019) 'Biofilm-stimulated epithelium modulates the inflammatory responses in co-cultured immune cells.', *Scientific reports*, 9(1), p. 15779. doi: 10.1038/s41598-019-52115-7.

Brusa, T. *et al.* (1987) 'The presence of methanobacteria in human subgingival plaque.', *Journal of clinical periodontology*, 14(8), pp. 470–1. doi: 10.1111/j.1600-051x.1987.tb02254.x.

Brusa, T. *et al.* (1993) 'Methanogens in the human intestinal tract and oral cavity', *Current microbiology*, 27(5), pp. 261–265. doi: 10.1007/BF01575989.

Bustin, S. and Huggett, J. (2017) 'qPCR primer design revisited.', *Biomolecular detection and quantification*, 14, pp. 19–28. doi: 10.1016/j.bdq.2017.11.001.

Byers, H. L. *et al.* (1999) 'Sequential deglycosylation and utilization of the N-linked, complex-type glycans of human alpha1-acid glycoprotein mediates growth of Streptococcus oralis.', *Glycobiology*, 9(5), pp. 469–79. doi: 10.1093/glycob/9.5.469.

Byers, H. L. *et al.* (2000) 'Isolation and characterisation of sialidase from a strain of Streptococcus oralis.', *Journal of medical microbiology*, 49(3), pp. 235–244. doi: 10.1099/0022-1317-49-3-235.

Ceri, H. *et al.* (1999) 'The Calgary Biofilm Device: new technology for rapid determination of antibiotic susceptibilities of bacterial biofilms.', *Journal of clinical microbiology*, 37(6), pp. 1771–6. doi: 10.1128/JCM.37.6.1771-1776.1999.

Chaban, B. *et al.* (2009) 'Development of cpn60-based real-time quantitative PCR assays for the detection of 14 Campylobacter species and application to screening of canine fecal samples.', *Applied and environmental microbiology*, 75(10), pp. 3055–61. doi: 10.1128/AEM.00101-09.

Chalmers, N. I. *et al.* (2008) 'Characterization of a Streptococcus sp.-Veillonella sp. community micromanipulated from dental plaque.', *Journal of bacteriology*, 190(24), pp. 8145–54. doi: 10.1128/JB.00983-08.

Chen, T. *et al.* (2010) 'The Human Oral Microbiome Database: a web accessible resource for investigating oral microbe taxonomic and genomic information.', *Database : the journal of biological databases and curation*, 2010(0), p. baq013.

doi: 10.1093/database/baq013.

Cheng, S. L. *et al.* (1985) 'Comparative study of six random oral spirochete isolates. Serological heterogeneity of Treponema denticola.', *Journal of periodontal research*. John Wiley & Sons, Ltd, 20(6), pp. 602–12. doi: 10.1111/j.1600-0765.1985.tb00844.x.

Chevalier, M., Ranque, S. and Prêcheur, I. (2018) 'Oral fungal-bacterial biofilm models in vitro: a review.', *Medical mycology*, 56(6), pp. 653–667. doi: 10.1093/mmy/myx111.

Christersson, L. A., Zambon, J. J. and Genco, R. J. (1991) 'Dental bacterial plaques. Nature and role in periodontal disease.', *Journal of clinical periodontology*, 18(6), pp. 441–6. doi: 10.1111/j.1600-051x.1991.tb02314.x.

Cisar, J. O. *et al.* (1984) 'Exclusive presence of lactose-sensitive fimbriae on a typical strain (WVU45) of Actinomyces naeslundii.', *Infection and immunity*, 46(2), pp. 453–8. doi: 10.1128/iai.46.2.453-458.1984.

Ciuffreda, L., Rodríguez-Pérez, H. and Flores, C. (2021) 'Nanopore sequencing and its application to the study of microbial communities.', *Computational and structural biotechnology journal*. The Authors, 19, pp. 1497–1511. doi: 10.1016/j.csbj.2021.02.020.

Cohen, M. and Varki, A. (2010) 'The sialome--far more than the sum of its parts.', *Omics : a journal of integrative biology*, 14(4), pp. 455–64. doi: 10.1089/omi.2009.0148.

Corby, P. M. *et al.* (2005) 'Microbial risk indicators of early childhood caries.', *Journal of clinical microbiology*, 43(11), pp. 5753–9. doi: 10.1128/JCM.43.11.5753-5759.2005.

Corfield, T. (1992) 'Bacterial sialidases--roles in pathogenicity and nutrition.', *Glycobiology*, 2(6), pp. 509–21. doi: 10.1093/glycob/2.6.509.

Crocker, P. R., Paulson, J. C. and Varki, A. (2007) 'Siglecs and their roles in the immune system.', *Nature reviews immunology*, 7(4), pp. 255–66. doi: 10.1038/nri2056.

Cross, B. W. and Ruhl, S. (2018) 'Glycan recognition at the saliva - oral microbiome interface.', *Cellular immunology*, 333, pp. 19–33. doi: 10.1016/j.cellimm.2018.08.008.

Dalmasso, M. *et al.* (2015) 'Isolation of a novel phage with activity against Streptococcus mutans biofilms.', *PloS one*, 10(9), p. e0138651. doi: 10.1371/journal.pone.0138651.

Deng, D. M. *et al.* (2009) 'Influence of Streptococcus mutans on Enterococcus faecalis biofilm formation.', *Journal of endodontics*. Elsevier Ltd, 35(9), pp. 1249–52. doi: 10.1016/j.joen.2009.05.038.

Deng, D. M., van Loveren, C. and ten Cate, J. M. (2005) 'Caries-preventive agents induce remineralization of dentin in a biofilm model.', *Caries research*, 39(3), pp. 216–23. doi: 10.1159/000084801.

Dewhirst, F. E. *et al.* (2010) 'The human oral microbiome.', *Journal of bacteriology*, 192(19), pp. 5002–17. doi: 10.1128/JB.00542-10.

Dhariwal, A. *et al.* (2017) 'MicrobiomeAnalyst: a web-based tool for comprehensive statistical, visual and meta-analysis of microbiome data.', *Nucleic acids research*, 45(W1), pp. W180–W188. doi: 10.1093/nar/gkx295.

Diaz, P. I. *et al.* (2006) 'Molecular characterization of subject-specific oral microflora during initial colonization of enamel.', *Applied and environmental microbiology*, 72(4), pp. 2837–48. doi: 10.1128/AEM.72.4.2837-2848.2006.

Diaz, P. I. *et al.* (2012) 'Using high throughput sequencing to explore the biodiversity in oral bacterial communities.', *Molecular oral microbiology*, 27(3), pp. 182–201. doi: 10.1111/j.2041-1014.2012.00642.x.

Diaz, P. I. *et al.* (2017) 'Mining the oral mycobiome: Methods, components, and meaning.', *Virulence*, 8(3), pp. 313–323. doi: 10.1080/21505594.2016.1252015.

Dietz, V. H. (1943) 'In vitro production of plaques and caries', *Journal of Dental Research*, 22, pp. 423–40. doi: 10.1177/002203454302200601.

Ding, Y. *et al.* (2014) 'Antimicrobial and anti-biofilm effect of Bac8c on major bacteria associated with dental caries and Streptococcus mutans biofilms.', *Peptides*, 52, pp. 61–7. doi: 10.1016/j.peptides.2013.11.020.

Do, T. *et al.* (2008) 'Evidence for recombination between a sialidase (nanH) of Actinomyces naeslundii and Actinomyces oris, previously named "Actinomyces naeslundii genospecies 1 and 2".', *FEMS microbiology letters*, 288(2), pp. 156–62. doi: 10.1111/j.1574-6968.2008.01336.x.

Doel, J. J. *et al.* (2005) 'Evaluation of bacterial nitrate reduction in the human oral cavity.', *European journal of oral sciences*, 113(1), pp. 14–9. doi: 10.1111/j.1600-0722.2004.00184.x.

Douglas, C. W. I. *et al.* (2014) 'Physiological adaptations of key oral bacteria.', *Advances in microbial physiology*. Edited by R. K. Poole. AMP, UK, Academic Press, 65, pp. 257–335. doi: 10.1016/bs.ampbs.2014.08.005.

Drescher, J. *et al.* (2010) 'Molecular epidemiology and spatial distribution of Selenomonas spp. in subgingival biofilms.', *European journal of oral sciences*. England, 118(5), pp. 466–74. doi: 10.1111/j.1600-0722.2010.00765.x.

Dupuy, A. K. *et al.* (2014) 'Redefining the human oral mycobiome with improved practices in amplicon-based taxonomy: discovery of Malassezia as a prominent commensal.', *PloS one*, 9(3), p. e90899. doi: 10.1371/journal.pone.0090899.

Dwek, R. A. (1996) 'Glycobiology: toward understanding the function of sugars.', *Chemical reviews*, 96(2), pp. 683-720fost. doi: 10.1021/cr940283b.

Van Dyke, T. E., Bartold, P. M. and Reynolds, E. C. (2020) 'The nexus between periodontal inflammation and dysbiosis.', *Frontiers in immunology*, 11, p. 511. doi: 10.3389/fimmu.2020.00511.

Dzink, J. L. *et al.* (1985) 'Gram negative species associated with active destructive periodontal lesions.', *Journal of clinical periodontology*, 12(8), pp. 648–59. doi: 10.1111/j.1600-051x.1985.tb00936.x.

Edlund, A. *et al.* (2013) 'An in vitro biofilm model system maintaining a highly reproducible species and metabolic diversity approaching that of the human oral microbiome.', *Microbiome*, 1(1), p. 25. doi: 10.1186/2049-2618-1-25.

Eisenberg, E. and Levanon, E. Y. (2013) 'Human housekeeping genes, revisited.', *Trends in genetics*, 29(10), pp. 569–74. doi: 10.1016/j.tig.2013.05.010.

Enkhtaivan, G. *et al.* (2017) 'Discovery of berberine based derivatives as anti-influenza agent through blocking of neuraminidase.', *Bioorganic & medicinal chemistry*, 25(20), pp. 5185–5193. doi: 10.1016/j.bmc.2017.07.006.

Eren, A. M. *et al.* (2014) 'Oligotyping analysis of the human oral microbiome.', *Proceedings of the national academy of sciences of the United States of America*, 111(28), pp. E2875-84. doi: 10.1073/pnas.1409644111.

Eren, A. M. *et al.* (2015) 'Minimum entropy decomposition: unsupervised oligotyping for sensitive partitioning of high-throughput marker gene sequences.', *The ISME journal*, 9(4), pp. 968–79. doi: 10.1038/ismej.2014.195.

Ericsson, I. *et al.* (1975) 'Experimental periodontal breakdown in the dog.', *European journal of oral sciences*, 83(3), pp. 189–92. doi: 10.1111/j.1600-0722.1975.tb01198.x.

Eriksson, L., Lif Holgerson, P. and Johansson, I. (2017) 'Saliva and tooth biofilm bacterial microbiota in adolescents in a low caries community.', *Scientific reports*, 7(1), p. 5861. doi: 10.1038/s41598-017-06221-z.

Esberg, A., Eriksson, L. and Johansson, I. (2022) 'Site- and time-dependent compositional shifts in oral microbiota communities.', *Frontiers in oral health*, 3(March), p. 826996. doi: 10.3389/froh.2022.826996.

Escapa, I. F. *et al.* (2018) 'New insights into human nostril microbiome from the Expanded Human Oral Microbiome Database (eHOMD): a resource for the microbiome of the human aerodigestive tract.', *mSystems*, 3(6). doi: 10.1128/mSystems.00187-18.

Exterkate, R. A. M., Crielaard, W. and Ten Cate, J. M. (2010) 'Different response to amine fluoride by Streptococcus mutans and polymicrobial biofilms in a novel high-throughput active attachment model.', *Caries research*, 44(4), pp. 372–9. doi: 10.1159/000316541.

Fernandez Y Mostajo, M. *et al.* (2017) 'A reproducible microcosm biofilm model of subgingival microbial communities.', *Journal of periodontal research*, 52(6), pp. 1021–1031. doi: 10.1111/jre.12473.

Ferrari, A. *et al.* (1994) 'Isolation and characterization ofMethanobrevibacter oralis sp. nov.', *Current microbiology*, 29(1), pp. 7–12. doi: 10.1007/BF01570184.

Finelli, A. *et al.* (2003) 'Use of in-biofilm expression technology to identify genes involved in Pseudomonas aeruginosa biofilm development.', *Journal of bacteriology*, 185(9), pp. 2700–10. doi: 10.1128/JB.185.9.2700-2710.2003.

Foster, J. S. and Kolenbrander, P. E. (2004) 'Development of a multispecies oral bacterial community in a saliva-conditioned flow cell', *Applied and environmental microbiology*, 70(7), pp. 4340–8. doi: 10.1128/AEM.70.7.4340.

Frencken, J. E. *et al.* (2017) 'Global epidemiology of dental caries and severe periodontitis - a comprehensive review.', *Journal of clinical periodontology*, 44 Suppl 1, pp. S94–S105. doi: 10.1111/jcpe.12677.

Frey, A M *et al.* (2018) 'Characterisation and pure culture of putative health-

associated oral bacterium BU063 (Tannerella sp. HOT-286) reveals presence of a potentially novel glycosylated S-layer.', *FEMS microbiology letters*, 365(17), pp. 1–8. doi: 10.1093/femsle/fny180.

Frey, Andrew M *et al.* (2018) 'Evidence for a carbohydrate-binding module (CBM) of Tannerella forsythia NanH sialidase, key to interactions at the host-pathogen interface.', *The biochemical journal*, 475(6), pp. 1159–1176. doi: 10.1042/BCJ20170592.

Frey, A. M. *et al.* (2019) 'Characterization of Porphyromonas gingivalis sialidase and disruption of its role in host-pathogen interactions.', *Microbiology*, 165(11), pp. 1181–1197. doi: 10.1099/mic.0.000851.

Friedrich, V. *et al.* (2017) 'Tannerella forsythia strains display different cell-surface nonulosonic acids: biosynthetic pathway characterization and first insight into biological implications.', *Glycobiology*, 27(4), pp. 342–357. doi: 10.1093/glycob/cww129.

Garnier, F. *et al.* (1997) 'Identification of clinically relevant viridans group streptococci to the species level by PCR.', *Journal of clinical microbiology*, 35(9), pp. 2337–41. doi: 10.1128/jcm.35.9.2337-2341.1997.

Gerits, E., Verstraeten, N. and Michiels, J. (2017) 'New approaches to combat Porphyromonas gingivalis biofilms.', *Journal of oral microbiology*, 9(1), p. 1300366. doi: 10.1080/20002297.2017.1300366.

Ghannoum, M. A. *et al.* (2010) 'Characterization of the oral fungal microbiome (mycobiome) in healthy individuals.', *PLoS pathogens*, 6(1), p. e1000713. doi: 10.1371/journal.ppat.1000713.

Gibbons, R. J. and Macdonald, J. B. (1960) 'Hemin and vitamin K compounds as required factors for the cultivation of certain strains of Bacteroides melaninogenicus.', *Journal of bacteriology*, 80(2), pp. 164–70. doi: 10.1128/jb.80.2.164-170.1960.

Gmür, R. and Guggenheim, B. (1983) 'Antigenic heterogeneity of Bacteroides intermedius as recognized by monoclonal antibodies.', *Infection and immunity*, 42(2), pp. 459–70. doi: 10.1128/iai.42.2.459-470.1983.

Goeres, D. M. *et al.* (2005) 'Statistical assessment of a laboratory method for growing biofilms.', *Microbiology*, 151(Pt 3), pp. 757–762. doi: 10.1099/mic.0.27709-0.

Grenier, D. (1992) 'Nutritional interactions between two suspected periodontopathogens, Treponema denticola and Porphyromonas gingivalis.', *Infection and immunity*, 60(12), pp. 5298–301. doi: 10.1128/iai.60.12.5298-5301.1992.

Griffen, A. L. *et al.* (2012) 'Distinct and complex bacterial profiles in human periodontitis and health revealed by 16S pyrosequencing.', *The ISME journal*, 6(6), pp. 1176–85. doi: 10.1038/ismej.2011.191.

Gross, E. L. *et al.* (2010) 'Bacterial 16S sequence analysis of severe caries in young permanent teeth.', *Journal of clinical microbiology*, 48(11), pp. 4121–8. doi: 10.1128/JCM.01232-10.

Guggenheim, B. *et al.* (2001) 'Validation of an in vitro biofilm model of supragingival plaque.', *Journal of dental research*, 80(1), pp. 363–70. doi: 10.1177/00220345010800011201.

Guggenheim, B. *et al.* (2009) 'In vitro modeling of host-parasite interactions: the "subgingival" biofilm challenge of primary human epithelial cells.', *BMC microbiology*, 9, p. 280. doi: 10.1186/1471-2180-9-280.

Gul, S. S. *et al.* (2016) 'A pilot study of active enzyme levels in gingival crevicular fluid of patients with chronic periodontal disease.', *Journal of clinical periodontology*, 43(8), pp. 629–36. doi: 10.1111/jcpe.12568.

Hajishengallis, G. (2011) 'Immune evasion strategies of Porphyromonas gingivalis.', *Journal of oral biosciences*, 53(3), pp. 233–240. doi: 10.2330/joralbiosci.53.233.

Hajishengallis, G. *et al.* (2011) 'Low-abundance biofilm species orchestrates inflammatory periodontal disease through the commensal microbiota and complement.', *Cell host & microbe*, 10(5), pp. 497–506. doi: 10.1016/j.chom.2011.10.006.

Hall, M. W. *et al.* (2017) 'Inter-personal diversity and temporal dynamics of dental, tongue, and salivary microbiota in the healthy oral cavity.', *NPJ biofilms and microbiomes*, 3(1), p. 2. doi: 10.1038/s41522-016-0011-0.

Hall, T. A. (1999) 'BIOEDIT: a user-friendly biological sequence alignment editor and analysis program for Windows 95/98/ NT', in *Nucleic acids symposium series*.

Hannig, C. and Hannig, M. (2009) 'The oral cavity-a key system to understand substratum-dependent bioadhesion on solid surfaces in man.', *Clinical oral investigations*, 13(2), pp. 123–39. doi: 10.1007/s00784-008-0243-3.

Harrison, J. J., Turner, R. J. and Ceri, H. (2005) 'High-throughput metal susceptibility testing of microbial biofilms.', *BMC microbiology*, 5, p. 53. doi: 10.1186/1471-2180-5-53.

Hasan, N. A. *et al.* (2014) 'Microbial community profiling of human saliva using shotgun metagenomic sequencing.', *PloS one*, 9(5), p. e97699. doi: 10.1371/journal.pone.0097699.

Håvarstein, L. S., Hakenbeck, R. and Gaustad, P. (1997) 'Natural competence in the genus Streptococcus: evidence that streptococci can change pherotype by interspecies recombinational exchanges.', *Journal of bacteriology*, 179(21), pp. 6589–94. doi: 10.1128/jb.179.21.6589-6594.1997.

He, X. *et al.* (2015) 'Cultivation of a human-associated TM7 phylotype reveals a reduced genome and epibiotic parasitic lifestyle.', *Proceedings of the national academy of sciences of the United States of America*, 112(1), pp. 244–9. doi: 10.1073/pnas.1419038112.

Heikema, A. P. *et al.* (2020) 'Comparison of Illumina versus Nanopore 16S rRNA gene sequencing of the human nasal microbiota.', *Genes*, 11(9). doi: 10.3390/genes11091105.

Hiranmayi, K. V. *et al.* (2017) 'Novel pathogens in periodontal microbiology.', *Journal of pharmacy & bioallied sciences*, 9(3), pp. 155–163. doi: 10.4103/jpbs.JPBS_288_16.

Van der Hoeven, J. S. and Camp, P. J. (1991) 'Synergistic degradation of mucin by Streptococcus oralis and Streptococcus sanguis in mixed chemostat cultures.', *Journal of dental research*, 70(7), pp. 1041–4. doi: 10.1177/00220345910700070401.

Hojo, K. *et al.* (2009) 'Bacterial interactions in dental biofilm development.', *Journal of dental research*, 88(11), pp. 982–90. doi: 10.1177/0022034509346811.

Holzer, C. T. *et al.* (1993) 'Inhibition of sialidases from viral, bacterial and mammalian sources by analogues of 2-deoxy-2,3-didehydro-N-acetylneuraminic acid modified at the C-4 position.', *Glycoconjugate journal*, 10(1), pp. 40–4. doi: 10.1007/BF00731185.

Hong, B.-Y. *et al.* (2015) 'Microbiome profiles in periodontitis in relation to host and disease characteristics.', *PloS one*, 10(5), p. e0127077. doi: 10.1371/journal.pone.0127077.

Hong, B. Y. *et al.* (2020) 'The Salivary Mycobiome Contains 2 Ecologically Distinct Mycotypes.', *Journal of dental research*, 99(6), pp. 730–738. doi: 10.1177/0022034520915879.

Honma, K., Mishima, E. and Sharma, A. (2011) 'Role of Tannerella forsythia NanH sialidase in epithelial cell attachment.', *Infection and immunity*, 79(1), pp. 393–401. doi: 10.1128/IAI.00629-10.

Hope, C. K. *et al.* (2012) 'Reducing the variability between constant-depth film fermenter experiments when modelling oral biofilm.', *Journal of applied microbiology*, 113(3), pp. 601–8. doi: 10.1111/j.1365-2672.2012.05368.x.

Hughes, C. V *et al.* (2003) 'Cloning and expression of alpha-D-glucosidase and N-acetyl-beta-glucosaminidase from the periodontal pathogen, Tannerella forsythensis (Bacteroides forsythus).', *Oral microbiology and immunology*, 18(5), pp. 309–12. doi: 10.1034/j.1399-302x.2003.00091.x.

Human microbiome project consortium (2012) 'Structure, function and diversity of the healthy human microbiome.', *Nature*, 486(7402), pp. 207–14. doi: 10.1038/nature11234.

Hyde, E. R. *et al.* (2014) 'Metagenomic analysis of nitrate-reducing bacteria in the oral cavity: implications for nitric oxide homeostasis.', *PloS one*, 9(3), p. e88645. doi: 10.1371/journal.pone.0088645.

Ito, R. *et al.* (2010) 'Hemagglutinin/adhesin domains of Porphyromonas gingivalis play key roles in coaggregation with Treponema denticola.', *FEMS immunology and medical microbiology*, 60(3), pp. 251–60. doi: 10.1111/j.1574-695X.2010.00737.x.

Jaccard, P. (1900) 'Contributions au problème de l'immigration post-glaciaire de la flore alpine', *Bulletin de la société vaudoise des sciences naturelles*, 37, pp. 547–579.

Jakubovics, N. S. *et al.* (2008) 'Role of hydrogen peroxide in competition and cooperation between Streptococcus gordonii and Actinomyces naeslundii.', *FEMS microbiology ecology*, 66(3), pp. 637–44. doi: 10.1111/j.1574-6941.2008.00585.x.

Jansen, H. J. *et al.* (1994) 'Degradation of immunoglobulin G by periodontal bacteria.', *Oral microbiology and immunology*, 9(6), pp. 345–51. doi:

10.1111/j.1399-302x.1994.tb00284.x.

Janus, M. M. *et al.* (2017) 'Candida albicans alters the bacterial microbiome of early in vitro oral biofilms.', *Journal of oral microbiology*, 9(1), p. 1270613. doi: 10.1080/20002297.2016.1270613.

Jäsberg, H. *et al.* (2016) 'Bifidobacteria inhibit the growth of Porphyromonas gingivalis but not of Streptococcus mutans in an in vitro biofilm model.', *European journal of oral sciences*, 124(3), pp. 251–8. doi: 10.1111/eos.12266.

Jenkinson, H. F. (2011) 'Beyond the oral microbiome.', *Environmental microbiology*, 13(12), pp. 3077–87. doi: 10.1111/j.1462-2920.2011.02573.x.

Jiang, W.-X. *et al.* (2015) 'The impact of various time intervals on the supragingival plaque dynamic core microbiome.', *PloS one*, 10(5), p. e0124631. doi: 10.1371/journal.pone.0124631.

Jordan, H. V and Keyes, P. H. (1964) 'Aerobic, gram-positive, filamentous bacteria as etiologic agents of experimental periodontal disease in hamsters.', *Archives of oral biology*, 9, pp. 401–14. doi: 10.1016/0003-9969(64)90025-1.

Juge, N., Tailford, L. and Owen, C. D. (2016) 'Sialidases from gut bacteria: a mini-review.', *Biochemical society transactions*, 44(1), pp. 166–75. doi: 10.1042/BST20150226.

Kaewsrichan, J., Douglas, C. W. I. and Teanpaisan, R. (2005) 'Characterization of minimal bacteriocin operon from Prevotella nigrescens ATCC 25261.', *Letters in applied microbiology*, 40(2), pp. 138–45. doi: 10.1111/j.1472-765X.2004.01639.x.

Kapatral, V. *et al.* (2002) 'Genome sequence and analysis of the oral bacterium Fusobacterium nucleatum strain ATCC 25586.', *Journal of bacteriology*, 184(7), pp. 2005–18. doi: 10.1128/JB.184.7.2005-2018.2002.

Karpathy, S. E. *et al.* (2007) 'Genome sequence of Fusobacterium nucleatum subspecies polymorphum - a genetically tractable fusobacterium.', *PloS one*, 2(7), p. e659. doi: 10.1371/journal.pone.0000659.

Kawamura, Y. *et al.* (1995) 'Determination of 16S rRNA sequences of Streptococcus mitis and Streptococcus gordonii and phylogenetic relationships among members of the genus Streptococcus.', *International journal of systematic bacteriology*, 45(2), pp. 406–8. doi: 10.1099/00207713-45-2-406.

Kilian, M. *et al.* (2016) 'The oral microbiome - an update for oral healthcare professionals.', *British dental journal*, 221(10), pp. 657–666. doi: 10.1038/sj.bdj.2016.865.

Kim, J. H. *et al.* (2014) 'Neuraminidase inhibitory activities of quaternary isoquinoline alkaloids from Corydalis turtschaninovii rhizome.', *Bioorganic & medicinal chemistry*, 22(21), pp. 6047–52. doi: 10.1016/j.bmc.2014.09.004.

Kinniment, S. L. *et al.* (1996) 'Development of a steady-state oral microbial biofilm community using the constant-depth film fermenter.', *Microbiology*, 142 (Pt 3(3), pp. 631–638. doi: 10.1099/13500872-142-3-631.

Kistler, J. O. *et al.* (2013) 'Bacterial community development in experimental gingivitis.', *PloS one*, 8(8), p. e71227. doi: 10.1371/journal.pone.0071227.

Kistler, J. O., Pesaro, M. and Wade, W. G. (2015) 'Development and pyrosequencing analysis of an in-vitro oral biofilm model.', *BMC microbiology*, 15(1), p. 24. doi: 10.1186/s12866-015-0364-1.

Kolenbrander, P. E. *et al.* (2010) 'Oral multispecies biofilm development and the key role of cell-cell distance.', *Nature reviews microbiology*, 8(7), pp. 471–80. doi: 10.1038/nrmicro2381.

Kolenbrander, P. E., Andersen, R. N. and Moore, L. V (1989) 'Coaggregation of Fusobacterium nucleatum, Selenomonas flueggei, Selenomonas infelix, Selenomonas noxia, and Selenomonas sputigena with strains from 11 genera of oral bacteria.', *Infection and immunity*, 57(10), pp. 3194–203. doi: 10.1128/iai.57.10.3194-3203.1989.

Kommerein, N. *et al.* (2017) 'An oral multispecies biofilm model for high content screening applications.', *PloS one*, 12(3), p. e0173973. doi: 10.1371/journal.pone.0173973.

Koyama, K. *et al.* (2010) 'Pharmacokinetics and disposition of CS-8958, a long-acting prodrug of the novel neuraminidase inhibitor laninamivir in rats.', *Xenobiotica; the fate of foreign compounds in biological systems*, 40(3), pp. 207–16. doi: 10.3109/00498250903447691.

Kozich, J. J. *et al.* (2013) 'Development of a dual-index sequencing strategy and curation pipeline for analyzing amplicon sequence data on the MiSeq Illumina sequencing platform.', *Applied and environmental microbiology*, 79(17), pp. 5112–20. doi: 10.1128/AEM.01043-13.

Kreth, J. *et al.* (2005a) 'Co-ordinated bacteriocin production and competence development: a possible mechanism for taking up DNA from neighbouring species.', *Molecular microbiology*, 57(2), pp. 392–404. doi: 10.1111/j.1365-2958.2005.04695.x.

Kreth, J. *et al.* (2005b) 'Competition and coexistence between Streptococcus mutans and Streptococcus sanguinis in the dental biofilm.', *Journal of bacteriology*, 187(21), pp. 7193–203. doi: 10.1128/JB.187.21.7193-7203.2005.

Krom, B. P., Kidwai, S. and Ten Cate, J. M. (2014) 'Candida and other fungal species: forgotten players of healthy oral microbiota.', *Journal of dental research*, 93(5), pp. 445–51. doi: 10.1177/0022034514521814.

Kuboniwa, M. *et al.* (2006) 'Streptococcus gordonii utilizes several distinct gene functions to recruit Porphyromonas gingivalis into a mixed community.', *Molecular microbiology*, 60(1), pp. 121–39. doi: 10.1111/j.1365-2958.2006.05099.x.

Kulik, E. M. *et al.* (2001) 'Identification of archaeal rDNA from subgingival dental plaque by PCR amplification and sequence analysis.', *FEMS microbiology letters*, 196(2), pp. 129–33. doi: 10.1111/j.1574-6968.2001.tb10553.x.

Kumar, P. S. *et al.* (2005) 'Identification of candidate periodontal pathogens and beneficial species by quantitative 16S clonal analysis.', *Journal of clinical microbiology*, 43(8), pp. 3944–55. doi: 10.1128/JCM.43.8.3944-3955.2005.

Kurniyati, K. *et al.* (2013) 'A surface-exposed neuraminidase affects complement resistance and virulence of the oral spirochaete Treponema denticola.', *Molecular*

microbiology, 89(5), pp. 842–56. doi: 10.1111/mmi.12311.

Lamont, E. I. *et al.* (2021) 'Modified SHI medium supports growth of a disease-state subgingival polymicrobial community in vitro.', *Molecular oral microbiology*, 36(1), pp. 37–49. doi: https://doi.org/10.1111/omi.12323.

Lamont, R. J., Koo, H. and Hajishengallis, G. (2018) 'The oral microbiota: dynamic communities and host interactions.', *Nature reviews microbiology*, 16(12), pp. 745–759. doi: 10.1038/s41579-018-0089-x.

Lazarevic, V. *et al.* (2010) 'Study of inter- and intra-individual variations in the salivary microbiota.', *BMC genomics*, 11(1), p. 523. doi: 10.1186/1471-2164-11-523.

Lederberg, J. and McCray, A. T. (2001) ''Ome Sweet 'Omics—a genealogical treasury of words', *Scientist*, 15(8).

Lee, S. F. *et al.* (2009) 'Immune response and alveolar bone resorption in a mouse model of Treponema denticola infection.', *Infection and immunity*, 77(2), pp. 694–8. doi: 10.1128/IAI.01004-08.

Leeuwenhoek, A. V. (1683) 'An abstract of a letter from Mr. Anthony Leewenhoeck writ to Sir C. W.', *Philosophical transactions of the Royal Society of London. Series B, biological sciences*, 13, pp. 74–81.

Leggett, R. M. *et al.* (2020) 'Rapid MinION profiling of preterm microbiota and antimicrobial-resistant pathogens.', *Nature microbiology*, 5(3), pp. 430–442. doi: 10.1038/s41564-019-0626-z.

Lepp, P. W. *et al.* (2004) 'Methanogenic Archaea and human periodontal disease.', *Proceedings of the national academy of sciences of the United States of America*, 101(16), pp. 6176–81. doi: 10.1073/pnas.0308766101.

Lethem, M. I. *et al.* (1990) 'The origin of DNA associated with mucus glycoproteins in cystic fibrosis sputum.', *The European respiratory journal*, 3(1), pp. 19–23. Available at: http://www.ncbi.nlm.nih.gov/pubmed/2107097.

Levine, M. J. *et al.* (1987) 'Structural aspects of salivary glycoproteins.', *Journal of dental research*, 66(2), pp. 436–41. doi: 10.1177/00220345870660020901.

Li, Chen *et al.* (2012) 'Abrogation of neuraminidase reduces biofilm formation, capsule biosynthesis, and virulence of Porphyromonas gingivalis.', *Infection and immunity*, 80(1), pp. 3–13. doi: 10.1128/IAI.05773-11.

Limsuwat, N. *et al.* (2016) 'Sialic acid content in human saliva and anti-influenza activity against human and avian influenza viruses.', *Archives of virology*, 161(3), pp. 649–56. doi: 10.1007/s00705-015-2700-z.

Liu, B. *et al.* (2012) 'Deep sequencing of the oral microbiome reveals signatures of periodontal disease.', *PloS one*, 7(6), p. e37919. doi: 10.1371/journal.pone.0037919.

Liu, G., Tang, C. M. and Exley, R. M. (2015) 'Non-pathogenic Neisseria: members of an abundant, multi-habitat, diverse genus.', *Microbiology*, 161(7), pp. 1297–1312. doi: 10.1099/mic.0.000086.

Loe, H., Theilade, E. and Jensen, S. B. (1965) 'Experimental gingivitis in man', *The Journal of periodontology*, 36, pp. 177–87. doi: 10.1902/jop.1965.36.3.177.

Lundberg, J. O., Weitzberg, E. and Gladwin, M. T. (2008) 'The nitrate-nitrite-nitric oxide pathway in physiology and therapeutics.', *Nature reviews. Drug discovery*, 7(2), pp. 156–67. doi: 10.1038/nrd2466.

Lundblad, A. (2015) 'Gunnar Blix and his discovery of sialic acids. Fascinating molecules in glycobiology.', *Upsala journal of medical sciences*, 120(2), pp. 104–12. doi: 10.3109/03009734.2015.1027429.

Luo, T. L. *et al.* (2019) 'Introducing BAIT (Biofilm Architecture Inference Tool): a software program to evaluate the architecture of oral multi-species biofilms.', *Microbiology*, 165(5), pp. 527–537. doi: 10.1099/mic.0.000761.

Ly, M. *et al.* (2014) 'Altered oral viral ecology in association with periodontal disease.', *mBio*, 5(3), pp. e01133-14. doi: 10.1128/mBio.01133-14.

Machuca, P. *et al.* (2010) 'Isolation of a novel bacteriophage specific for the periodontal pathogen Fusobacterium nucleatum.', *Applied and environmental microbiology*, 76(21), pp. 7243–50. doi: 10.1128/AEM.01135-10.

Macuch, P. J. and Tanner, A. C. R. (2000) 'Campylobacter species in health, gingivitis, and periodontitis.', *Journal of dental research*, 79(2), pp. 785–92. doi: 10.1177/00220345000790021301.

Maghini, D. G. *et al.* (2021) 'Improved high-molecular-weight DNA extraction, nanopore sequencing and metagenomic assembly from the human gut microbiome.', *Nature protocols*, 16(1), pp. 458–471. doi: 10.1038/s41596-020-00424-x.

Magitot, E. (1878) *Treatise on dental caries (Trans by Chandler TH)*. Boston: Osgood.

Mally, M. and Cornelis, G. R. (2008) 'Genetic tools for studying Capnocytophaga canimorsus.', *Applied and environmental microbiology*, 74(20), pp. 6369–77. doi: 10.1128/AEM.01218-08.

Mark Welch, J. L., Dewhirst, F. E. and Borisy, G. G. (2019) 'Biogeography of the oral microbiome: the site-specialist hypothesis.', *Annual review of microbiology*, 73, pp. 335–58. doi: 10.1146/annurev-micro-090817-062503.

Marsh, P. D. (2003) 'Are dental diseases examples of ecological catastrophes?', *Microbiology*, 149(Pt 2), pp. 279–294. doi: 10.1099/mic.0.26082-0.

Marsh, P. D. (2010) 'Microbiology of dental plaque biofilms and their role in oral health and caries', *Dental clinics of North America*, 54(3), pp. 441–54. doi: 10.1016/j.cden.2010.03.002.

Marsh, P. D. D. (1994) 'Microbial ecology of dental plaque and its significance in health and disease.', *Advances in dental research*, 8(2), pp. 263–71. doi: 10.1177/08959374940080022001.

McKimm-Breschkin, J. L. (2013) 'Influenza neuraminidase inhibitors: antiviral action and mechanisms of resistance.', *Influenza and other respiratory viruses*, 7 Suppl 1, pp. 25–36. doi: 10.1111/irv.12047.

Melchior, M. B., Fink-Gremmels, J. and Gaastra, W. (2007) 'Extended antimicrobial susceptibility assay for Staphylococcus aureus isolates from bovine mastitis growing in biofilms.', *Veterinary microbiology*, 125(1–2), pp. 141–9. doi:

10.1016/j.vetmic.2007.05.019.

Meyle, J. and Chapple, I. (2015) 'Molecular aspects of the pathogenesis of periodontitis.', *Periodontology 2000*, 69(1), pp. 7–17. doi: 10.1111/prd.12104.

Miles, A. A., Misra, S. S. and Irwin, J. O. (1938) 'The estimation of the bactericidal power of the blood.', *The Journal of hygiene*, 38(6), pp. 732–49. doi: 10.1017/s002217240001158x.

Miller, W. D. (1890) *The microorganisms of the human mouth*. Edited by W. D. MFG. Philadelphia: Philadelphia, Pa. : S.S. White Dental Manufacturing Co.

Millhouse, E. *et al.* (2014) 'Development of an in vitro periodontal biofilm model for assessing antimicrobial and host modulatory effects of bioactive molecules.', *BMC oral health*, 14, p. 80. doi: 10.1186/1472-6831-14-80.

Mira, A. *et al.* (2019) 'Development of an in vitro system to study oral biofilms in real time through impedance technology: validation and potential applications.', *Journal of oral microbiology*, 11(1), p. 1609838. doi: 10.1080/20002297.2019.1609838.

Mizan, S. *et al.* (2000) 'Cloning and characterization of sialidases with 2-6' and 2-3' sialyl lactose specificity from Pasteurella multocida.', *Journal of bacteriology*, 182(24), pp. 6874–83. doi: 10.1128/JB.182.24.6874-6883.2000.

Moncla, B. J. and Braham, P. (1989) 'Detection of sialidase (neuraminidase) activity in Actinomyces species by using 2'-(4-methylumbelliferyl)alpha-D-N-acetylneuraminic acid in a filter paper spot test.', *Journal of clinical microbiology*, 27(1), pp. 182–4. doi: 10.1128/jcm.27.1.182-184.1989.

Moncla, B. J., Braham, P. and Hillier, S. L. (1990) 'Sialidase (neuraminidase) activity among gram-negative anaerobic and capnophilic bacteria.', *Journal of clinical microbiology*, 28(3), pp. 422–5. doi: 10.1128/jcm.28.3.422-425.1990.

Moore, W. E. *et al.* (1983) 'Bacteriology of moderate (chronic) periodontitis in mature adult humans.', *Infection and immunity*, 42(2), pp. 510–5. doi: 10.1128/iai.42.2.510-515.1983.

Moss, E. L., Maghini, D. G. and Bhatt, A. S. (2020) 'Complete, closed bacterial genomes from microbiomes using nanopore sequencing.', *Nature biotechnology*, 38(6), pp. 701–707. doi: 10.1038/s41587-020-0422-6.

Naginyte, M. *et al.* (2019) 'Enrichment of periodontal pathogens from the biofilms of healthy adults.', *Scientific reports*, 9(1), p. 5491. doi: 10.1038/s41598-019-41882-y.

Naginyte M (2018) *Environmental effects on oral biofilm communities*. PhD thesis. University of Leeds.

Nagpal, D. *et al.* (2016) 'Detection and comparison of Selenomonas sputigena in subgingival biofilms in chronic and aggressive periodontitis patients.', *Journal of Indian society of periodontology*, 20(3), pp. 286–91. doi: 10.4103/0972-124X.181247.

Nasidze, I. *et al.* (2009) 'Global diversity in the human salivary microbiome.', *Genome research*, 19(4), pp. 636–43. doi: 10.1101/gr.084616.108.

Neilands, J. *et al.* (2019) 'Parvimonas micra stimulates expression of gingipains from Porphyromonas gingivalis in multi-species communities.', *Anaerobe*, 55, pp. 54–60. doi: 10.1016/j.anaerobe.2018.10.007.

Newman, G. M. *et al.* (2012) *Carranza's clinical periodontonlogy*. 11th edn. Saunders Elsevier.

Ng, H. M. *et al.* (2019) 'The role of Treponema denticola motility in synergistic biofilm formation With Porphyromonas gingivalis.', *Frontiers in cellular and infection microbiology*, 9, p. 432. doi: 10.3389/fcimb.2019.00432.

Nguyen-Hieu, T. *et al.* (2013) 'Methanogenic archaea in subgingival sites: a review.', *APMIS : acta pathologica, microbiologica, et immunologica Scandinavica*, 121(6), pp. 467–77. doi: 10.1111/apm.12015.

Nishimura, Y. *et al.* (1988) 'Siastatin B, a potent neuraminidase inhibitor: the total synthesis and absolute configuration', *Journal of the American chemical society*, 110(21), pp. 7249–7250. doi: 10.1021/ja00229a069.

Nobbs, A. H., Lamont, R. J. and Jenkinson, H. F. (2009) 'Streptococcus adherence and colonization.', *Microbiology and molecular biology reviews*, 73(3), pp. 407–50. doi: 10.1128/MMBR.00014-09.

Nocker, A. *et al.* (2007) 'Use of propidium monoazide for live/dead distinction in microbial ecology', *Applied and environmental microbiology*, 73(16), pp. 5111–7. doi: 10.1128/AEM.02987-06.

Nyvad, B. and Fejerskov, O. (1987) 'Scanning electron microscopy of early microbial colonization of human enamel and root surfaces in vivo.', *Scandinavian journal of dental research*, 95(4), pp. 287–96. doi: 10.1111/j.1600-0722.1987.tb01844.x.

Nyvad, B. and Kilian, M. (1990) 'Comparison of the initial streptococcal microflora on dental enamel in caries-active and in caries-inactive individuals.', *Caries research*, 24(4), pp. 267–72. doi: 10.1159/000261281.

Oppenheim, F. G. *et al.* (2007) 'Salivary proteome and its genetic polymorphisms.', *Annals of the New York academy of sciences*, 1098, pp. 22–50. doi: 10.1196/annals.1384.030.

Pamp, S. J., Sternberg, C. and Tolker-Nielsen, T. (2009) 'Insight into the microbial multicellular lifestyle via flow-cell technology and confocal microscopy.', *Cytometry. Part A : the journal of the international society for analytical cytology*, 75(2), pp. 90–103. doi: 10.1002/cyto.a.20685.

Park, J. H. *et al.* (2014) 'A periodontitis-associated multispecies model of an oral biofilm.', *Journal of periodontal & implant science*, 44(2), pp. 79–84. doi: 10.5051/jpis.2014.44.2.79.

Park, S.-N., Lim, Y. K. and Kook, J.-K. (2013) 'Development of quantitative real-time PCR primers for detecting 42 oral bacterial species.', *Archives of microbiology*, 195(7), pp. 473–82. doi: 10.1007/s00203-013-0896-4.

Paster, B. J. *et al.* (2001) 'Bacterial diversity in human subgingival plaque.', *Journal of bacteriology*, 183(12), pp. 3770–83. doi: 10.1128/JB.183.12.3770-3783.2001.

Paulson, J. C. and Kawasaki, N. (2011) 'Sialidase inhibitors DAMPen sepsis.', *Nature biotechnology*, 29(5), pp. 406–7. doi: 10.1038/nbt.1859.

Payment, S. A. *et al.* (2000) 'Immunoquantification of Human Salivary Mucins MG1 and MG2 in Stimulated whole Saliva: Factors Influencing Mucin levels', *Journal of dental research*, 79(10), pp. 1765–72. doi: 10.1177/00220345000790100601.

Pearce, E. I. F. and Major, G. N. (1978) 'The colorimetric analysis of sialic acid in human saliva and bovine salivary mucin.', *Journal of dental research*, 57(11–12), pp. 995–1002. doi: 10.1177/00220345780570111701.

Pérez-Brocal, V. and Moya, A. (2018) 'The analysis of the oral DNA virome reveals which viruses are widespread and rare among healthy young adults in Valencia (Spain).', *PloS one*, 13(2), p. e0191867. doi: 10.1371/journal.pone.0191867.

Periasamy, S. and Kolenbrander, P. E. (2009) 'Mutualistic biofilm communities develop with Porphyromonas gingivalis and initial, early, and late colonizers of enamel.', *Journal of bacteriology*, 191(22), pp. 6804–11. doi: 10.1128/JB.01006-09.

Periasamy, S. and Kolenbrander, P. E. (2010) 'Central role of the early colonizer Veillonella sp. in establishing multispecies biofilm communities with initial, middle, and late colonizers of enamel', *Journal of bacteriology*, 192(12), pp. 2965–72. doi: 10.1128/JB.01631-09.

Peters, A. C. and Wimpenny, J. W. T. (1988) 'A constant-depth laboratory model film fermentor', *Biotechnology and bioengineering*, 32(3), pp. 263–70. doi: 10.1002/bit.260320302.

Peters, B. A. *et al.* (2017) 'The oral fungal mycobiome: characteristics and relation to periodontitis in a pilot study', *BMC microbiology*, 17(1), p. 157. doi: 10.1186/s12866-017-1064-9.

Petersen, C. and Round, J. L. (2014) 'Defining dysbiosis and its influence on host immunity and disease.', *Cellular microbiology*, 16(7), pp. 1024–1033. doi: 10.1111/cmi.12308.

Peyyala, R. *et al.* (2011) 'Novel model for multispecies biofilms that uses rigid gas-permeable lenses', *Applied and environmental microbiology*, 77(10), pp. 3413–21. doi: 10.1128/AEM.00039-11.

Phansopa, C. *et al.* (2015) 'Characterization of a sialate-O-acetylesterase (NanS) from the oral pathogen Tannerella forsythia that enhances sialic acid release by NanH, its cognate sialidase.', *The biochemical journal*, 472(2), pp. 157–67. doi: 10.1042/BJ20150388.

Pigman, W., Elliott, H. C. and Laffre, R. O. (1952) 'An artificial mouth for caries research', *Journal of dental research*, 31(5), pp. 627–33. doi: 10.1177/00220345520310050501.

Pihlstrom, B. L., Michalowicz, B. S. and Johnson, N. W. (2005) 'Periodontal diseases.', *Lancet*, 366(9499), pp. 1809–20. doi: 10.1016/S0140-6736(05)67728-8.

Polak, D. *et al.* (2009) 'Mouse model of experimental periodontitis induced by Porphyromonas gingivalis / Fusobacterium nucleatum infection: bone loss and host response', *Journal of clinical periodontology*, 36(5), pp. 406–10. doi: 10.1111/j.1600-051X.2009.01393.x.

Popenoe, E. A. and Drew, R. M. (1957) 'The action of an enzyme of Clostridium perfringens on orosomucoid', *Journal of biological chemistry*, 228(2), pp. 673–83.

Porter, J. R. (1976) 'Antony van Leeuwenhoek: tercentenary of his discovery of bacteria', *Bacteriological reviews*, 40(2), pp. 260–69. doi: 10.1128/br.40.2.260-269.1976.

Potier, M. *et al.* (1979) 'Fluorometric assay of neuraminidase with a sodium (4-methylumbelliferyl-α-d-N-acetylneuraminate) substrate', *Analytical biochemistry*, 94(2), pp. 287–96. doi: 10.1016/0003-2697(79)90362-2.

Pratten *et al.* (1998) 'In vitro studies of the effect of antiseptic-containing mouthwashes on the formation and viability of Streptococcus sanguis biofilms', *Journal of applied microbiology*, 84(6), pp. 1149–55. doi: 10.1046/j.1365-2672.1998.00462.x.

Pride, D. T. *et al.* (2012) 'Evidence of a robust resident bacteriophage population revealed through analysis of the human salivary virome', *The ISME journal*, 6(5), pp. 915–26. doi: 10.1038/ismej.2011.169.

Quast, C. *et al.* (2012) 'The SILVA ribosomal RNA gene database project: improved data processing and web-based tools', *Nucleic acids research*, 41(D1), pp. D590-96. doi: 10.1093/nar/gks1219.

Quince, C. *et al.* (2017) 'Shotgun metagenomics, from sampling to analysis.', *Nature biotechnology*, 35(9), pp. 833–844. doi: 10.1038/nbt.3935.

Radaic, A. and Kapila, Y. L. (2021) 'The oralome and its dysbiosis: New insights into oral microbiome-host interactions', *Computational and structural biotechnology journal*, 19, pp. 1335–60. doi: 10.1016/j.csbj.2021.02.010.

Rahman, M. M. *et al.* (2015) 'Novel pH-dependent regulation of human cytosolic sialidase 2 (NEU2) activities by siastatin B and structural prediction of NEU2/siastatin B complex', *Biochemistry and biophysics reports*, 4, pp. 234–42. doi: 10.1016/j.bbrep.2015.09.017.

Ramseier, C. A. *et al.* (2009) 'Identification of pathogen and host-response markers correlated with periodontal disease.', *Journal of periodontology*, 80(3), pp. 436–46. doi: 10.1902/jop.2009.080480.

Ramsey, K. A., Rushton, Z. L. and Ehre, C. (2016) 'Mucin agarose gel electrophoresis: western blotting for high-molecular-weight glycoproteins', *Journal of visualized experiments*, (112), p. 54153. doi: 10.3791/54153.

Rausch, P. *et al.* (2019) 'Comparative analysis of amplicon and metagenomic sequencing methods reveals key features in the evolution of animal metaorganisms', *Microbiome*, 7(1), p. 133. doi: 10.1186/s40168-019-0743-1.

Ritz, H. L. (1967) 'Microbial population shifts in developing human dental plaque', *Archives of oral biology*, 12(12), pp. 1561–68. doi: 10.1016/0003-9969(67)90190-2.

Robbe, C. *et al.* (2003) 'Evidence of regio-specific glycosylation in human intestinal mucins.', *Journal of biological chemistry*, 278(47), pp. 46337–48. doi: 10.1074/jbc.M302529200.

Robin, C. (1853) *Histoire naturelle des végétaux parasites qui croissent sur l'homme et sur les animaux vivants*. chez JB Baillière.

Rognes, T. *et al.* (2016) 'VSEARCH: a versatile open source tool for metagenomics', *PeerJ*, 4, p. e2584. doi: 10.7717/peerj.2584.

Romero, E. L. *et al.* (1997) 'Sialic acid measurement by a modified Aminoff method: a time-saving reduction in 2-thiobarbituric acid concentration.', *Journal of biochemical and biophysical methods*, 35(2), pp. 129–34. doi: 10.1016/s0165-022x(97)00021-3.

Rossi-Tamisier, M. *et al.* (2015) 'Cautionary tale of using 16S rRNA gene sequence similarity values in identification of human-associated bacterial species', *International journal of systematic and evolutionary microbiology*, 65, pp. 1929–34. doi: 10.1099/ijs.0.000161.

Roy, S. *et al.* (2011) 'Role of sialidase in glycoprotein utilization by Tannerella forsythia', *Microbiology*, 157(11), pp. 3195–202. doi: 10.1099/mic.0.052498-0.

Roy, S. *et al.* (2012) 'Beta-hexosaminidase activity of the oral pathogen Tannerella forsythia influences biofilm formation on glycoprotein substrates', *FEMS immunology & medical microbiology*, 65(1), pp. 116–20. doi: 10.1111/j.1574-695X.2012.00933.x.

Rudney, J. D. *et al.* (2012) 'A reproducible oral microcosm biofilm model for testing dental materials', *Journal of applied microbiology*, 113(6), pp. 1540–53. doi: 10.1111/j.1365-2672.2012.05439.x.

Salli, K. M. and Ouwehand, A. C. (2015) 'The use of in vitro model systems to study dental biofilms associated with caries: a short review', *Journal of oral microbiology*, 7(1), p. 26149. doi: 10.3402/jom.v7.26149.

Sánchez, M. C. *et al.* (2011) 'Structure, viability and bacterial kinetics of an in vitro biofilm model using six bacteria from the subgingival microbiota', *Journal of periodontal research*, 46(2), pp. 252–60. doi: 10.1111/j.1600-0765.2010.01341.x.

Sansone, C. *et al.* (1993) 'The association of mutans streptococci and non-mutans streptococci capable of acidogenesis at a low pH with dental caries on enamel and root surfaces', *Journal of dental research*, 72(2), pp. 508–16. doi: 10.1177/00220345930720020701.

Satur, M. (2019) *Engineering improved specificity and activity into oral bacterial sialidases for glycan biotechnology applications*. PhD thesis, University of Sheffield.

Satur, M. J. *et al.* (2022) 'Structural and functional characterisation of a stable, broad-specificity multimeric sialidase from the oral pathogen Tannerella forsythia.', *The biochemical journal*, 479(17), pp. 1785–806. doi: 10.1042/BCJ20220244.

Schauer, R. (1982) 'Chemistry, metabolism, and biological functions of sialic acids.', *Advances in carbohydrate chemistry and biochemistry*, 40, pp. 131–234. doi: 10.1016/s0065-2318(08)60109-2.

Schloss, P. D. *et al.* (2009) 'Introducing mothur: open-source, platform-independent, community-supported software for describing and comparing microbial communities', *Applied and environmental microbiology*, 75(23), pp. 7537–41. doi: 10.1128/AEM.01541-09.

Schloss, P. D. (2018) 'Identifying and overcoming threats to reproducibility, replicability, robustness, and generalizability in microbiome research', *mBio*. Edited by J. Ravel, 9(3), pp. 1–13. doi: 10.1128/mBio.00525-18.

Schou, S., Holmstrup, P. and Kornman, K. S. (1993) 'Non-human primates used in

studies of periodontal disease pathogenesis: a review of the literature', *Journal of periodontology*, 64(6), pp. 497–508. doi: 10.1902/jop.1993.64.6.497.

Schramm, G. and Mohr, E. (1959) 'Purification of neuraminidase from Vibrio cholerae', *Nature*, 183(4676), pp. 1677–8. doi: 10.1038/1831677a0.

Schreiber, F. *et al.* (2010) 'Denitrification in human dental plaque', *BMC biology*, 8(1), p. 24. doi: 10.1186/1741-7007-8-24.

Schulze-Schweifing, K., Banerjee, A. and Wade, W. G. (2014) 'Comparison of bacterial culture and 16S rRNA community profiling by clonal analysis and pyrosequencing for the characterization of the dentine caries-associated microbiome', *Frontiers in cellular and infection microbiology*, 12(4), p. 164. doi: 10.3389/fcimb.2014.00164.

Sekot, G. *et al.* (2011) 'Potential of the Tannerella forsythia S-layer to delay the immune response', *Journal of dental research*, 90(1), pp. 109–14. doi: 10.1177/0022034510384622.

Serrage, H. J. *et al.* (2021) 'Understanding the matrix: the role of extracellular DNA in oral biofilms', *Frontiers in oral health*, 2, p. 640129. doi: 10.3389/froh.2021.640129.

Settem, R. P. *et al.* (2012) 'Fusobacterium nucleatum and Tannerella forsythia induce synergistic alveolar bone loss in a mouse periodontitis model', *Infection and immunity*, 80(7), pp. 2436–43. doi: 10.1128/IAI.06276-11.

Severi, E., Hood, D. W. and Thomas, G. H. (2007) 'Sialic acid utilization by bacterial pathogens.', *Microbiology*, 153, pp. 2817–22. doi: 10.1099/mic.0.2007/009480-0.

Shaddox, L. M. *et al.* (2010) 'Perpetuation of subgingival biofilms in an in vitro model', *Molecular oral microbiology*, 25(1), pp. 81–7. doi: 10.1111/j.2041-1014.2009.00549.x.

Shah, H. N. and Collins, M. D. (1988) 'Proposal for reclassification of Bacteroides asaccharolyticus, Bacteroides gingivalis, and Bacteroides endodontalis in a new genus, Porphyromonas', *International journal of systematic bacteriology*, 38(1), pp. 128–31. doi: 10.1099/00207713-38-1-128.

Sharma, A., Inagaki, S, *et al.* (2005) 'Synergy between Tannerella forsythia and Fusobacterium nucleatum in biofilm formation', *Oral microbiology and immunology*, 20(1), pp. 39–42. doi: 10.1111/j.1399-302X.2004.00175.x.

Sharma, A., Inagaki, S., *et al.* (2005) 'Tannerella forsythia -induced alveolar bone loss in mice involves leucine-rich-repeat BspA protein', *Journal of dental research*, 84(5), pp. 462–7. doi: 10.1177/154405910508400512.

Shori, D. K. *et al.* (2001) 'Altered sialyl- and fucosyl-linkage on mucins in cystic fibrosis patients promotes formation of the sialyl-Lewis X determinant on salivary MUC-5B and MUC-7', *Pflugers archiv European journal of physiology*, 443, pp. S55-61. doi: 10.1007/s004240100645.

Simpson, E. (1949) 'Measurement of diversity', *Nature*, 163(4148), p. 688. doi: 10.1038/163688a0.

Singh, A. K. *et al.* (2017) 'Streptococcus oralis neuraminidase modulates adherence to multiple carbohydrates on platelets', *Infection and immunity*, 85(3), pp. e00774-

16. doi: 10.1128/IAI.00774-16.

Soares, G. M. S. *et al.* (2015) 'Effects of azithromycin, metronidazole, amoxicillin, and metronidazole plus amoxicillin on an in vitro polymicrobial subgingival biofilm model', *Antimicrobial agents and chemotherapy*, 59(5), pp. 2791–98. doi: 10.1128/AAC.04974-14.

Socransky, S. S. *et al.* (1982) 'An approach to the definition of periodontal disease syndromes by cluster analysis', *Journal of clinical periodontology*, 9(6), pp. 460–71. doi: 10.1111/j.1600-051X.1982.tb02107.x.

Socransky, S. S. *et al.* (1998) 'Microbial complexes in subgingival plaque', *Journal of clinical periodontology*, 25(2), pp. 134–44. doi: 10.1111/j.1600-051X.1998.tb02419.x.

Socransky, S. S. and Haffajee, A. D. (2005) 'Periodontal microbial ecology', *Periodontology 2000*, pp. 135–187. doi: 10.1111/j.1600-0757.2005.00107.x.

Sogodogo, E. *et al.* (2019) 'First characterization of methanogens in oral cavity in Malian patients with oral cavity pathologies', *BMC oral health*, 19(1), p. 232. doi: 10.1186/s12903-019-0929-8.

Song, J. M., Lee, K. H. and Seong, B. L. (2005) 'Antiviral effect of catechins in green tea on influenza virus', *Antiviral research*, 68(2), pp. 66–74. doi: 10.1016/j.antiviral.2005.06.010.

Song, W. S. *et al.* (2017) 'Comparison of periodontitis-associated oral biofilm formation under dynamic and static conditions', *Journal of periodontal & implant science*, 47(4), p. 219. doi: 10.5051/jpis.2017.47.4.219.

Soro, V. *et al.* (2014) 'Axenic culture of a candidate division TM7 bacterium from the human oral cavity and biofilm interactions with other oral bacteria', *Applied and environmental microbiology*, 80(20), pp. 6480–89. doi: 10.1128/AEM.01827-14.

Stackebrandt, E. and Ebers, J. (2006) 'Taxonomic parameters revisited : tarnished gold standards', *Microbiology today*.

Stackebrandt, E. and Goebel, B. M. (1994) 'Taxonomic note: a place for DNA-DNA reassociation and 16S rRNA sequence analysis in the present species definition in bacteriology', *International journal of systematic and evolutionary microbiology*, 44(4), pp. 846–9. doi: 10.1099/00207713-44-4-846.

Stafford, G. *et al.* (2012) 'Sialic acid, periodontal pathogens and Tannerella forsythia: stick around and enjoy the feast!', *Molecular oral microbiology*, 27(1), pp. 11–22. doi: 10.1111/j.2041-1014.2011.00630.x.

Sun, Z. *et al.* (2022) 'Species-resolved sequencing of low-biomass or degraded microbiomes using 2bRAD-M.', *Genome biology*, 23(1), p. 36. doi: 10.1186/s13059-021-02576-9.

Tabak, L. A. *et al.* (1982) 'Role of salivary mucins in the protection of the oral cavity', *Journal of oral pathology and medicine*, 11(1), pp. 1–17. doi: 10.1111/j.1600-0714.1982.tb00138.x.

Takahashi, N. and Nyvad, B. (2008) 'Caries ecology revisited: microbial dynamics and the caries process', *Caries research*, 42(6), pp. 409–18. doi:

10.1159/000159604.

Takahashi, Y. *et al.* (1997) 'A specific cell surface antigen of Streptococcus gordonii is associated with bacterial hemagglutination and adhesion to α2-3-linked sialic acid- containing receptors', *Infection and Immunity*.

Takehara, S. *et al.* (2013) 'Degradation of MUC7 and MUC5B in human saliva.', *PloS one*, 8(7), p. e69059. doi: 10.1371/journal.pone.0069059.

Tanner, A. C. R. *et al.* (1986) 'Bacteroides forsythus sp. nov., a slow-growing, fusiform Bacteroides sp. from the human oral cavity', *International journal of systematic bacteriology*, 36(2), pp. 213–21. doi: 10.1099/00207713-36-2-213.

Tanner, A. C. R. *et al.* (2018) 'The caries microbiome: implications for reversing dysbiosis', *Advances in dental research*, 29(1), pp. 78–85. doi: 10.1177/0022034517736496.

Tao, R. *et al.* (2011) 'Antimicrobial and antibiofilm activity of pleurocidin against cariogenic microorganisms', *Peptides*, 32(8), pp. 1748–54. doi: 10.1016/j.peptides.2011.06.008.

Theilade, E. *et al.* (1966) 'Experimental gingivitis in man: II. A longitudinal clinical and bacteriological investigation', *Journal of periodontal research*, 1, pp. 1–13. doi: 10.1111/j.1600-0765.1966.tb01842.x.

Thompson, H. *et al.* (2009) 'An orthologue of Bacteroides fragilis NanH is the principal sialidase in Tannerella forsythia.', *Journal of bacteriology*, 191(11), pp. 3623–8. doi: 10.1128/JB.01618-08.

Thonard, J. C., Hefflin, C. M. and Steinberg, A. I. (1965) 'Neuraminidase activity in mixed culture supernatant fluids of human oral bacteria.', *Journal of bacteriology*, 89(3), pp. 924–5. doi: 10.1128/jb.89.3.924-925.1965.

Thurnheer, T. and Belibasakis, G. N. (2016) 'Incorporation of staphylococci into titanium-grown biofilms: an in vitro "submucosal" biofilm model for peri-implantitis.', *Clinical oral implants research*, 27(7), pp. 890–5. doi: 10.1111/clr.12715.

Thurnheer, T., Bostanci, N. and Belibasakis, G. N. (2016) 'Microbial dynamics during conversion from supragingival to subgingival biofilms in an in vitro model.', *Molecular oral microbiology*, 31(2), pp. 125–35. doi: 10.1111/omi.12108.

Thurnheer, T., Gmür, R. and Guggenheim, B. (2004) 'Multiplex FISH analysis of a six-species bacterial biofilm.', *Journal of microbiological methods*, 56(1), pp. 37–47. doi: 10.1016/j.mimet.2003.09.003.

Tildon, J. T. and Ogilvie, J. W. (1972) 'The esterase activity of bovine mercaptalbumin. The reaction of the protein with p-nitrophenyl acetate.', *The journal of biological chemistry*, 247(4), pp. 1265–71. doi: https://doi.org/10.1016/S0021-9258(19)45642-1.

Tonetti, M. S., Greenwell, H. and Kornman, K. S. (2018) 'Staging and grading of periodontitis: Framework and proposal of a new classification and case definition.', *Journal of periodontology*, 89(S1), pp. 159–72. doi: 10.1002/JPER.18-0006.

von Troil-Lindén, B. *et al.* (1995) 'Salivary levels of suspected periodontal pathogens in relation to periodontal status and treatment.', *Journal of dental research*, 74(11),

pp. 1789–95. doi: 10.1177/00220345950740111201.

Tuyau, J. E. and Sims, W. (1974) 'Neuraminidase activity in human oral strains of haemophili.', *Archives of oral biology*, 19(9), pp. 817–9. doi: 10.1016/0003-9969(74)90171-x.

Tyrrell, K. L. *et al.* (2002) 'Periodontal bacteria in rabbit mandibular and maxillary abscesses.', *Journal of clinical microbiology*, 40(3), pp. 1044–7. doi: 10.1128/JCM.40.3.1044-1047.2002.

Utter, D. R., Mark Welch, J. L. and Borisy, G. G. (2016) 'Individuality, Stability, and Variability of the Plaque Microbiome.', *Frontiers in microbiology*, 7, p. 564. doi: 10.3389/fmicb.2016.00564.

Valm, A. M., Mark Welch, J. L. and Borisy, G. G. (2012) 'CLASI-FISH: principles of combinatorial labeling and spectral imaging.', *Systematic and applied microbiology*, 35(8), pp. 496–502. doi: 10.1016/j.syapm.2012.03.004.

Varki, A. (1992) 'Diversity in the sialic acids.', *Glycobiology*, 2(1), pp. 25–40. doi: 10.1093/glycob/2.1.25.

Varki, A. (2001) 'Loss of N-glycolylneuraminic acid in humans: Mechanisms, consequences, and implications for hominid evolution', *American Journal of Physical Anthropology*. doi: 10.1002/ajpa.10018.

Varki, A. (2008) 'Sialic acids in human health and disease', *Trends in Molecular Medicine*. doi: 10.1016/j.molmed.2008.06.002.

Varki, A. and Diaz, S. (1983) 'A neuraminidase from Streptococcus sanguis that can release O-acetylated sialic acids.', *The Journal of biological chemistry*, 258(20), pp. 12465–71. Available at: http://www.ncbi.nlm.nih.gov/pubmed/6630194.

Varki, A. and Kornfeld, S. (2015) *Historical background and overview*, *Essentials of Glycobiology*. 4th edn. Cold Spring Harbor (NY): Cold Spring Harbor Laboratory Press. doi: 10.1101/glycobiology.3e.001.

Varki, Ajit and Schauer, R. (2009) 'Sialic acids', in Varki, A, Cummings, R. D., and Esko, J. D. (eds) *Essentials of Glycobiology*. 2nd edn. Cold Spring Harbor (NY): Cold Spring Harbor (NY): Cold Spring Harbor Laboratory Press. Available at: http://www.ncbi.nlm.nih.gov/books/NBK1920/.

Verma, D., Garg, P. K. and Dubey, A. K. (2018) 'Insights into the human oral microbiome.', *Archives of microbiology*, 200(4), pp. 525–40. doi: 10.1007/s00203-018-1505-3.

Volgenant, C. M. C. *et al.* (2016) 'Red and green fluorescence from oral biofilms.', *PloS one*, 11(12), p. e0168428. doi: 10.1371/journal.pone.0168428.

Vonnicolai, H. *et al.* (1983) 'Isolation and characterization of sialidase from Bacteroides fragilis', *FEMS microbiology letters*, 17(1–3), pp. 217–20. doi: 10.1111/j.1574-6968.1983.tb00404.x.

Wade, W. *et al.* (2016) 'Uncultured members of the oral microbiome.', *Journal of the California dental association*, 44(7), pp. 447–56. Available at: http://www.ncbi.nlm.nih.gov/pubmed/27514156.

Wade, W. G. (2013a) 'Characterisation of the human oral microbiome', *Journal of*

oral biosciences, 55(3), pp. 143–8. doi: 10.1016/j.job.2013.06.001.

Wade, W. G. (2013b) 'The oral microbiome in health and disease.', *Pharmacological research*, 69(1), pp. 137–43. doi: 10.1016/j.phrs.2012.11.006.

Wade, W. G. and Prosdocimi, E. M. (2020) 'Profiling of oral bacterial communities.', *Journal of dental research*, 99(6), pp. 621–29. doi: 10.1177/0022034520914594.

Walker, C. and Sedlacek, M. J. (2007) 'An in vitro biofilm model of subgingival plaque.', *Oral microbiology and immunology*, 22(3), pp. 152–61. doi: 10.1111/j.1399-302X.2007.00336.x.

Wang, Q. *et al.* (2007) 'Naive Bayesian classifier for rapid assignment of rRNA sequences into the new bacterial taxonomy.', *Applied and environmental microbiology*, 73(16), pp. 5261–7. doi: 10.1128/AEM.00062-07.

Wescombe, P. A. *et al.* (2009) 'Streptococcal bacteriocins and the case for Streptococcus salivarius as model oral probiotics.', *Future microbiology*, 4(7), pp. 819–35. doi: 10.2217/fmb.09.61.

Widziolek, M. *et al.* (2016) 'Zebrafish as a new model to study effects of periodontal pathogens on cardiovascular diseases.', *Scientific reports*, 6, p. 36023. doi: 10.1038/srep36023.

Winand, R. *et al.* (2019) 'Targeting the 16S rRNA Gene for Bacterial Identification in Complex Mixed Samples: Comparative Evaluation of Second (Illumina) and Third (Oxford Nanopore Technologies) Generation Sequencing Technologies.', *International journal of molecular sciences*, 21(1). doi: 10.3390/ijms21010298.

Wolfaardt, G. M. *et al.* (1994) 'Multicellular organization in a degradative biofilm community.', *Applied and environmental microbiology*, 60(2), pp. 434–46. doi: 10.1128/aem.60.2.434-446.1994.

Wright, T. L. *et al.* (1997) 'Effects of metronidazole on Porphyromonas gingivalis biofilms.', *Journal of periodontal research*, 32(5), pp. 473–7. doi: 10.1111/j.1600-0765.1997.tb00560.x.

Wu, Y. *et al.* (2011) 'In vivo and in vitro antiviral effects of berberine on influenza virus.', *Chinese journal of integrative medicine*, 17(6), pp. 444–52. doi: 10.1007/s11655-011-0640-3.

Wylie, K. M. *et al.* (2014) 'Metagenomic analysis of double-stranded DNA viruses in healthy adults.', *BMC biology*, 12(1), p. 71. doi: 10.1186/s12915-014-0071-7.

Wyss, C. (1989) 'Dependence of proliferation of Bacteroides forsythus on exogenous N-acetylmuramic acid.', *Infection and immunity*, 57(6), pp. 1757–9. doi: 10.1128/iai.57.6.1757-1759.1989.

Ximénez-Fyvie, L. a, Haffajee, a D. and Socransky, S. S. (2000) 'Comparison of the microbiota of supra- and subgingival plaque in health and periodontitis.', *Journal of clinical periodontology*, 27(9), pp. 648–57. doi: 10.1034/j.1600-051x.2000.027009648.x.

Yang, J. *et al.* (2009) 'Comparative structural and molecular characterization of ribitol-5-phosphate-containing Streptococcus oralis coaggregation receptor polysaccharides.', *Journal of bacteriology*, 191(6), pp. 1891–900. doi: 10.1128/JB.01532-08.

Yasunaga, A. *et al.* (2013) 'Monitoring the prevalence of viable and dead cariogenic bacteria in oral specimens and in vitro biofilms by qPCR combined with propidium monoazide.', *BMC microbiology*, 13, p. 157. doi: 10.1186/1471-2180-13-157.

Yoneda, S. *et al.* (2014) 'Ubiquitous sialometabolism present among oral fusobacteria.', *PloS one*, 9(6), p. e99263. doi: 10.1371/journal.pone.0099263.

Yu, S. *et al.* (2021) 'The sialidase inhibitor, DANA, reduces Porphyromonas gingivalis pathogenicity and exerts anti-inflammatory effects: An in vitro and in vivo experiment.', *Journal of periodontology*, 92(2), pp. 286–97. doi: 10.1002/JPER.19-0688.

Zalewska, a *et al.* (2000) 'Structure and biosynthesis of human salivary mucins.', *Acta biochimica Polonica*, 47(4), pp. 1067–79. Available at: http://www.ncbi.nlm.nih.gov/pubmed/11996097.

Zaura, E. *et al.* (2009) 'Defining the healthy "core microbiome" of oral microbial communities.', *BMC microbiology*, 9, p. 259. doi: 10.1186/1471-2180-9-259.

Zheng, W. *et al.* (2015) 'An accurate and efficient experimental approach for characterization of the complex oral microbiota.', *Microbiome*, 3, p. 48. doi: 10.1186/s40168-015-0110-9.

Chapter 8 – Appendices

8.1 Liquid and semi-solid mNOS growth medium (ATCC medium 1494) for *T. denticola* cultures

Volumes for 100 ml

Step 1- make volatile fatty acid (VFA) mix:
0.5 ml isobutyric acid- flammables cupboard in E26
0.5 ml 2-methylbutyric acid- flammables cupboard in E26
0.5 ml isovaleric acid- flammables cupboard in E26
0.5 ml valeric acid- flammables cupboard in E26
98 ml 0.1 M NaOH
Filter-sterilise and store at 4 ^{o}C

Step 2- make thiamine pyrophosphate volatile fatty acid (TPP-VFA) mix:
8.5 ml distilled water (dH_2O)
1.5 ml 0.2% thiamine pyrophosphate
1 ml VFA mix
Filter-sterilise and store at 4 ^{o}C

Step 3- make 100 ml mNOS:
1.25 g brain heart infusion
1 g trypticase peptone
0.25 g yeast extract
0.05 g sodium thioglycolate
0.1 g L-cysteine
0.025 g L-asparagine
0.2 g glucose
0.1 ml resazurin (0.1% w/v in dH_2O)
94 ml dH_2O
For semi-solid agar, add additionally 0.5 % agar and 0.5 % gelatin

Step 4- autoclave and then add:
2.67 ml filter-sterilised $NaHCO_3$ (7.5% w/v in dH_2O)
2 ml heat sterile inactivated human serum
2 ml filter-sterilised TPP-VFA mix

Step 5- if liquid mNOS broth, pour into sterile tubes. If semi-solid mNOS agar, pour cooled yet molten agar into sterile T25 tissue flasks or 7 ml bijou tubes.

Step 6- store at 4 ^{o}C.

8.2 Bacterial community liquid growth medium (modified mFUM medium from Ammann et al. (2013))

Composition of bacterial community liquid growth medium:
50 % autoclaved modified fluid universal medium (mFUM)
30 % sterile heat-inactivated human serum
Either 0.001 % (0.01 mg/ml) or 1 % (10 mg/ml) sterile bovine submaxillary gland mucin using (BSM)
Top up to 100 % with sterile phosphate buffer solution (PBS)

Volumes for 1L:

Step 1- make 133 mM Sørensen's buffer (pH 7.2)
Make 133 mM Na_2HPO_4 by adding 18.89 g to 1 L dH_2O
Make 133 mM KH_2PO_4 by adding 9.08 g to 0.5 L dH_2O
To get pH 7.2, mix 71.5 ml 133 mM Na_2HPO_4 to 28.5 ml 133 mM KH_2PO_4.

Step 2- make 67 mM Sørensen's buffer (pH 7.2) by diluting 1 in 2 with dH_2O.

Step 3- make 500 ml mFUM (Gmur and Guggenheim, 1983)
5 g tryptone
Either 0.005 g or 5 g bovine submaxillary mucin only if the mucin is being autoclaved
2.5 g yeast extract
1.5 g glucose
1 mg haemin
0.5 mg menadione
0.25 g cysteine hydrochloride
0.05 g dithiothreitol (DTT)
1.45 g NaCl
0.25 g Na_2CO_3
0.5 g KNO_3
0.225 g K_2HPO_4
0.225 g KH_2PO_4
0.45 g $(NH_4)_2SO_4$
0.094 g $MgSO_4.7H_2O$
Top up to 500 ml with *67 mM Sørensen's buffer (pH 7)*

Step 4: autoclave then add:
300 ml sterile heat-inactivated human serum
Filter-sterilised 1 % (w/v) mucin only if the mucin is being filter-sterilised
Top up to 500 1L with sterile PBS

Step 5: store at 4 °C.

8.3 Barcoded 27F-YM/338R-R fusion primers used in MiSeq sequencing

Table 8.1 Summary of the barcoded primers used in MiSeq sequencing.

Forward 27-FYM primers:

Barcode	Adapter sequence 5' -3' (i5 adaptor sequence)	Barcode sequence	Primer pad	Linker sequence	27F-YM primer sequence	Full primer sequence
SB501	AATGATACGGCGACCACCGAGATCTACAC	CTACTATA	AGTCAGTCTG	TC	AGAGTTTGATY MTGGCTCAG	AATGATACGGCGACCACCGAGATCTACACCTACTA TAAGTCAGTCTGTCAGAGTTTGATYMTGGCTCAG
SB502	AATGATACGGCGACCACCGAGATCTACAC	CGTTACTA	AGTCAGTCTG	TC	AGAGTTTGATY MTGGCTCAG	AATGATACGGCGACCACCGAGATCTACACCGTTAC TAAGTCAGTCTGTCAGAGTTTGATYMTGGCTCAG

Reverse 338R-R primers:

Barcode	Adapter sequence 5' -3' (i7 adaptor sequence)	Barcode sequence	Primer pad	Linker sequence	338R-R primer sequence	Full primer sequence
SA701	CAAGCAGAAGACGGCATACGAGAT	AACTCTCG	TATGGTAATT	CA	TGCTGCCTCCCG TAGRAGT	CAAGCAGAAGACGGCATACGAGATAACTCTCG TATGGTAATTCATGCTGCCTCCCGTAGRAGT
SA702	CAAGCAGAAGACGGCATACGAGAT	ACTATGTC	TATGGTAATT	CA	TGCTGCCTCCCG TAGRAGT	CAAGCAGAAGACGGCATACGAGATACTATGTC TATGGTAATTCATGCTGCCTCCCGTAGRAGT

SA704	CAAGCAGAAGACGGCATACGAGAT	CAGTGAGT	TATGGTAATT	CA	TGCTGCCTCCCG TAGRAGT	CAAGCAGAAGACGGCATACGAGATCAGTGAG TTATGGTAATTCATGCTGCCTCCCGTAGRAGT
SA705	CAAGCAGAAGACGGCATACGAGAT	CGTACTCA	TATGGTAATT	CA	TGCTGCCTCCCG TAGRAGT	CAAGCAGAAGACGGCATACGAGATCGTACTCA TATGGTAATTCATGCTGCCTCCCGTAGRAGT
SA706	CAAGCAGAAGACGGCATACGAGAT	CTACGCAG	TATGGTAATT	CA	TGCTGCCTCCCG TAGRAGT	CAAGCAGAAGACGGCATACGAGATCTACGCA GTATGGTAATTCATGCTGCCTCCCGTAGRAGT
SA707	CAAGCAGAAGACGGCATACGAGAT	GGAGACTA	TATGGTAATT	CA	TGCTGCCTCCCG TAGRAGT	CAAGCAGAAGACGGCATACGAGATGGAGACT ATATGGTAATTCATGCTGCCTCCCGTAGRAGT
SA708	CAAGCAGAAGACGGCATACGAGAT	GTCGCTCG	TATGGTAATT	CA	TGCTGCCTCCCG TAGRAGT	CAAGCAGAAGACGGCATACGAGATGTCGCTCG TATGGTAATTCATGCTGCCTCCCGTAGRAGT
SA709	CAAGCAGAAGACGGCATACGAGAT	GTCGTAGT	TATGGTAATT	CA	TGCTGCCTCCCG TAGRAGT	CAAGCAGAAGACGGCATACGAGATGTCGTAGT TATGGTAATTCATGCTGCCTCCCGTAGRAGT

8.4 Barcoded 27F-YM/1492R-D primers used in Nanopore sequencing

Table 8.2 Summary of the barcoded primers used in Nanopore sequencing.

Forward 27F-YM primers:

Barcode	Barcode sequence	27F-YM primer sequence	Full primer sequence
BC01	AAGAAAGTTGTCGGTGTCTTTGTG	AGAGTTTGATYMTGGCTCAG	AAGAAAGTTGTCGGTGTCTTTGTGAGAGTTTGATYMTGGCTCAG
BC02	TCGATTCCGTTTGTAGTCGTCTGT	AGAGTTTGATYMTGGCTCAG	TCGATTCCGTTTGTAGTCGTCTGTAGAGTTTGATYMTGGCTCAG
BC03	GAGTCTTGTGTCCCAGTTACCAGG	AGAGTTTGATYMTGGCTCAG	GAGTCTTGTGTCCCAGTTACCAGGAGAGTTTGATYMTGGCTCAG
BC04	TTCGGATTCTATCGTGTTTCCCTA	AGAGTTTGATYMTGGCTCAG	TTCGGATTCTATCGTGTTTCCCTAAGAGTTTGATYMTGGCTCAG
BC05	CTTGTCCAGGGTTTGTGTAACCTT	AGAGTTTGATYMTGGCTCAG	CTTGTCCAGGGTTTGTGTAACCTTAGAGTTTGATYMTGGCTCAG
BC06	TTCTCGCAAAGGCAGAAAGTAGTC	AGAGTTTGATYMTGGCTCAG	TTCTCGCAAAGGCAGAAAGTAGTCAGAGTTTGATYMTGGCTCAG
BC07	GTGTTACCGTGGGAATGAATCCTT	AGAGTTTGATYMTGGCTCAG	GTGTTACCGTGGGAATGAATCCTTAGAGTTTGATYMTGGCTCAG
BC08	TTCAGGGAACAAACCAAGTTACGT	AGAGTTTGATYMTGGCTCAG	TTCAGGGAACAAACCAAGTTACGTAGAGTTTGATYMTGGCTCAG
BC09	AACTAGGCACAGCGAGTCTTGGTT	AGAGTTTGATYMTGGCTCAG	AACTAGGCACAGCGAGTCTTGGTTAGAGTTTGATYMTGGCTCAG
BC10	AAGCGTTGAAACCTTTGTCCTCTC	AGAGTTTGATYMTGGCTCAG	AAGCGTTGAAACCTTTGTCCTCTCAGAGTTTGATYMTGGCTCAG
BC11	GTTTCATCTATCGGAGGGAATGGA	AGAGTTTGATYMTGGCTCAG	GTTTCATCTATCGGAGGGAATGGAAGAGTTTGATYMTGGCTCAG
BC12	CAGGTAGAAAGAAGCAGAATCGGA	AGAGTTTGATYMTGGCTCAG	CAGGTAGAAAGAAGCAGAATCGGAAGAGTTTGATYMTGGCTCAG
BC13	AGAACGACTTCCATACTCGTGTGA	AGAGTTTGATYMTGGCTCAG	AGAACGACTTCCATACTCGTGTGAAGAGTTTGATYMTGGCTCAG
BC14	AACGAGTCTCTTGGGACCCATAGA	AGAGTTTGATYMTGGCTCAG	AACGAGTCTCTTGGGACCCATAGAAGAGTTTGATYMTGGCTCAG
BC15	AGGTCTACCTCGCTAACACCACTG	AGAGTTTGATYMTGGCTCAG	AGGTCTACCTCGCTAACACCACTGAGAGTTTGATYMTGGCTCAG

BC16	CGTCAACTGACAGTGGTTCGTACT	AGAGTTTGATYMTGGCTCAG	CGTCAACTGACAGTGGTTCGTACTAGAGTTTGATYMTGGCTCAG
BC17	ACCCTCCAGGAAAGTACCTCTGAT	AGAGTTTGATYMTGGCTCAG	ACCCTCCAGGAAAGTACCTCTGATAGAGTTTGATYMTGGCTCAG
BC18	CCAAACCCAACAACCTAGATAGGC	AGAGTTTGATYMTGGCTCAG	CCAAACCCAACAACCTAGATAGGCAGAGTTTGATYMTGGCTCAG
BC19	GTTCCTCGTGCAGTGTCAAGAGAT	AGAGTTTGATYMTGGCTCAG	GTTCCTCGTGCAGTGTCAAGAGATAGAGTTTGATYMTGGCTCAG
BC20	TTGCGTCCTGTTACGAGAACTCAT	AGAGTTTGATYMTGGCTCAG	TTGCGTCCTGTTACGAGAACTCATAGAGTTTGATYMTGGCTCAG
BC21	GAGCCTCTCATTGTCCGTTCTCTA	AGAGTTTGATYMTGGCTCAG	GAGCCTCTCATTGTCCGTTCTCTAAGAGTTTGATYMTGGCTCAG
BC22	ACCACTGCCATGTATCAAAGTACG	AGAGTTTGATYMTGGCTCAG	ACCACTGCCATGTATCAAAGTACGAGAGTTTGATYMTGGCTCAG
BC23	CTTACTACCCAGTGAACCTCCTCG	AGAGTTTGATYMTGGCTCAG	CTTACTACCCAGTGAACCTCCTCGAGAGTTTGATYMTGGCTCAG
BC24	GCATAGTTCTGCATGATGGGTTAG	AGAGTTTGATYMTGGCTCAG	GCATAGTTCTGCATGATGGGTTAGAGAGTTTGATYMTGGCTCAG
BC25	GTAAGTTGGGTATGCAACGCAATG	AGAGTTTGATYMTGGCTCAG	GTAAGTTGGGTATGCAACGCAATGAGAGTTTGATYMTGGCTCAG
BC26	CATACAGCGACTACGCATTCTCAT	AGAGTTTGATYMTGGCTCAG	CATACAGCGACTACGCATTCTCATAGAGTTTGATYMTGGCTCAG
BC27	CGACGGTTAGATTCACCTCTTACA	AGAGTTTGATYMTGGCTCAG	CGACGGTTAGATTCACCTCTTACAAGAGTTTGATYMTGGCTCAG
BC28	TGAAACCTAAGAAGGCACCGTATC	AGAGTTTGATYMTGGCTCAG	TGAAACCTAAGAAGGCACCGTATCAGAGTTTGATYMTGGCTCAG
BC29	CTAGACACCTTGGGTTGACAGACC	AGAGTTTGATYMTGGCTCAG	CTAGACACCTTGGGTTGACAGACCAGAGTTTGATYMTGGCTCAG
BC30	TCAGTGAGGATCTACTTCGACCCA	AGAGTTTGATYMTGGCTCAG	TCAGTGAGGATCTACTTCGACCCAAGAGTTTGATYMTGGCTCAG
BC31	TGCGTACAGCAATCAGTTACATTG	AGAGTTTGATYMTGGCTCAG	TGCGTACAGCAATCAGTTACATTGAGAGTTTGATYMTGGCTCAG
BC32	CCAGTAGAAGTCCGACAACGTCAT	AGAGTTTGATYMTGGCTCAG	CCAGTAGAAGTCCGACAACGTCATAGAGTTTGATYMTGGCTCAG
BC33	CAGACTTGGTACGGTTGGGTAACT	AGAGTTTGATYMTGGCTCAG	CAGACTTGGTACGGTTGGGTAACTAGAGTTTGATYMTGGCTCAG
BC34	GGACGAAGAACTCAAGTCAAAGGC	AGAGTTTGATYMTGGCTCAG	GGACGAAGAACTCAAGTCAAAGGCAGAGTTTGATYMTGGCTCAG
BC35	CTACTTACGAAGCTGAGGGACTGC	AGAGTTTGATYMTGGCTCAG	CTACTTACGAAGCTGAGGGACTGCAGAGTTTGATYMTGGCTCAG
BC36	ATGTCCCAGTTAGAGGAGGAAACA	AGAGTTTGATYMTGGCTCAG	ATGTCCCAGTTAGAGGAGGAAACAAGAGTTTGATYMTGGCTCAG
BC37	GCTTGCGATTGATGCTTAGTATCA	AGAGTTTGATYMTGGCTCAG	GCTTGCGATTGATGCTTAGTATCAAGAGTTTGATYMTGGCTCAG
BC38	ACCACAGGAGGACGATACAGAGAA	AGAGTTTGATYMTGGCTCAG	ACCACAGGAGGACGATACAGAGAAAGAGTTTGATYMTGGCTCAG
BC39	CCACAGTGTCAACTAGAGCCTCTC	AGAGTTTGATYMTGGCTCAG	CCACAGTGTCAACTAGAGCCTCTCAGAGTTTGATYMTGGCTCAG
BC40	TAGTTTGGATGACCAAGGATAGCC	AGAGTTTGATYMTGGCTCAG	TAGTTTGGATGACCAAGGATAGCCAGAGTTTGATYMTGGCTCAG

BC70	ACCGAGATCCTACGAATGGAGTGT	AGAGTTTGATYMTGGCTCAG	ACCGAGATCCTACGAATGGAGTGTAGAGTTTGATYMTGGCTCAG
BC71	CCTGGGAGCATCAGGTAGTAACAG	AGAGTTTGATYMTGGCTCAG	CCTGGGAGCATCAGGTAGTAACAGAGAGTTTGATYMTGGCTCAG
BC72	TAGCTGACTGTCTTCCATACCGAC	AGAGTTTGATYMTGGCTCAG	TAGCTGACTGTCTTCCATACCGACAGAGTTTGATYMTGGCTCAG
BC73	AAGAAACAGGATGACAGAACCCTC	AGAGTTTGATYMTGGCTCAG	AAGAAACAGGATGACAGAACCCTCAGAGTTTGATYMTGGCTCAG
BC74	TACAAGCATCCCAACACTTCCACT	AGAGTTTGATYMTGGCTCAG	TACAAGCATCCCAACACTTCCACTAGAGTTTGATYMTGGCTCAG
BC75	GACCATTGTGATGAACCCTGTTGT	AGAGTTTGATYMTGGCTCAG	GACCATTGTGATGAACCCTGTTGTAGAGTTTGATYMTGGCTCAG
BC76	ATGCTTGTTACATCAACCCTGGAC	AGAGTTTGATYMTGGCTCAG	ATGCTTGTTACATCAACCCTGGACAGAGTTTGATYMTGGCTCAG
BC77	CGACCTGTTTCTCAGGGATACAAC	AGAGTTTGATYMTGGCTCAG	CGACCTGTTTCTCAGGGATACAACAGAGTTTGATYMTGGCTCAG
BC78	AACAACCGAACCTTTGAATCAGAA	AGAGTTTGATYMTGGCTCAG	AACAACCGAACCTTTGAATCAGAAAGAGTTTGATYMTGGCTCAG
BC79	TCTCGGAGATAGTTCTCACTGCTG	AGAGTTTGATYMTGGCTCAG	TCTCGGAGATAGTTCTCACTGCTGAGAGTTTGATYMTGGCTCAG
BC80	CGGATGAACATAGGATAGCGATTC	AGAGTTTGATYMTGGCTCAG	CGGATGAACATAGGATAGCGATTCAGAGTTTGATYMTGGCTCAG
BC81	CCTCATCTTGTGAAGTTGTTTCGG	AGAGTTTGATYMTGGCTCAG	CCTCATCTTGTGAAGTTGTTTCGGAGAGTTTGATYMTGGCTCAG
BC82	ACGGTATGTCGAGTTCCAGGACTA	AGAGTTTGATYMTGGCTCAG	ACGGTATGTCGAGTTCCAGGACTAAGAGTTTGATYMTGGCTCAG
BC83	TGGCTTGATCTAGGTAAGGTCGAA	AGAGTTTGATYMTGGCTCAG	TGGCTTGATCTAGGTAAGGTCGAAAGAGTTTGATYMTGGCTCAG
BC84	GTAGTGGACCTAGAACCTGTGCCA	AGAGTTTGATYMTGGCTCAG	GTAGTGGACCTAGAACCTGTGCCAAGAGTTTGATYMTGGCTCAG
BC85	AACGGAGGAGTTAGTTGGATGATC	AGAGTTTGATYMTGGCTCAG	AACGGAGGAGTTAGTTGGATGATCAGAGTTTGATYMTGGCTCAG
BC86	AGGTGATCCCAACAAGCGTAAGTA	AGAGTTTGATYMTGGCTCAG	AGGTGATCCCAACAAGCGTAAGTAAGAGTTTGATYMTGGCTCAG
BC87	TACATGCTCCTGTTGTTAGGGAGG	AGAGTTTGATYMTGGCTCAG	TACATGCTCCTGTTGTTAGGGAGGAGAGTTTGATYMTGGCTCAG
BC88	TCTTCTACTACCGATCCGAAGCAG	AGAGTTTGATYMTGGCTCAG	TCTTCTACTACCGATCCGAAGCAGAGAGTTTGATYMTGGCTCAG
BC89	ACAGCATCAATGTTTGGCTAGTTG	AGAGTTTGATYMTGGCTCAG	ACAGCATCAATGTTTGGCTAGTTGAGAGTTTGATYMTGGCTCAG
BC90	GATGTAGAGGGTACGGTTTGAGGC	AGAGTTTGATYMTGGCTCAG	GATGTAGAGGGTACGGTTTGAGGCAGAGTTTGATYMTGGCTCAG
BC91	GGCTCCATAGGAACTCACGCTACT	AGAGTTTGATYMTGGCTCAG	GGCTCCATAGGAACTCACGCTACTAGAGTTTGATYMTGGCTCAG
BC92	TTGTGAGTGGAAAGATACAGGACC	AGAGTTTGATYMTGGCTCAG	TTGTGAGTGGAAAGATACAGGACCAGAGTTTGATYMTGGCTCAG
BC93	AGTTTCCATCACTTCAGACTTGGG	AGAGTTTGATYMTGGCTCAG	AGTTTCCATCACTTCAGACTTGGGAGAGTTTGATYMTGGCTCAG
BC94	GATTGTCCTCAAACTGCCACCTAC	AGAGTTTGATYMTGGCTCAG	GATTGTCCTCAAACTGCCACCTACAGAGTTTGATYMTGGCTCAG

BC95	CCTGTCTGGAAGAAGAATGGACTT	AGAGTTTGATYMTGGCTCAG	CCTGTCTGGAAGAAGAATGGACTTAGAGTTTGATYMTGGCTCAG
BC96	CTGAACGGTCATAGAGTCCACCAT	AGAGTTTGATYMTGGCTCAG	CTGAACGGTCATAGAGTCCACCATAGAGTTTGATYMTGGCTCAG

Reverse 1492R-D primers:

Barcode	Barcode sequence	1492R-D primer sequence	Full primer sequence
BC01	AAGAAAGTTGTCGGTGTCTTTGTG	CGGDTACCTTGTTACGACTT	AAGAAAGTTGTCGGTGTCTTTGTGCGGDTACCTTGTTACGACTT
BC02	TCGATTCCGTTTGTAGTCGTCTGT	CGGDTACCTTGTTACGACTT	TCGATTCCGTTTGTAGTCGTCTGTCGGDTACCTTGTTACGACTT
BC03	GAGTCTTGTGTCCCAGTTACCAGG	CGGDTACCTTGTTACGACTT	GAGTCTTGTGTCCCAGTTACCAGGCGGDTACCTTGTTACGACTT
BC04	TTCGGATTCTATCGTGTTTCCCTA	CGGDTACCTTGTTACGACTT	TTCGGATTCTATCGTGTTTCCCTACGGDTACCTTGTTACGACTT
BC05	CTTGTCCAGGGTTTGTGTAACCTT	CGGDTACCTTGTTACGACTT	CTTGTCCAGGGTTTGTGTAACCTTCGGDTACCTTGTTACGACTT
BC06	TTCTCGCAAAGGCAGAAAGTAGTC	CGGDTACCTTGTTACGACTT	TTCTCGCAAAGGCAGAAAGTAGTCCGGDTACCTTGTTACGACTT
BC07	GTGTTACCGTGGGAATGAATCCTT	CGGDTACCTTGTTACGACTT	GTGTTACCGTGGGAATGAATCCTTCGGDTACCTTGTTACGACTT
BC08	TTCAGGGAACAAACCAAGTTACGT	CGGDTACCTTGTTACGACTT	TTCAGGGAACAAACCAAGTTACGTCGGDTACCTTGTTACGACTT
BC09	AACTAGGCACAGCGAGTCTTGGTT	CGGDTACCTTGTTACGACTT	AACTAGGCACAGCGAGTCTTGGTTCGGDTACCTTGTTACGACTT
BC10	AAGCGTTGAAACCTTTGTCCTCTC	CGGDTACCTTGTTACGACTT	AAGCGTTGAAACCTTTGTCCTCTCCGGDTACCTTGTTACGACTT
BC11	GTTTCATCTATCGGAGGGAATGGA	CGGDTACCTTGTTACGACTT	GTTTCATCTATCGGAGGGAATGGACGGDTACCTTGTTACGACTT
BC12	CAGGTAGAAAGAAGCAGAATCGGA	CGGDTACCTTGTTACGACTT	CAGGTAGAAAGAAGCAGAATCGGACGGDTACCTTGTTACGACTT
BC13	AGAACGACTTCCATACTCGTGTGA	CGGDTACCTTGTTACGACTT	AGAACGACTTCCATACTCGTGTGACGGDTACCTTGTTACGACTT
BC14	AACGAGTCTCTTGGGACCCATAGA	CGGDTACCTTGTTACGACTT	AACGAGTCTCTTGGGACCCATAGACGGDTACCTTGTTACGACTT
BC15	AGGTCTACCTCGCTAACACCACTG	CGGDTACCTTGTTACGACTT	AGGTCTACCTCGCTAACACCACTGCGGDTACCTTGTTACGACTT

BC16	CGTCAACTGACAGTGGTTCGTACT	CGGDTACCTTGTTACGACTT	CGTCAACTGACAGTGGTTCGTACTCGGDTACCTTGTTACGACTT
BC17	ACCCTCCAGGAAAGTACCTCTGAT	CGGDTACCTTGTTACGACTT	ACCCTCCAGGAAAGTACCTCTGATCGGDTACCTTGTTACGACTT
BC18	CCAAACCCAACAACCTAGATAGGC	CGGDTACCTTGTTACGACTT	CCAAACCCAACAACCTAGATAGGCCGGDTACCTTGTTACGACTT
BC19	GTTCCTCGTGCAGTGTCAAGAGAT	CGGDTACCTTGTTACGACTT	GTTCCTCGTGCAGTGTCAAGAGATCGGDTACCTTGTTACGACTT
BC20	TTGCGTCCTGTTACGAGAACTCAT	CGGDTACCTTGTTACGACTT	TTGCGTCCTGTTACGAGAACTCATCGGDTACCTTGTTACGACTT
BC21	GAGCCTCTCATTGTCCGTTCTCTA	CGGDTACCTTGTTACGACTT	GAGCCTCTCATTGTCCGTTCTCTACGGDTACCTTGTTACGACTT
BC22	ACCACTGCCATGTATCAAAGTACG	CGGDTACCTTGTTACGACTT	ACCACTGCCATGTATCAAAGTACGCGGDTACCTTGTTACGACTT
BC23	CTTACTACCCAGTGAACCTCCTCG	CGGDTACCTTGTTACGACTT	CTTACTACCCAGTGAACCTCCTCGCGGDTACCTTGTTACGACTT
BC24	GCATAGTTCTGCATGATGGGTTAG	CGGDTACCTTGTTACGACTT	GCATAGTTCTGCATGATGGGTTAGCGGDTACCTTGTTACGACTT
BC25	GTAAGTTGGGTATGCAACGCAATG	CGGDTACCTTGTTACGACTT	GTAAGTTGGGTATGCAACGCAATGCGGDTACCTTGTTACGACTT
BC26	CATACAGCGACTACGCATTCTCAT	CGGDTACCTTGTTACGACTT	CATACAGCGACTACGCATTCTCATCGGDTACCTTGTTACGACTT
BC27	CGACGGTTAGATTCACCTCTTACA	CGGDTACCTTGTTACGACTT	CGACGGTTAGATTCACCTCTTACACGGDTACCTTGTTACGACTT
BC28	TGAAACCTAAGAAGGCACCGTATC	CGGDTACCTTGTTACGACTT	TGAAACCTAAGAAGGCACCGTATCCGGDTACCTTGTTACGACTT
BC29	CTAGACACCTTGGGTTGACAGACC	CGGDTACCTTGTTACGACTT	CTAGACACCTTGGGTTGACAGACCCGGDTACCTTGTTACGACTT
BC30	TCAGTGAGGATCTACTTCGACCCA	CGGDTACCTTGTTACGACTT	TCAGTGAGGATCTACTTCGACCCACGGDTACCTTGTTACGACTT
BC31	TGCGTACAGCAATCAGTTACATTG	CGGDTACCTTGTTACGACTT	TGCGTACAGCAATCAGTTACATTGCGGDTACCTTGTTACGACTT
BC32	CCAGTAGAAGTCCGACAACGTCAT	CGGDTACCTTGTTACGACTT	CCAGTAGAAGTCCGACAACGTCATCGGDTACCTTGTTACGACTT
BC33	CAGACTTGGTACGGTTGGGTAACT	CGGDTACCTTGTTACGACTT	CAGACTTGGTACGGTTGGGTAACTCGGDTACCTTGTTACGACTT
BC34	GGACGAAGAACTCAAGTCAAAGGC	CGGDTACCTTGTTACGACTT	GGACGAAGAACTCAAGTCAAAGGCCGGDTACCTTGTTACGACTT
BC35	CTACTTACGAAGCTGAGGGACTGC	CGGDTACCTTGTTACGACTT	CTACTTACGAAGCTGAGGGACTGCCGGDTACCTTGTTACGACTT
BC36	ATGTCCCAGTTAGAGGAGGAAACA	CGGDTACCTTGTTACGACTT	ATGTCCCAGTTAGAGGAGGAAACACGGDTACCTTGTTACGACTT
BC37	GCTTGCGATTGATGCTTAGTATCA	CGGDTACCTTGTTACGACTT	GCTTGCGATTGATGCTTAGTATCACGGDTACCTTGTTACGACTT
BC38	ACCACAGGAGGACGATACAGAGAA	CGGDTACCTTGTTACGACTT	ACCACAGGAGGACGATACAGAGAACGGDTACCTTGTTACGACTT
BC39	CCACAGTGTCAACTAGAGCCTCTC	CGGDTACCTTGTTACGACTT	CCACAGTGTCAACTAGAGCCTCTCCGGDTACCTTGTTACGACTT
BC40	TAGTTTGGATGACCAAGGATAGCC	CGGDTACCTTGTTACGACTT	TAGTTTGGATGACCAAGGATAGCCCGGDTACCTTGTTACGACTT

BC70	ACCGAGATCCTACGAATGGAGTGT	CGGDTACCTTGTTACGACTT	ACCGAGATCCTACGAATGGAGTGTCGGDTACCTTGTTACGACTT
BC71	CCTGGGAGCATCAGGTAGTAACAG	CGGDTACCTTGTTACGACTT	CCTGGGAGCATCAGGTAGTAACAGCGGDTACCTTGTTACGACTT
BC72	TAGCTGACTGTCTTCCATACCGAC	CGGDTACCTTGTTACGACTT	TAGCTGACTGTCTTCCATACCGACCGGDTACCTTGTTACGACTT
BC73	AAGAAACAGGATGACAGAACCCTC	CGGDTACCTTGTTACGACTT	AAGAAACAGGATGACAGAACCCTCCGGDTACCTTGTTACGACTT
BC74	TACAAGCATCCCAACACTTCCACT	CGGDTACCTTGTTACGACTT	TACAAGCATCCCAACACTTCCACTCGGDTACCTTGTTACGACTT
BC75	GACCATTGTGATGAACCCTGTTGT	CGGDTACCTTGTTACGACTT	GACCATTGTGATGAACCCTGTTGTCGGDTACCTTGTTACGACTT
BC76	ATGCTTGTTACATCAACCCTGGAC	CGGDTACCTTGTTACGACTT	ATGCTTGTTACATCAACCCTGGACCGGDTACCTTGTTACGACTT
BC77	CGACCTGTTTCTCAGGGATACAAC	CGGDTACCTTGTTACGACTT	CGACCTGTTTCTCAGGGATACAACCGGDTACCTTGTTACGACTT
BC78	AACAACCGAACCTTTGAATCAGAA	CGGDTACCTTGTTACGACTT	AACAACCGAACCTTTGAATCAGAACGGDTACCTTGTTACGACTT
BC79	TCTCGGAGATAGTTCTCACTGCTG	CGGDTACCTTGTTACGACTT	TCTCGGAGATAGTTCTCACTGCTGCGGDTACCTTGTTACGACTT
BC80	CGGATGAACATAGGATAGCGATTC	CGGDTACCTTGTTACGACTT	CGGATGAACATAGGATAGCGATTCCGGDTACCTTGTTACGACTT
BC81	CCTCATCTTGTGAAGTTGTTTCGG	CGGDTACCTTGTTACGACTT	CCTCATCTTGTGAAGTTGTTTCGGCGGDTACCTTGTTACGACTT
BC82	ACGGTATGTCGAGTTCCAGGACTA	CGGDTACCTTGTTACGACTT	ACGGTATGTCGAGTTCCAGGACTACGGDTACCTTGTTACGACTT
BC83	TGGCTTGATCTAGGTAAGGTCGAA	CGGDTACCTTGTTACGACTT	TGGCTTGATCTAGGTAAGGTCGAACGGDTACCTTGTTACGACTT
BC84	GTAGTGGACCTAGAACCTGTGCCA	CGGDTACCTTGTTACGACTT	GTAGTGGACCTAGAACCTGTGCCACGGDTACCTTGTTACGACTT
BC85	AACGGAGGAGTTAGTTGGATGATC	CGGDTACCTTGTTACGACTT	AACGGAGGAGTTAGTTGGATGATCCGGDTACCTTGTTACGACTT
BC86	AGGTGATCCCAACAAGCGTAAGTA	CGGDTACCTTGTTACGACTT	AGGTGATCCCAACAAGCGTAAGTACGGDTACCTTGTTACGACTT
BC87	TACATGCTCCTGTTGTTAGGGAGG	CGGDTACCTTGTTACGACTT	TACATGCTCCTGTTGTTAGGGAGGCGGDTACCTTGTTACGACTT
BC88	TCTTCTACTACCGATCCGAAGCAG	CGGDTACCTTGTTACGACTT	TCTTCTACTACCGATCCGAAGCAGCGGDTACCTTGTTACGACTT
BC89	ACAGCATCAATGTTTGGCTAGTTG	CGGDTACCTTGTTACGACTT	ACAGCATCAATGTTTGGCTAGTTGCGGDTACCTTGTTACGACTT
BC90	GATGTAGAGGGTACGGTTTGAGGC	CGGDTACCTTGTTACGACTT	GATGTAGAGGGTACGGTTTGAGGCCGGDTACCTTGTTACGACTT
BC91	GGCTCCATAGGAACTCACGCTACT	CGGDTACCTTGTTACGACTT	GGCTCCATAGGAACTCACGCTACTCGGDTACCTTGTTACGACTT
BC92	TTGTGAGTGGAAAGATACAGGACC	CGGDTACCTTGTTACGACTT	TTGTGAGTGGAAAGATACAGGACCCGGDTACCTTGTTACGACTT
BC93	AGTTTCCATCACTTCAGACTTGGG	CGGDTACCTTGTTACGACTT	AGTTTCCATCACTTCAGACTTGGGCGGDTACCTTGTTACGACTT
BC94	GATTGTCCTCAAACTGCCACCTAC	CGGDTACCTTGTTACGACTT	GATTGTCCTCAAACTGCCACCTACCGGDTACCTTGTTACGACTT

BC95	CCTGTCTGGAAGAAGAATGGACTT	CGGDTACCTTGTTACGACTT	CCTGTCTGGAAGAAGAATGGACTTCGGDTACCTTGTTACGACTT
BC96	CTGAACGGTCATAGAGTCCACCAT	CGGDTACCTTGTTACGACTT	CTGAACGGTCATAGAGTCCACCATCGGDTACCTTGTTACGACTT

8.5 DNA gels from validating bacterium-specific primer sets

A. oris specific primers

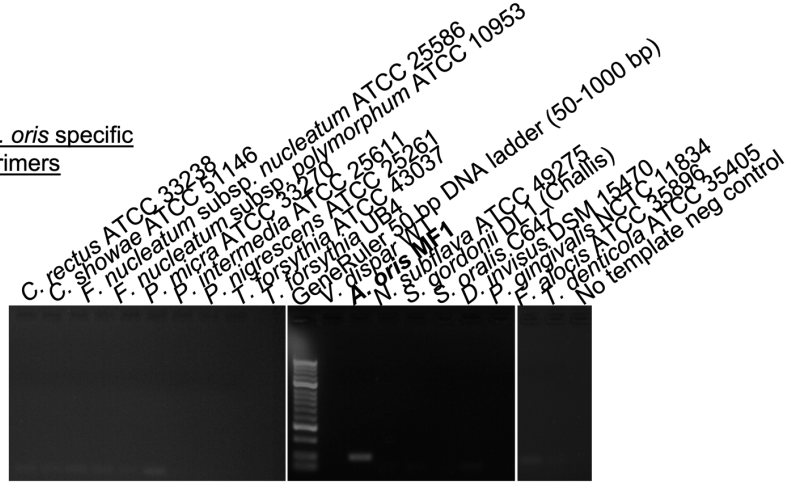

C. rectus specific primers

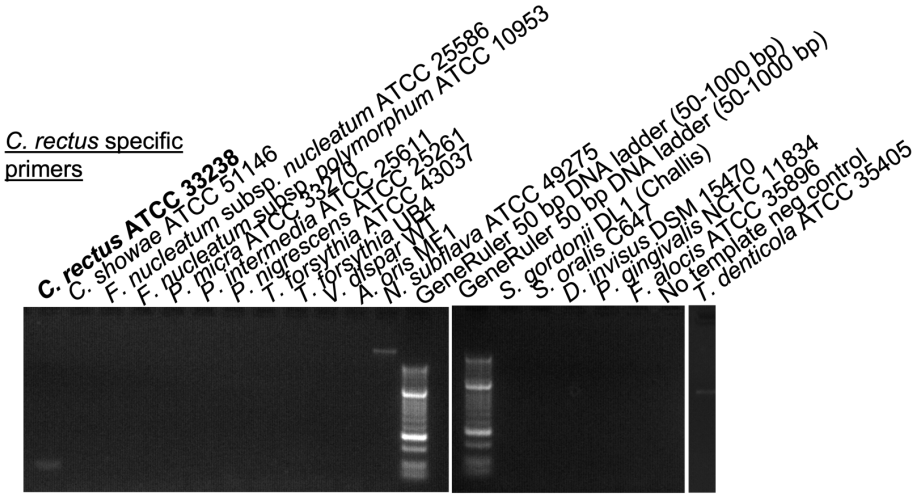

C. showae specific primers

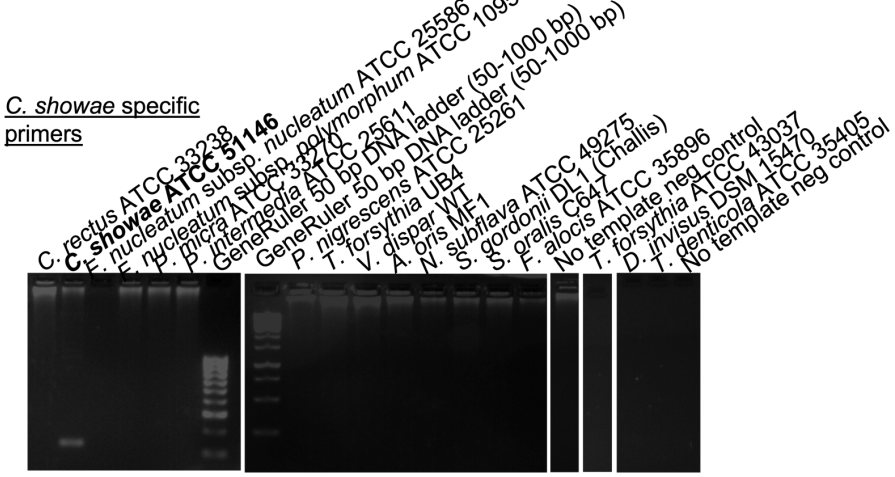

D. invisus specific primers

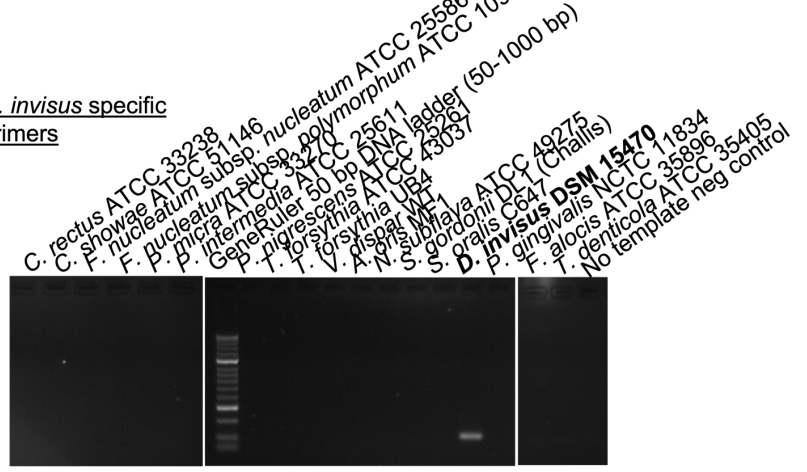

F. alocis specific primers

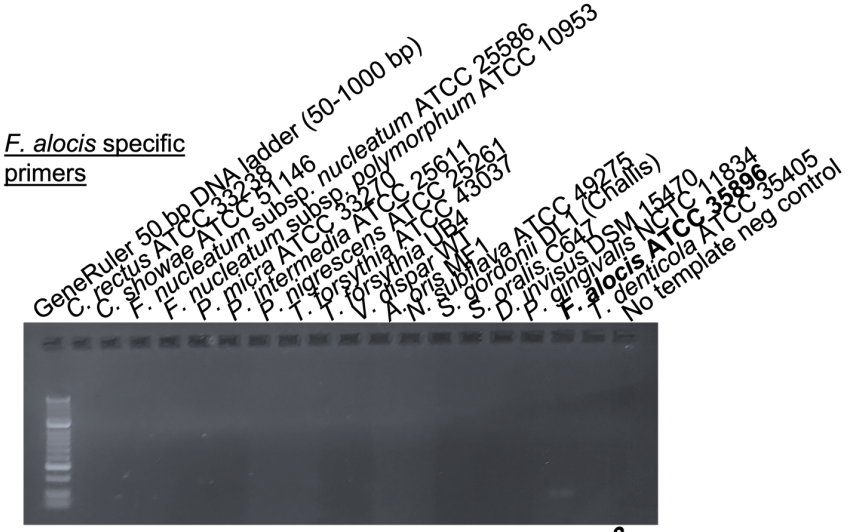

F. nucleatum subsp. *nucleatum* specific primers

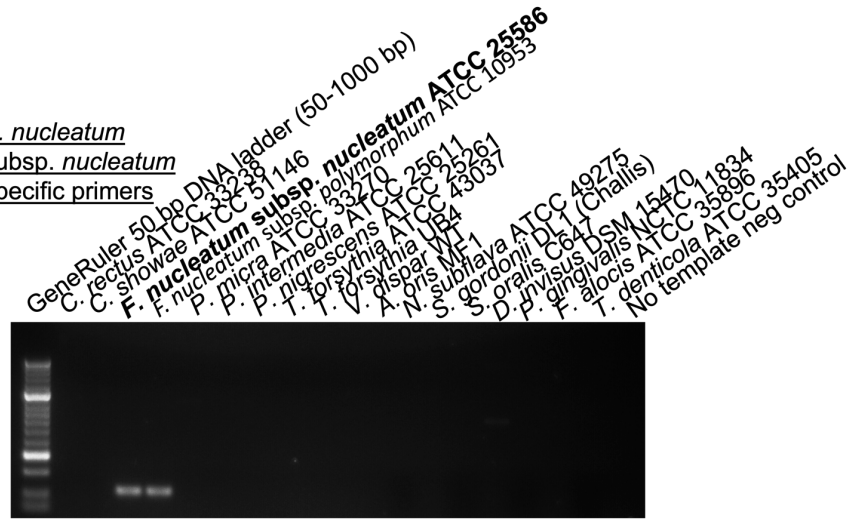

F. nucleatum subsp. *polymorphum* specific primers

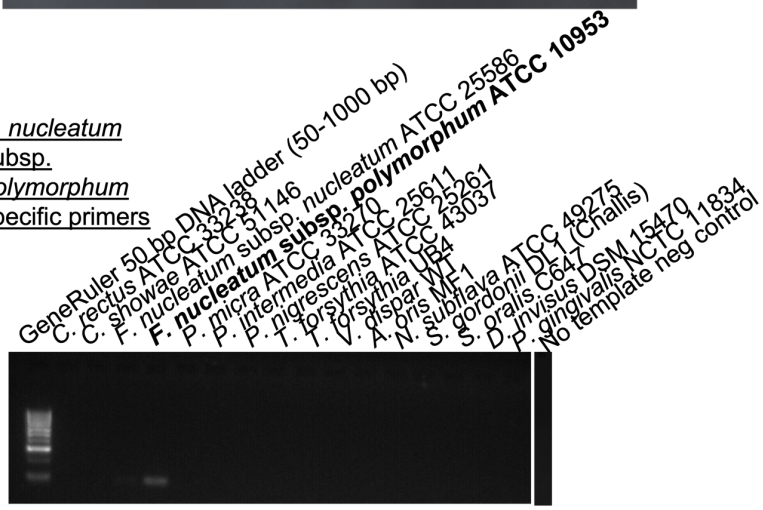

Note: *F. alocis* ATCC 35896 and *T. denticola* ATCC 35405 was not tested here due to the non-differentiation between the *F. nucleatum* subspecies.

N. subflava specific primers

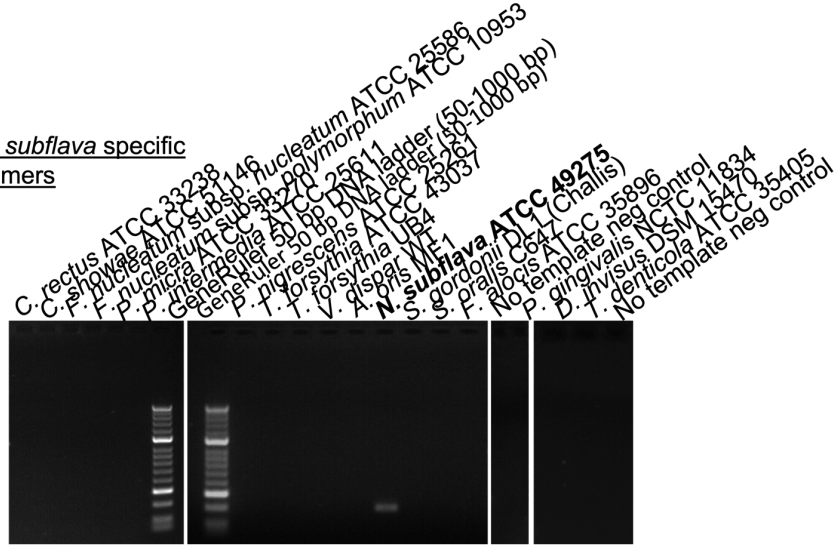

P. micra specific primers

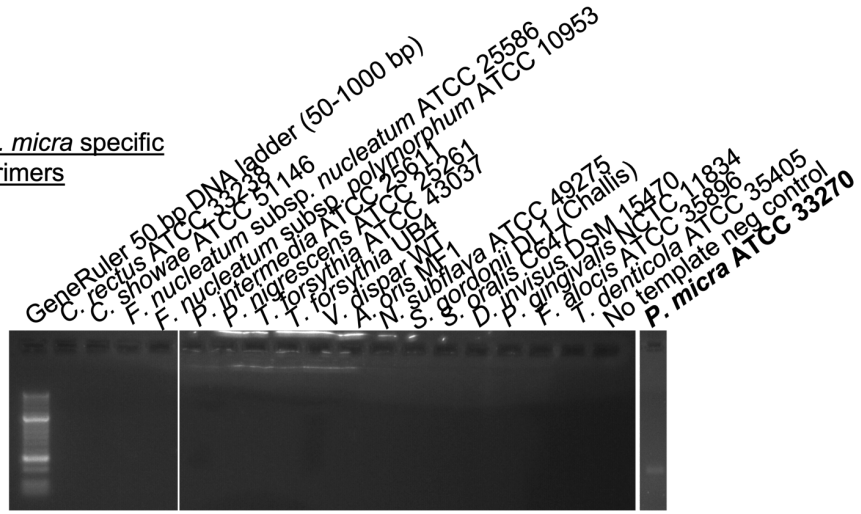

P. gingivalis specific primers

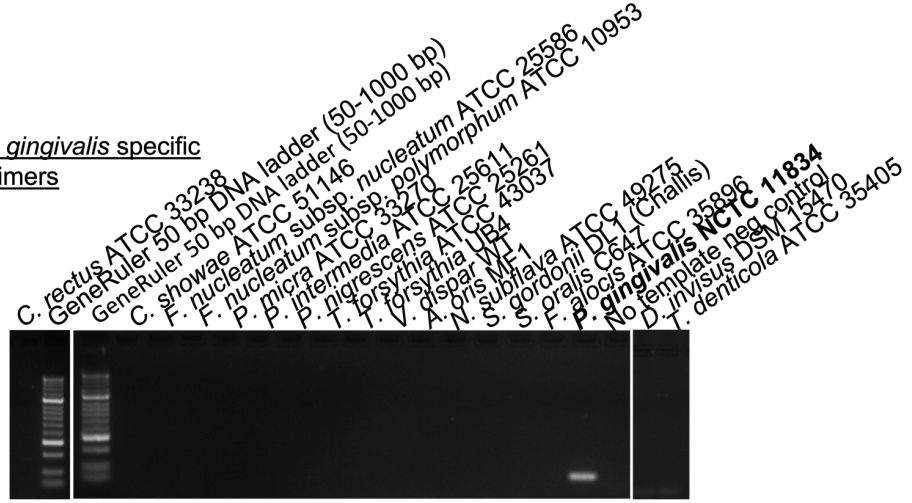

P. intermedia specific primers

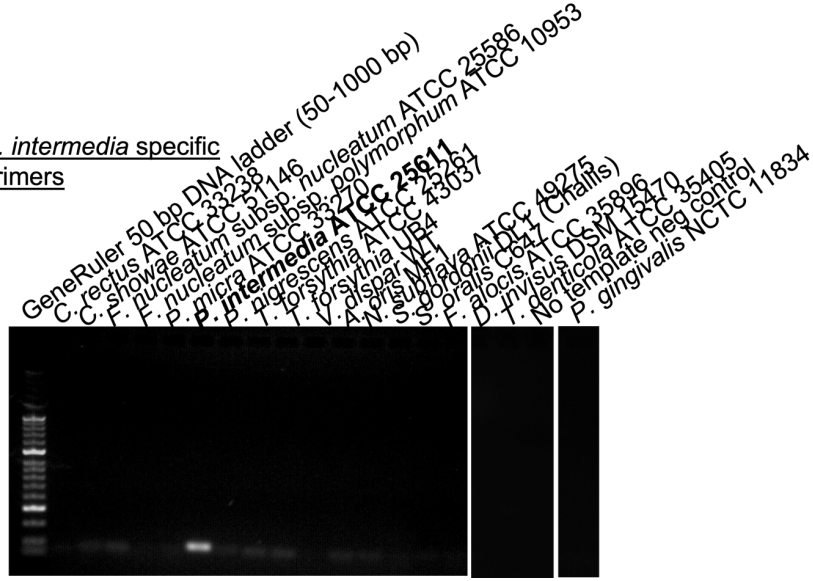

P. nigrescens specific primers

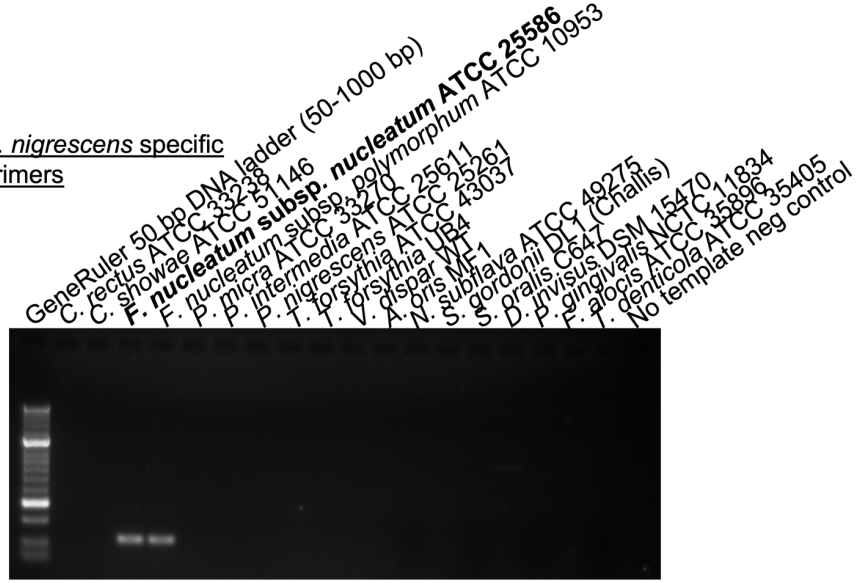

S. gordonii specific primers

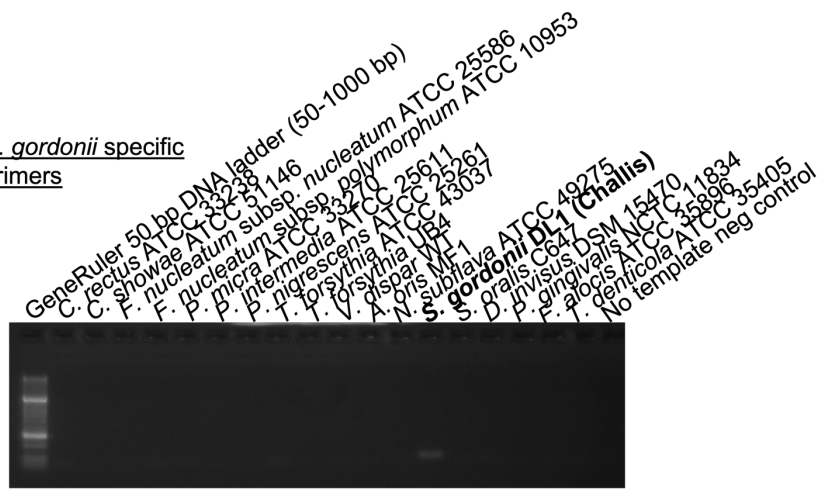

S. oralis specific primers

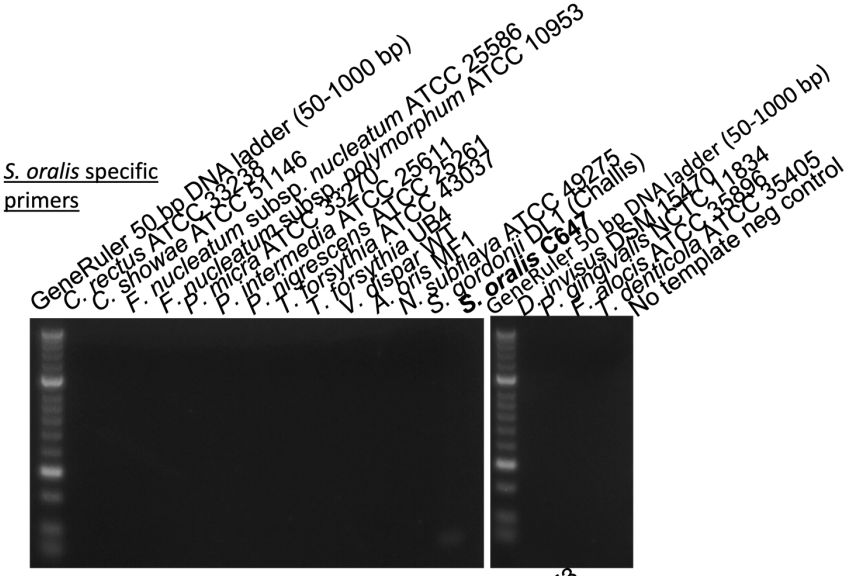

T. forsythia ATCC 43037 specific primers

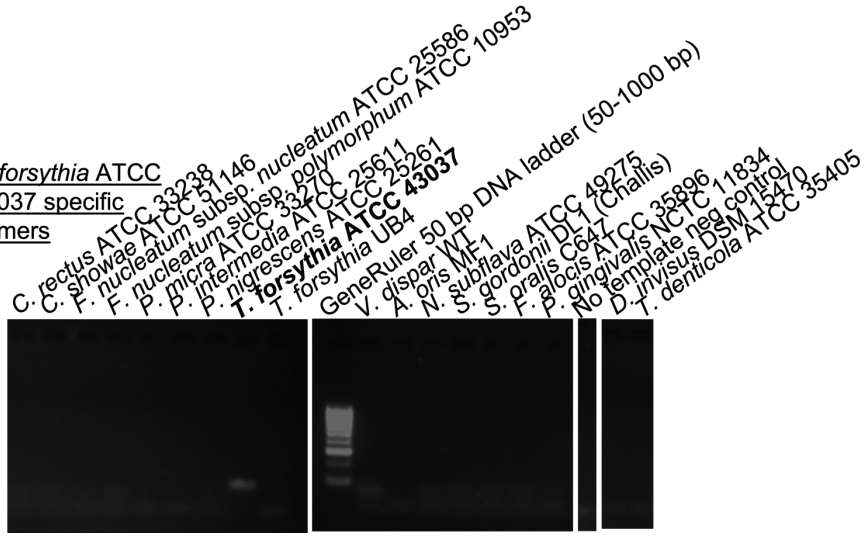

T. forsythia UB4 specific primers

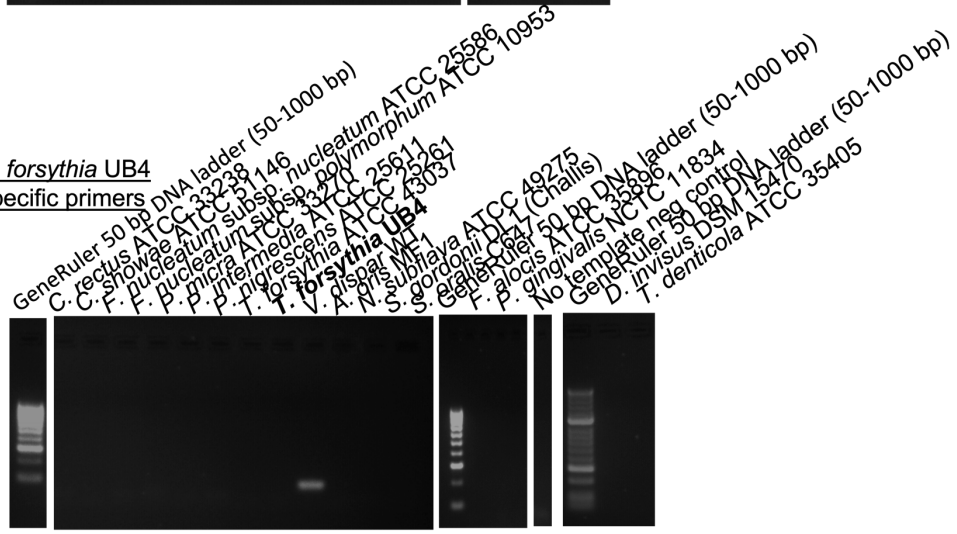

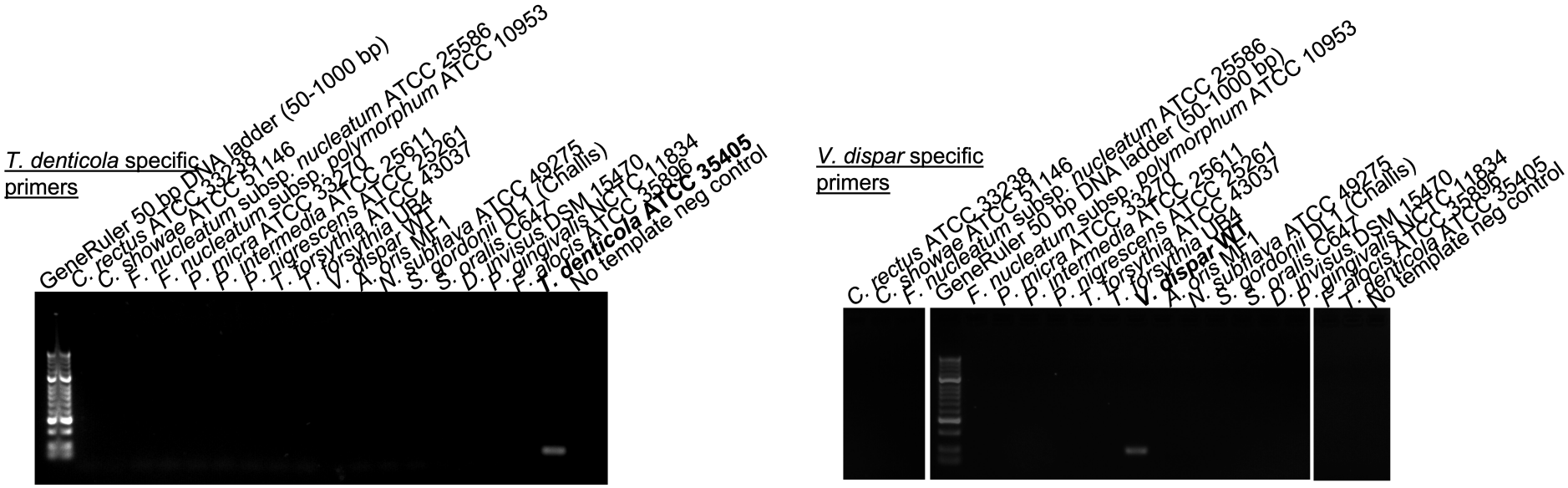

Figure 8.1 DNA electrophoresis gels conducted for the validation of bacterium-specific primer sets. The bacterium of interest in each gel is highlighted in bold.